225
Advances in Polymer Science

Advances in Polymer Science

Recently Published and Forthcoming Volumes

Polymer Libraries

Volume Editors: Michael A.R. Meier
Dean C. Webster

With contributions by

N. Adams · C.R. Becer · K.L. Beers · M.J. Fasolka
M.A.R. Meier · U.S. Schubert · C.M. Stafford
D.C. Webster

Springer

Editors

Prof. Dr. Michael A.R. Meier
University of Potsdam
Institute of Chemistry
Laboratory of Sustainable Organic Synthesis
Karl-Liebknecht-Str. 24
2514476 Golm/Potsdam
Germany
michael.meier@uni-potsdam.de

Prof. Dean C. Webster
Department of Coatings
    and Polymeric Materials
North Dakota State University
PO Box 6050, Dept 2760
Fargo, ND 58108, USA
dean.webster@ndsu.edu

Advances in Polymer Sciences
Also Available Electronically

Advances in Polymer Sciences is included in Springer's eBook package *Chemistry and Materials Science*. If a library does not opt for the whole package the book series may be bought on a subscription basis. Also, all back volumes are available electronically.

For all customers who have a standing order to the print version of *Advances in Polymer Sciences*, we offer the electronic version via SpringerLink free of charge.

If you do not have access, you can still view the table of contents of each volume and the abstract of each article by going to the SpringerLink homepage, clicking on "Browse by Online Libraries", then "Chemical Sciences", and finally choose *Advances in Polymer Science*.

You will find information about the

– Editorial Board
– Aims and Scope
– Instructions for Authors
– Sample Contribution

at springer.com using the search function by typing in *Advances in Polymer Sciences*.

Color figures are published in full color in the electronic version on SpringerLink.

Aims and Scope

The series *Advances in Polymer Science* presents critical reviews of the present and future trends in polymer and biopolymer science including chemistry, physical chemistry, physics and material science. It is addressed to all scientists at universities and in industry who wish to keep abreast of advances in the topics covered.

Review articles for the topical volumes are invited by the volume editors. As a rule, single contributions are also specially commissioned. The editors and publishers will, however, always be pleased to receive suggestions and supplementary information. Papers are accepted for *Advances in Polymer Science* in English.

In references *Advances in Polymer Sciences* is abbreviated as *Adv. Polym. Sci.* and is cited as a journal.

Special volumes are edited by well known guest editors who invite reputed authors for the review articles in their volumes.

Impact Factor in 2008: 6.802; Section "Polymer Science": Rank 2 of 73

Preface

This is truly an exciting time to be in the field of polymer science. Advances in polymerization methods are providing polymer scientists with the ability to specify and control polymer composition, structure, architecture, and molecular weight to a degree that was not possible just a decade ago. This, in turn, is resulting in many novel application possibilities of polymers ranging from drug delivery systems and nanolithography to stimuli-responsive materials and many others. In addition, many of the application areas of polymers – such as coatings, adhesives, thermoplastics, composites, and personal care – are also taking advantage of the ability to design polymers during their development efforts. Not to forget, many of these applications of polymers involve mixing polymers with solvents, catalysts, colorants, and many other ingredients to prepare a formulated product.

However, the tuning of polymer composition and structure as well as polymer formulations to optimize the final performance properties can be challenging, especially since in many cases several interacting variables need to be optimized simultaneously. This is where the methodologies and techniques of combinatorial and high-throughput experimentation to synthesize and characterize polymer libraries can be an invaluable approach. Simply put, a polymer library is a collection of multiple polymer samples having a systematic variation in one or more variables related to composition, structure, or process. Various methods and strategies have been explored to efficiently prepare a large number of polymer samples and also to screen these samples for key properties of interest. In this way, a broad range of compositions can be prepared and evaluated in a similar time frame required to prepare one or two samples, significantly increasing the efficiency of the experimental process. In addition, because the variable space is explored more thoroughly and in more detail than when using conventional laboratory methods, often materials having a unique combination of properties are identified.

While the use of these methods can be shown to be of benefit to a large number of polymer research programs, the widespread implementation of these concepts has not been realized. Thus, we would encourage those working in complex polymer systems to carefully consider the examples provided in this volume and identify how these could be implemented in their research work.

In Chap. 1, we provide an introduction to the strategies that have been reported for the preparation and characterization of polymer libraries and then highlight

a few selected examples where polymer libraries have been effectively used to identify novel materials. In Chap. 2, Becer and Schubert describe the preparation of polymers using controlled/living polymerization methods. Automated reactors have been used both to optimize the synthetic conditions and for preparing libraries of novel block copolymers. Next, Fasolka, Stafford, and Beers describe strategies used to study the interfaces of polymer systems using a gradient combinatorial approach. In the gradient approach, a single physical sample is prepared that has a systematic change in properties such as composition, thickness, surface energy, etc. A number of truly unique and creative methods have been developed to prepare the samples and characterize the gradient libraries for properties such as adhesion, surface energy, modulus, and so on. Finally, one of the challenges in the use of combinatorial and high-throughput methods is in the analysis and modeling of the data obtained. In Chap. 4, Adams discusses various approaches and especially the challenges involved in the modeling of the polymer data which may be generated using combinatorial and high-throughput experiments.

While providing a compendium of work done in the past, our primary aim is that this volume will provide inspiration and motivation for polymer scientists to employ combinatorial and high-throughput methods in their research efforts and generate even greater and novel discoveries from their research work.

In addition, we would like to thank all those who have contributed to this volume to make it a success: C. Remzi Becer, Ulrich S. Schubert, Michael J. Fasolka, Christopher M. Stafford, Kathryn L. Beers, and Nico Adams. Without your excellent contributions, this volume would not have been a reality.

Potsdam, Germany   *Michael A.R. Meier*
Fargo, ND, USA   *Dean C. Webster*
Spring 2010

Contents

Polymer Libraries: Preparation and Applications

Dean C. Webster and Michael A.R. Meier

Abstract Polymer libraries offer straightforward opportunities for the investigation of structure–property relationships and for a more thorough understanding of certain research problems. Furthermore, if combined with high-throughput methods for their preparation as well as screening, they offer the additional advantage of time savings and/or the reduction of experimental efforts. Thus, the herein discussed methods of polymer library preparation and selected literature examples of polymer libraries describe efficient and state-of-the-art methods to tackle difficult research challenges in polymer and materials science.

Keywords Combinatorial materials research · High-throughput screening · Library preparation · Polymer library · Property screening

Contents

————————————

D.C. Webster (✉)
Coatings and Polymeric Materials, North Dakota State University, 1735 NDSU Research Park Drive, Fargo, ND 58102, USA
email:dean.webster@ndsu.edu

M.A.R. Meier
University of Potsdam, Institute of Chemistry, Karl-Liebknecht-Str. 24-25, 14476 Golm, Germany
email:michael.meier@uni-potsdam.de

1 Introduction

Polymers are highly tailorable materials and polymers having unique combinations of properties or can perform a specific function (e.g. drug delivery) are desirable. In addition to variations in composition and molecular weight, different polymer architectures, such as block, graft, star, dendrimer, etc., are also possible. Identifying a specific polymer that has the desired properties can be a challenging task due to the large number of variations possible.

Therefore, polymer libraries, in combination with high-throughput screening techniques, are highly useful tools for the evaluation of (quantitative) structure–property relationships and/or the identification of "hits" of certain desired properties of the evaluated materials. These tools help researchers to understand their research problems more thoroughly by, e.g., finding optimal process conditions or product performance within a reduced amount of time and/or experimental effort.

After the introduction of combinatorial and high-throughput approaches in pharmaceutical and catalysis research programs, these methods also became available to the polymer/materials scientist at the beginning of this new century [1–3]. Therefore, new and specially adopted preparation and high-throughput screening techniques had to be developed, taking the requirements of the fields into account [4]. Examples include parallel synthetic equipment that can handle highly viscous polymer melts and solutions as well as screening techniques for polymer molecular weights and molecular weight distributions. Only this development made it possible to prepare and screen polymer libraries within a reasonable amount of time, opening the possibility to address scientific questions that would otherwise be difficult to tackle.

In order to find the desired hits and/or structure–property relationships, the design of a polymer library as well as the availability of suitable screening methods are crucial. The researchers have to ask themselves which experimental factors will have an influence and what are reasonable ranges for these factors to be tested. After this screening process, a further optimization of the screening outcome might be necessary and, finally, a model might be developed and tested for its robustness. Traditionally, such optimizations are performed stepwise, one parameter at a time. Unfortunately, this approach can lead to results that are far from the optimum (compare Fig. 1, left), since interaction between the investigated factors are most likely not identified. The advantage of high-throughput approaches on the other hand is the possibility to screen the complete parameter set, making the identification of hits as well as optimal process parameters easier (Fig. 1, right).

Before setting up the experiments, or preparing a library, a suitable experimental design has to be chosen [5, 6]. One of the most commonly used designs for polymer libraries are still the statistical full factorial designs and fractional factorial designs. Both have in common the systematic variation of experimental factors in a set of discrete levels, whereby the latter consist of a carefully chosen subset (fraction) of the full factorial design. Increasing the amount of simultaneously investigated parameters exponentially increases the experimental as well as data handling efforts
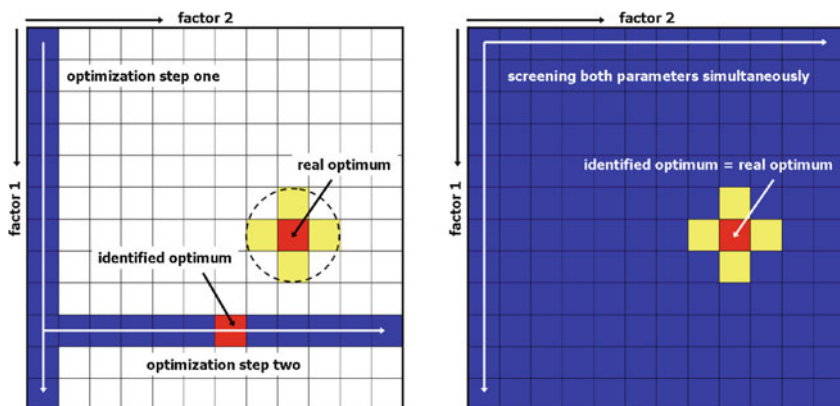
Fig. 1 Classical step-by-step optimization (*left*) compared to simultaneous screening of all parameters (*right*)

and can, at a certain point, not even be tackled with high-throughput approaches. For these problems, design-of-experiments approaches that utilize statistical experimental designs and allow for the reduction of the number of experiments to be performed without compromising the information content of the generated data have to be applied [5, 6].

Within the following sections we will give a brief overview of the available high-throughput methods for the preparation and screening of polymer libraries and then focus our discussion on well recognized literature examples of polymer libraries.

2 Polymer Library Preparation

Polymer libraries are generally not prepared for their own sake, but rather in order to explore some key property of the investigated materials. The technique used to prepare a given polymer library is often dictated by the method(s) to be used to screen or characterize the library compositions for the key properties of interest.

Concepts for the preparation of polymer libraries have followed two general pathways. One method involves the preparation of a single specimen wherein independent variables are varied spatially across the sample dimensions. The use of this technique for polymer systems has been led by researchers at the National Institute of Standards and Technology (NIST) in the USA. For example, the phase behavior of binary polymer blends has been studied as a function of composition and temperature by preparing a single sample having varying polymer blend composition along one spatial dimension and placing the sample on a temperature stage having a gradient in the orthogonal direction [7]. Illustrated in Fig. 2, the composition gradient was prepared by slowly filling a syringe from a stirred reservoir of the first polymer while a solution of the second polymer was added, creating a change in composition over time.
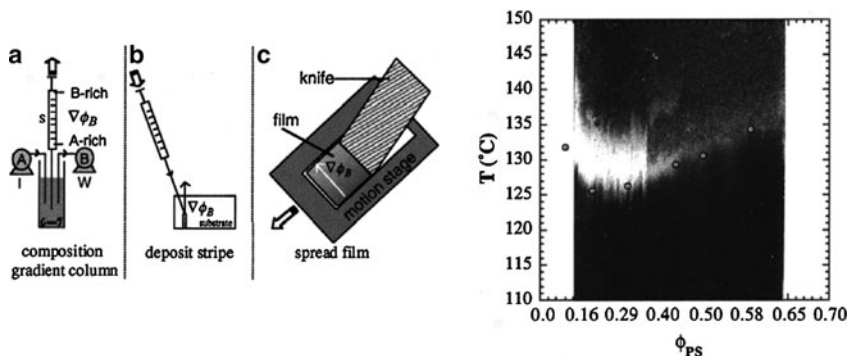
Fig. 2 Formation of polymer blend gradient film and phase behavior. Reprinted with permission from [7]. (Copyright 2000 American Chemical Society)

Then the content of the syringe was dispensed in a strip on a glass slide and a doctor blade was used to spread the solution in the orthogonal direction. The phase behavior of the blend can be determined directly by visual inspection of the sample (Fig. 2, right). Similarly, it was also possible to create gradients in both polymer blend composition and film thickness by accelerating the movement of the doctor blade when spreading the blend solution [8].

The group of Genzer et al. have used surface-initiated polymerization to create samples having gradients in surface grafting density [9–11] and molecular weight [12]. Surfaces of grafted block copolymers having orthogonal variation in the individual block lengths have also been prepared [13, 14].

The Beers group at NIST have demonstrated the preparation of surface-grafted copolymers having a compositional gradient by filling a narrow channel with a gradient in monomer composition followed by atom-transfer radical polymerization (ATRP) using a surface-grafted initiator (Fig. 3) [15]. This results in a gradient of statistical copolymers having a systematic change in composition from one end of the sample to the other. Block copolymer brush gradients could be synthesized using a two-step technique [16]. The first block was polymerized using surface-initiated ATRP. Then using the first block as macroinitiator, the second block was polymerized to have a gradient in block length.

To study the effects of composition on the photopolymerization behavior of acrylates, the group of Bowman et al. prepared gradient libraries where acrylate composition was varied in one dimension and light exposure was varied using a moveable shutter in the orthogonal direction [17–21]. An FTIR microscope was used to characterize the conversion across the samples and the data from multiple libraries was then used to derive kinetic models for the photopolymerization.

While the gradient approach is attractive for studying many phenomena, for many studies it is desired to prepare a library of discrete (individual) polymer samples having a systematic variation in composition, molecular weight, crosslink density, or architecture. Using discrete samples frees one from the two (or possibly three) spatial dimensions of the gradient library, allowing for experimental designs having three, four, or more variables.
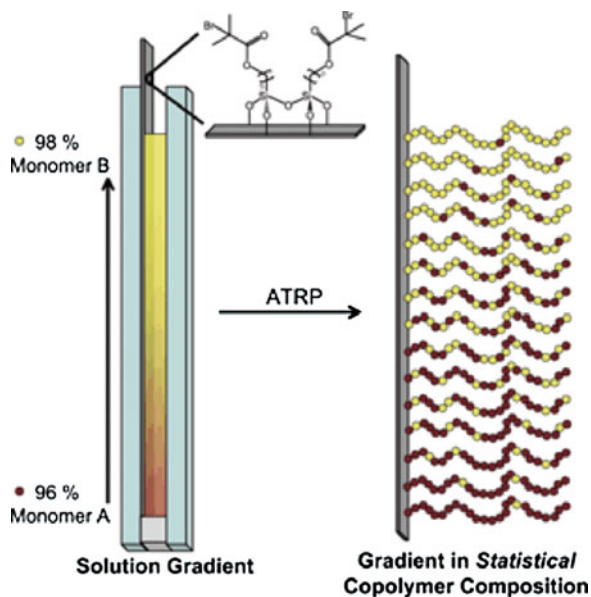
Fig. 3 Preparation of surface-grafted polymer brush composition gradient. Reprinted with permission from [15]. (Copyright 2006 Wiley-VCH Verlag GmbH & Co)

One approach to preparing polymer samples for a combinatorial study could involve using conventional laboratory synthesis methods to prepare the desired polymers one at a time. There are many studies reported in the literature where a series of polymers having some systematic variation in composition or other property were prepared and characterized. However, this approach has limitations in time and resources and becomes unattractive when the synthesis of large numbers of polymers is required.

If the chemistry is amenable, it is possible to synthesize a large number of small samples of polymers by simply mixing the ingredients in either small vials or multiwell plates. For example, Brocchini et al. prepared a library of 112 polymers by mixing the monomers in individual vials which were placed in a water bath [22]. Akinc et al. synthesized a library of 24 unique poly(β-amino esters) via the conjugate addition of acrylates and amines by mixing the monomers in sample vials fitted with stir bars [23]. To speed up this process, a liquid handling robot can be used to dispense the raw materials into an array of vials [24].

Another approach to the preparation of polymer libraries is to conduct individual polymer synthesis reactions in parallel in small individual reactors. To speed up the process, automated parallel synthesizers designed for use in combinatorial chemistry have been adapted and reactor systems specifically designed for polymer synthesis have also been commercialized (Fig. 4). These reactor systems can automate many of the steps needed to prepare a library of polymers, including dispensing of monomers and other reagents according to the desired recipe, controlling the heating and cooling steps and performing the required purification steps.
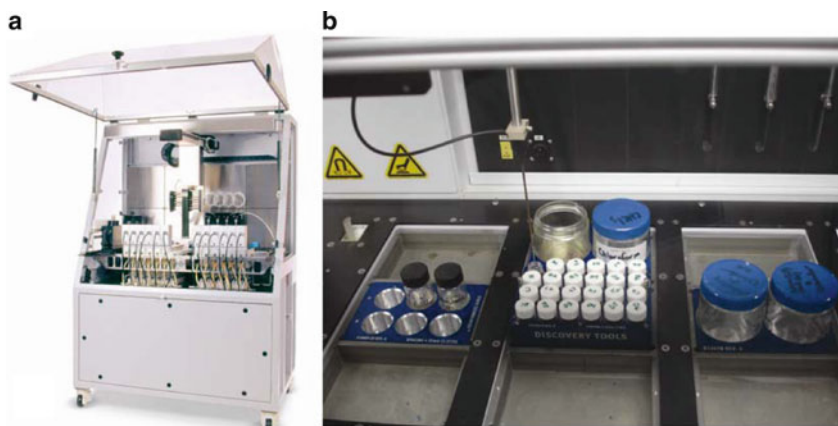
Fig. 4 Illustration of (**a**) Chemspeed automated synthesizer and (**b**) Symyx batch polymerization system for synthesis of discrete polymer libraries. Reprinted with permission from [90]. (Copyright 2007 Taylor & Francis Group, http://www.informaworld.com)

The group of Schubert et al. has demonstrated the utility of using automated chemical synthesizers for carrying out many different types of polymerizations including controlled radical polymerizations [25–33], cationic ring-opening polymerization [34–38], and anionic polymerization [39, 40]. In addition, block copolymers [41–46] and supramolecular polymers [47–49] have also been synthesized. The Webster group has used a simple batch polymerization system to synthesize functional siloxane and siloxane-polycaprolactone block copolymers via ring-opening polymerization [50, 51], and also to carry out conventional and controlled free radical polymerization [52–55]. Rojas et al. have reported that it is challenging to conduct step-growth polymerization to high and reproducible molecular weight using an automated reactor system since, in order to obtain high molecular weight polymers when two or more monomers are used, equivalent stoichiometry between the monomers, and therefore precise dispensing of the monomers into the individual reactors, is required [56]. Liquid dispensing of the monomers in solution was found to be more precise than dispensing the solid powders. An alternative approach is to convert the polymerization from a step-growth (condensation) reaction of monomers to an entropically-driven ring-opening polymerization [57].

A limitation of these simple reactor systems is that agitation is typically by vortexing or magnetic stirring, thus polymerizations have to be carried out in solution at relatively low viscosity. Newer reactor systems have been designed that employ mechanical mixing, allowing for conducting polymerizations at higher viscosity including multi-step processes [58]. Some of these automated synthesizers can be programmed to withdraw samples periodically during the polymerization reaction for further analysis, so the course of the reaction can be followed and the reaction kinetics evaluated [59].

Following polymer synthesis, in many cases it is necessary to convert the polymer into a solid film for property screening. Solutions of thermoplastic polymers can be deposited directly onto the required substrate and the solvent evaporated to leave the polymer film. Libraries of thermoset polymers are prepared by dispensing and mixing the required components, which can include polymers, crosslinkers, solvents, catalysts, etc., using an automated dispensing and mixing system. The mixtures are then deposited on an appropriate substrate, usually in an array format, followed by the curing of the library of samples. A number of methods can be used to deposit the formulation libraries including using a liquid handling pipette to deposit the samples into the wells of a microtiter plate or other multiwell substrate [60, 61], ink-jet printing [62–65], microcontact printing [66–68], or using an automated device for depositing and spreading the materials on a substrate [69–71].

3 Selected Examples

In recent years, many examples of polymer libraries applying high-throughput experimentation concepts for the fast and reliable determination of structure–property relationships were reported in the literature.

Kohn et al. were probably the first to make use excessively of these concepts and reported in 1997 on a "combinatorial approach for polymer design" [22]. Therefore, 14 tyrosine-derived diphenols and eight diacids were reacted with each other in up to 32 parallel polymerization reactions to obtain a 112-membered library of strictly alternating A–B type copolymers with predictable and systematic material property variations. These polymerizations were conducted in separate reactions vessels in a water bath in a 0.2 g scale yielding enough material after purification for the establishment basic material properties as well as certain biological properties. For instance, it was shown that the glass transition temperature (T_g) as well as the air–water contact angle of the polymers increased as the number of carbon or oxygen atoms in the polymer backbone and pendent chain decreased in a defined fashion to mention only a few of the found structure–property correlations (Fig. 5).

Moreover, a linear correlation was obtained between cell proliferation and air–water contact angles when polymers having an identical backbone structure but different pendent chains were grouped together. In general, cell proliferation significantly decreased as the polymer surface became more hydrophobic. In contrast, for those polymers having oxygen-containing diacids in the backbone, cell proliferation was far less sensitive to surface hydrophobicity. In fact, all polymers having oxygen-containing diacids in their backbone were uniformly good fibroblast growth substrates irrespective of their air–water contact angle. In subsequent investigations, models for both protein adsorption onto and cellular response to polymeric surfaces were derived from the discussed 112-membered library using computed descriptors that are only based on the polymer structures and their glass transition temperatures (T_g) [72]. Finally, a variety of other biologically important parameters, such as gene expression levels or protein adsorption, were evaluated for this

Fig. 5 Glass transition temperature variation within a library of 112 copolymers. Reprinted with permission from [22]. (Copyright 1997 American Chemical Society)

polymer library and it was attempted to correlate the outcome of these tests to the chemical structure of the investigated polymers [73–75]. These examples clearly demonstrate that a designed (targeted) library of polymeric materials is a very useful tool to evaluate structure–property relationships and to develop computational models. The knowledge obtained can subsequently be applied for the preparation of materials with certain designed properties with a reduced amount of effort and time [76].

Later, several authors adopted this general library preparation technique to their specific needs and reported on the synthesis of different polymer libraries prepared via step-growth polymerization techniques [77–79]. For instance, *Candida antarctica* lipase in acetonitrile was shown to catalyze efficiently the polycondensation of a variety of diol monomers, including aliphatic and aromatic diols, as well as carbohydrates, nucleic acids, and a natural steroid diol, with straight chain diesters to form a library of high molecular weight polymers [79]. Moreover, a linearly varying compositional library of 100 different biodegradable polyanhydride random copolymers was prepared via polycondensation [77]. It was argued that these materials are promising carriers for controlled drug delivery and indeed the authors could show that the rate of release of a model dye could be correlated to the copolymer composition.

In an equally distinguished example, Langer et al. demonstrated the synthesis of a 140-membered library of degradable polymers from diacrylate and amine monomers (compare Fig. 6) that were polymerized via aza-Michael addition chemistry [80].

The library was screened for DNA-complexing materials as well as gene delivery vectors, revealing several new materials that were able to condense DNA

Fig. 6 Monomers used for the construction of a 140-membered library of degradable polymers. Structures redrawn from [80]

into small enough structures to be internalized by cells and releasing the DNA in a transcriptionally active form. Further investigation of this library by in vitro transfections screening methods identified two candidates with very high transfection levels and revealed, due to this highly systematic approach, first correlations between the chemical structure of the polymers and their performance [81]. Subsequently, the synthesis and screening of a library of 2,350 structurally unique, degradable, cationic polymers from a larger subset of similar monomers (compare Fig. 6) became feasible by using automated fluid-handling systems [24]. In particular, a high-throughput, cell-based screening method could thus identify 46 new polymers that transfect with a higher efficiency than conventional nonviral delivery systems such as poly(ethyleneimine). Last, but not least, Langer et al. reported the in vitro screening of a 500-membered poly(β-amino esters) library for transfection efficiency and cytotoxicity [82]. Some vectors surpassed the best commercially available nonviral vectors for in vitro and in vivo gene transfer, and it was observed that the direct administration of one of these poly(β-amino ester)s complexed to DNA encoding the toxin DT-A could effectively inhibit tumor growth in mice.

In the area of conjugated polymers, Lavastre et al. reported a high-throughput approach for the preparation and screening of poly(arylene ethynylene)s [83]. Therefore, Pd-catalyzed carbon–carbon coupling reactions between 12 dihalogenated and 8 diethynyl monomers were performed in parallel, yielding a 96-membered polymer library that was screened for its fluorescent properties in solution as well as in thin films utilizing plate reader technology. The authors conclude that their HTE approach was successfully applied for the fast discovery of potential new candidates for OLEDs and led to the detection of polymers showing a red, green, or blue solid-sate fluorescence [83].

Moreover, libraries of dendrimers and other branched polymer architectures were successfully prepared and investigated. In 2001 Hawker et al. presented a strategy to prepare multiarm star polymers using nitroxide-mediated "living" radical polymerization [84]. Therefore, a macroinitiator together with a monofunctional and a bifunctional monomer were reacted resulting in the formation of cross-linked moieties with random spacers of the monofunctional monomer, which effectively knit together the polymeric arms of the macroinitiator leading to formation of soluble star polymers. Since too many parameters had to be investigated for this polymerization, only a high-throughput approach enabled the researchers to achieve their goal [84]. Later, the same group reported a library of highly branched, 3-dimensional, dendron functional core cross-linked star polymers via a similar approach [85]. Moreover, dendrimer libraries were prepared via click-chemistry [86] as well as via classical approaches [87]. Especially the click-chemistry approach led to a library of functionalized dendritic macromolecules in extremely high yields using no protecting group strategies and only minimal purification steps [86]. Therefore, this strategy presents a significant advance compared to traditional approaches not only for the synthesis of dendrimer libraries but polymer libraries in general. Last, but not least, a small library of star-shaped block copolymers was shown to behave as unimolecular micelles and to transfer guest molecules from a water to a chloroform phase [45]. This behavior was screened using plate reader technology and the encapsulation behavior could be correlated to the polymer architecture. At a later stage, it could be shown that these polymers encapsulated a large variety of different guest molecules [46], they were able to stabilize metal nano-particles that were potent catalysts for C–C coupling reactions [88], and the encapsulated guest molecules could also be transported within these nano-carriers [89].

High-throughput approaches are frequently applied to the synthesis and evaluation of coating libraries [90]. Representative examples include, for instance, the preparation of acrylate based coatings and their subsequent evaluation by high-throughput screening techniques [91]. Thus, 48-element coatings libraries were prepared as 8×6 arrays and evaluated for their abrasion resistance applying self-developed test methods leading to an important productivity improvement of at least 10 times over a conventional coating development process [91]. Moreover, Webster et al. have worked on coating libraries with reduced adhesion for applications as anti-fouling coatings [52, 92, 93]. For instance, an acrylic polyol library was synthesized using batch solution polymerization of the monomers using the three monomers butyl methacrylate, *n*-butyl acrylate, and 2-hydroxyethyl acrylate to obtain polyols of varying compositions [52]. The resulting 24-membered polyol library was characterized using high-throughput gel permeation chromatography and differential scanning calorimetry (DSC). Subsequently, this library was formulated into siloxane-polyurethane coatings and the resulting coatings were tested for pseudo-barnacle adhesion revealing that most of the investigated materials showed very low adhesion [52]. Later, the same authors reported on the development of an automated imaging software tool that quantifies bacterial and algal percent coverage on coating arrays and argued that surface coverage is a highly relevant parameter when down-selecting coatings on the basis of their fouling-release potential [92]. The presented

screening method, in combination with other high-throughput screening techniques, would ultimately allow a reduction of 200–300 coating formulations to only approximately 10 formulations that need to be subjected to full ocean testing [92]. Thus, these high-throughput coating testing methods not only save time, but also significantly reduce the time required and the expenses necessary for full evaluation of a certain class of materials.

More specific libraries, such as polymer thin film (gradient) libraries or libraries prepared via controlled polymerization techniques, are not part of this overview, but will be discussed in detail in other chapters of this book [94, 95].

References

1. Webster DC (2008) Combinatorial and high-throughput methods in macromolecular materials research and development. Macromol Chem Phys 209:237–246
2. Hoogenboom R, Meier MAR, Schubert US (2003) Combinatorial methods, automated synthesis and high-throughput screening in polymer research: past and present. Macromol Rapid Commun 24:15–32
3. Meier MAR, Hoogenboom R, Schubert US (2004) Combinatorial methods, automated synthesis and high-throughput screening in polymer research: the evolution continues. Macromol Rapid Commun 25:21–33
4. Schmatloch S, Meier MAR, Schubert US (2003) Instrumentation for combinatorial and high-throughput polymer research: a short overview. Macromol Rapid Commun 24:33–46
5. Cawse JN (2001) Experimental strategies for combinatorial and high-throughput materials development. Acc Chem Res 34:213–221
6. Harmon L (2003) Experiment planning for combinatorial materials discovery. J Mater Sci 38:4479–4485
7. Meredith JC, Karim A, Amis EJ (2000) High-throughput measurement of polymer blend phase behavior. Macromolecules 33:5760–5762
8. Meredith JC, Smith AP, Karim A, Amis EJ (2000) Combinatorial materials science for polymer thin-film dewetting. Macromolecules 33:9747–9756
9. Wu T, Efimenko K, Vlcek P, Subr V, Genzer J (2003) Formation and properties of anchored polymers with a gradual variation of grafting densities on flat substrates. Macromolecules 36:2448–2453
10. Wu T, Tomlinson M, Efimenko K, Genzer J (2003) A combinatorial approach to surface anchored polymers. J Mater Sci 38:4471–4477
11. Wu T, Efimenko K, Genzer J (2002) Combinatorial study of the mushroom-to-brush crossover in surface anchored polyacrylamide. J Am Chem Soc 124:9394–9395
12. Tomlinson MR, Genzer J (2003) Formation of grafted macromolecular assemblies with a gradual variation of molecular weight on solid substrates. Macromolecules 36:3449–3451
13. Bhat RR, Tomlinson MR, Genzer J (2005) Orthogonal surface-grafted polymer gradients: a versatile combinatorial platform. J Polym Sci Part B Polym Phys 43:3384–3394
14. Tomlinson MR, Genzer J (2005) Evolution of surface morphologies in multivariant assemblies of surface-tethered diblock copolymers after selective solvent treatment. Langmuir 21:11552–11555
15. Xu C, Barnes SE, Wu T, Fischer DA, DeLongchamp DM, Batteas JD, Beers KL (2006) Solution and surface composition gradients via microfluidic confinement: fabrication of a statistical-copolymer-brush composition gradient. Adv Mater 18:1427–1430
16. Xu C, Wu T, Batteas JD, Drain CM, Beers KL, Fasolka MJ (2006) Surface-grafted block copolymer gradients: effect of block length on solvent response. Appl Surf Sci 252:2529–2534

17. Johnson PM, Reynolds TB, Stansbury JW, Bowman CN (2005) High throughput kinetic analysis of photopolymer conversion using composition and exposure time gradients. Polymer 46:3300–3306
18. Johnson PM, Stansbury JW, Bowman CN (2008) High-throughput kinetic analysis of acrylate and thiol-ene photopolymerization using temperature and exposure time gradients. J Polym Sci Part A Polym Chem 46:1502–1509
19. Johnson PM, Stansbury JW, Bowman CN (2007) Photopolymer kinetics using light intensity gradients in high-throughput conversion analysis. Polymer 48:6319–6324
20. Johnson PM, Stansbury JW, Bowman CN (2007) Alkyl chain length effects on copolymerization kinetics of a monoacrylate with hexanediol diacrylate. J Comb Chem 9:1149–1156
21. Johnson PM, Stansbury JW, Bowman CN (2008) Kinetic modeling of a comonomer photopolymerization system using high-throughput conversion data. Macromolecules 41:230–237
22. Brocchini S, James K, Tangpasuthadol V, Kohn J (1997) A combinatorial approach for polymer design. J Am Chem Soc 119:4553–4554
23. Akinc A, Anderson Daniel G, Lynn David M, Langer R (2003) Synthesis of poly(β-amino ester)s optimized for highly effective gene delivery. Bioconjug Chem 14:979–988
24. Anderson DG, Lynn DM, Langer R (2003) Semi-automated synthesis and screening of a large library of degradable cationic polymers for gene delivery. Angew Chem, Int Ed 42:3153–3158
25. Becer CR, Paulus RM, Hoogenboom R, Schubert US (2006) Optimization of the nitroxide-mediated radical polymerization conditions for styrene and *tert*-butyl acrylate in an automated parallel synthesizer. J Polym Sci Part A Polym Chem 44:6202–6213
26. Eggenhuisen TM, Becer CR, Fijten MWM, Eckardt R, Hoogenboom R, Schubert US (2008) Libraries of statistical hydroxypropyl acrylate containing copolymers with LCST properties prepared by NMP. Macromolecules 41:5132–5140
27. Fijten MWM, Meier MAR, Hoogenboom R, Schubert US (2004) Automated parallel investigations/optimizations of the reversible addition-fragmentation chain transfer polymerization of methyl methacrylate. J Polym Sci Part A Polym Chem 42:5775–5783
28. Fijten MWM, Paulus RM, Schubert US (2005) Systematic parallel investigation of RAFT polymerizations for eight different (meth)acrylates: a basis for the designed synthesis of block and random copolymers. J Polym Sci Part A Polym Chem 43:3831–3839
29. Paulus RM, Fijten MWM, de la Mar MJ, Hoogenboom R, Schubert US (2005) Reversible addition-fragmentation chain transfer polymerization on different synthesizer platforms. QSAR Comb Sci 24:863–867
30. Zhang H, Abeln CH, Fijten MWM, Schubert US (2006) High-throughput experimentation applied to atom-transfer radical polymerization: automated optimization of the copper catalysts removal from polymers. e-Polymers
31. Zhang H, Fijten MWM, Hoogenboom R, Reinierkens R, Schubert US (2003) Application of a parallel synthetic approach in atom-transfer radical polymerization: set-up and feasibility demonstration. Macromol Rapid Commun 24:81–86
32. Zhang H, Fijten MWM, Hoogenboom R, Schubert US (2003) Atom-transfer radical polymerization of methyl methacrylate utilizing an automated synthesizer. ACS Symp Ser 854:193–205
33. Zhang H, Marin V, Fijten MWM, Schubert US (2004) High-throughput experimentation in atom-transfer radical polymerization: a general approach toward a directed design and understanding of optimal catalytic systems. J Polym Sci Part A Polym Chem 42:1876–1885
34. Adams N, Gans B-JD, Kozodaev D, Sanchez C, Bastiaansen CWM, Broer DJ, Schubert US (2006) High-throughput screening and optimization of photoembossed relief structures. J Comb Chem 8:184–191
35. Hoogenboom R, Fijten MWM, Schubert US (2004) Parallel kinetic investigation of 2-oxazoline polymerizations with different initiators as basis for designed copolymer synthesis. J Polym Sci Part A Polym Chem 42:1830–1840
36. Hoogenboom R, Fijten MWM, Schubert US (2004) The effect of temperature on the living cationic polymerization of 2-phenyl-2-oxazoline explored utilizing an automated synthesizer. Macromol Rapid Commun 25:339–343

37. Hoogenboom R, Fijten MWM, Wijnans S, Van den Berg AMJ, Thijs HML, Schubert US (2006) High-throughput synthesis and screening of a library of random and gradient copoly(2-oxazoline)s. J Comb Chem 8:145–148
38. Hoogenboom R, Thijs HML, Fijten MWM, Schubert US (2007) Synthesis, characterization, and cross-linking of a library of statistical copolymers based on 2-"soy alkyl"-2-oxazoline and 2-ethyl-2-oxazoline. J Polym Sci Part A Polym Chem 45:5371–5379
39. Guerrero-Sanchez C, Abeln C, Schubert US (2005) Automated parallel anionic polymerizations: enhancing the possibilities of a widely used technique in polymer synthesis. J Polym Sci Part A Polym Chem 43:4151–4160
40. Guerrero-Sanchez C, Schubert US (2004) Towards automated parallel anionic polymerizations. Polymeric Mater Sci Eng 90:647–648
41. Becer CR, Hahn S, Fijten MWM, Thijs HML, Hoogenboom R, Schubert US (2008) Libraries of methacrylic acid and oligo(ethylene glycol) methacrylate copolymers with LCST behavior. J Polym Sci Part A Polym Chem 46:7138–7147
42. Fijten MWM, Kranenburg JM, Thijs HML, Paulus RM, Van Lankvelt BM, D Hullu J, Springintveld M, Thielen DJG, Tweedie CA, Hoogenboom R, VanVliet KJ, Schubert US (2007) Synthesis and structure–property relationships of random and block copolymers: a direct comparison for copoly(2-oxazoline)s. Macromolecules 40:5879–5886
43. Hoeppener S, Wiesbrock F, Hoogenboom R, Thijs HML, Schubert US (2006) Morphologies of spin-coated films of a library of diblock copoly(2-oxazoline)s and their correlation to the corresponding surface energies. Macromol Rapid Commun 27:405–411
44. Meier MAR, Aerts SNH, Staal BBP, Rasa M, Schubert US (2005) PEO-b-PCL block copolymers: synthesis, detailed characterization, and selected micellar drug encapsulation behavior. Macromol Rapid Commun 26:1918–1924
45. Meier MAR, Gohy J-F, Fustin C-A, Schubert US (2004) Combinatorial synthesis of star-shaped block copolymers: host-guest chemistry of unimolecular reversed micelles. J Am Chem Soc 126:11517–11521
46. Meier MAR, Schubert US (2005) Combinatorial evaluation of the host-guest chemistry of star-shaped block copolymers. J Comb Chem 7:356–359
47. Lohmeijer BGG, Wouters D, Yin Z, Schubert US (2004) Block copolymer libraries using supramolecular strategies. Polym Mater Sci Eng 90:723–724
48. Schmatloch S, Van den Berg AMJ, Fijten MMW, Schubert US (2004) Automated parallel synthesis of metallo-supramolecular polymers. Polym Mater Sci Eng 90:645–646
49. Schmatloch S, van den Berg AMJ, Fijten MWM, Schubert US (2004) A high-throughput approach towards tailor-made water-soluble metallo-supramolecular polymers. Macromol Rapid Commun 25:321–325
50. Ekin A, Webster DC (2006) Library synthesis and characterization of 3-aminopropyl-terminated poly(dimethylsiloxane)s and poly(e-caprolactone)-b-poly(dimethylsiloxane)s. J Polym Sci Part A Polym Chem 44:4880–4894
51. Ekin A, Webster DC. (2006) Synthesis and characterization of novel hydroxyalkyl carbamate and dihydroxyalkyl carbamate terminated poly(dimethylsiloxane) oligomers and their block copolymers with poly(e-caprolactone). Macromolecules 39:8659–8668
52. Pieper R, Ekin A, Webster DC, Casse F, Callow JA, Callow M. E. (2007) A combinatorial approach to study the effect of acrylic polyol composition on the pProperties of crosslinked siloxane-polyurethane fouling-release coatings. J Coatings Techn Res 4:453–461
53. Webster DC, Bennett J, Kuebler S, Kossuth MB, Jonasdottir S (2004) High throughput workflow for the development of coatings. J Coatings Tech 1:34–39
54. Nasrullah MJ, Webster DC (2006) Polymerization of styrene and t-butyl acrylate by atom-transfer radical polymerization – high throughput approach. Polymer Prepr 47:217–218
55. Nastrullah MJ, Ekin A, Bahr JA, Gallagher-Lein C, Webster DC (2006) Practical and automated high throughput approach: atom-transfer radical polymerization of styrene and t-butyl acrylate. PMSE Prepr 95:10–12
56. Rojas R, Harris NK, Piotrowska K, Kohn J (2009) Evaluation of automated synthesis for chain and step-growth polymerizations: can robots replace the chemists? J Poly Sci Part A Polym Chem 47:48–58

57. Kamau SD, Hodge P, Williams RT, Stagnaro P, Conzatti L (2008) High throughput synthesis of polyesters using entropically-driven ring-opening polymerizations. J Comb Chem 10:644–654
58. Nasrullah MJ, Bahr JA, Gallagher-Lein C, Webster DC, Roesler RR, Schmitt P (2009) Automated parallel polyurethane dispersion synthesis and characterization J Coatings Tech Res 6:1–10
59. Hoogenboom R, Fijten MWM, Abeln CH, Schubert US (2004) High-throughput investigation of polymerization kinetics by online monitoring of GPC and GC. Macromol Rapid Commun 25:237–242
60. Cawse JN, Olson D, Chisholm BJ, Brennan M, Sun T, Flanagan W, Akhave J, Mehrabi A, Saunders D (2003) Combinatorial chemistry methods for coating development V: generating a combinatorial array of uniform coatings samples. Prog Org Coatings 47:128–135
61. Chisholm B, Potyrailo R, Cawse J, Shaffer R, Brennan M, Molaison C, Whisenhunt D, Flanagan B, Olson D, Akhave J, Saunders D, Mehrabi A, Licon M (2002) The development of combinatorial chemistry methods for coating development I. Overview of the experimental factory. Prog Org Coatings 45:313–321
62. de Gans B-J, Duineveld PC, Schubert US (2004) Inkjet printing of polymers: state-of-the-art and future developments. Adv Mater 16:203–213
63. de Gans B-J, Kazancioglu E, Meyer W, Schubert US (2004) Ink-jet printing polymers and polymer libraries using micropipettes. Macromol Rapid Commun 25:292–296
64. de Gans B-J, Schubert US (2003) Inkjet printing of polymer micro-arrays and libraries: instrumentation, requirements, and perspectives. Macromol Rapid Commun 24:659–666
65. Tekin E, de Gans B-J, Schubert US (2004) Ink-jet printing of polymers – from single dots to thin film libraries. J Mater Chem 14:2627–2632
66. Anderson DG, Levenberg S, Langer R (2004) Nanoliter-scale synthesis of arrayed biomaterials and application to human embryonic stem cells. Nat Biotech 22:863–866
67. Diaz-Mochon JJ, Bialy L, Keinicke L, Bradley M (2005) Combinatorial libraries – from solution to 2D microarrays. Chem Commun 1384–1386
68. Tourniaire G, Collins J, Campbell S, Mizomoto H, Ogawa S, Thaburet J-F, Bradley M (2006) Polymer microarrays for cellular adhesion. Chemical Commun 2118–2120
69. Schmatloch S, Bach H, van Benthem RATM, Schubert US (2004) High-throughput experimentation in organic coating and thin film research: state-of-the-art and future perspectives. Macromol Rapid Commun 25:95–107
70. Iden R, Schrof W, Hadeler J, Lehmann S (2003) Combinatorial materials research in the polymer industry: speed versus flexibility. Macromol Rapid Commun 24:63–72
71. Majumdar P, Christianson DA, Roesler RR, Webster DC (2006) Optimization of coating film deposition when using an automated high throughput coating application unit. Prog Org Coatings 56:169–177
72. Smith JR, Kholodovych V, Knight D, Welsh WJ, Kohn J (2005) QSAR models for the analysis of bioresponse data from combinatorial libraries of biomaterials. QSAR Comb Sci 24:99–113
73. Weber N, Bolikal D, Bourke SL, Kohn J (2004) Small changes in the polymer structure influence the adsorption behavior of fibrinogen on polymer surfaces: validation of a new rapid screening technique. J Biomed Mater Res Part A 68A:496–503
74. Smith JR, Seyda A, Weber N, Knight D, Abramson S, Kohn J (2004) Integration of combinatorial synthesis, rapid screening, and computational modeling in biomaterials development. Macromol Rapid Commun 25:127–140
75. Abramson SD, Alexe G, Hammer PL, Kohn J (2005) A computational approach to predicting cell growth on polymeric biomaterials. J Biomed Mater Res Part A 73A:116–124
76. Meier MAR, Schubert US (2006) Selected successful approaches in combinatorial materials research. Soft Matter 2:371–376. This paragraph was partially reproduced by permission of The Royal Society of Chemistry:http://dx.doi.org/10.1039/b518304a
77. Vogel BM, Cabral JT, Eidelman N, Narasimhan B, Mallapragada SK (2005) Parallel synthesis and high throughput dissolution testing of biodegradable polyanhydride copolymers. J Comb Chem 7:921–928
78. Reynolds CH (1999) Designing diverse and focused combinatorial libraries of synthetic polymers. J Comb Chem 1:297–306

79. Kim D-Y, Dordick JS (2001) Combinatorial array-based enzymatic polyester synthesis. Biotechnol Bioeng 76:200–206
80. Lynn DM, Anderson DG, Putnam D, Langer R (2001) Accelerated discovery of synthetic transfection vectors: parallel synthesis and screening of a degradable polymer library. J Am Chem Soc 123:8155–8156
81. Akinc A, Lynn DM, Anderson DG, Langer R (2003) Parallel synthesis and biophysical characterization of a degradable polymer library for gene delivery. J Am Chem Soc 125:5316–5323
82. Anderson DG, Peng W, Akinc A, Hossain N, Kohn A, Padera R, Langer R, Sawicki JA (2004) A polymer library approach to suicide gene therapy for cancer. Proc Natl Acad Sci U S A 101:16028–16033
83. Lavastre O, Illitchev I, Jegou G, Dixneuf PH (2002) Discovery of new fluorescent materials from fast synthesis and screening of conjugated polymers. J Am Chem Soc 124:5278–5279
84. Bosman AW, Heumann A, Klaerner G, Benoit D, Frechet JMJ, Hawker CJ (2001) High-throughput synthesis of nanoscale materials: structural optimization of fFunctionalized one-step star polymers. J Am Chem Soc 123:6461–6462
85. Connal LA, Vestberg R, Hawker CJ, Qiao GG (2007) Synthesis of dendron functionalized core cross-linked star polymers. Macromolecules 40:7855–7863
86. Malkoch M, Schleicher K, Drockenmuller E, Hawker CJ, Russell TP, Wu P, Fokin VV (2005) Structurally diverse dendritic libraries: a highly efficient functionalization approach using click-chemistry. Macromolecules 38:3663–3678
87. Percec V, Mitchell CM, Cho W-D, Uchida S, Glodde M, Ungar G, Zeng X, Liu Y, Balagurusamy VSK, Heiney PA (2004) Designing libraries of first generation AB3 and AB2 self-assembling dendrons via the primary structure generated from combinations of (AB)y-AB3 and (AB)y-AB2 building blocks. J Am Chem Soc 126:6078–6094
88. Meier MAR, Filali M, Gohy J-F, Schubert US (2006) Star-shaped block copolymer stabilized palladium nanoparticles for efficient catalytic Heck cross-coupling reactions. J Mater Chem 16:3001–3006
89. Rasa M, Meier MAR, Schubert US (2007) Transport of guest molecules by unimolecular micelles evidenced in analytical ultracentrifugation experiments. Macromol Rapid Commun 28:1429–1433
90. Webster DC, Chisholm BJ, Stafslien SJ (2007) Mini-review: combinatorial approaches for the design of novel coating systems. Biofouling 23:179–192
91. Potyrailo RA, Chisholm BJ, Olson DR, Brennan MJ, Molaison CA (2002) Development of combinatorial chemistry methods for coatings: high-throughput screening of abrasion resistance of coatings libraries. Anal Chem 74:5105–5111
92. Ribeiro E, Stafslien SJ, Casse F, Callow JA, Callow ME, Pieper RJ, Daniels JW, Bahr JA, Webster DC (2008) Automated image-based method for laboratory screening of coating libraries for adhesion of algae and bacterial biofilms. J Comb Chem 10:586–594
93. Casse F, Ribeiro E, Ekin A, Webster DC, Callow JA, Callow ME (2007) Laboratory screening of coating libraries for algal adhesion. Biofouling 23:267–276
94. Becer CR, Schubert US (2009) Parallel optimization and high-throughput preparation of well-defined copolymer libraries using controlled/"living" polymerization methods. Adv Polym Sci DOI 10.1007/12_2009_16
95. Fasolka MJ, Stafford CM, Beers KL (2009) Gradient and microfluidic library approaches to polymer interfaces. Adv Polym Sci DOI 10.1007/12_2009_17

Parallel Optimization and High-Throughput Preparation of Well-Defined Copolymer Libraries Using Controlled/"Living" Polymerization Methods

C. Remzi Becer and Ulrich S. Schubert

Abstract This chapter highlights the application of controlled/"living" polymerization (CLP) techniques in automated parallel synthesizers for both optimizing reaction parameters as well as preparing copolymer libraries. Special attention is given to the use of CLP techniques for constructing well-defined copolymer libraries. Furthermore, alternative strategies for the preparation of block copolymer libraries are discussed.

Keywords Automated parallel synthesis · Block copolymers · High-throughput experimentation · Polymer libraries · Random copolymers

Contents

C.R. Becer and U.S. Schubert (✉)
Laboratory of Macromolecular Chemistry and Nanoscience, Eindhoven University of Technology, Den Dolech 2, 5612, AZ, Eindhoven, The Netherlands
and
Laboratory of Organic and Macromolecular Chemistry, Friedrich-Schiller-University Jena, Humboldtstr., 10, 07743 Jena, Germany
and
Dutch Polymer Institute, John F. Kennedylaan 2, 5612, AB, Eindhoven, The Netherlands
e-mail:r.becer@tue.nl;ulrich.schubert@uni-jena.de

Abbreviations

AA	Acrylic acid
AcBr	Acetyl bromide
AcCl	Acetyl chloride
AcI	Acetyl iodide
AFM	Atomic force microscopy
AIBN	α,α-Azobisisobutyronitrile
Amor	*N*-Acryoyl morpholine
ATRP	Atom transfer radical polymerization
BEB	(1-Bromo ethyl) benzene
bpy	$4,4'$-Dialkyl substituted bipyridine
BrEB*i*B	2-Bromo-2-methylpropanoyl bromide
CBDB	2-Cyano-2-butyl dithio benzoate
CLP	Controlled/"living" polymerization
CROP	Cationic ring opening polymerization
CRP	Controlled radical polymerization
CTA	Chain transfer agent
DMA	*N*,*N*-Dimethyl acrylamide
DMAc	*N*,*N*-Dimethyl acetamide
DMAEMA	*N*,*N*-Dimethyl aminoethyl acrylamide
DMF	*N*,*N*-Dimethyl formamide
DP	Degree of polymerization
DSC	Differential scanning calorimetry
EEA	1-Ethoxy ethyl acrylate
EBIB	Ethyl-2-bromo-*iso*-butyrate
EtOx	2-Ethyl-2-oxazoline
GC	Gas chromatography
HPA	2-Hydoxypropyl acrylate
*i*PrOx	2-*iso*-Propyl-2-oxazoline
LCST	Lower critical solution temperature
MA	Methyl acrylate
MAA	Methacrylic acid
MADIX	Macromolecular design via the interchange of xanthates
MBP	Methyl bromo propionate
MMA	Methyl methacrylate
MeOMA	2-Methoxyethyl 2-methylacrylate
MeO$_2$MA	2-(2-Methoxyethoxy)ethyl 2-methylacrylate

MeOx	2-Methyl-2-oxazoline
M_n	Number average molar mass
nBA	*n*-Butyl acrylate
NIPAM	*N*-Isopropyl acrylamide
NMP	Nitroxide mediated polymerization
NMR	Nuclear magnetic resonance
NonOx	2-Nonyl-2-oxazoline
OEGMA	Oligo(ethyleneglycol) methyl ether methacrylate
OEGEMA	Oligo(ethylene glycol) ethyl ether methacrylate
PAA	Poly(acrylic acid)
PDI	Polydispersity index
PEEA	Poly(1-ethoxyethyl acrylate)
PEG	Poly(ethyleneglycol)
PEO	Poly(ethylene oxide)
PheOx	2-Phenyl-2-oxazoline
PDMAEMA	Poly(*N*,*N*-dimethyl aminoethyl methacrylate)
PMA	Poly(methyl acrylate)
PMMA	Poly(methyl methacrylate)
PnBA	Poly(*n*-butyl acrylate)
PSt	Poly(styrene)
P*t*BA	Poly(*tert*-butyl acrylate)
RAFT	Reversible addition-fragmentation chain transfer
SEC	Size exclusion chromatography
s-BuLi	*sec*-Butyllithium
SPE	Solid phase extraction
SoyOx	2-"Soyalkyl"-2-oxazoline
St	Styrene
*t*BA	*tert*-Butyl acrylate
TEMPO	2,2,6,6-Tetramethyl-1-piperidinyloxy stable radical
T_g	Glass transition temperature
TGA	Thermal gravimetric analysis
TsCl	*p*-Toluene sulfonyl chloride

1 Introduction

Tailor-made macromolecules have come into the focus of polymer science to overcome the challenges of a number of complex applications from the nano to the macro scale. Materials scientists have been designing and synthesizing tailor-made macromolecules specific for each application. These materials are composed of different monomeric units, chemical functionalities, and topologies. The challenge has been to control precisely the position of the functionality on the polymer, to determine the necessary ratio of monomeric units, as well as to understand the effect of the molecular architecture on the material performance.

The development of controlled/"living" polymerization (CLP) techniques has opened a new window to researchers to gain control successfully over the synthesis of well-defined polymeric structures [1–5]. However, each polymerization technique requires specific catalysts, initiators, and optimum reaction conditions for different monomers. Optimization and understanding the effect of each input variable on the polymerization kinetics or the obtained macromolecule can be performed by the use of high-throughput experimentation techniques. There is no doubt that screening a wide range of reaction parameters will allow researchers to define the most efficient synthesis conditions for successfully designing and preparing tailor-made polymers. Following the identification of the optimum reaction parameters, systematic sets of copolymers can be synthesized to elucidate structure-property relationships. Alternatively, gradient thin film libraries allow screening the effect of two or more parameters on a relatively small scale [6–8]. There are several methods to create gradient thin film libraries, e.g., flow-coating and ink jet printing [9, 10]. Countless data sets are being obtained by analysis of large polymer libraries and these data sets allow pinpointing of the best performance materials [11–15].

In this chapter, we will focus on the use of CLP techniques for the synthesis of systematic copolymer libraries using high-throughput approaches. Prior to that, automated parallel optimization reactions that have been performed for different CLP techniques will be discussed. At the end of this chapter there will be a highlight on the latest synthetic approaches to synthesize well-defined polymer libraries.

2 Parallel Optimization of Controlled/"Living" Polymerizations

Absolute structural control over the polymer chain represents the primary target in modern synthetic polymer chemistry. In practice, the term "well-defined" is commonly used for polymers that exhibit low polydispersity indices; however their structural composition should also be known in some detail. Important key features can be listed such as the chemical structures of the initiating and the end groups, monomer composition, number of repeating units as well as topology. Different synthetic approaches have been developed to gain control over the architecture. Ionic and radical polymerization techniques have been the most promising ones to provide the desired macromolecules. There is still the need to develop and optimize these techniques further, not only to improve the synthesis procedures but also to provide a deeper insight into the fundamentals of polymerization mechanisms.

Researchers have already invested several decades to elucidate the effect of input variables on the polymerization kinetics and the polymer structures. Many research groups have devoted their resources to obtaining reproducible data on polymerization kinetics. One of the methods to achieve that is to conduct several experiments in parallel to keep most reaction inputs constant and to minimize unpredictable environmental effects. In these series of experiments it appeared to be necessary to apply

automated parallel synthesis platforms and standardized experimental protocols in order to provide extended and comparable data sets within a short period of time.

2.1 Radical Polymerization Techniques

Starting from 1956, living ionic polymerizations became the major interest for the synthesis of well-defined polymers. Szwarc reported that in the anionic polymerization of styrene (St) the polymer chains grew until all the monomer was consumed; the chains continued to grow upon addition of more monomer [16].

According to the IUPAC definition, ionic polymerization is a type of chain polymerization where the kinetic-chain carriers are ions or ion pairs [17]. However, these techniques have some limitations such as the necessity of extreme purity of the chemicals and the reaction medium, incompatibility between the reactive centers and monomers, and the sensitivity to certain chemical functionalities that limits the monomer selection. These challenges directed researchers to discover or develop alternative polymerization techniques. One of the alternative polymerization routes is radical polymerization since it is less discriminating regarding the types of polymerizable vinyl monomers and more tolerant to several functionalities. The most common method is free radical polymerization, which results in polymers with broad molar mass distributions. However, polymers with relatively high polydispersity indices may be of some advantage in industrial processing. For instance, low molar mass polymer chains in polymers with broad molar mass distributions provide a plasticizer effect during processing. However, these ill-defined polymers are not suited for advanced applications and are also not suitable for understanding structure-property relationships.

As a consequence of the free radical polymerization kinetics, the termination rates are extremely fast in comparison to the slow initiation rates. This results in the formation of high molar mass chains at the initial stage of the polymerization and decreasing molar masses in the latter stages due to the decrease in the monomer concentration. Under these circumstances, broad molar mass distributions are inevitable.

There were several attempts to gain better control on the free radical polymerization process [18, 19]. One of these methods was named the "iniferter" method. The compounds used in this technique can serve as *ini*tiator, trans*fer* agent and *ter*minating agent [20–22]. Another technique is based on the use of bulky organic compounds such as diaryl or triarylmethyl derivatives [23–25]. The main disadvantages of these systems comprise slow initiation, slow exchange, direct reaction of counter radicals with monomers, and their thermal decomposition. Therefore, these techniques did not offer the desired level of control over the polymerization.

Relatively new controlled radical polymerization (CRP) methods, which were discovered in the mid-1990s, focused on establishing a precise equilibrium between the active and dormant species. Three approaches, namely atom transfer radical

polymerization (ATRP) [1, 2], nitroxide mediated polymerization (NMP) [3, 26], and reversible addition fragmentation chain transfer (RAFT) [4, 27], out of several others, have attracted the most attention due to their success in providing relatively stable chain end functionalities that can be reactivated for subsequent block copolymerizations or post polymerization modifications.

2.1.1 Atom Transfer Radical Polymerization

ATRP has become the most widely applied CRP technique due to its simple mechanism and commercially available reagents. This technique was first reported in 1995, independently by Sawamoto and Matyjaszewski [28, 29]. The polymerization mechanism is based on the reversible redox reaction between alkyl halides and transition metal complexes. Scheme 1 illustrates the mechanism of normal ATRP.

The simplicity of the polymerization reaction is the result of intense research carried out by several groups on the importance and the fundamentals of each parameter. In particular, Matyjaszewski et al. have spent great effort on the construction of numerous comparison charts on the activity of initiators and ligands that are used in ATRP [30–32]. These published comparison tables represent the summary of hundreds of single experiments and are now a very important and reliable source of data for the ATRP technique.

It is obvious that automated parallel synthesis robots provide a great advantage to the researcher that has necessarily to keep all secondary parameters constant throughout the screening reactions. These commercially available robotic systems have been constantly tested not only by its producers but also by academic groups to verify the reproducibility of the high-throughput experimentation setups. Recently, we have reported a standard protocol on the automated kinetic investigation of controlled/living radical polymerization of various monomers as a first step to obtain comparable results independent of the research group [33].

Automated parallel experiments were carried out to rapidly screen and optimize the reaction conditions for ATRP of methyl methacrylate (MMA) [34]. A set of 108 different reactions was designed for this purpose. Different initiators and different metal salts have been used, namely ethyl-2-bromo-*iso*-butyrate (EBIB), methyl bromo propionate (MBP), (1-bromo ethyl) benzene (BEB), and *p*-toluene sulfonyl chloride (TsCl), and CuBr, CuCl, CuSCN, $FeBr_2$, and $FeCl_2$, respectively. 2,2′-Bipyridine and its derivatives were used as ligands. The overall reaction scheme and the structure of the used reagents are shown in Scheme 2.

$$R\text{-}X \ + \ M_t^n/\text{Ligand} \ \underset{k_{deact}}{\overset{k_{act}}{\rightleftharpoons}} \ \overset{\overset{(+M) \ k_p}{\curvearrowright}}{R\bullet} \ + \ M_t^{n+1}/\text{Ligand}$$
$$\downarrow k_t$$
$$R\text{-}R \ / \ R^H \ \& \ R^=$$
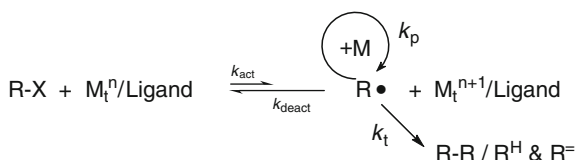
Scheme 1 General mechanism of atom transfer radical polymerization (ATRP)
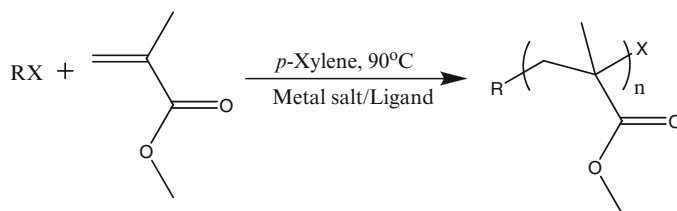
RX = EBIB, MBP, BEB, TsCl
Metal salt = CuBr, CuCl, CuSCN, $FeBr_2$, $FeCl_2$
Ligand = bpy, dMbpy, dHbpy, dTbpy, 4,5'-dMbpy, 5,5'-dMbpy, 4Mbpy, 6Mbpy
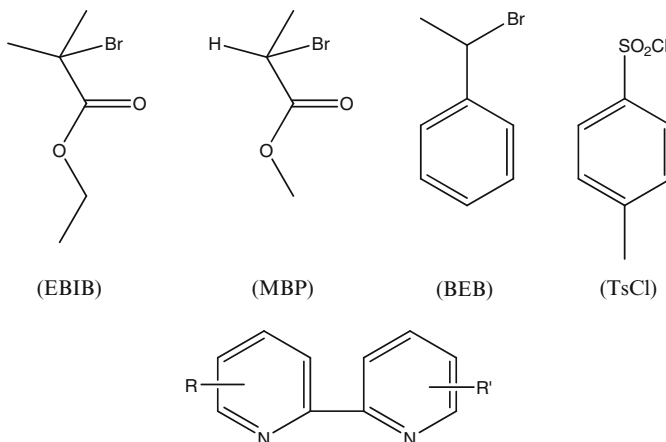
$R_4 = R_{4'} = $ H (bpy), CH_3 (dMbpy), n-C_6H_{13} (dHbpy), n-C_9H_{19} (dNbpy), n-$C_{13}H_{27}$ (dTbpy)
$R_4 = R_{5'} = CH_3$ (4,5'-dMbpy), $R_5 = R_{5'} = CH_3$ (5,5'-dMbpy)
$R_4 = CH_3$ and R' = H (4-Mbpy), $R_6 = CH_3$ and R' = H (6-Mbpy)

Scheme 2 Schematic representation of the ATRP of MMA using different initiators, ligands and metal salts. $[MMA]_0 : [initiator]_0 : [metal\ salt]_0 : [ligand]_0 = 150:1:1:2$ and MMA : p-xylene = 1:2 v/v

High-throughput experimentation of the ATRP of MMA was carried out in a Chemspeed ASW2000 automated synthesizer to screen rapidly and to optimize the reaction conditions. Two reactor blocks were used in parallel and each block consisted of 16 reaction vessels equipped with a double jacket heater. The typical layout of the automated synthesis platform is illustrated in Fig. 1. There are several locations for the reactor blocks in the platform and most commonly one or two blocks are used in parallel in order to keep the high-throughput workflow running without any bottlenecks. The stock solution rack is equipped with an argon inlet to keep the stock solutions under inert conditions. A solid phase extraction (SPE) unit, which is equipped with alumina columns, is used to remove the metal salt from the aliquots. The samples intended for characterization are transferred into small vials
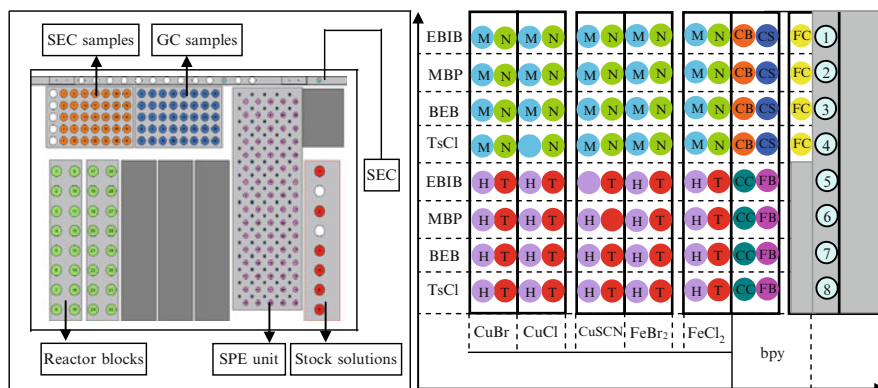
Fig. 1 Schematic representation of the automated synthesizer and combinations of metal salts, initiators and ligands used in this study. The symbols used in this figure are as follows: dMbpy, M; dHbpy, N; dTbpy, T; CuBr, CB; CuCl, CC; CuSCN, CS; FeBr$_2$, FB; FeCl$_2$, FC; CuBr + ligand + TsCl (ligand = $4,5'$ − dMbpy, 1; $5,5'$ − dMbpy, 2; 4Mbpy, 3; and 6Mbpy, 4), and CuCl + ligand + TsCl (ligand = $4,5'$ − dMbpy, 5; $5,5'$ − dMbpy, 6; 4Mbpy, 7; and 6Mbpy, 8). (Reprinted with permission from [34]. Copyright (2004) John Wiley & Sons, Inc.)

arranged in racks and the racks are transferred to the autosampler of the analytical instruments, such as gas chromatography (GC) or gas chromatography coupled with mass spectrometry (GC–MS), or size exclusion chromatography (SEC). In addition, there is an injection port for online SEC measurements. The technical details and further explanation on this system can be found in several reviews [35–40]. It should be noted that the computer-based planning and robotic performing of the reactions as well as the utilization of fast characterization techniques significantly decreased the research time for the designed library from several months to two weeks. The experimental results obtained could be compared and used for elucidation of structure-property relationships of monomer, initiator, and catalytic systems since all the reactions were carried under the same conditions.

Three main parameters were used to evaluate the efficiency of the polymerization, namely monomer conversion (C_{MMA}), initiation efficiency of the reaction ($f = M_{n,theo}/M_{n,SEC}$), and polydispersity index (PDI). These results are depicted in Fig. 2. It is obvious that the Cu(I)-catalyzed systems are more effective than the Fe(II)-catalyzed systems under the studied conditions. It was concluded that a bipyridine based ligand with a critical length of the substituted alkyl group (e.g., dHbpy) shows the best performance in Cu(I)-mediated systems. Besides, Cu(I) halide-mediated ATRP with $4,5'$-Mbpy as the ligand and TsCl as the initiator was better controlled than that with dMbpy as the ligand, and polymers with much lower PDI values were obtained in the former case.

Another challenge in ATRP is to remove the catalyst prior to the analysis of the polymers. In the case of automated sample withdrawing, this leads to the necessity of an automated purification system. For this purpose, an SPE unit was utilized
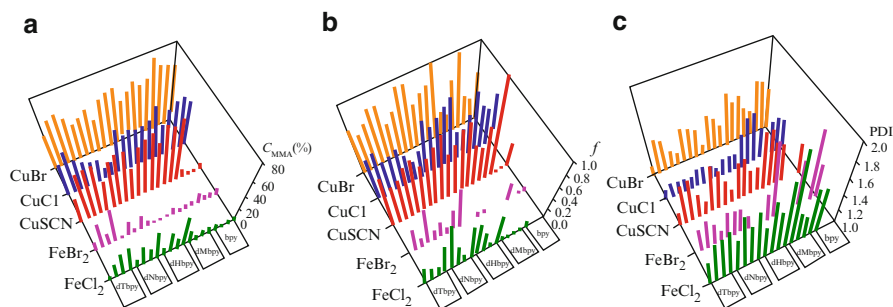
Fig. 2 Effects of metal salts, ligands, and initiators on C_{MMA}s (**a**), f (**b**), PDIs (**c**) of the polymers in the atom transfer radical polymerization (ATRP) of methyl methacrylate (MMA) in p-xylene at 90°C. $[MMA]_0$:$[initiator]_0$:$[metal\ salt]_0$:$[ligand]_0$ = 150:1:1:2, MMA/p-xylene = 1:2 v/v. EBIB, MBP, BEB, and TsCl were used as initiator from right to left in each ligand column, respectively (Reprinted with permission from [34]. Copyright (2004) John Wiley & Sons, Inc.)
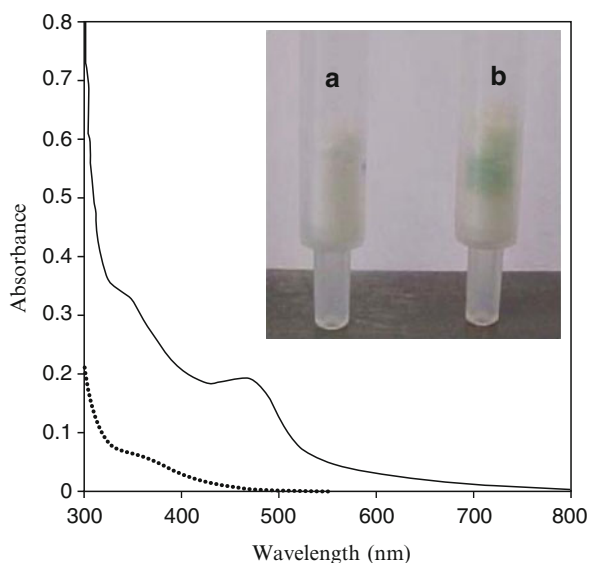
Fig. 3 UV-vis spectra of unpurified (*solid line*) and purified (*dashed line*) polymers in acetonitrile at same concentrations. (Reprinted with permission from [42]. Copyright (2003) John Wiley & Sons, Inc.)

to purify the aliquots [41, 42]. Different column materials were investigated and deactivated aluminum oxide gave the best results. As shown in Fig. 3, the absorption band of the sample decreased significantly after the purification.

2.1.2 Nitroxide Mediated Polymerization

Nitroxide mediated polymerization is one of the most environmentally friendly CRP techniques and has a relatively simple polymerization mechanism since there is no need for a catalyst [3]. Solomon, Rizzardo and Moad have demonstrated the reaction between 2,2,6,6-tetramethyl-1-piperidinyloxy stable radical (TEMPO) and vinyl monomers in the range of the free radical polymerization temperature (40–60 °C) [43]. Since then, two different NMP concepts have been developed, namely the bimolecular and the unimolecular process, respectively. Georges et al. described the bimolecular process for the preparation of low PDI value polystyrene initiated by benzoylperoxide and mediated by TEMPO [44]. Following that, unimolecular initiators have been developed that have the similar concept of well-defined initiators in living anionic and cationic processes [45, 46]. In unimolecular polymerizations, the initiator and the mediator are combined in a single molecule (e.g., alkoxyamines) that also simplifies the polymerization kinetics. The investigation on stable free nitroxide compounds were started with TEMPO and extended to several different types of nitroxide-containing compounds [3], such as phosphonate derivatives [47] or arenes [48]. The use of alkoxyamines allows the greatest degree of control over the final polymeric structure with well-defined functional end groups. A schematic representation of the NMP of St initiated by *N*-(2-methylpropyl)-*N*-(1-diethylphosphono-2,2-dimethylpropyl)-*O*-(2-carboxylprop-2-yl) hydroxylamine (Bloc Builder™) is illustrated in Scheme 3. Bloc Builder™ is an efficient alkoxyamine for styrenics as well as acrylates and currently commercially available from Arkema.

A systematic investigation has been performed on the homopolymerization of St and *tert*-butyl acrylate (*t*BA) in an automated parallel synthesizer [49]. The Chemspeed Accelerator SLT106™ was used in order to screen the effect of the polymerization temperature by the use of an individually heated reactor block. These blocks allow conducting up to 16 parallel reactions each at different temperatures, heated by electrical heating and controlled by an individual heat sensor in every reactor. The determination of the optimum polymerization temperature for a specific nitroxide compound plays a crucial role in the control of the polymer chain growth. Relatively high temperatures will cause an increase in the apparent radical concentration which will lead to increased side reactions such as termination by coupling or disproportionation. An example of this behavior is visible in Fig. 4. The apparent polymerization rates were increased by higher temperatures. Higher monomer conversions were obtained at shorter reaction periods; however, the PDI values of the polymers were increased above 1.4. The optimum polymerization temperature range using this type of alkoxyamine (Bloc Builder™) was reported to be in the range of 110–125 °C.

The most critical point of all CRP techniques is to gain absolute control over the activation and deactivation of the reactive chain end. This can be simply controlled by altering the polymerization temperature or increasing the deactivator concentration. Thus, additional stable free-nitroxide compounds can be added to the
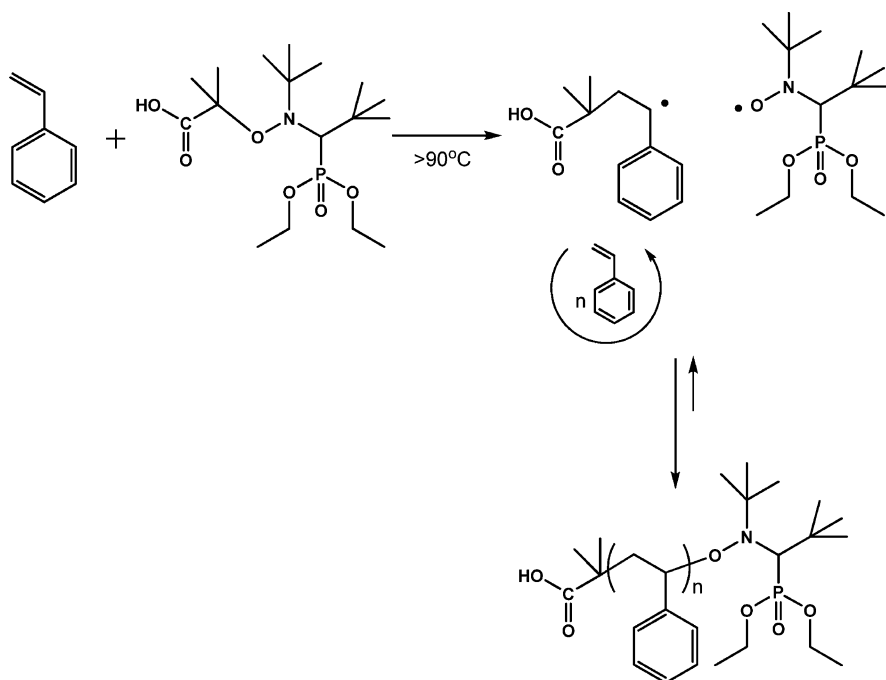
Scheme 3 Schematic representation of the nitroxide mediated polymerization (NMP) of styrene (St)
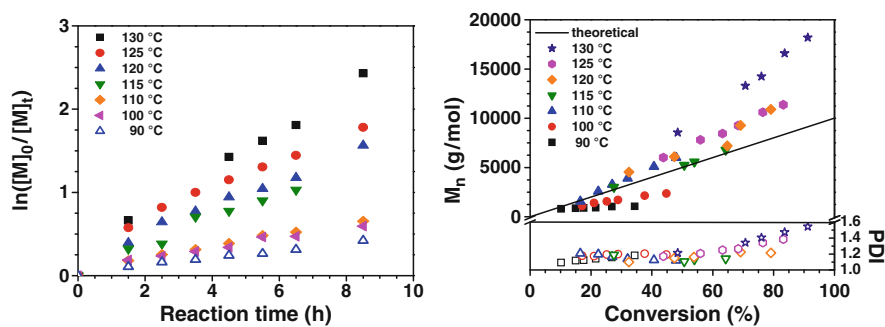
Fig. 4 Semilogarithmic kinetic plot for the NMP of styrene (St) initiated by Bloc Builder[TM] (*left*), M_n and PDI values vs conversion plot at different polymerization temperatures (*right*). (Reprinted with permission from [49]. Copyright (2006) John Wiley & Sons, Inc.)

polymerization medium besides the alkoxyamine initiator. This effect has been investigated in detail for different types of monomers as shown in Scheme 4 [50].

Based on the optimization reactions described, the polymerization temperature was kept constant at 110 °C for the NMP of *N,N*-dimethyl acrylamide (DMA), *N*-acryoyl morpholine (Amor), and 2-hydoxypropyl acrylate (HPA). However, it

Scheme 4 Schematic representation of the chemical structures of the monomers N,N-dimethyl acrylamide (DMA), N-acryoylmorpholine, and 2-hydroxypropyl acrylate

was necessary to add an excess of free nitroxide to obtain better control over the polydispersity of the polymers. On the other hand, the excess of free nitroxide dramatically decreased the apparent polymerization rate. Parallel optimization reactions were conducted for the monomers depicted in Scheme 4 in order to identify the right balance between the polymerization rate and sufficient control over the polydispersity. Some representative results from that report are illustrated in Fig. 5. All the reactions were performed in N,N-dimethyl formamide (DMF) as solvent, at a polymerization temperature of 110°C, a monomer concentration of 2 M, and a monomer to initiator ratio of 100:1. The free nitroxide (SG-1) ratio was varied from 0 up to 20% with respect to the amount of initiator (Bloc Builder™). Apparently, the polymerization rate of Amor was decreased by increasing amounts of SG-1, as shown in Fig. 5a. However, the lowest PDI values were obtained with the highest amount of SG-1 (20%) (Fig. 5b). Similar trends of the molar masses and the PDI values were observed for the polymerization of DMA and HPA. According to the kinetic results, the apparent rates of Amor, DMA, and HPA were found to be $16.0 \times 10^{-4} \, \mathrm{L \, mol^{-1} \, s^{-1}}, 7.7 \times 10^{-4} \, \mathrm{L \, mol^{-1} \, s^{-1}}$, and $4.3 \times 10^{-4} \, \mathrm{L \, mol^{-1} \, s^{-1}}$, respectively. In the case of copolymerization of these monomers, there will be different distributions of monomers throughout the polymeric chain depending on their reactivity. The optimization of key parameters and the determination of the polymerization rate constants provide critical knowledge on the construction of polymer libraries.

2.1.3 Reversible Addition Fragmentation Chain Transfer

The first well established RAFT polymerization using thiocarbonylthio compounds was reported by CSIRO in 1998 [51]. Subsequently, another group reported a similar mechanism using xanthate RAFT agent; they named this technique macromolecular

Fig. 5 Semilogarithmic kinetic plot of Amor (*top left*), molar mass and PDI value vs conversion plots for Amor (*top right*), *N*,*N*-dimethyl acrylamide (DMA) (*bottom left*), and 2-hydoxypropyl acrylate (HPA) (*bottom right*). (Reprinted with permission from [50]. Copyright (2008) American Chemical Society)

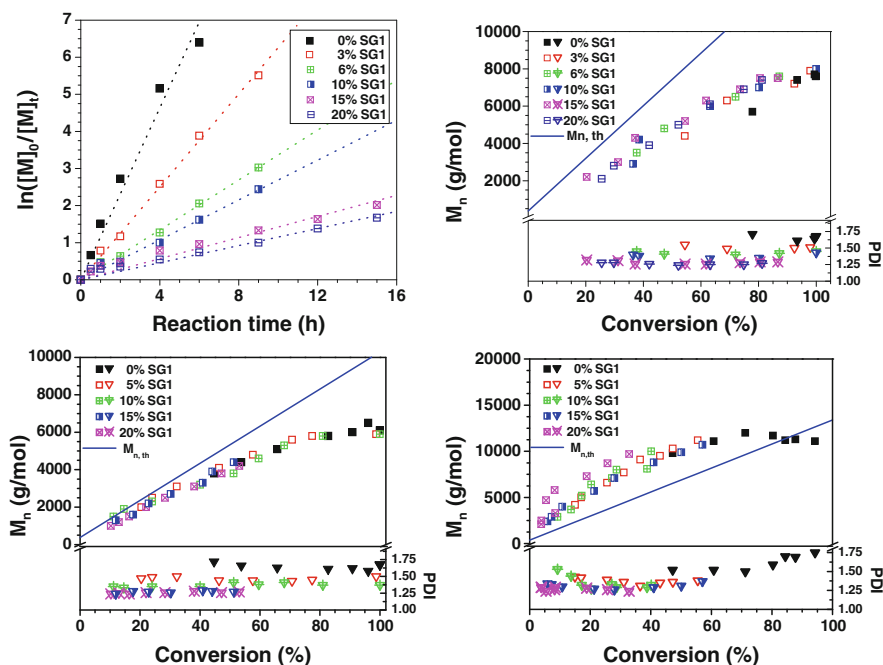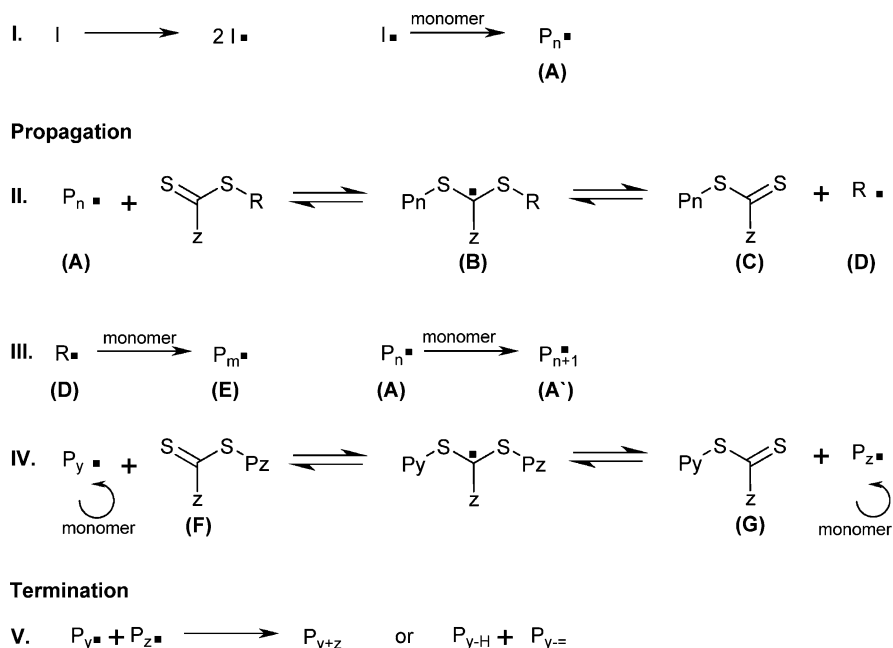design via the interchange of xanthates (MADIX) [52, 53]. RAFT polymerization has several advantages over other CRP techniques. The most significant advantage is the compatibility of the technique with a wide range of monomers, such as St, acrylates, methacrylates, and derivatives. This large number of monomers provides the opportunity of creating well-defined polymer libraries by the combination of different monomeric units. The mechanism of the RAFT polymerization comprises a sequence of addition-fragmentation processes as shown in Scheme 5.

The initiation and radical–radical termination reactions occur as in conventional free radical polymerization. This is followed by the addition of the propagating species (A) to the chain transfer agent (CTA), which leads to the formation of an intermediate species (B). Therefore, a new radical (D) can be released to form new propagating chains (E). In step IV, rapid equilibrium between active propagating radicals and the corresponding dormant species provides equal probability for all chains to grow and allows for the production of polymers with low PDI values. Termination reactions occur via combination or disproportionation (step V) to some extent, but can be largely eliminated by maintaining appropriate conditions that control the apparent radical concentration.

I.   I $\longrightarrow$ 2 I•   I• $\xrightarrow{\text{monomer}}$ P_n•
                                                                    (A)

Propagation

II. P_n• + $\rightleftharpoons$ $\rightleftharpoons$ + R•

         (A)   **(B)**   **(C)**   **(D)**

III.   R• $\xrightarrow{\text{monomer}}$ P_m• P_n• $\xrightarrow{\text{monomer}}$ P_{n+1}•
          (D)   **(E)**   **(A)**   **(A`)**

IV. P_y• + $\rightleftharpoons$ $\rightleftharpoons$ + P_z•
          monomer   **(F)**   **(G)**   monomer

Termination

V. P_y• + P_z• $\longrightarrow$ P_{y+z} or $P_{y\text{-}H}$ + $P_{y\text{-}=}$

Scheme 5 Schematic representation of the mechanism of the RAFT polymerization

Some of the most important critical points in RAFT polymerizations are the relative concentrations of the free radical initiator, the CTA, and the monomer, since these will establish the delicate balance between the dormant and active species. Acrylate and methacrylate derivatives can be successfully polymerized using 2-cyano-2-butyl dithio benzoate (CBDB) as a CTA. However, the amount of free radical initiator (α, α-azobisisobutyronitrile (AIBN) is used in general) compared to CTA determines the rate of control over the polymerization. Therefore, eight different acrylates or methacrylates were polymerized with different ratios of CTA to AIBN [54]. The structures of the monomers and the design of the experiment are shown in Fig. 6.

A reactor block consisting of 16 reactors was divided into 4 zones with 4 different CTA to initiator ratios, and 4 different acrylates or methacrylates were used in each set of experiments. The polymerization of *tert*-butyl methacrylate was repeated four times to demonstrate the reproducibility of the polymerization in an automated parallel synthesizer. Structural analysis of the polymers revealed that there was less than 10% deviation in the number average molar mass (M_n) and the PDI values.

The polymerization of four different acrylates at four different CTA to initiator ratios are shown in Fig. 7, as a representative example. The increased ratio of CTA to AIBN resulted in improved PDI values; however, there is a decrease
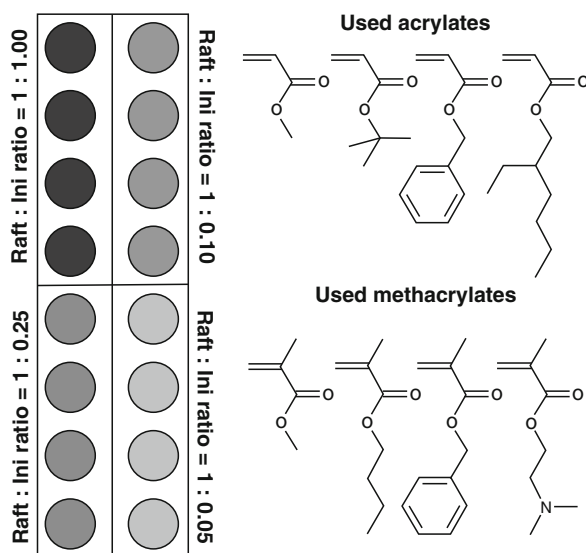
Fig. 6 Schematic representation of the design of experiment and the structures of the used (meth)acrylates. (Reprinted with permission from [54]. Copyright (2005) John Wiley & Sons, Inc.)
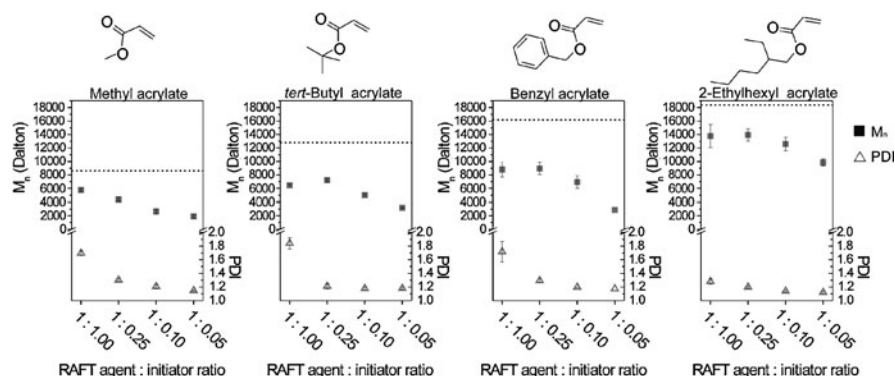
Fig. 7 M_n and PDI values vs CTA to α,α-azobisisobutyronitrile (AIBN) ratio plots for different acrylates. (Reprinted with permission from [54]. Copyright (2005) John Wiley & Sons, Inc.)

observed in the M_n of the polymers. All polymerizations were conducted at 70 °C for 10 h. Due to the different initiator concentrations, the rate of polymerization differs and a significant decrease occurs in the molar mass for a certain reaction time. Nevertheless, this systematic study not only proved the reproducibility of the RAFT polymerization of several (meth)acrylates but also provided the optimum ratio of CTA to initiator to be used in further reactions.

2.2 Ionic Polymerization Techniques

2.2.1 Anionic Polymerization

Anionic polymerization represents a powerful technique for synthesizing polymers with low PDI values, thus providing good control over the chain length. This method leads to less side reactions than radical polymerizations. For instance, unlike in radical polymerization, there is no termination by the combination of two active chains. However, the mechanism is more sensitive to impurities and functional groups, and therefore applicable for only a limited class of monomers.

It still represents a great challenge to conduct anionic polymerizations in an automated parallel synthesizer. Above all, the technique requires an intensive purification of the reagents and the polymerization medium in order to obtain well-defined polymers. Therefore, a special procedure has been described for the inertization of the reactors [55]. It is called "chemical cleaning," which is essentially rinsing all the reactors with *sec*-butyllithium (*s*-BuLi) prior to the reaction in order to eliminate all chemical impurities. This process can be performed in an automated manner. Due to the extreme sensitivity of the polymerization technique to oxygen, moisture, and impurities, detailed investigations on the inertization procedure and the reproducibility of the experiments need to be conducted.

The inertization procedure applied for the Chemspeed ASW2000 robot was started with flushing the hood with argon overnight while the reactors were heated up to 140°C and were exposed to six cycles of vacuum (25 min)-argon (5 min) to eliminate oxygen and moisture completely. Afterwards, *s*-BuLi in cyclohexane was added to all reactors and vortexed for 1.5 h at room temperature and 30 min at 50°C with fresh cyclohexane solutions. As a final step, the washing solution was aspirated from all the reactors and one more vacuum–argon cycle was applied to finalize the inertization of the automated parallel synthesizer for the anionic polymerization.

The reproducibility of the reaction was examined by performing the parallel anionic polymerization of St. The polymerizations were performed in cyclohexane and initiated by *s*-BuLi. The obtained polymers were analyzed by SEC and the difference between the results was less than 3%. This corresponds to less than 5% deviation after calculating the real concentration of the initiator in the reactors by a double titration method [56].

Once the robotic system and procedure passed the optimization and reproducibility tests for a certain type of reaction, the researcher has the chance to move on to the most delightful part of a high-throughput experimentation workflow that is to follow the reaction kinetics of the reaction by withdrawing several samples under comparable conditions. The characterization of these samples allows the determination of the apparent rate constants and activation energies in a very reproducible way. As an example, the anionic polymerization of St in cyclohexane initiated by *s*-BuLi under different reaction conditions was investigated. Several samples were withdrawn during the reaction into small vials which were prefilled with 25 μL of

Fig. 8 Semilogarithmic kinetic plot of the anionic polymerization of St (*left*) and molar mass and PDI values vs conversion plot (*right*). (Reprinted with permission from [55]. Copyright (2005) John Wiley & Sons, Inc.)

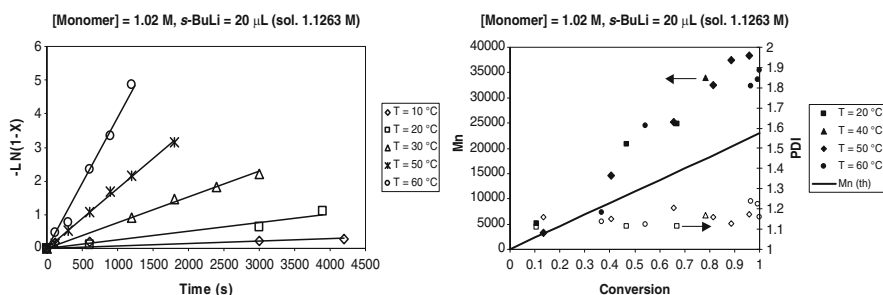**Table 1** Values of the activation energy reported in the literature for the propagation reaction of the anionic polymerization of styrene (St) in different solvents

| Solvent	Activation energy $(kJ \, mol^{-1})$	Reference
Ethylbenzene	75	[57]
Benzene	59.9	[58]
Toluene	64.8	[59]
Toluene	59.9	[60]
Cyclohexane	63 ± 2	[55]

methanol to quench the polymerization. The monomer conversion and molar masses of each sample were determined by GC and SEC measurements. Figure 8 illustrates a representative example of the results obtained from these reactions.

Based on these results, the activation energy of the anionic polymerization of St in cyclohexane was determined as $63 \pm 2 \, kJ \, mol^{-1}$ [55]. The results obtained were comparable to the literature results obtained with other solvents and are summarized in Table 1.

2.2.2 Cationic Ring Opening Polymerization

The living cationic ring opening polymerization (CROP) of 2-oxazolines was first reported in the 1960s [61, 62]. The polymerization can be initiated by an electrophile such as benzyl halides, acetyl halides, and tosylate or triflate derivatives. The typical polymerization mechanism for 2-alkyl-2-oxazoline initiated by methyl tosylate is shown in Scheme 6.

The alkyl group attached at the 2 position of the 2-oxazoline provides extraordinary possibilities for variations in the monomer structure and the proper-
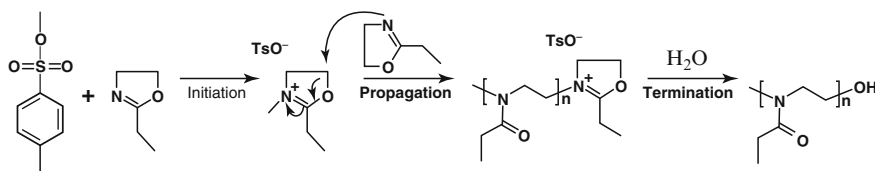
Scheme 6 Schematic representation of the CROP of 2-ethyl-2-oxazoline (EtOx) initiated by the methyl tosylate

ties. This monomer family is a good candidate for high-throughput experimentation and allows creating different copolymer libraries by a combination of 2-oxazolines with different side groups. However, the typical required polymerization times for this type of monomers were previously in the range of 10–20 h. Nevertheless, the reaction time for 2-ethyl-2-oxazoline (EtOx) in acetonitrile could be reduced from 6 h under standard conditions (oil bath heating, reflux at 82 °C) to less than 1 min (at 200 °C) under microwave irradiation. Thus, a high-throughput experimentation workflow could be applied for CROP of 2-oxazolines. Several reaction parameters, such as temperature, pressure, and solvent were investigated under microwave irradiation and using automated parallel synthesizers [63–67].

The living CROP of 2-methyl, 2-ethyl, 2-nonyl, and 2-phenyl-2-oxazolines (PheOx) were investigated at different temperatures in the range 80–200 °C using a single mode microwave synthesizer [68]. The reaction rates were enhanced by a factor of up to 400. The livingness of the polymerization over the whole range of polymerization temperatures was examined by following the first-order kinetics of the monomer consumption. The semilogarithmic kinetic plots for 2-methyl-2-oxazoline (MeOx), EtOx, 2-nonyl-2-oxazoline (NonOx), and PhOx are shown in Fig. 9. All reactions show a linear increase which is an indication of a living polymerization. Besides, each sample was characterized by SEC, and a linear increase in their M_n was observed.

The apparent rate constants for CROP of each monomer at each investigated temperature were calculated and the corresponding activation energy plots were obtained. These plots are shown in Fig. 10 and they exhibit good agreement between theoretical and experimental data. It was concluded that a temperature of 140 °C represents the optimum polymerization temperature since it leads to almost perfect agreement with the theoretical values [69].

There are numerous reports available on the optimization of reaction conditions of 2-oxazolines. For instance, the effect of solvent, temperature, pressure, monomer to initiator ratio, and many other critical parameters have been investigated to obtain the optimum conditions [64–68]. Besides these parameters, the initiator structure has also a great effect on the polymerization. The investigation on different initiator structures provided the necessary kinetic parameters for the use of functional initiators [69]. Heterofunctional initiators have been used in polymer science for the combination of different types of monomers that can be polymerized with different polymerization techniques, such as ATRP and CROP [70–72].
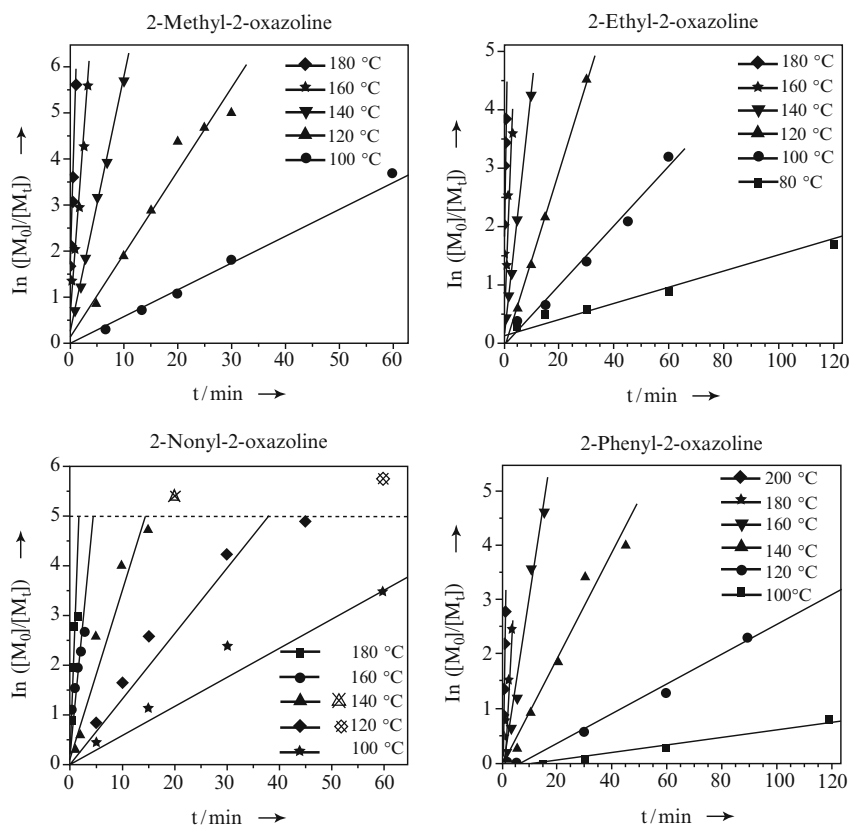
Fig. 9 Semilogarithmic kinetic plots for different 2-oxazolines at various temperatures. (Reprinted with permission from [68]. Copyright (2005) American Chemical Society)

For instance, the CROP of EtOx using four different acetyl halide type of initiators showed that the rate of polymerization increases with the decreased basicity of the counter ion: acetyl iodide < acetyl bromide < acetyl chloride. The apparent rates of polymerization of EtOx with different initiators are listed in Table 2.

3 Synthesis of Well-Defined Copolymer Libraries

3.1 Preparation via Controlled Radical Polymerization Techniques

Free radical polymerization remains the most versatile technique due to its compatibility with a wide range of monomers, its compatibility with protic and aqueous media, and experimentally less demanding conditions. Development of
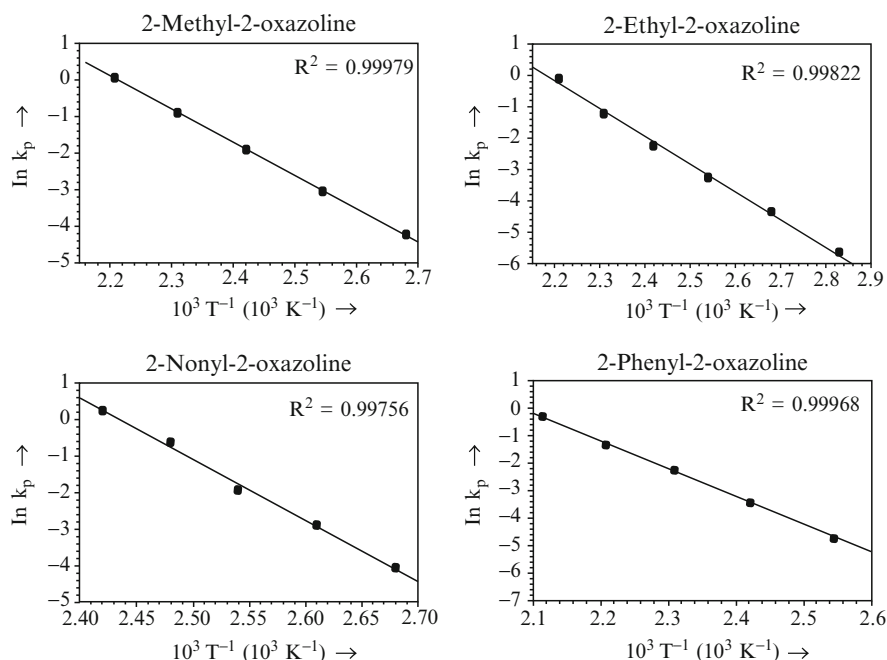
2-Methyl-2-oxazoline

$R^2 = 0.99979$

2-Ethyl-2-oxazoline

$R^2 = 0.99822$

2-Nonyl-2-oxazoline

$R^2 = 0.99756$

2-Phenyl-2-oxazoline

$R^2 = 0.99968$

Fig. 10 Arrhenius plots for the polymerization of various 2-oxazolines in acetonitrile. (Reprinted with permission from [68]. Copyright (2005) American Chemical Society)

Table 2 Polymerization rates (in 10^{-3} L mol^{-1} s^{-1}) of CROP of EtOx with different initiators at various temperatures – acetyl chloride (AcCl), acetyl bromide (AcBr), acetyl iodide (AcI), and 2-bromo-2-methylpropanoyl bromide (BrEBiB)

Initiator	80°C	90°C	100°C	120°C	140°C	160°C	180°C	200°C	220°C
AcCl	–	–	–	–	–	11.4	47.4	111.3	126.8
AcBr	–	–	7.8 ± 0.1	15 ± 1	54 ± 4	149 ± 1	342 ± 18	–	–
AcI	3.5 ± 0.3	7.7 ± 0.3	14.3 ± 0.1	42 ± 1	150 ± 9	351 ± 1	–	–	–
BrEBiB	–	–	7.9	24.9	44.6	202	351	–	–

controlled/"living" radical polymerization techniques combined the advantages of "living" polymerizations and free radical polymerizations. Thus, tailor-made macromolecules could be synthesized from a variety of monomeric units bearing different functional side groups. These special side groups bring an additional property to the polymeric material and influence the whole material properties such as solubility, mechanical properties, thermal properties as well as optical properties.

The combination of different monomeric units at various ratios generates totally new materials, in most cases with the expected properties and rarely with unexpected, superior properties. Therefore, the investigation of series of polymers in parallel has a great importance not only to elucidate structure-property relationships but also to be able to realize "magic" compositions.

3.1.1 Random Copolymer Libraries

Copolymers containing oligo(ethyleneglycol) methyl ether methacrylate (OEGMA) and methacrylic acid (MAA) were synthesized via RAFT polymerization in an automated synthesizer [73]. OEGMA containing polymers exhibit a phase transition behavior upon changes in temperature. This thermoresponsive behavior is based on the formation or breakage of hydrogen bonds between OEGMA units and water molecules at a critical temperature which is also known as lower critical solution temperature (LCST). Polymers with LCST behavior show a sudden and reversible change from hydrophilic to hydrophobic behavior that makes them attractive for usage as "smart" switchable materials in applications ranging from, e.g., drug delivery systems, soft actuators or valves, coatings to textile materials.

Thermoresponsive polymers have in common hydrogen donor or acceptor groups mostly present on their side chains. The most well-known and investigated structures can be listed as N-isopropyl acrylamide (NIPAM), N,N-dimethyl aminoethyl acrylamide (DMAEMA), 2-iso-propyl-2-oxazoline (iPrOx), and oligo(ethylene glycol) methacrylates [74]. Monomers composed of relatively short poly(ethyleneglycol) (PEG) chains and radically polymerizable methacrylate moieties represent versatile building blocks for thermoresponsive materials. Some of the OEGMA based on monomers, i.e., 2-methoxyethyl 2-methylacrylate (MeOMA), Me_2OMA, $OEGEMA_{246}$, $OEGMA_{475}$, and $OEGMA_{1100}$), are commercially available and their chemical structures are schematically depicted in Scheme 7.

The monomers in Scheme 7 show increased hydrophilicity with increased side chain length, and thereby the cloud points are expected to be higher. A wide range of LCST values could be achieved by combining OEGMA monomers having short and
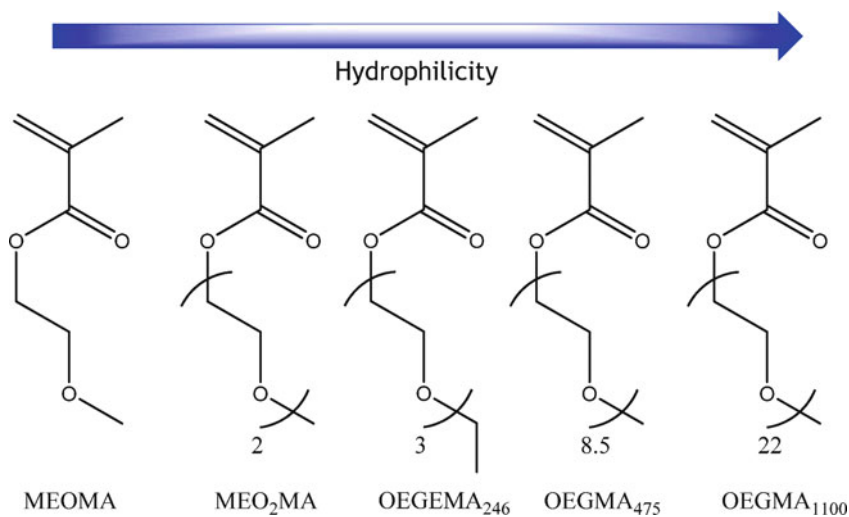
Scheme 7 Schematic representation of the chemical structures of monomers which may exhibit thermoresponsive behavior
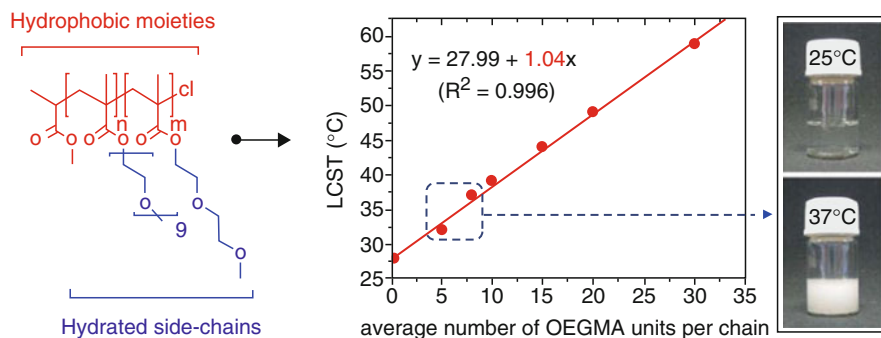
Hydrophobic moieties

$y = 27.99 + 1.04x$
$(R^2 = 0.996)$

LCST (°C)

average number of OEGMA units per chain

Hydrated side-chains

25°C

37°C

Fig. 11 Plots of the measured lower critical solution temperature (LCST) as a function of the theoretical average number of OEGMA$_{475}$ units per chain for a series of P(MeO$_2$MA-*co*-OEGMA$_{475}$) copolymers of various composition. Hydrophobic and hydrophilic molecular regions on the copolymer are indicated in *red* and *blue*, respectively. (Reprinted with permission from [76]. Copyright (2008) John Wiley & Sons, Inc.)

long PEG side chains. Lutz et al. have investigated a series of these combinations to determine the right balance between hydrophilicity and hydrophobicity [75]. As shown in Fig. 11, the combination of OEGMA$_{475}$ and 2-(2-methoxyethoxy)ethyl 2-methylacrylate (MeO$_2$MA) building blocks at various ratios results in thermoresponsive polymers with cloud points in the range 27–60 °C [76].

Further detailed studies on the LCST properties of OEGMA based polymers have been conducted by Schubert et al. Several homopolymer and copolymer libraries of the monomers listed in Scheme 7 have been synthesized in an automated parallel synthesizer using the RAFT polymerization process [74]. Homopolymers with different chain lengths were prepared to understand the effect of the chain length on the LCST behavior of this class of monomers. As expected, polymers containing longer PEG chains as side groups revealed relatively higher cloud point temperatures than the others. For instance, cloud points for P(MeO$_2$MA), P(OEGMA$_{246}$), and P(OEGMA$_{475}$) were found to be 21.8, 21.6, and 89.8 °C, respectively. All the polymers were prepared with a 100 to 1 monomer to initiator ratio and their corresponding cloud points were measured in a buffer solution of pH 7. As the number of hydrogen bond forming functionalities increases in the macromolecule, the energy required to break these bonds also increases. Therefore, homopolymers with longer PEG side chains required higher temperatures in order to break the hydrogen bonds and, as a result, precipitate in the solution. However, homopolymers of P(MAA) and P(OEGMA$_{1100}$) with up to 100 repeating units did not show LCST behavior due to their highly hydrophilic structures.

Copolymers of MAA and OEGMA were prepared via RAFT polymerization in ethanol. A systematic parallel synthesis was performed to obtain copolymers containing different ratios of two monomers. Therefore, a complete screening in composition of P(MAA)-*r*-(OEGMA)$_n$ copolymers was elaborated from 0% OEGMA$_n$ to 100% OEGMA$_n$. As representative examples, the M_n and PDI values of two libraries, namely P(MAA)-*r*-(OEGMA$_{475}$) and P(MAA)-*r*-(OEGMA$_{1100}$),
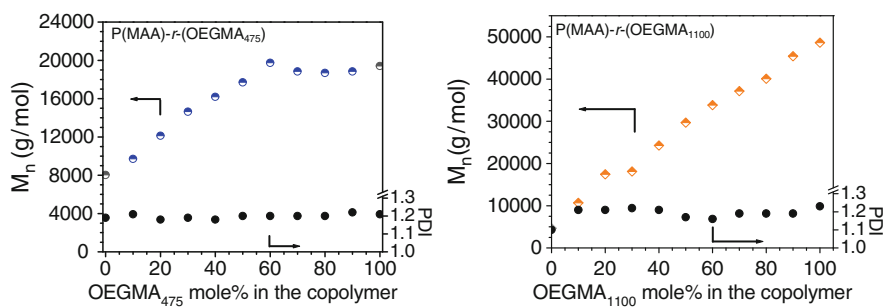
Fig. 12 M_n and PDI values data of copolymers synthesized with different comonomer feed ratios. (Reprinted with permission from [73]. Copyright (2008) John Wiley & Sons, Inc.)
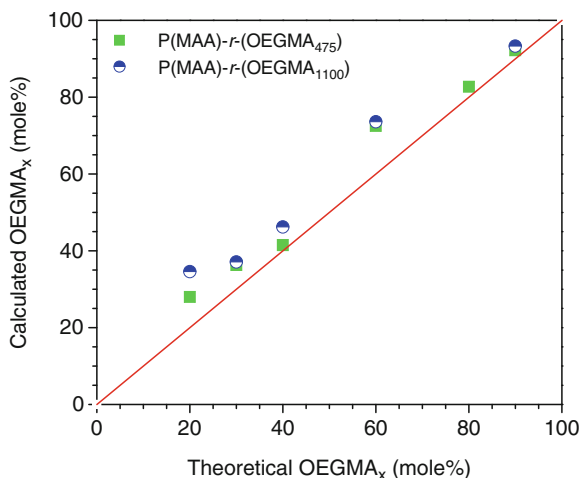

Fig. 13 Theoretical composition vs calculated composition. (Reprinted with permission from [73]. Copyright (2008) John Wiley & Sons, Inc.)

are depicted in Fig. 12. The $M_{n,GPC}$ values of the copolymers increased linearly with increasing $OEGMA_n$ content whereas the PDI values remained below 1.3.

Depending on the length of the side chain of the $OEGMA_n$ monomers, their corresponding reactivity ratios are expected to be different. This may result in slight differences in the copolymer composition. Therefore, it is necessary to quantify the amount of each repeating unit in the copolymer. Based on ^1H NMR spectroscopy measurements the content of MAA and $OEGMA_n$ could be determined. Thus, the amount of $OEGMA_n$ repeating units in P(MAA)-r-(OEGMA)$_n$ copolymers were found to be slightly higher than the theoretical values, as depicted in Fig. 13.

The LCST properties of P(MAA)-r-(OEGMA$_{475}$) and P(MAA)-r-(OEGMA$_{1100}$) libraries were determined in buffer solutions with different pH values. As illustrated in Fig. 14, the copolymer library of P(MAA)-r-(OEGMA$_{475}$) revealed cloud points from 25 to 90°C at pH values of 2 and 4, respectively. It was mentioned

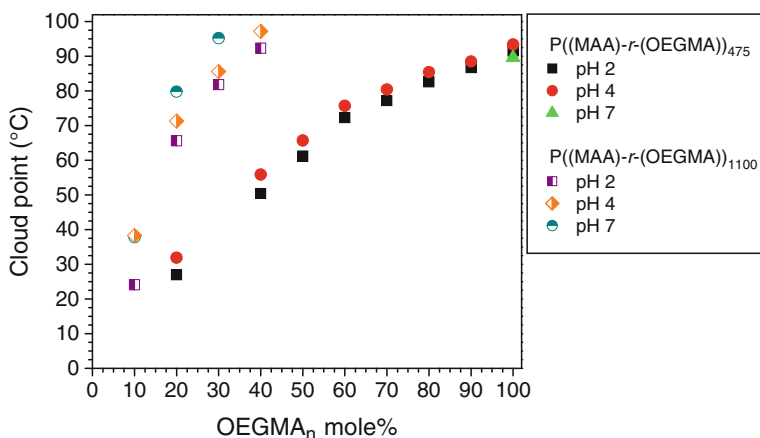**Fig. 14** Cloud points of P(MAA)-*r*-(OEGMA$_{475}$) and P(MAA)-*r*-(OEGMA$_{1100}$) copolymer libraries at different pH values. (Reprinted with permission from [73]. Copyright (2008) John Wiley & Sons, Inc.)

previously that homopolymers of P(MAA) and P(OEGMA)$_{1100}$ did not show any LCST due to their highly hydrophilic structures. However, the copolymers of these two monomers do exhibit cloud points at certain comonomer compositions. Besides, these polymers were found to be double-responsive to both temperature and pH values. For instance, the copolymer P(MAA)$_{0.9}$-*r*-(OEGMA$_{1100}$)$_{0.1}$ is soluble at pH 4 whereas it is not soluble at pH 2 in water at 37 °C. The determination of these "magic" compositions is easily feasible by screening large libraries of polymers for the best performance.

The phase transition is directly related to the hydrophilic/hydrophobic balance in a copolymer and controlling the polymer composition provides a highly effective way of tuning the LCST. Another example of responsive polymer libraries was based on the combination of 2-hydroxypropyl acrylate and DMA or *N*-acryloyl morpholine [50]. The nitroxide mediated copolymerization conditions were chosen on the basis of the kinetic investigation of the homopolymerizations, as discussed in this chapter (see, e.g., Sect. 2.1.2).

The copolymers obtained for the P(Amor)-*stat*-(HPA) library (Scheme 8) revealed relatively low PDI values in the range from 1.16 to 1.32 and increasing M$_{n,GPC}$ values with increasing HPA content, as listed in Table 3. The observed copolymerization rates for both monomers decreased with increasing HPA content due to the slower HPA-SG1 dissociation and association kinetics. The copolymer compositions were calculated from the monomer conversions obtained by GC as well as from ^{1}H NMR spectroscopy of the precipitated polymers.

The thermal transition behavior within the P(Amor)-*stat*-(HPA) copolymer library was investigated using differential scanning calorimetry (DSC). For all members of this library, single glass transition temperatures (T$_g$) were obtained, which is an indication of a good mixing of the two different monomers. The homopolymer
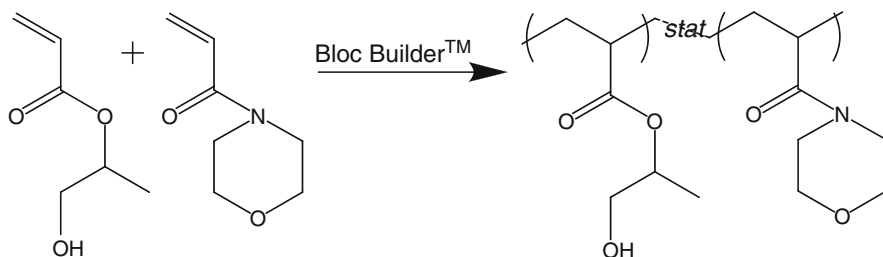
Scheme 8 Schematic representation of the synthesis of statistical copolymers of 2-hydroxypropyl acrylate (mixture of isomers) and *N*-acryloyl morpholine

Table 3 Copolymerization results of the p(Amor-*stat*-HPA) library

Name[a]	Conversion[b] (%) Amor/HPA	Mn[c] (g mol^{-1})	PDI[c]	Composition GC[b] (mol%) Amor/HPA	Composition NMR[d] (mol%) Amor/HPA
A100	70/0[e]	6,900	1.32	100/0	100/0
A90H10	63/69	7,700	1.27	89/11	90/10
A80H20	48/51	7,200	1.22	79/21	78/22
A70H30	56/53	8,300	1.26	71/29	68/32
A60H40	45/38	8,100	1.21	64/36	58/42
A50H50	45/42	8,500	1.23	52/48	47/53
A40H60	37/28	8,300	1.20	47/53	38/62
A30H70	37/31	8,800	1.20	34/66	29/72
A20H80	34/28	8,400	1.20	23/77	18/82
A10H90	28/20	8,100	1.16	13/87	7/93
H100	0/22	8,200	1.16	0/100	0/100

[a] Names indicate the monomer feed: A50H50 = p(Amor$_{50}$-*stat*-HPA$_{50}$)
[b] Calculated by GC using monomer/DMF ratios
[c] Of precipitated polymer, determined by GPC in DMAc using p(MMA) calibration
[d] ^{1}H NMR spectra were recorded in CDCl$_3$
[e] Conversion calculated by ^{1}H NMR spectroscopy

of P(Amor) exhibits a T_g of 146.5 °C whereas it was found as 21.7 °C for P(HPA). Their copolymers exhibited T_g values in between these temperatures, as listed in Table 4. The cloud points were determined by turbidimetry measurements in a parallel turbidimetry instrument (Crystal16, Avantium Technologies). This instrument measures the turbidity from the transmission of red light through the sample vial as a function of temperature. One of the alternative techniques to measure turbidity is UV-Vis spectroscopy which requires at least 1 h per sample and per cycle. However, the Crystal16 turbidimeter is capable of measuring 16 samples in parallel and repeating as many cycles as programmed. Thus, the turbidimetry property of the samples could be determined in an accelerated manner. As can be seen in Table 4, the cloud points of the P(Amor)-*stat*-(HPA) copolymers could be tuned from 20 to 90 °C by varying the comonomer composition.

Table 4 Thermal and lower critical solution temperature (LCST) properties for the copolymers of the p(Amor-*stat*-HPA) library

Name	Composition[a] Amor/HPA (wt%)	T_g^{b} (°C)	Cloud point[c] 0.5 wt% (°C)	Cloud point[c] 1.0 wt% (°C)
A100	100/0	146.5	Soluble	Soluble
A90H10	90/10	130.6	Soluble	Soluble
A80H20	80/20	106.4	Soluble	Soluble
A70H30	69/31	95.8	Soluble	Soluble
A60H40	60/40	84.0	Soluble	88.0
A50H50	49/51	75.2	79.5	65.9
A40H60	40/60	61.4	62.7	53.0
A30H70	30/70	51.8	49.2	38.3
A20H80	19/82	41.7	41.5	30.9
A10H90	8/82	31.3	33.9	25.3
H100[d]	0/100	21.7	26.7	21.4[d]

[a] Calculated from ^{1}H NMR spectroscopy
[b] Mid-temperature
[c] 50% transmittance point in first heating curve
[d] p(HPA) synthesized with 15 h reaction time
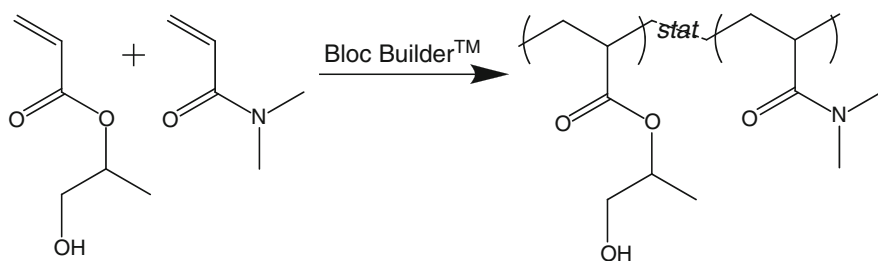
Scheme 9 Schematic representation of the synthesis of statistical copolymers of 2-hydroxypropyl acrylate (mixture of isomers) and DMA

The copolymers obtained for the P(DMA)-*stat*-(HPA) (Scheme 9) library revealed relatively low PDI values below 1.3 and increasing $M_{n,GPC}$ values with increasing HPA content, as listed in Table 5. It should be noted that a poly(methyl methacrylate) (PMMA) calibration was used for the calculation of the $M_{n,GPC}$ values and this causes an overestimation for HPA containing polymers. The copolymer compositions were calculated from the ^{1}H NMR spectra; however, this method was not suitable for reliable conversion determination since the DMA-*CH$_3$* groups overlap in the ^{1}H NMR spectra not only with the HPA-*OH* group but also with broad backbone signals, which obstruct any reliable integration. Therefore, elemental analysis was used as an alternative method for the calculation of the molecular composition of the copolymers.

Similarly, the thermal transition behavior of the members of the P(DMA)-*stat*-(HPA) copolymer library was investigated using DSC. For all members of this library, single T_g were obtained, which is an indication of a good mixing of the two

Table 5 Copolymerization results of the p(DMA-*stat*-HPA) library

Name[a]	Conversion[b] (%) DMA/HPA	Mn^c (g mol^{-1})	PDI[c]	Composition NMR[d] (mol%) DMA/HPA	Composition EA (mol%) DMA/HPA
D100	53/0	4,500	1.23	100/0	100/0
D90H10	60/93	6,800	1.20	85/15	88/12
D80H20	46/36	6,500	1.23	75/25	78/22
D70H30	67/73	8,400	1.27	69/31	68/32
D60H40	57/56	8,500	1.24	53/48	59/41
D50H50	66/53	9,800	1.27	46/54	50/50
D40H60	58/53	9,600	1.26	33/67	41/59
D30H70	82/29	10,900	1.24	28/72	32/68
D20H80	57/44	10,700	1.22	18/82	22/78
D10H90	71/48	10,500	1.20	9/91	12/88
H100	0/33	11,100	1.21	0/100	0/100

[a] Names indicate monomer feed: D50H50 = p(DMA$_{50}$-*stat*-HPA$_{50}$)
[b] Calculated by GC using monomer/DMF ratios
[c] Determined by GPC in DMAc using p(MMA) calibration
[d] ^{1}H NMR spectra recorded in CDCl$_3$

Table 6 Thermal and LCST properties for the copolymers of the p(DMA-*stat*-HPA) library

Name	Composition[a] DMA/HPA (wt%)	T_g^b (°C)	Cloud point[c] 0.5 wt% (°C)	Cloud point[c] 1.0 wt% (°C)
D100	100/0	111.4	Soluble	Soluble
D90H10	85/15	97.6	Soluble	Soluble
D80H20	73/27	87.7	Soluble	Soluble
D70H30	62/38	79.7	Soluble	Soluble
D60H40	52/48	63.4	Soluble	Soluble
D50H50	43/57	58.8	Soluble	82.9
D40H60	34/66	51.6	71.6	62.3
D30H70	26/74	44.6	55.8	48.7
D20H80	18/82	36.0	46.7	38.6
D10H90	10/90	30.5	35.3	28.5
H100	0/100	21.7	26.7	21.4

[a] Calculated from elemental analysis
[b] Mid-temperature
[c] 50% transmittance point in first heating curve

different monomer structures. The homopolymer of P(DMA) has a T_g of 111.4 °C whereas a T_g of 21.7 °C was measured for P(HPA). Besides, their copolymers exhibited T_g values in between these temperatures, as listed in Table 6. The T_g of P(DMA)-*stat*-(HPA) copolymers show a positive deviation from the Fox equation, which is an indication of the presence of some weak hydrogen bonding of the hydroxyl group of HPA with the amide group of DMA. The cloud points were

determined by turbidimetry in the Crystal16. The phase transition temperature of P(DMA)-*stat*-(HPA) copolymers could be tuned from 20 to 90 °C by varying the comonomer composition.

3.1.2 Block Copolymer Libraries

The synthesis of well-defined block copolymers has been a challenge for decades. Block copolymers consist of segments with different solubility typically resulting in phase separation [77, 78] and solution aggregation behavior [79–81]. The efforts to synthesize them have strongly accelerated the development of CLP techniques. Several catalysts, functional initiators, and CTAs have been investigated for different classes of monomers to synthesize well-defined block copolymers. RAFT polymerization represents one of the most versatile techniques that can be applied for a wide range of monomers not only in organic solvents but also in aqueous media.

Poly(acrylic acid) (PAA) is a water soluble polymer that has been used in various applications. Direct synthesis of well-defined PAA-containing polymers has been a challenge for CRP techniques because of the acid-containing monomer. So far, RAFT polymerization and NMP techniques could be successfully employed for unprotected acrylic acid (AA) [82, 83]. Even though it is possible to polymerize AA directly, the applied polymerization solvents had to be polar, implying that block copolymers with a variety of apolar monomers cannot be synthesized in a straightforward manner. Therefore, the protected analogues of AA, e.g., *t*BA [84] and benzyl acrylate [85], are often used for the polymerization and deprotected following the polymerization [86]. Du Prez et al. investigated a new route toward near-monodisperse PAA and derived block copolymer structures by the RAFT polymerization of 1-ethoxy ethyl acrylate (EEA) [87].

The temperature optimization for the RAFT polymerization of EAA revealed an optimum reaction temperature of 70 °C. Block copolymers with a poly(methyl acrylate) (PMA), a poly(*n*-butyl acrylate) (PnBA), a PMMA, or a poly(N,N-dimethyl aminoethyl methacrylate) (PDMAEMA) first block and a poly(1-ethoxyethyl acrylate) (PEEA) second block were successfully synthesized in an automated synthesizer. The synthesis robot was employed for the preparation of 16 block copolymers consisting of 25 units of the first block composed of PMA (exp. 1–4), PnBA (exp. 5–8), PMMA (exp. 9–13), and PDMAEMA (exp. 13–16) and a second block of PEEA consisting of 25, 50, 75, or 100 units, respectively. The first blocks were polymerized for 3 h and a sample from each reaction was withdrawn for SEC analysis. Subsequently, EAA was added and the reactions were continued for 12 h. The molar masses and PDI values of the obtained block copolymers are shown in Fig. 15.

The composition of the resulting block copolymers was further characterized by ^{1}H NMR spectroscopy and the results are summarized in Table 7. The integral values of the aromatic resonances of the RAFT agent were applied to calculate the number average degree of polymerization (DP) for the monomers present in the block copolymers. Deprotection of the PEEA containing block copolymers was performed in CHCl$_3$ by heating to 80 °C for 3 h. The solutions exhibited a cloudy
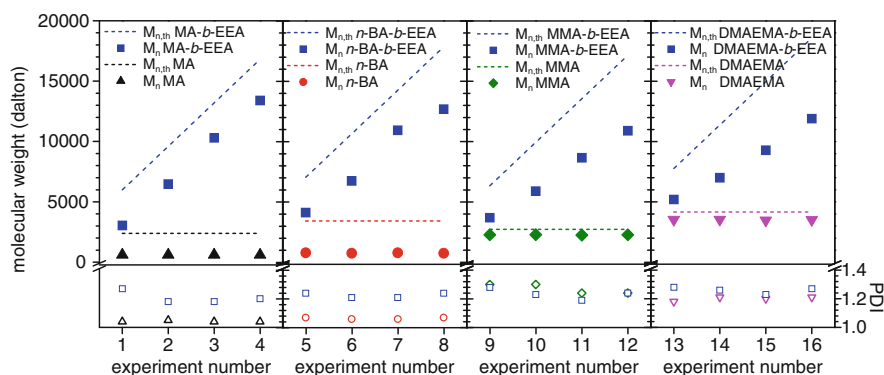
Fig. 15 Number average molar masses ($M_{n,GPC}$) and PDI values obtained for the first blocks and for the final copolymers of PMA, PnBA, PMMA, or PDMAEMA (25 units) with PEEA (25, 50, 75, and 100 units for 100% conversion). All $M_{n,GPC}$ values are calculated against PMMA standards. SEC eluent $CHCl_3$:NEt_3:i-PrOH. (Reprinted with permission from [87]. Copyright (2005) American Chemical Society)

Table 7 Compositions of the synthesized copolymers as determined by ^{1}H NMR spectroscopy

Exp	Mon A	$DP_{A,th}$	$DP_{EEA,th}$	$f_{EEA,th}$	$DP_{A,NMR}$	$DP_{EEA,NMR}$	$f_{EEA,NMR}$
1	MA	25	25	0.5	19	9	0.32
2	MA	25	50	0.67	17	22	0.56
3	MA	25	75	0.75	18	35	0.66
4	MA	25	100	0.8	20	52	0.72
5	n-BA	25	25	0.5	18	20	0.53
6	n-BA	25	50	0.67	18	44	0.71
7	n-BA	25	75	0.75	19	73	0.79
8	n-BA	25	100	0.8	22	87	0.80
9	MMA	25	25	0.5	23	6	0.21
10	MMA	25	50	0.67	23	12	0.34
11	MMA	25	75	0.75	23	20	0.47
12	MMA	25	100	0.8	23	32	0.58
13	DMAEMA	25	25	0.5	22	8	0.27
14	DMAEMA	25	50	0.67	22	20	0.48
15	DMAEMA	25	75	0.75	22	35	0.61
16	DMAEMA	25	100	0.8	22	51	0.70

appearance which is an indication of the PAA formation. ^{1}H NMR spectroscopy revealed 85–100% deprotection for selected copolymers.

NMP is as successful as RAFT polymerization for the construction of block copolymers. A small library of block copolymers comprised of poly(styrene) (PSt) and poly(*tert*-butyl acrylate) (P*t*BA) was designed and the schematic representation of the reaction is depicted in Scheme 10 [49]. Prior to the block copolymerization, the optimization reactions for the homopolymerization of St and *t*-BA were performed as discussed in this chapter (e.g., see Sect. 2.1.2). Based on these results,
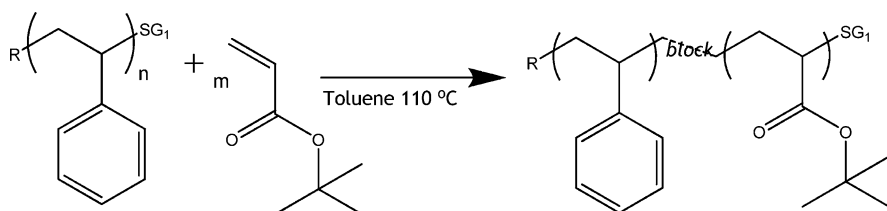
Scheme 10 Schematic representation of the nitroxide mediated block copolymerization of P(St)-b-(t-BA)

Table 8 Block copolymerization of poly(styrene)-b-(tert-butyl acrylate) at different macroinitiator to monomer ratios. $PS_n(n)$ = degree of polymerization of the PS macroinitiator

Run	PS_n (n)	Initiator/t-BA	Time (h)	Conversion (%)	$M_{n,theo}$ (g mol^{-1})	$M_{n,GPC}$ (g mol^{-1})	PDI (M_w/M_n)
1	50	1:50	20	65	13,600	6,700	1.17
2	50	1:100	20	18	7,500	6,600	1.12
3	50	1:150	20	40	10,300	14,800	1.33
4	78	1:50	20	10	9,400	8,900	1.10
5	78	1:100	14	15	10,200	9,900	1.09
6	78	1:150	20	23	11,100	11,100	1.15
7	120	1: 50	14	11	14,800	14,800	1.13
8	120	1:100	14	10	14,100	15,600	1.10
9	120	1:150	14	13	14,500	17,300	1.11

PS macroinitiators were prepared with chain lengths of 50, 78, and 120, respectively. These three different PS macroinitiators were reacted with different amount of t-BA to obtain a 3×3 library of P(St)-b-(t-BA). The resulting block copolymers were characterized by SEC to determine the $M_{n,GPC}$ and PDI values, which are listed in Table 8.

3.2 Preparation via Ionic Polymerization Techniques

Ionic polymerization techniques are very powerful for the construction of well-defined block copolymers having controlled architectures, microstructures and molar masses, narrow molar mass distributions, and chemical and compositional homogeneity. Under the appropriate experimental conditions, anionic polymerizations are associated with the absence of any spontaneous termination or chain transfer reactions. One important limitation of ionic polymerizations is the demanding experimental conditions required to achieve a living polymerization system and its applicability to a rather narrow range of monomers. However, recent developments not only in polymerization kinetics and reagents but also in synthesis methods and instrumentation have allowed extending the utility of the method to a broader range of monomers.

3.2.1 Random Copolymer Libraries

A library of random copolymers comprised of MeOx, EtOx, and NonOx has been established, and the properties of the members have been studied [88]. Systematic copolymerization studies and corresponding structure-property investigations have been performed in detail by Schubert et al. For this purpose, nine copolymers were synthesized with 0–100 mol% (steps of 12.5 mol%) of the second monomer, resulting in 27 polymerizations for three different combinations of MeOx, EtOx, and NonOx. The monomer conversion was followed by GC measurements. As shown in Fig. 16, the content of the second monomer increases linearly with increasing mole fraction of the second monomer, whereas the content of the first monomer decreases linearly.

The resulting semilogarithmic kinetic plots for the 50 mol% copolymerizations are depicted in Fig. 17. The linearity in these first-order plots indicates a constant concentration of the living polymer chains as expected for a living polymerization. The plots also revealed a slightly higher reactivity of MeOx in comparison to EtOx and NonOx. To elucidate further the copolymer compositions, the reactivity ratios were determined from the relation between fraction of monomer A in the monomer feed (f_1) and the incorporated fraction of monomer A at both ~20 and ~60% monomer conversion. The corresponding reactivity ratios calculated for MeOx, EtOx, and NonOx using two different methods, namely the Mayo-Lewis terminal model and the extended Kelen–Tüdös, are listed in Table 9.

The synthesis of statistical copolymers consisting of EtOx and 2-"soyalkyl"-2-oxazoline (SoyOx) via a microwave assisted CROP procedure was reported by Schubert et al. [89]. The SoyOx monomer is based on soybean fatty acids and has an average of 1.5 double bonds per monomer unit. The designed polymer
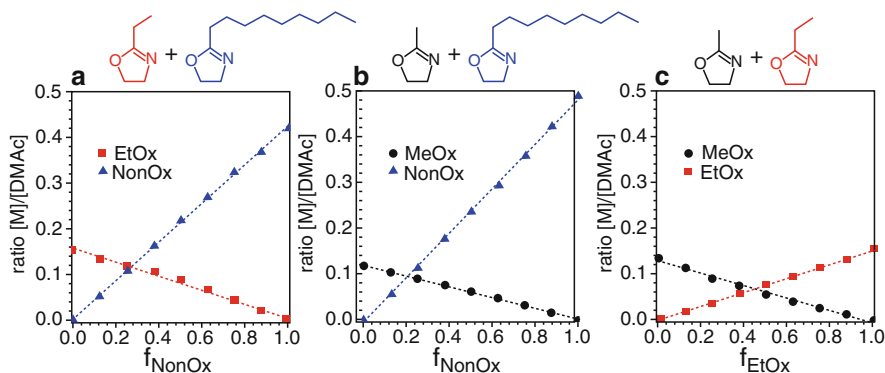

Fig. 16 Ratios of monomer to solvent ([M]/[DMAc]) obtained by GC for t = 0 samples of the different copolymerizations plotted against fraction of the second monomer (f): EtOx:NonOx (**a**), MeOx:NonOx (**b**), MeOx:EtOx (**c**). These graphs clearly demonstrate the gradual change in monomer composition within the investigated library. (Reprinted with permission from [88]. Copyright (2006) American Chemical Society)
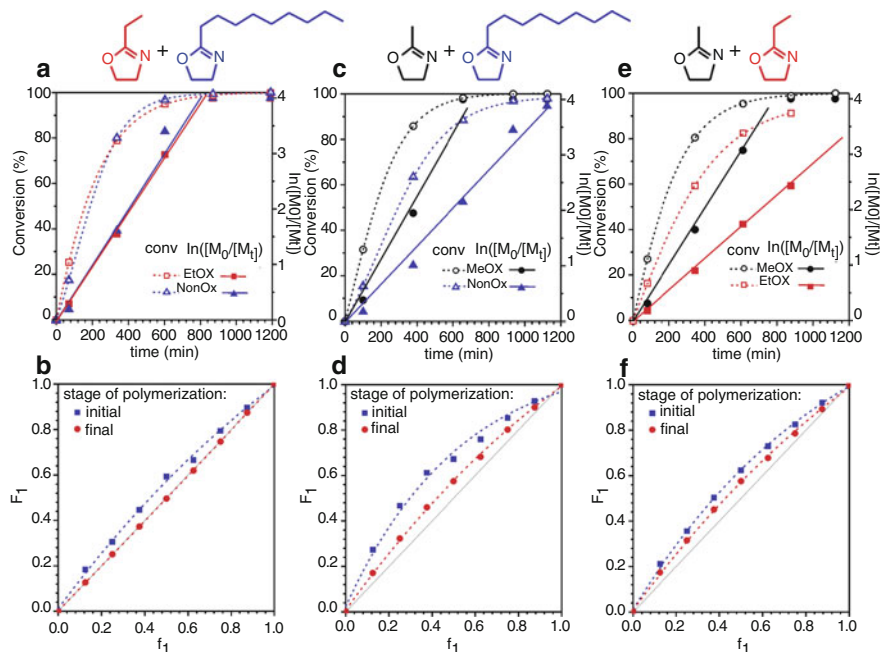
Fig. 17 *Top row*: conversion $(\ln([M]_0/[M]_t))$ against time plots for 50 mol% copolymerizations (**a**, **c**, **e**). *Bottom row*: relationship between the monomer feed (f_1) and the actual monomer incorporation (F_1) at the initial ($\sim$20% conversion) and final ($>$50% conversion) polymerization stages (**b**, **d**, **f**). Both conversion and monomer incorporation are shown for EtOx:NonOx (**a**, **b**), MeOx:NonOx (**c**, **d**), and MeOx:EtOx (**e**, **f**) copolymerizations. (Reprinted with permission from [88]. Copyright (2006) American Chemical Society)

Table 9 Reactivity ratios determined for 2-oxazoline copolymerizations utilizing both the Mayo-Lewis terminal model (MLTD) and the extended Kelen–Tüdös (KT) method. Initial defines $\sim$20% conversion and final defines $>$50% conversion

$M_1:M_2$	Method	Initial r_1	Initial r_2	Final r_1	Final r_2
EtOx:NonOx	MLTM	1.2 ± 0.2	0.7 ± 0.1	0.97 ± 0.01	0.99 ± 0.01
EtOx:NonOx	KT	1.23 ± 0.13	0.60 ± 0.05	0.91 ± 0.05	0.94 ± 0.03
MeOx:NonOx	MLTM	1.8 ± 0.3	0.3 ± 0.1	1.26 ± 0.05	0.66 ± 0.03
MeOx:NonOx	KT	1.94 ± 0.15	0.25 ± 0.04	1.83 ± 0.04	0.46 ± 0.02
MeOx:EtOx	MLTM	1.52 ± 0.1	0.54 ± 0.03	1.18 ± 0.04	0.65 ± 0.02
MeOx:EtOx	KT	1.67 ± 0.04	0.51 ± 0.04	1.63 ± 0.05	0.52 ± 0.04

library consisted of a series of copolymers in which the monomer composition was systematically varied allowing the determination of structure-property relationships. The monomer structures and the polymerization mechanism are depicted in Scheme 11.

The polymerization mixtures consisting of EtOx, SoyOx, methyl tosylate, and acetonitrile were automatically prepared utilizing the liquid handling system of
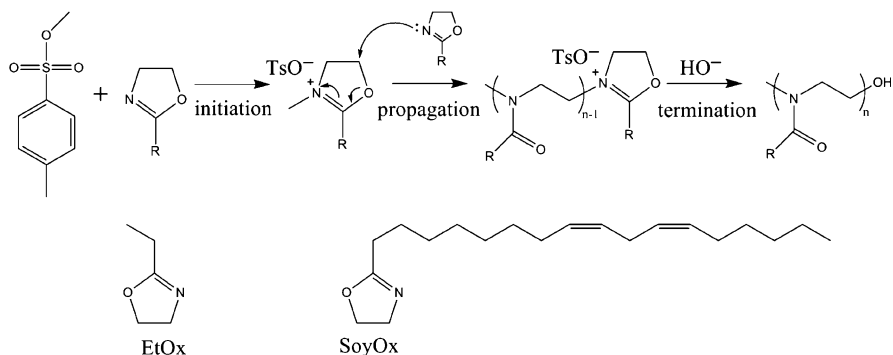
Scheme 11 Schematic representation of the polymerization mechanism as well as the EtOx and 2-"soyalkyl"-2-oxazoline (SoyOx) monomer structures

Table 10 Structural characterization of the synthesized P(EtOx)-*stat*-(SoyOx) copolymers

| Entry | $f_{SoyOx,th}$ | ~40% conversion | | | Full conversion | | |
		f_{SoyOx} [a]	$M_{n,GPC}$ [b]	PDI	f_{SoyOx} [a]	$M_{n,GPC}$ [b]	PDI
1	0	–	–	–	0	5,500	1.11
2	0.05	–	–	–	0.04	6,250	1.16
3	0.10	0.06	4,700	1.12	0.08	6,900	1.15
4	0.15	–	–	–	0.13	8,000	1.15
5	0.20	0.20	5,300	1.19	0.18	8,500	1.19
6	0.25	–	–	–	0.22	9,450	1.16
7	0.30	0.29	6,550	1.16	0.28	11,100	1.12
8	0.40	0.41	7,050	1.17	0.38	11,300	1.19
9	0.50	0.51	7,250	1.17	0.48	12,100	1.26
10	0.60	0.63	7,950	1.18	0.58	12,700	1.31
11	0.70	0.76	7,550	1.31	0.70	14,400	1.28
12	0.80	0.88	9,100	1.24	0.81	13,100	1.43
13	0.90	0.85	7,500	1.38	0.91	13,000	1.54
14	1.00	–	–	–	1.0	15,000	1.75

[a] Determined by ^{1}H NMR spectroscopy
[b] M_n values are given in Dalton

the ASW2000 synthesis robot. The total degree of polymerization was aimed for 100 and compositions of EtOx and SoyOx were altered in steps of 10 mol%. The prepared vials were placed in the autosampler of the microwave synthesizer and were irradiated one by one for a predefined reaction time and temperature. The structural characterizations of the resulting polymers were performed by SEC as well as ^{1}H NMR spectroscopy measurements and are summarized in Table 10. The reactivity ratios of EtOx and SoyOx were examined and it could be concluded that both monomers have slightly higher reactivity to itself than to the other monomer. The Mayo-Lewis terminal model with nonlinear least square fitting of the data revealed reactivity ratios of $r_{EtOx} = 1.4 \pm 0.3$ and $r_{SoyOx} = 1.7 \pm 0.3$. These values
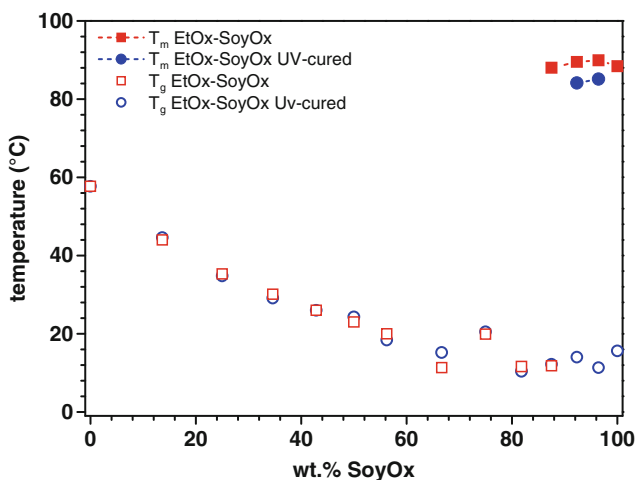
Fig. 18 Thermal properties (T_g and T_m) of the P(EtOx)-*stat*-(SoyOx) copolymer before and after UV-curing. (Reprinted with permission from [89]. Copyright (2007) John Wiley & Sons, Inc.)

indicate that two different monomers will be present almost in a random fashion, whereby small clusters of the same monomer may be present in the polymer chains.

The unsaturated side chain of the SoyOx repeating units could be used for cross-linking well-defined P(EtOx)-*stat*-(SoyOx) copolymers. Thus, the effect of cross-linking on the thermal properties of the polymers was investigated. The thermal properties of the synthesized P(EtOx)-*stat*-(SoyOx) copolymers before and after UV-curing are illustrated in Fig. 18.

3.2.2 Block Copolymer Libraries

A library of 4 chain extended homopolymers and 12 diblock copoly(2-oxazoline)s was prepared from 2-methyl, 2-ethyl, 2-nonyl, PheOx in a very short period of time [90]. The CROP was initiated by methyl tosylate and performed in acetonitrile at 140°C in a single-mode microwave synthesizer. A total number of $100(50 + 50)$ repeating units was incorporated into the respective polymer chains. The concentration of the solutions and predefined polymerization times for each monomer and comonomer are summarized in Table 11.

The structural characterization of the resulting diblock copolymers was performed by means of SEC, ^{1}H NMR spectroscopy, thermal gravimetric analysis (TGA), and DSC. In most of the cases the PDI values were found to be lower than 1.3. However, the calculation of the molar masses of the diblock copolymers was not straightforward since the calibration standards (PEG, PS, and PMMA) used in SEC systems do not provide accurate data. Moreover, the folding behavior of the different block copolymers significantly influence the hydrodynamic volume and,

Table 11 Reaction time for the preparation of the diblock copoly(2-oxazolines). In each cell, the corresponding entries indicate the initial concentration of the first monomer (first line), and the reaction times for the polymerization of the first and the second monomer, respectively (second line)

First monomer	Second monomer			
	MeOx	EtOx	NonOx	PhOx
MeOx	4 M	4 M	4 M	4 M
	400 s + 400 s	400 s + 500 s	400 s + 400 s	400 s + 1,800 s
EtOx	4 M	4 M	4 M	4 M
	500 s + 400 s	500 s + 500 s	500 s + 400 s	500 s + 1,800 s
NonOx	2 M	2 M	2 M	2 M
	800 s + 800 s	800 s + 1,000 s	800 s + 800 s	800 s + 3,600 s
PhOx	3 M	3 M	3 M	3 M
	2,400 s + 600 s	2,400 s + 800 s	2,400 s + 600 s	2,400 s + 2,400 s

Table 12 Theoretical number average molar masses (M_n^{th}) and polydispersity indices for the for chain extended and 12 diblock copoly(2-oxazolines). In each cell, the first and second entry for the PDI values results from the GPC measurements in different eluents, chloroform and N,N-dimethyl formamide (DMF), respectively

First monomer	Second monomer			
	MeOx	EtOx	NonOx	PheOx
MeOx	$M_n^{th} = 8.5$ kDa	$M_n^{th} = 9.2$ kDa	$M_n^{th} = 14.2$ kDa	$M_n^{th} = 11.6$ kDa
	PDI: –/1.16	PDI: –/1.17	PDI: –/–	PDI: –/1.25
EtOx	$M_n^{th} = 9.2$ kDa	$M_n^{th} = 9.9$ kDa	$M_n^{th} = 14.8$ kDa	$M_n^{th} = 12.3$ kDa
	PDI: –/1.18	PDI: 1.12/1.16	PDI: 1.15/–	PDI: 1.27/1.19
NonOx	$M_n^{th} = 14.2$ kDa	$M_n^{th} = 14.8$ kDa	$M_n^{th} = 19.7$ kDa	$M_n^{th} = 17.2$ kDa
	PDI: –/–	PDI: 1.64/–	PDI: 1.14/–	PDI: 1.24/–
PhOx	$M_n^{th} = 11.6$ kDa	$M_n^{th} = 12.3$ kDa	$M_n^{th} = 17.2$ kDa	$M_n^{th} = 14.7$ kDa
	PDI: –/1.18	PDI: 1.35/1.19	PDI: 1.28/–	PDI: 1.27/1.16

consequently, the M_n. Theoretical M_n and PDI values of the synthesized diblock copolymer library are summarized in Table 12.

The glass-transition temperatures and the corresponding specific heats were measured three times for each sample in order to enable the calculation of the standard deviations, which were in the range of ±3% or lower. Apparently, the kind of substituent greatly influences the T_g values, and rigid substituents (phenyl or methyl) or flexible substituents (ethyl or nonyl) cause an increase or decrease in corresponding T_g values, respectively. The measured T_g values are plotted in Fig. 19.

A library of 30 triblock copolymers was synthesized from 2-methyl, 2-ethyl, 2-nonyl, and PheOx in a single mode microwave synthesizer [92]. The polymers exhibited narrow PDI values and showed slight deviations from the targeted monomer ratio of 33:33:33. The design of the experiments is shown in Scheme 12.
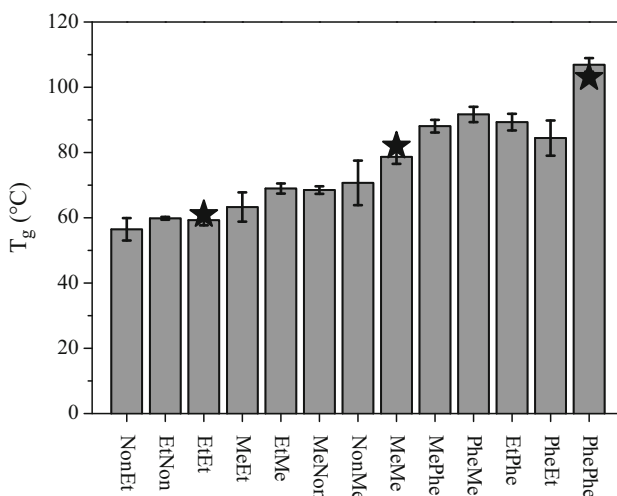
Fig. 19 Glass-transition temperatures for the chain extended and the diblock copoly(2-oxazoline)s (the *error bars* represent the range of standard deviation). $Non_{50}Non_{50}$, $Non_{50}Phe_{50}$, and $Phe_{50}Non_{50}$ did not exhibit a glass transition temperature (T_g). The stars represent the literature values for $Me_{50}Me_{50}$, $Et_{50}Et_{50}$, and $Non_{50}Non_{50}$, respectively. (Reprinted with permission from [90]. Copyright (2005) American Chemical Society)
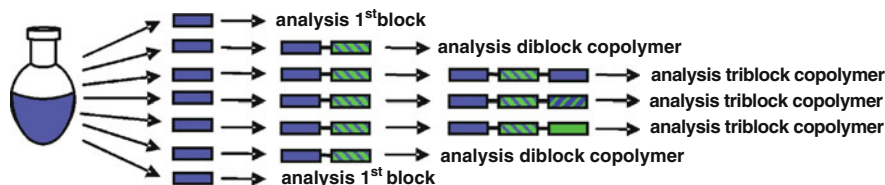
Scheme 12 Schematic representation of the synthetic procedure that was applied for the preparation of three triblock copolymers with the same first and second blocks

The designed set of 2-oxazoline monomers that was used for the synthesis of the triblock copolymers (MeOx, EtOx, PheOx, and NonOx) yielded polymers of different polarity [91]. P(MeOx) and P(EtOx) are hydrophilic, whereas P(PheOx) and P(NonOx) are hydrophobic. All possible combinations of these four different monomers would result in 64 different structures. However, all polymers that would have two times the same block after each other were excluded since they do represent diblock copolymers. Additionally, some structures, which have NonOx as the first block and EtOx or MeOx as the second block, were excluded due to extensive side reactions. Consequently, 30 different triblock copolymers were synthesized, and they are listed in Table 13 with their corresponding structural characterization.

The T_g values of all investigated triblock copolymers are plotted in Fig. 20. The increasing trend in the measured values is due to the incorporation of monomers with rigid substituent such as methyl or phenyl. Moreover, the T_g values did not

Table 13 Number of incorporated monomer units into the 30 triblock copoly(2-oxazoline)s resulting from combined ^{1}H NMR spectroscopy analyses (top) of the model [A and AB (block co) polymers] and final polymers as well as the measured number average molar masses (Mn,SEC/PDI; bottom). ^{1}H NMR spectra were recorded in CDCl$_3$ or CD$_2$Cl$_2$ (PhOx containing polymers) and GPC analyses were performed using DMF (with 5 mM NH$_4$PF$_6$) as eluent. M$_n$,GPC was calculated utilizing poly(methyl methacrylate) (PMMA) standards

1st–2nd block	3rd block			
	MeOx	EtOx	PhOx	NonOx
MeOx-EtOx				
MeOx-PhOx	33:31:33	33:33:36	–	33:30:32
	14.1 kDa/1.22	13.9 kDa/1.15		10.2 kDa/1.21
MeOx-NonOx	33:28:33	33:30:37	33:29:29	–
	9.9 kDa/1.20	10.0 kDa/1.21	10.6 kDa/1.27	
EtOx-MeOx	–	33:33:33	33:29:27	33:34:31
		10.9 kDa/1.32	12.4 kDa/1.23	9.5 kDa/1.28
EtOx-PhOx	33:31:30	33:30:33	–	33:30:36
	16.2 kDa/1.20	15.3 kDa/1.24		11.4 kDa/1.22
EtOx-NonOx	33:33:37	33:33:33	33:33:31	–
	10.1 kDa/1.27	9.9 kDa/1.22	11.3 kDa/1.25	
PhOx-MeOx	–	33:35:35	33:27:33	33:31:31
		15.3 kDa/1.21	15.2 kDa/1.19	9.1 kDa/1.23
PhOx-EtOx	33:35:34	–	33:42:33	33:38:38
	17.8 kDa/1.32		19.1 kDa/1.28	14.1 kDa/1.21
PhOx-NonOx	33:38:34	33:45:37	33:36:33	–
	9.7 kDa/1.21	8.8 kDa/1.21	11.6 kDa/1.22	
NonOx-PhOx	33:23:27	33:26:24	–	33:32:33
	7.2 kDa/1.40	7.8 kDa/1.33		10.3 kDa/1.38[a]

[a] GPC measurement with CHCl$_3$:NEt$_3$:2-PrOH (94:4:2) as eluent (PS calibration)

depend on the order of the blocks. It should also be noted that none of the triblock copolymers showed more than one T$_g$ value, indicating that there was no macroscopic phase separation occurring in the bulk state. This is most likely due to the relatively short segments (33 repeating units) that were incorporated.

3.3 Supramolecular Synthesis – LEGO® Approach

An alternative route to prepare well-defined block copolymers is first to prepare the homopolymers with functional groups and then to connect them by noncovalent interactions [92–99]. A systematic 4 × 4 library of block copolymers based on PSt and PEG connected by an asymmetrical octahedral *bis*(terpyridine) ruthenium complex at the block junction was reported [78]. Moreover, the thin film morphology of this library was investigated.
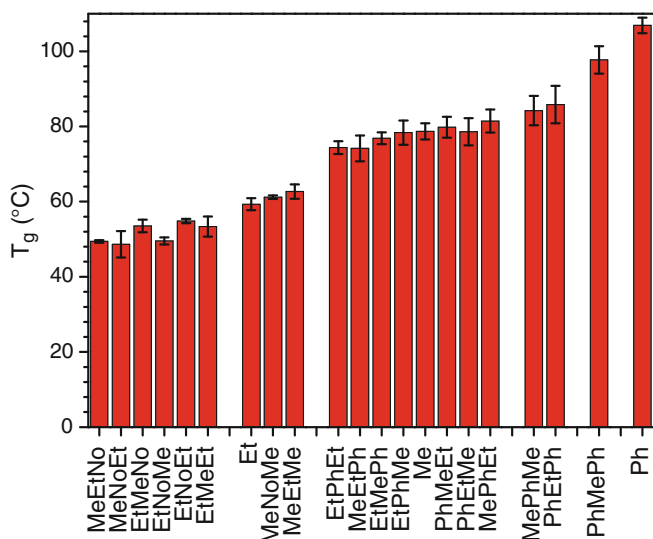
Fig. 20 Glass transition temperatures of the triblock copoly(2-oxazoline)s and the P(MeOx), P(EtOx), and P(PheOx) homopolymers, sorted in ascending order. The polymers that contained (at least) one block of P(NonOx) and P(PheOx) at the same time did not exhibit any T_g in differential scanning calorimetry (DSC). (Me = P(MeOx), Et = P(EtOx), Non = P(NonOx), and Ph = P(PheOx)). (Reprinted with permission from [91]. Copyright (2006) American Chemical Society)

Functional homopolymers can be synthesized by essentially two different methods. The first and more preferred way is to use a functional initiator which will ensure a high rate of chain end functionality. For instance, the polymerization of St initiated by a unimolecular terpyridine-functionalized nitroxide initiator yields well-defined PS homopolymers. The second technique is based on post-polymerization modifications. In this case, the reaction between mPEG and chloroterpyridine yields terpyridine-functionalized PEG building blocks, as illustrated in Scheme 13.

The theoretical molar masses and the corresponding volume fractions of PS, the metal complex, and PEG content of the block copolymers are summarized in Table 14. The metal complex has been treated as the third block. All block copolymers have been purified by preparative SEC and column chromatography, with isolated yields between 10% and 80%. The expected ratios (within 10% error) for all components in the library were obtained from the integration of ^{1}H NMR spectrum.

The morphology of this supramolecular diblock copolymer library has been investigated by means of atomic force microscopy (AFM) measurements. As illustrated in Fig. 21, at first glance different morphologies were obtained for different compositions. However, interpreting the phase behavior of supramolecular block copolymers is not straightforward. There are several important parameters that play a role in the phase behavior. For instance, the amorphous phase of PEG, the crystalline phase of PEG, the metal complex, and the amorphous PSt contribute to
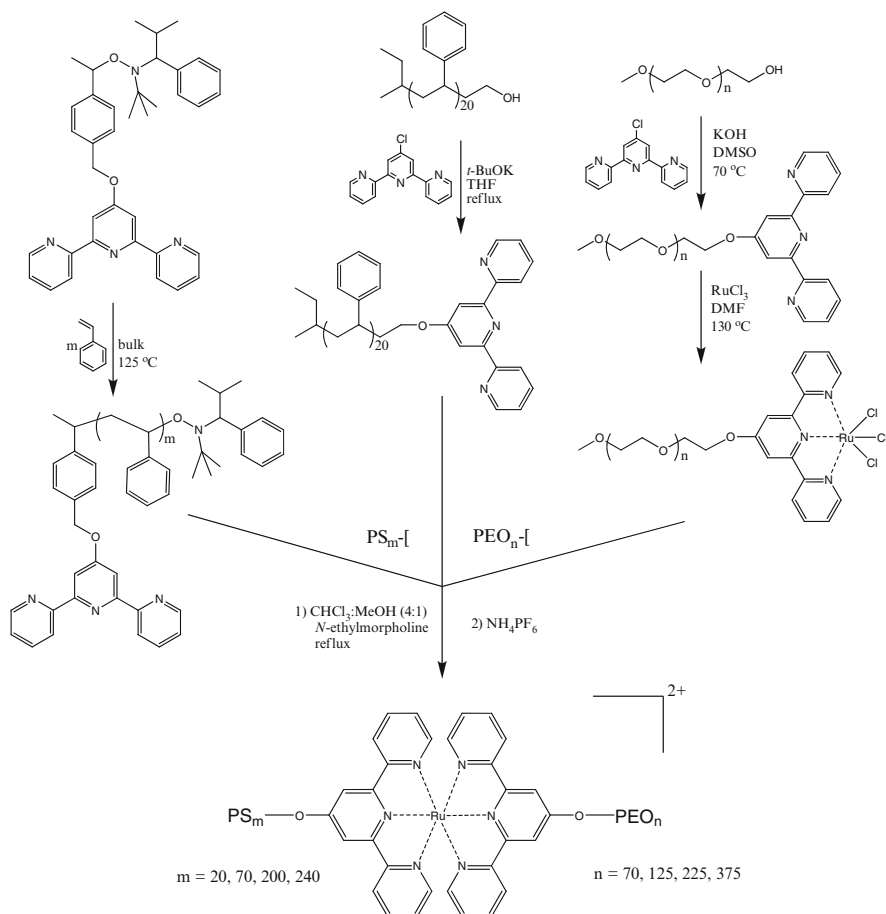
Scheme 13 Schematic representation of the synthetic route towards a library of PSt_m-[Ru]-PEO_n block copolymers, where m and n denote the degree of polymerization (DP) of PSt and PEO, respectively, and where -[Ru]- represents the bis(terpyridine) ruthenium complex

the phase contrast. Besides, the final morphology is greatly affected by competitions between self-organization, crystallization of the PEG block and vitrification of the PSt block [100].

4 Conclusion

Automated parallel synthesizers provide high-quality experimental data in relatively short periods of time. High-throughput experimentation techniques have become an inevitable reality in the field of polymer science, since there is a large
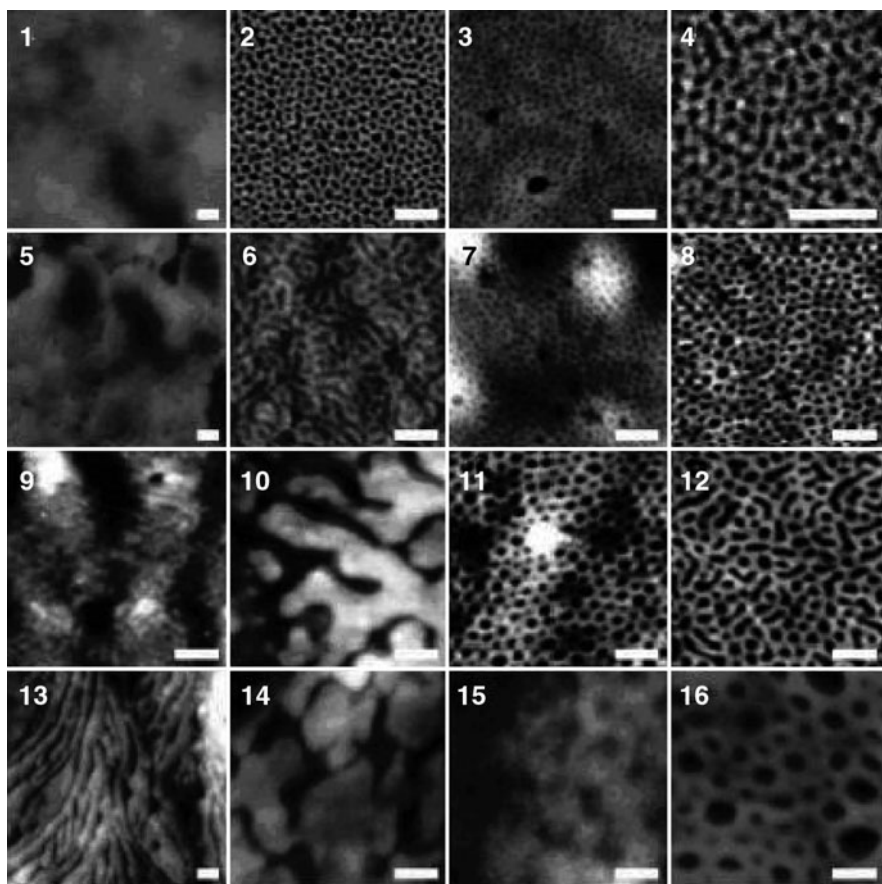
Fig. 21 Atomic force microscopy (AFM) phase images of all block copolymers in the library after spin coating from 2% w/v solution in toluene. No annealing has been performed. The *scale bar* represents 100 nm. (Reprinted with permission from [78]. Copyright (2005) Royal Society of Chemistry)

parameter space not only including the reaction parameters but also the use of different monomers, catalysts, and polymerization techniques. The application of CLP techniques in automated synthesizers have been demonstrated by several re-search groups. These techniques enable the synthesis of well-defined homo, block, or random copolymers and even more complex architectures such as graft, star, or dendritic shaped polymers.

The combination of CLP techniques and high-throughput experimentation tools accelerates the research in this field significantly. Besides, on the data collected, the construction of 3D-plots and extensive databases will provide the basis for deeper understanding of the underlying principles. As a consequence, the elucidation of quantitative structure-property relationships will be feasible.

Table 14 The block copolymers in the library are displayed in the table by name, by theoretical molar masses and by the volume fractions of PSt, -[Ru]-, and poly(ethylene oxide) (PEO) (annotated between brackets)

	PS$_{20}$-[	PS$_{70}$-[	PS$_{200}$-[	PS$_{240}$-[
PEO$_{70}$-[RuCl$_3$	PS$_{20}$-[Ru]-PEO$_{70}$ Mn = 6,100 Da (35:16:49) **1**	PS$_{70}$-[Ru]-PEO$_{70}$ Mn = 11,400 Da (65:8:27) **2**	PS$_{200}$-[Ru]-PEO$_{70}$ Mn = 25,100 Da (84:4:12) **3**	PS$_{240}$-[Ru]-PEO$_{70}$ Mn = 29,300 Da (87:3:10) **4**
PEO$_{125}$-[RuCl$_3$	PS$_{20}$-[Ru]-PEO$_{125}$ Mn = 8,400 Da (25:11:64) **5**	PS$_{70}$-[Ru]-PEO$_{125}$ Mn = 13,700 Da (54:7:39) **6**	PS$_{200}$-[Ru]-PEO$_{125}$ Mn = 27,400 Da (77:4:19) **7**	PS$_{240}$-[Ru]-PEO$_{125}$ Mn = 31,600 Da (80:3:17) **8**
PEO$_{225}$-[RuCl$_3$	PS$_{20}$-[Ru]-PEO$_{225}$ Mn = 12,800 Da (16:8:76) **9**	PS$_{70}$-[Ru]-PEO$_{225}$ Mn = 18,100 Da (41:5:54) **10**	PS$_{200}$-[Ru]-PEO$_{225}$ Mn = 31,800 Da (67:3:30) **11**	PS$_{240}$-[Ru]-PEO$_{225}$ Mn = 36,000 Da (71:3:26) **12**
PEO$_{375}$-[RuCl$_3$	PS$_{20}$-[Ru]-PEO$_{375}$ Mn = 19,400 Da (11:5:84) **13**	PS$_{70}$-[Ru]-PEO$_{375}$ Mn = 24,700 Da (31:4:65) **14**	PS$_{200}$-[Ru]-PEO$_{375}$ Mn = 38,400 Da (56:3:41) **15**	PS$_{240}$-[Ru]-PEO$_{375}$ Mn = 42,600 Da (60:2:38) **16**

References

1. Kamigaito M, Ando T, Sawamoto M (2001) Metal-catalyzed living radical polymerization. Chem Rev 101:3689–3745
2. Matyjaszewski K, Xia JH (2001) Atom transfer radical polymerization. Chem Rev 101:2921–2990
3. Hawker CJ, Bosman AW, Harth E (2001) New polymer synthesis by nitroxide mediated living radical polymerizations. Chem Rev 101:3661–3688
4. Moad G, Rizzardo E, Thang SH (2005) Living radical polymerization by the RAFT process. Aust J Chem 58:379–410
5. Hadjichristidis N, Pitsikalis M, Pispas S et al. (2001) Polymers with complex architecture by living anionic polymerization. Chem Rev 101:3747–3792
6. de Gans BJ, Duineveld P, Schubert US (2004) Ink-jet printing of polymers: state of the art and future developments. Adv Mater 16:203–213
7. Tekin E, Smith PJ, Schubert US (2008) Inkjet printing of functional materials: from polymers to nanoparticles and molecules. Soft Matter 4:703–713
8. de Gans BJ, Schubert US (2003) Ink-jet printing of polymer microarrays and libraries: requirements, possibilities and available instrumentation. Macromol Rapid Commun 24:659–666
9. Meredith JC, Smith AP, Karim A et al. (2000) Combinatorial materials science for polymer thin-film dewetting. Macromolecules 33:9747–9756
10. Smith AP, Douglas JF, Meredith JC et al. (2001) High-throughput characterization of pattern formation in symmetric diblock copolymer films. J Polym Sci Part B Polym Phys 39:2141–2158

11. Webster DC (2008) Combinatorial and high-throughput methods in macromolecular materials research and development. Macromol Chem Phys 209:237–246
12. Green JJ, Langer R, Anderson DG (2008) A combinatorial polymer library approach yields insight into nonviral gene delivery. Acc Chem Res 41:749–759
13. Lynn DM, Anderson DG, Putnam D et al. (2001) Accelerated discovery of synthetic transfection vectors: parallel synthesis and screening of a degradable polymer library. J Am Chem Soc 123:8155–8156
14. Reynolds CH (1999) Designing diverse and focused combinatorial libraries of synthetic polymers. J Comb Chem 1:297–306
15. Anderson DG, Peng W, Akinc A, Hossain N, Kohn A, Padera R, Langer R, Sawicki JA (2004) A polymer library approach to suicide gene therapy for cancer. Proc Nat Acad Sci USA 101:16028–16033
16. Szwarc M (1956) Living polymers. Nature 178:1168–1169
17. IUPAC (1997) Compendium of chemical terminology, (the "Gold Book"), 2nd edn. In: McNaught AD, Wilkinson A (eds) Blackwell, Oxford (XML on-line corrected version: http://goldbook.iupac.org (2006-) created by M. Nic, J. Jirat, B. Kosata; updates compiled by A. Jenkins. ISBN 0–9678550–9–8)
18. Moad G, Solomon DH (1995) The chemistry of free radical polymerization. Elsevier Science, Bath
19. Sawamoto M, Kamigaito M (1999) In: Schlueter D (ed) Synthesis of polymers. VCH, Weinheim
20. Otsu T, Matsumoto A (1998) Controlled synthesis of polymers using the iniferter technique: developments in living radical polymerization. Adv Polym Sci 136:75–137
21. Ajayaghosh A, Francis R (1998) Narrow polydispersed reactive polymers by a photoinitiated free radical polymerization approach. Controlled polymerization of methyl methacrylate. Macromolecules 31:1436–1438
22. Ajayaghosh A, Francis R (1999) A xanthate-derived photoinitiator that recognizes and controls the free radical polymerization pathways of methyl methacrylate and styrene. J Am Chem Soc 121:6599–6606
23. Borsig E, Lazar M, Capla M (1967) Polymerization of methyl methacrylate initiated by 3,3,4,4-tetraphenyl hexane and 1,1,2,2-tetraphenyl cyclopentane. Makromol Chem 105:212
24. Sebenik A (1998) Living free-radical block copolymerization using thio-iniferters. Prog Polym Sci 23:875–917
25. Qin SH, Qiu KY, Swift G et al. (1999) "Living" radical polymerization of methyl methacrylate with diethyl 2,3-dicyano-2,3-diphenylsuccinate as a thermal iniferter. J Polym Sci Part A Polym Chem 37:4610–4615
26. Moad G, Rizzardo E (1995) Alkoxyamine-initiated living radical polymerization: factors affecting alkoxyamine homolysis rates. Macromolecules 28:8772–8728
27. Moad G, Rizzardo E, Thang SH (2008) Toward living radical polymerization. Acc Chem Res 41:1133–1142
28. Wang JS, Matyjaszewski K (1995) Controlled living radical polymerization – atom transfer radical polymerization in the presence of transition metal complexes. J Am Chem Soc 117:5614–5615
29. Kato M, Kamigaito M, Sawamoto M et al. (1995) Polymerization of methyl methacrylate with the carbon-tetrachloride dichlorotris(triphenylphosphine)-ruthenium(II) methylaluminum bis(2,6-di-tert-butylphenoxide) initiating system – possibility of living radical polymerization. Macromolecules 28:1721–1723
30. Kwak Y, Matyjaszewski K (2008) Effect of initiator and ligand structures on ATRP of styrene and methyl methacrylate initiated by alkyl dithiocarbamate. Macromolecules 41:6627–6635
31. Tang W, Matyjaszewski K (2007) Effects of initiator structure on activation rate constants in ATRP. Macromolecules 40:1858–1863
32. Tang W, Kwak Y, Braunecker W et al. (2008) Understanding atom transfer radical polymerization: effect of ligand and initiator structures on the equilibrium constants. J Am Chem Soc 130:10702–10713

33. Becer CR, Groth AM, Paulus RM et al. (2008) Protocol for automated kinetic investigation/optimization of the RAFT polymerization of various monomers. QSAR Comb Sci 27:977–983
34. Zhang HQ, Marin V, Fijten MWM et al. (2004) High-throughput experimentation in ATRP: a general approach toward a directed design and understanding of optimal catalytic systems. J Polym Sci Part A Polym Chem 42:1876–1885
35. Meier MAR, Schubert US (2006) Selected successful approaches in combinatorial materials research. Soft Matter 2:371–376
36. Meier MAR, Hoogenboom R, Schubert US (2004) Combinatorial methods, automated synthesis and high-throughput screening in polymer research: the evolution continues. Macromol Rapid Commun 25:21–33
37. Hoogenboom R, Meier MAR, Schubert US (2003) Combinatorial methods, automated synthesis and high-throughput screening in polymer research: past and present. Macromol Rapid Commun 24:15–32
38. Meier MAR, Schubert US (2004) Combinatorial polymer research and high-throughput experimentation: powerful tools for the discovery and evaluation of new materials. J Mater Chem 14:3289–3299
39. Zhang HQ, Hoogenboom R, Meier MAR et al. (2005) Combinatorial and high-throughput approaches in polymer science. Meas Sci Technol 16:203–211
40. Guerrero-Sanchez G, Paulus RM, Fijten MWM et al. (2006) High-throughput experimentation in synthetic polymer chemistry: from RAFT and anionic polymerizations to process development. Appl Surf Sci 252:2555–2561
41. Zhang HQ, Abeln CH, Fijten MWM et al. (2006) High-throughput experimentation applied to atom transfer radical polymerization: automated optimization of the copper catalysts removal from polymers. e-polymers 8:1–9
42. Zhang HQ, Fijten MWM, Hoogenboom R et al. (2003) Application of a parallel synthetic approach in atom transfer radical polymerization: set up and feasibility demonstration. Macromol Rapid Commun 24:81–86
43. Moad G, Rizzardo E, Solomon DH (1982) Selectivity of the reaction of free radicals with styrene. Macromolecules 15:909–914
44. Georges MK, Veregin RPN, Kazmaier PM et al. (1993) Narrow molecular weight resins by a free radical polymerization process. Macromolecules 26:2987–2988
45. Hawker CJ (1994) Molecular weight control by a living free radical process. J Am Chem Soc 116:11185–11186
46. Hawker CJ, Barclay GG, Orellana A et al. (1996) Initiating systems for nitroxide-mediated "living" free radical polymerizations: synthesis and evaluation. Macromolecules 29:5245–5254
47. Benoit D, Grimaldi S, Robin S et al. (2000) Kinetics and mechanism of controlled free-radical polymerization of styrene and *n*-butyl acrylate in the presence of an acyclic beta-phosphonylated nitroxide. J Am Chem Soc 122:5929–5939
48. Benoit D, Chaplinski V, Braslau R et al. (1999) Development of a universal alkoxyamine for "living" free radical polymerizations. J Am Chem Soc 121:3904–3920
49. Becer CR, Paulus RM, Hoogenboom R et al. (2006) Optimization of the NMRP conditions for styrene and *tert*-butylacrylate in an automated parallel synthesizer. J Polym Sci Part A Polym Chem 44:6202–6213
50. Eggenhuisen TM, Becer CR, Fijten MWM et al. (2008) Libraries of statistical hydroxypropyl acrylate containing copolymers with LCST properties prepared by NMP. Macromolecules 41:5132–5140
51. Chiefari J, Chong YK, Ercole F (1998) Living free radical polymerization by reversible addition-fragmentation chain transfer – the RAFT process. Macromolecules 31:5559–5562
52. Corpart P, Charmot D, Biadatti T et al. (1999) Block polymer synthesis by controlled radical polymerization. (WO9858974) Chem Abstr 130:82018
53. Chapon P, Mignaud C, Lizarraga G et al. (2003) Automated parallel synthesis of MADIX (co)polymers. Macromol Rapid Commun 24:87–91

54. Fijten MWM, Paulus RM, Schubert US (2005) Systematic parallel investigation of RAFT polymerizations for eight different (meth)acrylates: a basis for the designed synthesis of block and random copolymers. J Polym Sci Part A Polym Chem 43:3831–3839

55. Guerrero-Sanchez C, Abeln C, Schubert US (2005) Automated parallel anionic polymerizations: enhancing the possibilities of a widely used technique in polymer synthesis. J Polym Sci Part A Polym Chem 43:4151–4160

56. Gilman H, Jaubein AH (1941) The quantitative analysis of alkyllithium compounds. J Am Chem Soc 66:1515–1516

57. Hadjichristidis N, Iatrou H, Pispas S et al. (2000) Anionic polymerization: high vacuum techniques. J Polym Sci Part A Polym Chem 38:3211–3234

58. Glusker DL, Lysloff I, Stiles E (1961) Mechanism of anionic polymerization of methyl methacrylate II. Use of molecular weight distributions to establish a mechanism. J Polym Sci 49:315–334

59. Auguste S, Edwards HGM, Johnson AF et al. (1996) Anionic polymerization of styrene and butadiene initiated by n-butyllithium in ethylbenzene: determination of the propagation rate constants using Raman spectroscopy and gel permeation chromatography. Polymer 37:3665–3673

60. Wang GM, van Beylen M (2003) Influence of π-complexing agents on the anionic polymerization of styrene with lithium as counterion in cyclohexane. 1. Effect of durene. Polymer 44:6205–6210

61. Tomalia DA, Sheetz DP (1966) Homopolymerization of 2-alkyl and 2-aryl-2-oxazolines. J Polym Sci Part A Polym Chem 4:2253–2265

62. Seelinger W, Aufderhaar E, Diepers W et al. (1966) Recent synthesis and reactions of cyclic imidic esters. Angew Chem 20:913–927

63. Hoogenboom R, Fijten MWM, Paulus RM et al. (2006) Accelerated pressure synthesis and characterization of 2-oxazoline block copolymers. Polymer 47:75–84

64. Hoogenboom R, Fijten MWM, Schubert US (2004) The effect of temperature on the living cationic polymerization of 2-phenyl-2-oxazoline explored utilizing an automated synthesizer. Macromol Rapid Commun 25:339–343

65. Hoogenboom R, Fijten MWM, Schubert US (2004) Parallel kinetic investigation of 2-oxazoline polymerizations with different initiators as basis for designed copolymer synthesis. J Polym Sci Part A Polym Chem 42:1830–1840

66. Hoogenboom R, Wiesbrock F, Leenen MAM et al. (2005) Accelerating the living polymerization of 2-nonyl-2-oxazoline by implementing a microwave synthesizer into a high-throughput experimentation workflow. J Comb Chem 7:10–13

67. Hoogenboom R, Paulus RM, Fijten MWM et al. (2005) Concentration effects in the CROP of 2-ethyl-2-oxazoline in *N,N*-dimethyl acetamide. J Polym Sci Part A Polym Chem 43:1487–1497

68. Wiesbrock F, Hoogenboom R, Leenen MAM et al. (2005) Investigation of the living cationic ring-opening polymerization of 2-methyl, 2-ethyl, 2-nonyl, and 2-phenyl-2-oxazoline in a single-mode microwave reactor. Macromolecules 38:5025–5034

69. Paulus RM, Becer CR, Hoogenboom R et al. (2008) Acetyl halide initiator screening for the cationic ring opening polymerization of 2-ethyl-2-oxazoline. Macromol Chem Phys 209:794–800

70. Yagci Y, Tasdelen MA (2006) Mechanistic transformations involving living and controlled/living polymerization methods. Prog Polym Sci 31:1133–1170

71. Bernaerts KV, Du Prez FE (2006) Dual/heterofunctional initiators for the combination of mechanistically distinct polymerization techniques. Prog Polym Sci 31:671–722

72. Becer CR, Paulus RM, Hoppener S et al. (2008) Synthesis of poly(2-ethyl-2-oxazoline)-*b*-poly(styrene) copolymers via a dual initiator route combining cationic ring opening polymerization and atom transfer radical polymerization. Macromolecules 41:5210–5215

73. Becer CR, Hahn S, Fijten MWM et al. (2008) Libraries of MAA and OEGMA copolymers with LCST behavior. J Polym Sci Part A Polym Chem 46:7138–7147

74. Fournier D, Hoogenboom R, Thijs HML, Paulus RM, Schubert US (2007) Tunable pH- and temperature-sensitive copolymer libraries by RAFT of methacrylates. Macromolecules 40:915–920

75. Lutz JF, Hoth A (2006) Preparation of ideal PEG analogues with a tunable thermosensitivity by controlled radical copolymerization of 2-(2-methoxyethoxy)ethyl methacrylate and oligo(ethylene glycol) methacrylate. Macromolecules 39:893–896

76. Lutz JF (2008) Polymerization of oligo(ethylene glycol) (meth)acrylates: toward new generations of smart biocompatible materials. J Polym Sci Part A Polym Chem 46:3459–3470

77. Thomas EL, Anderson DM, Henkee CS et al. (1988) Periodic area-minimizing surfaces in block copolymers. Nature 334:598–601

78. Lohmeijer BGG, Wouters D, Yin ZH et al. (2004) Block copolymer libraries: modular versatility of the macromolecular Lego (R) system. Chem Commun 24:2886–2887

79. Pochan DJ, Chen Z, Cui H et al. (2004) Toroidal triblock copolymer assemblies. Science 306:94–97

80. Jain S, Bates FS (2003) On the origins of morphological complexity in block copolymer surfactants. Science 300:460–464

81. Gohy JF (2005) Block copolymer micelles. Adv Polym Sci 190:65–136

82. Ladaviere C, Dorr N, Claverie JP (2001) Controlled radical polymerization of acrylic acid in protic media. Macromolecules 34:5370–5372

83. Couvreur L, Lefay C, Belleney J (2003) First nitroxide-mediated controlled free-radical polymerization of acrylic acid. Macromolecules 36:8260–8267

84. Haddleton DM, Crossman MC, Dana BH et al. (1999) Atom transfer polymerization of methyl methacrylate mediated by alkylpyridylmethan-imine type ligands, copper(I) bromide, and alkyl halides in hydrocarbon solution. Macromolecules 32:2110–2119

85. Butun V, Vamvakaki M, Billingham NC et al. (2000) Synthesis and aqueous solution properties of novel neutral/acidic block copolymers. Polymer 41:3173–3182

86. Mori H, Muller AHE (2003) New polymeric architectures with (meth)acrylic acid segments. Prog Polym Sci 28:1403–1439

87. Hoogenboom R, Schubert US, van Camp W et al. (2005) RAFT polymerization of 1-ethoxy ethyl acrylate: a novel route toward near-monodisperse poly(acrylic acid) and derived block copolymer structures. Macromolecules 38:7653–7659

88. Hoogenboom R, Fijten MWM, Wijnans S et al. (2006) High-throughput synthesis and screening of a library of random and gradient copoly(2-oxazoline)s. J Comb Chem 8:145–148

89. Hoogenboom R, Fijten MWM, Thijs HML et al. (2007) Synthesis, characterization, and cross-linking of a library of statistical copolymers based on 2-"soy alkyl"-2-oxazoline and 2-ethyl-2-oxazoline. J Polym Sci Part:A Polym Chem 45:5371–5379

90. Wiesbrock F, Hoogenboom R, Leenen M et al. (2005) Microwave-assisted synthesis of a 4 × 2-membered library of diblock copoly(2-oxazoline)s and chain-extended homo poly(2-oxazoline)s and their thermal characterization. Macromolecules 38:7957–7966

91. Hoogenboom R, Wiesbrock F, Huang H et al. (2006) Microwave-assisted cationic ring-opening polymerization of 2-oxazolines: a powerful method for the synthesis of amphiphilic triblock copolymers. Macromolecules 39:4719–4725

92. Lohmeijer BGG, Schubert US (2002) Supramolecular engineering with macromolecules: an alternative concept for block copolymers. Angew Chem Int Ed 41:3825–3829

93. Lohmeijer BGG, Schubert US (2005) The LEGO toolbox: supramolecular building blocks by NMP. J Polym Sci Part A Polym Chem 43:6331–6344

94. Lohmeijer BGG, Schubert US (2003) Water-soluble building blocks for metallo-supramolecular polymers: synthesis, complexation and decomplexation studies of poly(ethyleneoxide) moities. Macromol Chem Phys 204:1072–1078

95. Gohy JF, Lohmeijer BGG, Schubert US (2003) From supramolecular block copolymers to advanced nano-objects. Chem Eur J 9:3472–3479

96. Meier MAR, Lohmeijer BGG, Schubert US (2003) Characterization of defined metal containing supramolecular block copolymers. Macromol Rapid Commun 24:852–857

97. Lohmeijer BGG, Schubert US (2004) Expanding the supramolecular polymer LEGO system: nitroxide mediated living free radical polymerization for metallo-supramolecular block copolymers with a polystyrene block. J Polym Sci Part A Polym Chem 42:4016–4027
98. Gohy JF, Lohmeijer BGG, Alexeev A, Wang XS, Manners I, Winnik MA, Schubert US (2004) Cylindrical micelles from the aqueous self-assembly of an amphiphilic poly(ethylene oxide)-b-poly(ferrocenylsilane) (PEO-b-PFS) block copolymer with a metallo-supramolecular linker at the block junction. Chem Eur J 20:4315–4323
99. Hofmeier H, El-ghayoury A, Schenning APH, Schubert US (2004) New supramolecular polymers containing both terpyridine metal complexes and quadruple hydrogen bonding units. Chem Commun 318–319
100. Zhu L, Chen Y, Zhang AQ et al. (1999) Phase structures and morphologies determined by competitions among self-organization, crystallization, and vitrification in a disordered poly(ethylene oxide)-b-polystyrene diblock copolymer. Phys Rev B Condens Matter 60:10022–10031

Gradient and Microfluidic Library Approaches to Polymer Interfaces*

Michael J. Fasolka, Christopher M. Stafford, and Kathryn L. Beers

Abstract We present an overview of research conducted at the National Institute of Standards and Technology aimed at developing and applying combinatorial and high-throughput measurement approaches to polymer surfaces, interfaces and thin films. Topics include (1) the generation of continuous gradient techniques for fabricating combinatorial libraries of film thickness, temperature, surface chemistry and polymer blend composition, (2) high-throughput measurement techniques for assessing the mechanical properties and adhesion of surfaces, interfaces and films, and (3) microfluidic approaches to synthesizing and analyzing libraries of interfacially-active polymer species.

Contents

M.J. Fasolka (✉), C.M. Stafford, and K.L. Beers
Materials Science and Engineering Laboratory, National Institute of Standards and Technology, Gaithersburg, MD 20899, USA
e-mail: mfasolka@nist.gov; chris.stafford@nist.gov; kathryn.beers@nist.gov

1 Introduction: Surfaces and Interfaces in Polymer Science and Engineering

The success of a huge range of polymer-based technologies, including advanced coatings and adhesives, electronics materials, complex fluid formulations and biomaterials, hinges on the ability to produce tailored polymer surfaces and interfaces. This is because surface and interfacial properties govern key aspects of product structure and performance, such as film and multilayer stability, mechanical reliability, adhesion, expression of functional moieties, component dispersion, and domain orientation, among others. Research dedicated to the understanding and engineering of these factors is extensive, and has proceeded for a number of decades; this is due to the fact that both the origins and effects of surface and interfacial properties are complex, depend upon a large number of variables, and can be difficult to predict. Both the importance and complexity of surface and interfacial science and engineering make them excellent targets for combinatorial and high-throughput approaches. Indeed, some of the first uses of these methods for polymeric materials systems focused on the formulation and performance testing of coatings [1], the behavior of which depend greatly on surface and interfacial effects.

Starting in the late 1990s, and continuing for the following 10 years, the National Institute of Standards and Technology (NIST) built and executed a research program that developed combinatorial methods aimed largely at addressing scientific and engineering challenges in polymer surfaces, interfaces and thin films. The NIST program, organized through the NIST Combinatorial Methods Center (NCMC, www.nist.gov/combi), concentrated on meeting two measurement-related needs in establishing combinatorial approaches for polymer surfaces and interfaces: the design and implementation of appropriate library fabrication and synthesis methods, and the development of high-throughput testing techniques to asses these libraries. This review surveys the research conducted through the NCMC with a focus on methodology, technique development and descriptions of supporting case studies in polymer surfaces, interfaces and films. The paper will start with a discussion of continuous gradient techniques, where NIST was a pioneer in polymer materials. The fabrication of gradient libraries for surfaces and interfaces will be considered next, including techniques for making continuous spreads in film thickness and composition, surface chemistry and surface energy and temperature. Application studies will include film stability and wetting, polymer self-assembly, polymer brush behavior

and measurements, biomaterials surface engineering. The next section will consider NIST-developed high-throughput approaches to measuring surface, interface and film performance properties. These include rapid measurement of film modulus, adhesion, and interfacial strength. Applications examples include mechanical testing of ultrathin film systems, ultrasoft polymers, engineering adhesives and relatively weak adhesive interactions. The final section will consider microfluidic and continuous microreactor approaches to polymer library fabrication and the high-throughput measurement of such systems. The primary focus will be on methods to produce systematic libraries of interfacially-active polymer species, such as block copolymers and macromolecular surfactants. Measurement applications will include microfluidic assessments of complex fluid structure, in particular solution self-assembly, and of fluid mixture properties such as interfacial tension.

2   Continuous Gradient Library Techniques

A key challenge in combinatorial research is the creation of specimen *libraries* that exhibit a diversity of composition, processing conditions and other parameters over prescribed ranges. A common design for achieving this is the so-called "discrete" library, which consists of a large collection of individual sub-specimens. The main advantage of the discrete approach is the ability to incorporate a great number of different parameters in a single library – in this sense the design is versatile. However, since the library parameter space is divided into discrete sub-specimens, each with a single set of parameters, it is possible to "skip over" what may be important or interesting combinations of variables. Another disadvantage is that the fabrication of discrete libraries can depend upon complex, often expensive, equipment.

An alternate library design and fabrication strategy, and the one we focus on in this article, is the continuous gradient [2]. In this scheme, diversity is created by fabricating a specimen that gradually and continuously changes in a given parameter as a function of position (or as we will discuss later, as a function of time). Two or three continuous gradients can be combined in a single system. An illustration of a binary continuous gradient library can be seen in Fig. 1. Because they are continuous, and there are no "gaps" in the parameter space, gradient libraries present clear advantages for comprehensively examining and mapping the effect of the graded properties. For example, a binary gradient library exhibits every possible combination of the two graded parameters. As such, the gradient library design is excellent for mapping property correlation, and for identifying optimal conditions or critical phenomena that may exist only over a small range or at a specific parameter combination. Indeed, for materials scientists, gradient libraries can be a natural experimental design, since they are quite similar to the phase diagrams they use to represent two and three parameter systems.

A key aspect of gradient libraries is that they reside on a single substrate, and this has several advantages. Foremost, gradient libraries yield an entire set of systematic results from a single compound experiment. In this sense, they are "self-reporting",

Fig. 1 Illustration of a 2D continuous gradient combinatorial library that exhibits gradual and systematic changes in two variables
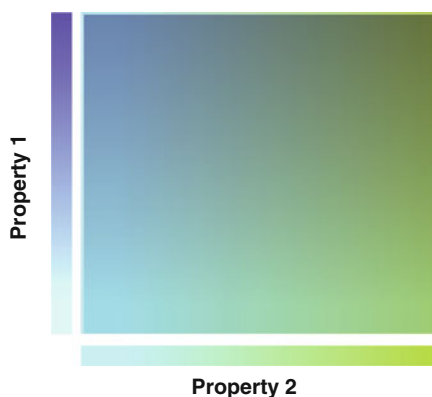
meaning that they can illuminate trends and express key results without extensive analysis (our example of a single specimen phase diagram, discussed below, will illustrate this point). Moreover, because the entire library undergoes identical processing, "sample to sample" errors (inherent to combining single measurements on individual specimens) can be reduced. Finally, gradient libraries can often be produced with simple, inexpensive equipment, which makes this approach accessible to academic laboratories and small companies.

3 Gradient Library Fabrication Methods and Application Examples

Gradient libraries generally assume a planar form, and are supported by a substrate. Often the library is a material deposited onto the substrate as a thin coating, or it can be achieved through chemical modification of the substrate itself. This geometry naturally gears gradient libraries for the examination of thin films, coatings and of the interfacial properties that govern these systems. At NIST, our goal was to create a suite of gradient library fabrication technologies that would be a combinatorial platform for examining polymer thin film physics phenomena including wetting and stability, blend phase behavior, self-assembly, and confinement effects.

3.1 Flow Coating: Polymer Film Thickness Gradients

Film thickness can govern the morphology, stability, and surface-chemical expression of polymeric thin films. NIST researchers developed a process for producing gradients, termed flow coating, which is a modified blade-casting technique [3–5]. Flow coater instrumentation and the flow coating process are illustrated in Fig. 2. To create the library, a dilute solution of polymer in solvent (1–5% mass fraction) is injected into the gap between a doctor blade positioned over a flat substrate
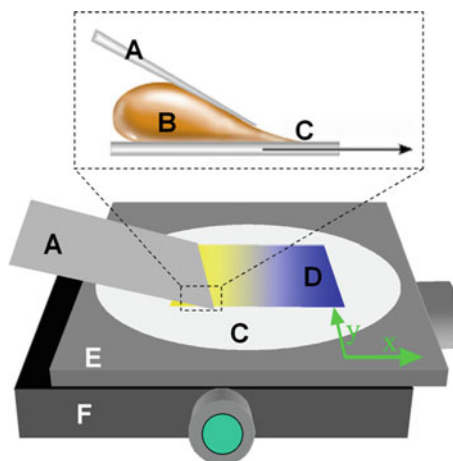
(e.g., silicon wafer) mounted on a computer-controlled translation stage. The stage/substrate is accelerated beneath the stationary blade in the *x*-direction as shown in Fig. 2. As the stage accelerates, increasing amounts of solution are deposited along the substrate. Subsequent solvent evaporation results in a gradient polymer film thickness library. As demonstrated by Stafford et al. [5], the range and slope of the thickness gradient can be precisely tuned through the stage velocity profile, solution concentration, and gap height.

Films produced via flow coating can be from ≈ 20 to ≈ 1 mm in thickness. A typical library will double in thickness over about 40 mm in length. In the range of 50–600 nm, libraries exhibit constant slopes of ≈ 1–10 nm mm^{-1}, depending upon processing parameters. In the NIST instrument, thickness gradients are characterized via spot interferometry. In this scheme, stacked translation stages (including the stage used to produce the specimen) raster the sample beneath the interferometer footprint, resulting in a 2D map of film thickness. With careful instrument construction and operation [5], thickness libraries created via flow coating are linear along the *x*-direction, and level along the *y*-direction (to about 3% of the average film thickness at a point *x*), but 2D thickness characterization may be necessary for the most quantitative combinatorial analysis.

When used with polymer solutions in the few percent by mass range, the flow coating instrument creates films that are comparable in thickness and roughness to those created by spin casting, i.e. ranging from ≈ 10 to 500 nm thickness, with root-mean-squared roughness ≤ 1 nm. However, it should be noted that spin casting typically drives solvent from the system much faster than with flow coating and this can affect the film morphology [6]. Recently, de Gans and coworkers [7] demonstrated a "sector" spin casting technique for creating discrete polymer film libraries. In this technique, a metal template is used to divide a round substrate into pie-slice shaped sectors, into which a series of polymer solutions can be deposited and cast. By varying spin speed and solution concentration, a discrete film thickness library could be built; moreover, the method can be used to cast discrete compositional libraries of, for example, polymer blends. Another route for discrete

film library fabrication is ink jetting, which has been explored by several groups [8–11]. As with sector spin coating, this technique can be used to create compositional spreads. However, ink jetting does not seem to offer the deposition control necessary to produce well-behaved thickness libraries, since ink jetted spots typically exhibit irregular thickness profiles due to "coffee ring" and other drying effects.

3.2 Gradient Hot Stage: Temperature Processing Libraries

Polymer thin film properties are often governed or modified by high-temperature annealing and processing, with most phenomena (phase transitions, dewetting, melting etc.) occurring below about 300°C. Accordingly, a temperature gradient with modest range can create a useful map of the effect of temperature on polymer film libraries. This concept has been examined in the literature [12], and in past decades several companies have used this concept to produce gradient hot-stages for applications that include melting-point determination. In recent years, NIST researchers designed a gradient hotstage with the aim of producing a flexible instrument that could accommodate libraries of various lengths, and that had a tunable temperature profile [13–15].

Figure 3 illustrates the NIST gradient hot stage design. The instrument consists of an aluminum sample platen ($10\,cm \times 15\,cm \times 0.5\,cm$) perforated with two slots (along *x*). Two aluminum blocks, fitted with heating/cooling channels, are attached to the bottom of the platen through the slots. This set-up enables control of the inter-block distance, which allows the positions of the heating/cooling sources to be matched with length of the specimen library. The blocks hold cylindrical heating cartridges or accommodate plumbing for fluid-mediated cooling.
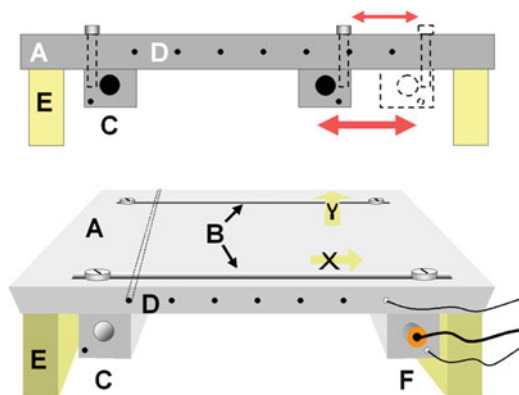

Fig. 3 NCMC gradient hot stage: **A** sample platen; **B** slots for mounting/positioning of heating/cooling blocks; **C** block with channel for heating/cooling element with thermocouple ports for temperature control; **D** thermocouple ports for gradient characterization; **E** ceramic blocks for mounting hot stage; **F** block with cylindrical heating element and thermocouple installed. (Reproduced with permission from [13])

Proportional–integral–derivative (PID) temperature controllers maintain the block temperatures, measured through integrated thermocouples. By heating (or cooling) each block to a constant temperature, a temperature gradient is produced across the platen. Ceramic supports insulate the device, so it can be mounted on, for example, a microscope translation stage or other observation instrument. The range and slope of the temperature gradient are tailored through the block distance and the temperatures of the heating/cooling sources. Remarkably, for modest temperature ranges ($\approx 200\,^\circ$C) the temperature profile is linear [14] along the gradient (x-direction), and level perpendicular to the gradient (y-direction), so measurements of the temperatures at the ends stage are sufficient to characterize the gradient. However, in the NIST instrument, thermocouple ports drilled into the platen edge enable temperature measurements along the gradient. Using this device, typical temperature gradients span intervals of about $100\,^\circ$C over a total range of room temperature to about $300\,^\circ$C.

In conjunction with both in situ and ex situ automated measurements, a gradient hot stage can be a powerful tool for examining the role of temperature on film microstructure, morphology development kinetics, phase transitions and performance. For example, Lucas et al. [15] recently used the NIST gradient hot stage to map the effect of temperature processing on the structure and performance of organic semiconductor films. In this study, polythiophene thin films were annealed on a temperature gradient that crossed the bulk liquid-crystal transition of the material. The resulting film library exhibited a range of morphologies across this transition, which could be observed via atomic force microscopy (AFM) conducted along the library. In addition, this team employed an automated probe station to measure the field effect mobility along the specimen, resulting in a map of the material's electronic performance. With this strategy, and using a single specimen, the authors were able both to identify the annealing temperature that gave optimal performance, and to determine how the mobility was correlated with film microstructure. In a similar scheme, Eidelman and coworkers [16] used the gradient hot stage in conjunction with automated Fourier transform infrared (FTIR) microspectroscopy and high-throughput adhesion testing to map correlations between curing temperature, degree of curing and surface tack of model epoxy adhesive formulations. By combining a temperature gradient, flow coating, and automated optical microscopy, Beers et al. [14] were able to examine simultaneously the roles of temperature and thickness on the crystallization rate of isotactic polystyrene. In this study, flow coating was used to create a film thickness library of the polymer, which was placed orthogonal to a temperature gradient. Automated micrographs were collected across a grid of points on the library, each of which represented a different combination of thickness and crystallization temperature. Time sequences of crystallite growth were built by repeating the cycle of micrograph acquisition over a few hours, which yielded a 2D map of crystallization rates as a function of thickness and temperature. In addition, analysis of the library via AFM and optical microscopy allowed the researchers to observe several thickness dependent transitions in crystallite morphology.

3.3   Surface Energy and Surface Chemistry Libraries

A key factor that governs the behavior of polymer thin films is its interaction
with an underlying substrate. In combination with other factors, surface energy
and chemistry of the substrate can cause film instability and dewetting, shifts in
thermodynamic and morphological transitions, changes in nano-domain orientation,
and modifications in the expression of chemical moieties at the substrate/film in-
terface and free film surface. In addition, surface energy/chemistry can affect the
mobility, growth and morphology of adsorbed cells in biological systems. NIST
researchers have developed two main strategies for creating libraries of substrate
surface energy/chemistry, which are useful for screening the effect of this factor on
the behavior of overlying films and other materials. First, we will discuss the use
of graded ultraviolet light–ozone (UV–ozone) exposure to fabricate surface energy
libraries, and some of the combinatorial studies that resulted from this capability.
Then, in the next section, we will consider more sophisticated surface chemistry
libraries fabricated through surface-initiated polymerization, and the use of these
graded polymer "brush" layers for high-throughput analysis.

It is well known that exposure of organic molecules to ozone generated from
ultraviolet–light (UV–ozone) can cause a variety of oxidative reactions – this
is the basis of UV–ozone surface cleaning devices. For alkyl chain molecules,
UV–ozonolysis leads first to the formation of oxygen containing moieties, typi-
cally starting at the chain ends, with the eventual consumptive oxidation of the
molecules at long exposures. Since the degree of oxidation is dependent upon
the UV–ozone dosage, this process can be harnessed to create a gradient surface
energy library. There are several ways to create the gradient in UV–ozone exposure
needed to accomplish such libraries. In one strategy, NIST researchers [17, 18]
used a UV–ozone flood source (185 and 254 nm light) to illuminate a planar sub-
strate through a graded neutral density filter, which systematically decreased the
amount of transmitted light as a function of position. The substrate was a native
oxide-terminated silicon wafer, treated with a self-assembled monolayer (SAM) of
n-octyldimethylchlorosilane (ODS).

As shown in Fig. 4a for an ODS treated substrate, the library exhibits a system-
atic change in water contact angle along its length. Roberson and coworkers [17]
also used more sophisticated contact angle measurements to yield the polar and
dispersive parts of the total surface energy (Fig. 4b). These measurements demon-
strate that the UV–ozone treatment changes the polar part of the surface energy,
while leaving the dispersive part relatively unchanged. Time-of-flight secondary ion
mass spectrometry measurements across the library show that the UV–ozonolysis
gradually imparts the hydrophobic, methyl-terminated, ODS SAM layer with a va-
riety of oxygen containing end-groups, but these were primarily –COOH terminated
species. The growing number of –COOH terminated species along the library results
in its increasing hydrophilicity (i.e. lower water contact angles) as shown in Fig. 4.

More recently, NIST researchers [13, 19] developed a device to more precisely
generate surface energy libraries using OV-ozonolysis. Pictured in Fig. 5, this de-
vice achieves graded UV–ozonolysis through a computer-driven translation stage,

Fig. 4 Water contact angle data (**a**) and surface energy data (**b**) from a surface energy library produced through the graded UV–ozonolysis of an ODS self-assembled monolayer on silicon. (Reproduced with permission from [17])
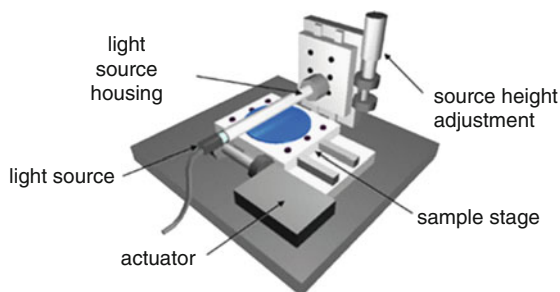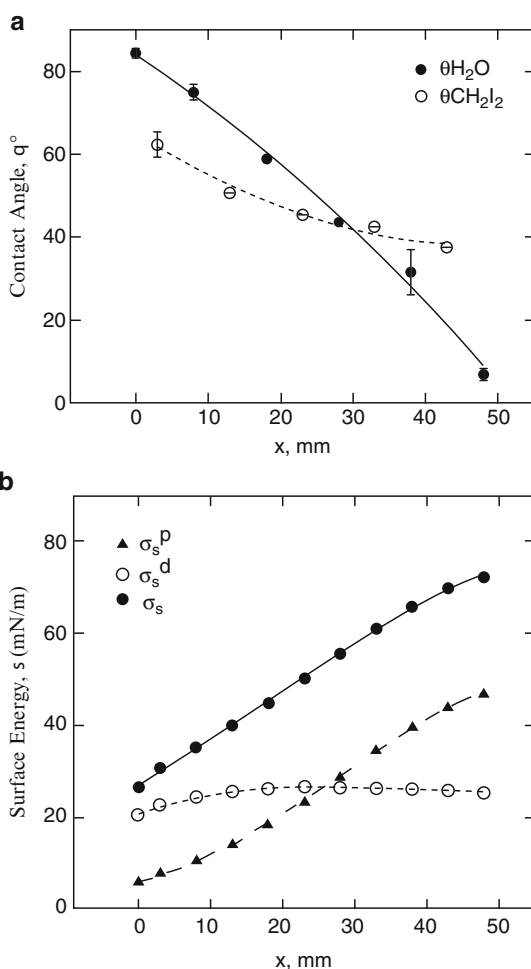

Fig. 5 Illustration of NIST Gradient UV–Ozone device for generating surface energy libraries on substrates functionalized with hydrophobic SAM species. The sample stage accelerates the specimen (*blue*) beneath a slit-source of UV light. (Reproduced with permission from [12])

which accelerates the silanized substrate beneath a 185 nm/254 nm UV wand-source projected through a 2 mm-wide slit aperture cut into the cylindrical lamp housing. The gap between the aperture and the substrate is controlled through a micro-positioner incorporated into the fixed lamp mount. Using these exposure-mediated methods on ODS treated silicon, surface energy gradients can span any interval between $20\,\mathrm{mJ\,m^{-2}}$ and $75\,\mathrm{mJ\,m^{-2}}$, over a tunable length of 1–5 cm. Water contact angles typically span $100°$ to less than $10°$.

The main advantage of this approach is the ability to determine the stage acceleration profile via computer control [19]. As opposed to a graded density filter (which represents a single static exposure "function") any mathematical function can be fed into the stage motion routine. This enables users to tune the length, steepness and shape of the surface energy profile in the library. Indeed, this sort of control can be used to create a well-behaved surface energy gradient profile, which can ease its application in combinatorial screening. For example, this capability can be used to create libraries that have a linear surface energy gradient, rather than the sigmoidal surface energy profile that results from a linear exposure function (as in Fig. 4). In this sense, this method also presents an advantage over techniques for creating surface chemistry gradients via diffusion mediated deposition of SAM species (see for example [20–22]), since these techniques also result in a steep, sigmoidal gradient profile. However, diffusion techniques and controlled immersion methods [23] offer the possibility of creating more chemically diverse mixed SAM gradient libraries via the simultaneous graded deposition of two SAM species [24, 25], or through a backfill sequence [26, 27].

The graded UV–ozonolysis approach to surface energy library fabrication is a powerful tool for examining the role of substrate-polymer interactions on film phenomena such as dewetting and block copolymer self-assembly. Ashley et al. [28], used this approach to determine the surface energy dependence of the stability and dewetted morphology of polystyrene films. In conjunction with an orthogonal temperature gradient, and automated optical microscopy, this team was rapidly able to map the dewetting behavior of five polystyrene specimens that varied in their molecular mass. The library approach enabled the team to observe the surface energy and temperature bounding conditions for film stability, since the dewetted portions of the film could be easily screened. Indeed, the authors discovered that, for the range of molecular mass they considered, these boundary conditions could be collapsed to a common "master curve", which suggests that a universal surface energy and temperature-dependent dewetting behavior is exhibited by this system.

A number of researchers have used surface energy libraries to examine the self-assembly of block copolymer species in thin films. It is well known that substrate-block interactions can govern the orientation, wetting symmetry and even the pattern motif of self-assembled domains in block copolymer films [29]. A simple illustration of these effects in diblock copolymer films is shown schematically in Fig. 6. However, for most block copolymer systems the exact surface energy conditions needed to control these effects are unknown, and for many applications of self-assembly (e.g., nanolithography) such control is essential.
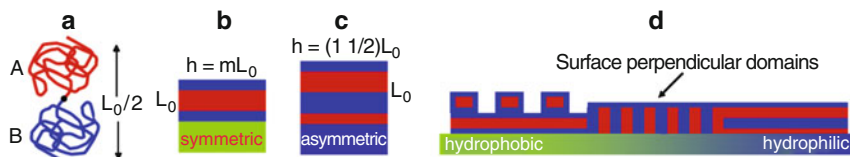
Fig. 6 Illustration of surface energy effects on the self-assembly of thin films of volume symmetric diblock copolymer (**a**). Sections **b** and **c** show surface-parallel block domains orientation that occur when one block preferentially wets the substrate. Symmetric wetting (**b**) occurs when the substrate and free surface favor interactions with one block B, which is more hydrophobic. Asymmetric wetting (**c**) occurs when blocks A and B are favored by the substrate and free surface, respectively. For some systems, a "neutral" substrate surface energy, which favors neither block, results in a self-assembled domains oriented perpendicular to the film plane (**d**). L_0 is the equilibrium length-scale of pattern formation in the diblock system
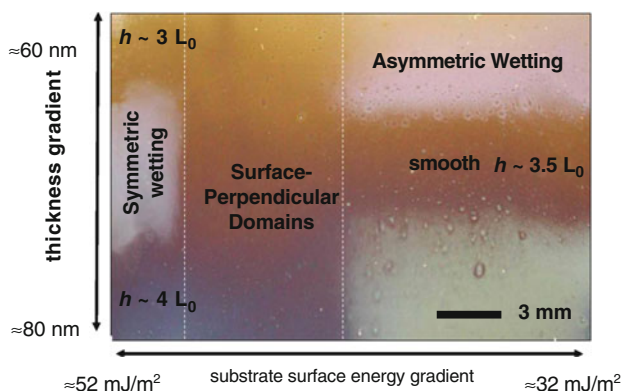

Fig. 7 2D thickness-surface energy gradient library for mapping the effects of these parameters on the self-assembly of PS-b-PMMA block copolymer thin films. See text for a full description. L_0 is the equilibrium self-assembly period and h is the film thickness. *Dashed white lines* delineate the "neutral" surface energy region, which exhibits nanostructures oriented perpendicular to the substrate plane. (Derived from [18] with permission)

To address this problem, Smith and coworkers [18] combined flow coating and surface energy gradients to generate a single specimen that maps the effects of film thickness and surface interactions on the self-assembly of polystyrene-b-poly(methyl methacrylate) (PS-b-PMMA) thin films. This thin film library is shown in Fig. 7. As demonstrated by this photograph of the specimen, the formation of microscopic "island and hole" structures, which make areas of the film hazy, make the library "self-reporting" via simple visual inspection. These surface features only occur when the block domains are oriented parallel to the surface, and they have a specific thickness-dependence, i.e. they disappear when the film thickness is an exact integral (or $n + 1/2$ integral) of the equilibrium period (L_0) of the diblock self-assembly. Examination of the thickness-dependence enabled the authors to determine the wetting symmetry of the surface-parallel self-assembly in these areas (see Fig. 6 caption). Moreover, the range of "neutral" substrate

surface energy is clearly indicated by the vertical band of film in which there is a lack of hazy bands regardless of film thickness. This range of surface energy causes the domains to orient perpendicular to the film surface. In this study, Smith et al. used the method to examine rapidly the molecular mass dependence of the width of the neutral surface region, which is a measurement of the diblock's susceptibility to surface interactions. Moreover, a separate gradient analysis of the thickness-dependence of the "island and hole" structures in diblock films yielded observations of a new labyrinthine form of this surface phenomenon [30].

Other teams used the surface energy gradient approach to examine the more complex thin film self-assembly of three component triblock copolymers. For example, Ludwigs et al. [31] used the technique to screen for surface energy dependent morphological shifts in a PS-b-poly(vinylpyridine)-b-poly(*tert*-butyl methacrylate) triblock films. Remarkably, in a single library experiment, the authors observed that the system exhibited a perforated lamella motif in thin films regardless of the substrate surface energy. This finding has interesting implications for lithographic applications, since it indicates that this laterally structured nanopattern can be formed on almost any smooth substrate material. More recently, Epps and coworkers [32] performed a similar study of a polyisoprene-b-PS-b-poly(ethylene oxide) triblock films. As with the work of Ludwigs et al., this examination showed that, regardless of the surface energy of the substrate, the triblock formed a different morphology in thin films to that in the bulk, in this case three-layered surface-parallel lamella. However, the authors observed that, at long annealing times, the lamellar films unexpectedly dewet the substrate over a specific range of surface energy. Using a high-throughput technique developed to pluck film specimens from the library [33] the team could examine the buried film–substrate interface via automated X-ray surface spectroscopy methods. Using this data, the unexpected phenomenon was determined to be a form of surface energy dependent autophobic dewetting that had not been observed previously. In both of these studies, it is unlikely that these key observations could have been made as readily without the comprehensive scope of the gradient library approach.

The UV–ozone gradient exposure approach can also be used to fabricate more complex libraries. For example, Julthongpiput and coworkers [34, 35] employed the technique to create libraries that exhibit a graded chemical micropattern. As illustrated in Fig. 8, these combinatorial test substrates consist of a pattern of micron-scale lines that exhibit a continuous gradient in surface energy differences against a constant surface energy matrix. On one end of the specimen the lines are strongly hydrophobic while the substrate matrix is hydrophilic SiO_2. The lines become increasingly more hydrophobic towards the other end of the library until they are chemically indistinguishable from the matrix. The library is fabricated through a vapor-mediated soft lithography [34] of an ODS SAM which is then treated to a graded UV–ozonolysis with the device shown in Fig. 5. The library design includes two calibration strips that express the changing and static surface energy of the SAM pattern lines and matrix respectively. Accordingly, the surface energy differences along the patterned region can be determined by contact angle measurements along the calibration strips.
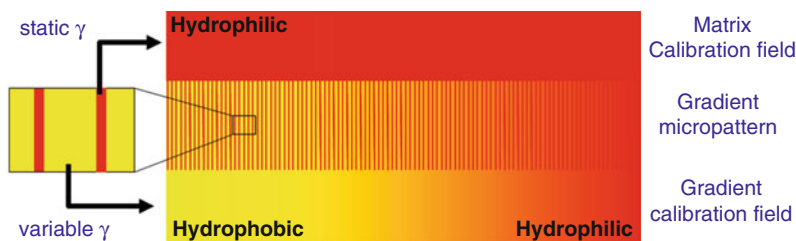
Fig. 8 Illustration of a gradient micropattern library. The central band of the library exhibits a micropattern that gradually changes the chemical differences between the striped domains and the matrix until the surface is chemically homogeneous. The bands on the top and bottom of the library are the calibration fields for static matrix and gradient respectively. γ is surface energy

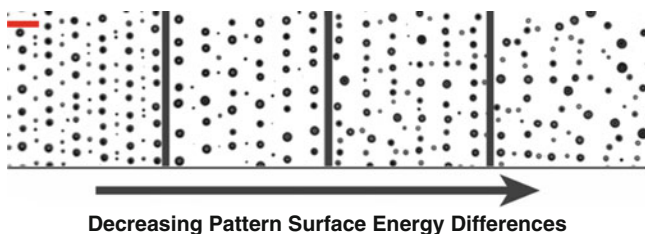**Decreasing Pattern Surface Energy Differences**

Fig. 9 Optical micrographs of dewetted polystyrene droplets collected from points along a chemical gradient library. Scale bar (*red*) is approximately 20 µm. As discussed in the text, this library was used to examine the transition between pattern directed dewetting (*left micrographs*) and isotropic dewetting from a homogeneous surface (*right micrograph*). (Reproduced with permission from [35])

The gradient micropattern library is a unique combinatorial tool for examining the effects of substrate chemical heterogeneity on surface, interface and thin film phenomenon. Julthongpiput et al. [35] recently demonstrated this library as a means to determine how the chemical differences between the stripes can drive the rupture, dewetting and patterning of overlying polystyrene thin films. In this study, automated optical microscopy was employed to collect 1,700 contiguous optical micrographs of polystyrene droplets that formed as a result of dewetting from the gradient micropattern substrate. A small, representative selection of these images is shown in Fig. 9. Automated image analysis was used to examine the droplet arrangements, in particular their registry with the underlying pattern. Through this data, the team could determine the range of surface energy differences that resulted in "pattern directed" dewetting, i.e. film instability, rupture and droplet alignment caused by the underlying stripes. In particular, the library showed that chemical differences between $14\,\mathrm{mJ\,m^{-2}}$ and $20\,\mathrm{mJ\,m^{-2}}$ resulted in the best droplet alignment. Moreover, the library data showed that when the pattern chemical differences dropped below $7\,\mathrm{mJ\,m^{-2}}$, the droplets had an isotropic arrangement indicative of dewetting from a homogeneous surface. This key observation, which precisely illuminates the minimum surface-chemical heterogeneity needed to induce film dewetting, would have been very difficult to make using traditional "single specimen" methods.

Another variation and application of the UV–ozone surface energy library was demonstrated recently by Gallant et al. [36]. In this work, the surface energy library is used as a facile platform for further modification by the "click" chemistry [37] route. In particular, the graded –COOH terminated SAM molecules produced by the UV–ozonolysis are reacted with a bifunctional cross-linker terminated with both amino and alkyne functional groups. The result is a library that has an increasing density of SAM chains with alkyne functionality. Through the click chemistry scheme, the alkyne can react with a huge variety of azido-derivatized biofunctional molecules. Accordingly, this versatile scheme enables continuous gradients in the grafting density of a number of bioactive species. The authors demonstrated this approach by creating a library that continuously varied the concentration of surface-bound RGD peptide molecules. This gradient was used to measure the effect of RGD density on cell adhesion and morphology. Using automated fluorescence microscopy, the team was able to measure cell behavior under a huge number of RGD concentrations, and determine the RGD densities that resulted in the most number of adhered cells, and the most extensive cell spreading. Such data is critical when designing surfaces for cell scaffolds and other biomaterials applications.

The general approach of graded radiation exposure can also be used to examine light driven processes such as photopolymerization [19]. For example, Lin-Gibson and coworkers used this library technique to examine structure-property relationships in photopolymerized dimethacrylate networks [38] and to screen the mechanical and biocompatibility performance of photopolymerized dental resins [39]. In another set of recent studies, Johnson and coworkers combined graded light exposure with temperature and composition gradients to map and model the photopolymerization kinetics of acrylates, thiolenes and a series of co-monomer systems [40–42].

3.4 Gradient Polymer Brush Libraries

While UV–ozone-generated surface energy libraries are simple to implement, they pose limitations in terms of both stability and chemical diversity. Chlorosilane SAMs modified via UV–ozonolysis are susceptible to degradation under light exposure, oxygen, humidity, and high-temperature, and thus must be used within a few hours of fabrication. Moreover, without further modification (as in the example from Gallant and coworkers above), this route generally results in a gradient only between –CH$_3$ and –COOH functionalities. In order to create more robust and diverse surface chemistry gradients, NIST researchers turned to surface-initiated polymerization (SIP) techniques [43, 44] to create libraries of grafted polymer "brushes" that would systematically change in their molecular composition and architecture. In this endeavor, the pioneering work of Genzer and coworkers [45–48] provided examples to build upon, including the creation of gradient libraries of polymer brush length and grafting density.

SIP involves the growth of a polymer chain from an initiator moiety that has been covalently tethered to a surface. The advent of this reaction approach, along

with advances in polymer synthesis routes, have enabled the creation of densely packed polymer "brush" layers that can exhibit a huge variety of macromolecular compositions, architectures and functional groups [49, 50]. Because this covalently bound layer can result in overlapping polymer coils, surface coverage is enhanced. Moreover, some polymer types and architectures offer the possibility of generating surfaces with advanced functionality including, chemical switching, reversible wetting and bioactivity [51, 52]. The potential chemical diversity and technological promise of polymer brushes present opportunities for new library fabrication methods, and for applications of combinatorial techniques. In the following passages, we will discuss how NIST researchers examined both of these opportunities.

SIP-driven polymer brush library fabrication leverages the fact that the polymerization initiation species are permanently bound to the substrate. Since the initiators are tethered, controlled delivery of monomer solution to different areas of the substrate results in a grafted polymer library. In NIST work, initiators bound via chlorosilane SAMs to silicon substrates were suitable for conducting controlled atom transfer radical polymerization (ATRP) [53] and traditional UV free radical polymerization [54, 55]. Suitable monomers are delivered in solution to the surface via microfluidic channels, which enables control over both the monomer solution composition and the time in which the solution is in contact with the initiating groups. After the polymerization is complete, the microchannel is removed from the substrate (or vice versa). This fabrication scheme, termed microchannel confined SIP (μ-SIP), is shown in Fig. 10. In these illustrations, and in the examples discussed below, the microchannels above the substrate are approximately 1 cm wide, 5 cm long, and 300–500 μm high.
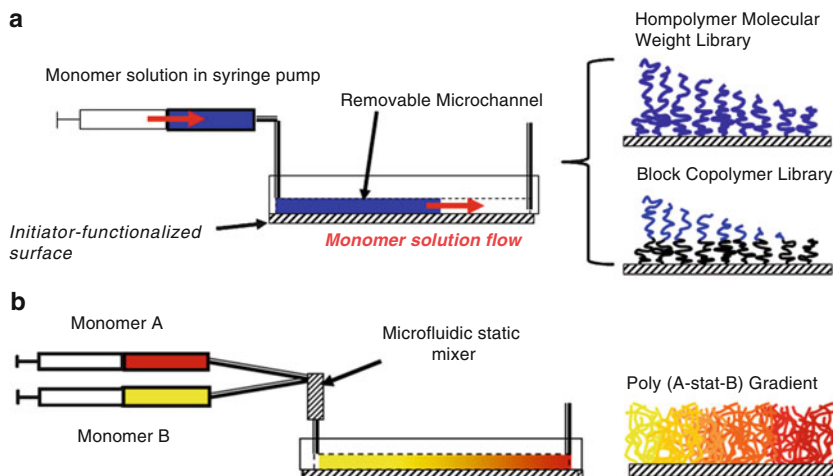

Fig. 10 Illustrations of the microchannel confined surface-initiated polymerization (μ-SIP) route for producing gradient polymer brush libraries: **a** route for making polymer molecular weight and block copolymer libraries; **b** route for making statistical copolymer libraries. *Red arrows* show the flow of monomer solution from a syringe pump used to gradually fill the microchannel. See text for details

As illustrated in Fig. 10a, and described by Xu and coworkers [56], the most basic implementation of μ-SIP involves a gradual filling of the microchannel with monomer solution under polymerization conditions. Depending on the rate of the polymerization and the desired library design, the microchannel is filled using a computer-controlled syringe over 5–40 min. Accordingly, beginning from the microchannel feed, the substrate is exposed to the monomer solution for a decreasing length of time, which is equivalent to a decreasing polymerization period along the library. This process results in a grafted polymer library that gradually decreases in its molecular mass and is evidenced by decreasing film thickness, as demonstrated in Fig. 11a for a poly(*N*,*N*-dimethylaminoethyl methacrylate) (PDMAEMA) homopolymer [56]. If a living polymerization route (such as ATRP) is used to grow constant-length polymers from the substrate, a similar process can be employed with a second monomer solution to fabricate a block copolymer library in which the second block gradually decreases in its length. As shown in Fig. 11b, Xu and coworkers [57, 58] demonstrated this technique by fabricating a series of grafted block copolymer libraries consisting of poly(*n*-butyl methacrylate) (PnBMA) and PDMAEMA. An application of these libraries will be discussed below. A variation of this approach can be used to create a gradient in polymer grafting density. As demonstrated by Mei et al. [59], this involves creating a gradient in surface-bound initiator concentration, which is achieved by gradually introducing initiator-SAM solution along the substrate. Subsequent immersion in the monomer solution results in a library that systematically varies the lateral spacing of tethered polymer chains. A similar technique for creating grafting density libraries has been published by Wu and coworkers [47].

As illustrated in Fig. 10b, a more sophisticated *statistical copolymer* gradient library can also be fabricated through the μ-SIP method [60]. The key to this library is a microfluidic mixer, positioned between two monomer solution feeds and the microchannel. The mixer serves to combine a ramped flow of these solutions in which the relative amount of one solution is decreased and the other increased over time. The result of this ramped input is that the microchannel is filled with a gradient monomer solution composition. Because of the narrow height dimensions of the channel, cross diffusion of the monomers is suppressed, and the solution gradient can persist over a few hours. Accordingly, during a period of polymerization, the monomer concentration profile is transferred to grafted polymer chains on the substrate. The resulting statistical copolymer brush gradient gradually changes from nearly 100% of one monomer to 100% of the other along the library. Composition data from a PnBMA-s-PDMAEMA statistical copolymer library, collected via near edge X-ray absorption fine structure (NEXAFS) spectroscopy, can be seen in Fig. 11c [60]. This achievement is exciting since it represents a way of producing surface chemistry libraries that exhibit both the reliability and enhanced coverage of covalently bound polymer brushes, and the potential for creating chemical gradients that exhibit the extensive chemical and architectural functionality available from advanced polymerization routes. In addition, a key feature of grafted statistical copolymers is that they present stable and intimate blends of disparate chemical species. Since the different monomers are bound within the same chains, the system
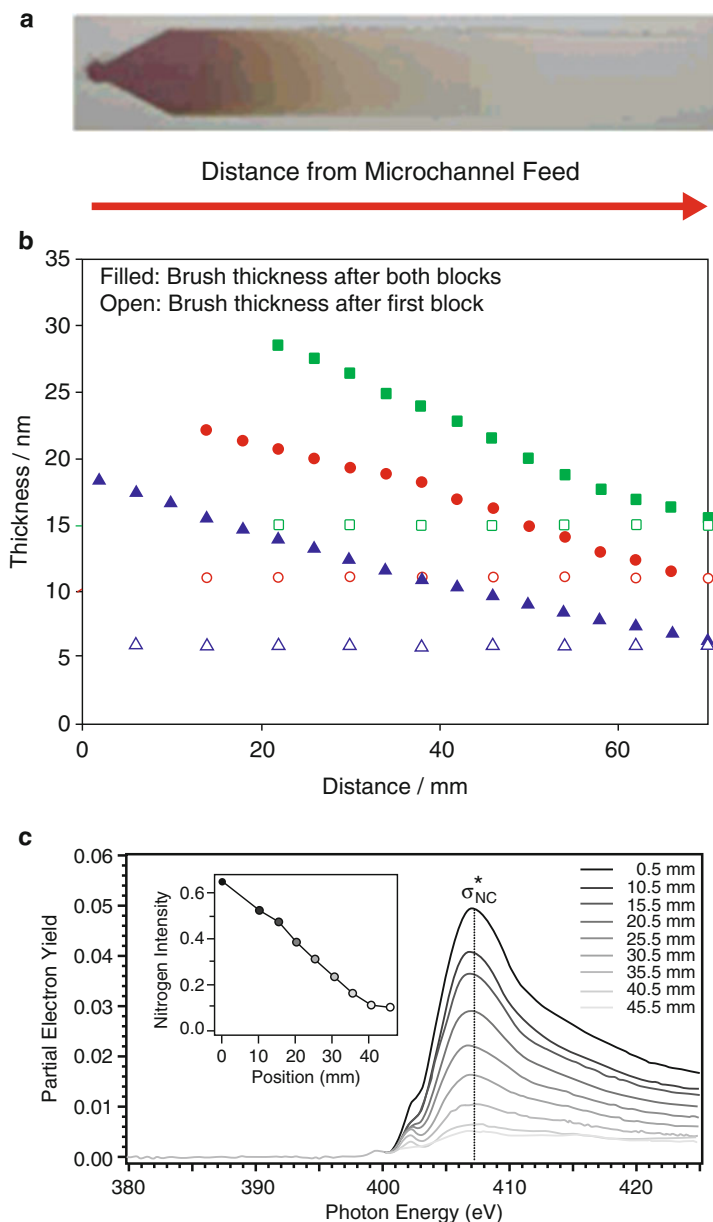
Fig. 11 Data from polymer brush libraries generated by μ-SIP: **a** photograph of molecular weight gradient of grafted PDMAEMA. The entire library is approximately 50 mm long. The brush thickness ranges from approximately 60 to 0 nm from left to right. (Reproduced with permission from [56]); **b** thickness data (ellipsometry) from a PnBMA-b-PDMAEMA block copolymer library after the growth of the PnBMA block (*open symbols*) and the PDMAEMA block (*closed symbols*). (Reproduced with permission from [58]); **c** NEXAFS data along PnBMA-s-PDMAEMA statistical copolymer gradient library. The decreasing nitrogen edge electron intensity signal demonstrates that the DMAEMA segment content of the statistical copolymer systematically decreases along the library. (Reproduced with permission from [60])

will not undergo lateral clustering typical of mixed homopolymer brushes [61], or segment segregation seen in block copolymer brushes [45, 58], both of which can cause spatial chemical heterogeneities on the scale of 10 nm or more. Accordingly, if local surface-chemical homogeneity is needed from a surface chemistry gradient library, statistical copolymer gradients present an advantage.

Grafted homopolymer and copolymer gradient libraries have a tremendous potential for the high-throughput examination of both brush properties and applications involving grafted polymer layers. For example, NIST researchers Xu et al. [57, 58] used such libraries to examine the ability of grafted block copolymers to change their surface segment expression under different environments. This "switching" behavior can be harnessed to create "smart" coatings and surfaces that change their wetting, adhesion, and other properties in response to environmental triggers. The NIST study examined environmental response of the series of PnBMA-b-PDMAEMA block copolymer libraries shown in Fig. 11b. In this system, the PDMAEMA (top) block segments are preferentially solvated by water, while hexane is a preferential solvent for the PnBMA (bottom) blocks. Basically, the gradient experiment involved an assessment of the expression of PnBMA and PDMAEMA segments at the surface of the brush after the library was treated with water and then hexane. Water contact angle measurements along the library were used to estimate the degree of segment surface expression, based on the known equilibrium water contact angles for the pure polymer species (about 90° for PnBMA and approximately 65° for PDMAEMA). The results of these experiments for three libraries, each with a different PnBMA block length, can be seen in Fig. 12. In this plot, the brush is shown to "switch" its surface expression of segments between the block species when the measured contact angle changes due to water or hexane exposure. If the contact angle remains the same, it indicates that the segments were unable to significantly rearrange. The power of the gradient approach to this system is that it clearly outlines how molecular parameters govern the diblock switching behavior. In addition, it provides a view of narrow windows of optimal response that would be quite difficult to observe in single specimens. The library shows that longer PDMAEMA blocks suppress switching, while longer PnBMA blocks enhance the system's ability to rearrange. In addition, the library illuminates the narrow ranges of molecular architecture that result in the maximum changes in segment expression at the surface. For example, for the data shown in red this optimal switching occurs in a window of top block thickness that is only 4 nm wide.

Grafted polymer libraries were also used by NIST researchers to achieve a variety of other measurements. For example, Mei and coworkers [59] leveraged their gradient in polymer grafting density to assess brush biocompatibility. In particular, they used this approach map the effect of poly(2-hydroxyethyl methacrylate) grafting density on the level of fibronectin adsorption and subsequent cell binding. The library enabled the team to determine rapidly the complex correlations between polymer grafting density, fibronectin coverage and cell adhesion, as well as the optimal surface conditions for cell proliferation. In another emerging example, Patton and coworkers [62] demonstrated how μ-SIP can be leveraged to measure rapidly and reliably copolymer reactivity ratios, which link the composition
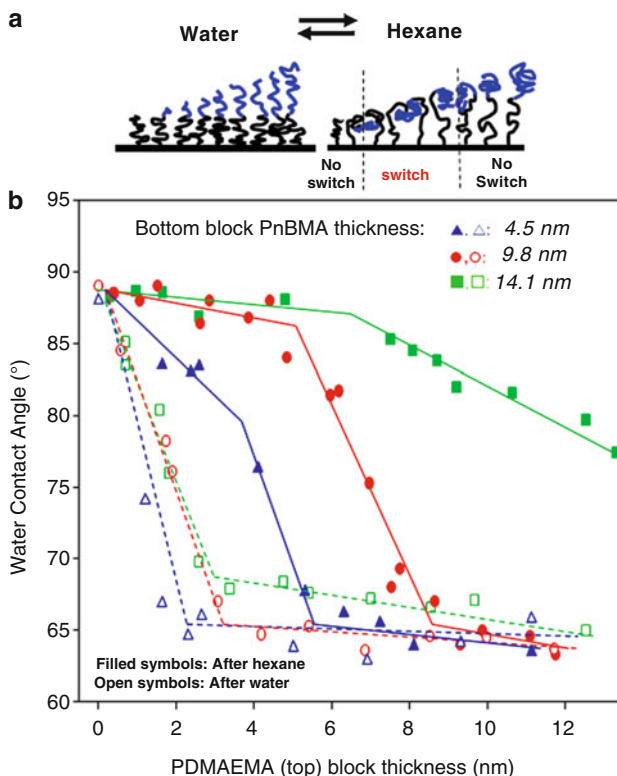
Fig. 12 Surface expression of block segments in block copolymer gradient libraries after treatment to two solvents. See text for details: **a** illustration of surface expression of PnBMA (*black*) and PDMAEMA (*blue*) block copolymer brush segments after water and hexane treatments; **b** water contact angle data from three PnBMA-b-PDMAEMA block copolymer gradient libraries after hexane (*filled symbols*) and water (*open symbols*) treatments. (Derived from [58] with permission)

of mixed monomer polymerization solutions to the composition of copolymer species. Knowledge of reactivity ratios is extremely important for synthesizing polymers with tailored composition and architecture, but they are difficult and time-consuming to measure. The researchers showed that by measuring the composition of the monomer solution in the microchannel (e.g., via a fiber optic Raman spectroscopy probe) and correlating it to the composition of the statistical copolymer brush created on the surface (measured by X-ray photoelectron spectroscopy, XPS), reactivity ratios could be determined. While the published study involved a series of discrete specimens, the extension of the measurement approach to gradient libraries is straightforward. This team is currently establishing protocols to reliably achieve this by combining Raman spectroscopy along a μ-SIP solution gradient and automated XPS data collected from a gradient statistical copolymer library of the type illustrated in Fig. 10b.

3.5 Polymer Blend Composition Gradients

In "hard" materials, such as metals or oxides, the creation of composition gradients is enabled by the excellent atomic-level mixing inherent to co-sputtering, co-evaporation and other co-deposition techniques [63]. The creation of composition spreads in polymers can be more difficult, since the size of macromolecules and the higher viscosity of their solutions can inhibit the proper mixing required for reliable libraries. At NIST, Meredith and coworkers addressed this challenge by combining the flow coating apparatus with an automated syringe-based deposition of blended polymer solutions [3]. A schematic of this approach can be seen in Fig. 13. To start, solutions of the polymers (A and B in the figure) to be blended are prepared using a common solvent. These solutions are fed, and then continuously mixed, in a common vessel (Fig. 13a). The solution feeds are ramped over time such that the mixed solution begin with 100% B solution and ends with 100% A solution. As the composition of the mixed solution changes, a narrow bore syringe is used to collect gradually an aliquot from the vessel, capturing a column of solution that has a gradient in its composition from top to bottom. The narrow bore of the syringe inhibits mixing long enough so that it can be deposited as a strip onto a flat substrate (Fig. 13b). Then the flow coater blade (moving at constant velocity) is used to spread the strip into a thin film with level thickness (Fig. 13c). When the solvent evaporates, the resulting rectangular film library has a gradient in polymer composition that ranges from nearly 100% A to nearly 100% B.

There are some limitations to this technique. First, proper mixing can only be achieved with dilute, low viscosity polymer solutions (perhaps a few percent polymer by mass), so the final films are at most a few hundred nanometers thick. This can be a problem if confinement will create undesired effects in the blend behavior.
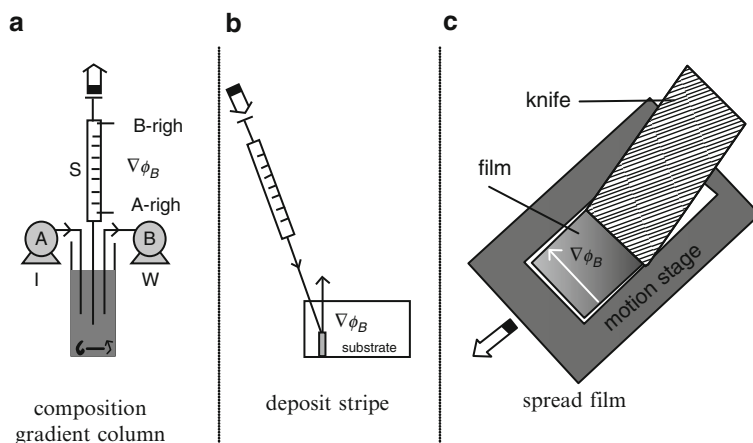

Fig. 13 Illustration of a method for producing polymer blend composition gradient libraries. A and B are the polymer solutions to be blended. φ_B is the relative volume concentration of the B polymer solution. See text for details. (Reproduced with permission from [3])
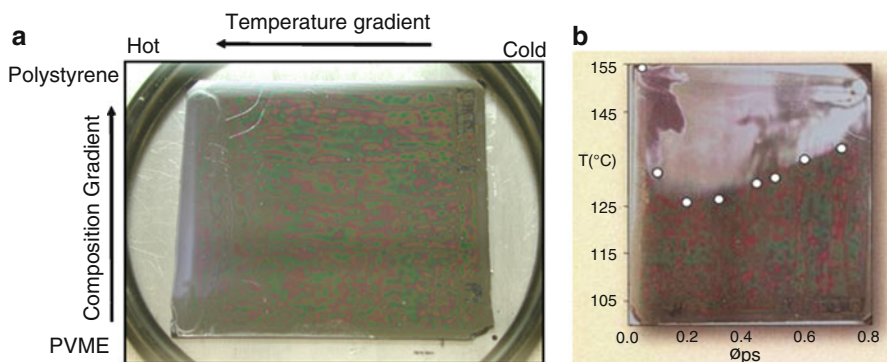
Fig. 14 Creation of a single specimen polymer blend phase diagram from orthogonal polymer composition and temperature gradients. The polymers are polystyrene and poly(vinyl methyl ether) (PVME): **a** composition library placed orthogonal to a temperature gradient; **b** completed gradient library polymer blend phase diagram. White points are data derived from traditional measurement for comparison. See text for details. (**b** reproduced with permission from [3])

In addition, the method only works for polymer pairs that can be blended in a common solvent. Nevertheless, this can be an extremely powerful method for assessing the behavior and performance of polymer blends. For example, Meredith et al. demonstrated the application of this approach to the high-throughput analysis of polymer blend phase behavior. Using polystyrene (PS) and poly(vinylmethylether) (PVME) as a test system, these authors created a single specimen polymer phase diagram by placing a PS-PVME gradient library on a gradient hot stage, as shown in Fig. 14. After annealing over the range of temperatures across the gradient hot stage, the library developed a hazy region, indicative of phase separated polymer domains. Where the polymer remained mixed, the film retained its smooth, as-cast appearance. As shown in Fig. 14b, these hazy and smooth regions delineate the miscibility gap of the PS-PVME blend system. The resulting polymer blend phase diagram library captures the entirety of this system's phase behavior in a single specimen.

Several research teams have employed this method for the high-throughput investigation of more complex polymer blend behavior and performance. For example, Karim and coworkers [64] used the method to screen the shifts in polymer miscibility induced by the addition of clay nanoparticles. In another study, a blend system slated for biomaterials applications was examined by Meredith et al. [65]. In this work, after the gradient phase diagram was created and cooled, cells were seeded across the library. A subsequent stain for cell viability indicated at which locations across the library cells adhered and propagated. Thus, in a single library experiment, the researchers could create a comprehensive map of which blend compositions and morphologies were biocompatible. More recently, Simon and coworkers [66] adapted this method to create microporous 3D gradient polymer blend specimens to investigate tissue scaffold materials. Instead of spreading a graded polymer concentration solution on a flat substrate, the researchers deposited it along a trough filled with salt crystals. Freeze-drying to remove the solvent and dissolution of the

salt resulted in a porous monolith (roughly $1\,cm \times 1\,cm \times 5\,cm$ in dimension) that gradually changed in its composition from one end to the other. A first application of this technique resulted in the identification of the optimal level of iodinated polymer additive needed to create contrast in X-ray imaging measurements (e.g., X-ray tomography) of polymer tissue scaffolds [67]. In this study, the gradient polymer blend composition library was fabricated so that it gradually increased in the level of iodinated species along its length. A single X-ray radiography image of the entire library thus provided a comprehensive map of X-ray adsorption levels as a function of position. Using only two such libraries, they were able to determine the minimal levels of contrast agents required for four X-ray imaging processes. By traditional methods, similar optimization would have required preparation of nearly 100 specimens, followed by many hours of imaging measurements.

4 High-Throughput Materials Testing: Surfaces, Interfaces, and Thin Films

In order to tailor the function and properties of next-generation coatings and adhesives, industry researchers need to understand and control the complex interactions of material interfaces. However, the properties of interfaces are often difficult to measure, since they are complex in their structure and chemistry, and depend on the interplay between multiple variables. Consequently, high-throughput measurements of surfaces, interfaces, and thin films are essential for developing structure-property relationships of coatings and adhesives generated using combinatorial strategies such as those presented in the previous sections. The NIST program has focused on enabling measurements of intrinsic properties of polymer films such as the Young's modulus, an extensive property of a material, as well as extrinsic properties such as adhesion, which depends on a multitude of factors such as modulus, surface energy, and surface roughness. In designing these types of measurement platforms, we discovered that some approaches are amenable to performing highly-parallel measurements on combinatorial libraries; thus, we could provide rapid, multiple-point measurements of a particular response. However, other approaches, due the very nature of the measurement method itself, did not lend themselves to parallel measurements; thus, we incorporated high-throughput, single point measurements of combinatorial libraries into our experimental design. In the following sections, examples of each type of measurement workflow will be highlighted.

4.1 Thin Film Mechanical Properties

Nanotechnology promises to revolutionize a growing set of materials applications ranging from technology sectors such as semiconductor manufacturing, advanced sensors and coatings, to biomedical sectors such as drug delivery and implant

devices. However, the quest to engineer materials on the nanoscale (e.g., in the form of ultrathin films) is met with the daunting task of measuring the physical and mechanical properties of these systems. Given that the material properties of thin films can be drastically different from that of the bulk material, understanding the mechanical properties of nanofilms is especially critical not only for engineering robust fabrication techniques but also for defining application thresholds and operating windows. Maintaining or even improving device performance and reliability while concurrently shortening overall time-to-market is strongly dependent on the ability to rapidly and quantitatively measure the mechanical properties of thin films and coatings. At NIST, we developed several combinatorial and high-throughput measurement platforms that probe the mechanical properties of thin film libraries. In particular, we incorporated combinatorial libraries into an established methodology based on deformation of a thin film on a copper grid to investigate crazing and fracture in thin coatings. We also pioneered a new methodology based on surface wrinkling to rapidly measure the elastic modulus of thin films and coatings. These two measurement platforms underscore many of the challenges and opportunities presented by combinatorial and high-throughput experimental design.

4.1.1 Crazing in Thin Polymer Films

Upon application of strain, polymeric materials can undergo local deformation and yielding processes such as crazing, which leads to the formation of small fibrils and microvoids. These fibrils and microvoids effectively increase the fracture toughness of the material by absorbing energy prior to large-scale cracking in the material [68]. Since many applications of polymers employ thin coatings that are exposed to relatively large stress fields, it is imperative to understand crazing in thin film geometries. The copper grid technique [69] applies a uniaxial strain to a thin polymer film mounted onto a ductile copper grid (see Fig. 15). Due to plastic deformation of the copper, a portion of the applied strain is transferred to and remains in the
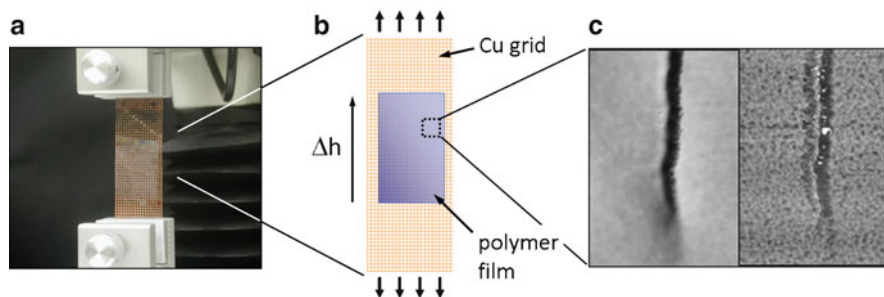

Fig. 15 a Digital image of a copper grid-supported thin polystyrene film clamped in a uniaxial tensile machine. **b** Schematic of a thickness gradient film mounted for conducting a copper grid strain test. **c** AFM images (height and phase) of a craze tip after deformation. (Derived from [70] with permission)

attached polymer film, even after the sample has been removed from the tensile testing instrument. This feature allows for the quantitative assessment of craze microstructure, craze distribution and film integrity. Observation of specimen deformation is achieved by monitoring the material suspended across the grid holes. The fracture processes within each grid space act independently and represent individual experiments. Accordingly, copper grid testing of gradient specimens enables parallel screening of craze behavior over the parameter spaced embodied by a combinatorial library. The ability to analyze rapidly multiple combinations of variables affecting crazing on a single sample eliminates potential variability and measurement error associated with sample preparation, processing and storage, while at the same time increasing measurement efficiency. Shallow thickness gradients allow comparatively uniform films to be presented across each grid square, thus yielding the equivalent of up to 30 or more different films that can be analyzed under identical conditions. The grid holes orthogonal to the thickness gradient can provide statistics of the crazing process, or a second gradient, such as film composition or crystallinity, can be incorporated into the film, thereby greatly increasing the parameter space studied. Using this technique, NIST researchers demonstrated that this method provides quantitative characterization of craze dimensions in glassy polymer films. Interestingly, those results indicated that craze widening and micronecking mechanisms are quantitatively continuous in films with thickness greater than 50 nm [70].

4.1.2 Thin Film Modulus Measurements

While the copper grid test captures the crazing and fracture behavior of thin polymer films, it does not provide any measure of the fundamental mechanical properties of these materials (e.g., the elastic modulus). The most common method for probing the modulus of thin coatings and films is instrument indentation (nanoindentation or AFM), which has proven extremely valuable in the field of hard materials such as metallic and ceramic materials. Despite the success of instrumented indentation, there continues to be a number of technical issues impeding accurate indentation measurements on thin polymer films, the most notable being the so-called substrate effect which necessitates that the indentation depth be less than 10% of the total film thickness. Such shallow indentation depths become increasingly impractical or difficult as the film thickness approaches 100 nm or less. Furthermore, when studying polymer films, it is difficult to detect when the indenter establishes contact with the surface due to the extremely low loads encountered with softer materials (MPa to GPa).

To address this measurement need, NIST researchers developed a novel methodology based on surface wrinkling to assess the mechanical properties of thin polymer films [71, 72]. Surface wrinkling occurs upon compression of a bilayer laminate comprised of a stiff, thin coating supported by a thick, soft substrate. In order to minimize the applied strain energy, the system undergoes a mechanical instability having a defined wavelength (λ), which can be related to the elastic modulus of the stiff coating by

$$\bar{E}_f = 3\bar{E}_s \left(\frac{\lambda}{2\pi h_f}\right)^3 \tag{1}$$

where h is the thickness, $\bar{E} = E/(1 - v^2)$ is the plane-strain modulus (E is the elastic modulus, v is the Poisson's ratio, and the subscripts "f" and "s" denote the film and substrate, respectively). In nearly all studies to date, NIST researchers and others have employed crosslinked poly(dimethyl siloxane) (PDMS, $E \approx 2\,\mathrm{MPa}$) as the substrate. Because the substrate modulus (E_s) and film thickness (h_f) can both be independently measured by traditional techniques, the wavelength of the wrinkling provides a window for measuring of the modulus of the stiff, thin coating (E_f). The wavelength of the wrinkling instability can be measured rapidly by a number of techniques such as laser light diffraction, optical microscopy, or AFM. In the case of light diffraction, the sample can be rastered across the beam to map out the mechanical properties of the entire film, providing rapid analysis of, for example, a gradient library. Conversely, if the sample is uniform, a multitude of images can be acquired to improve the statistics of a single measurement.

Figure 16 demonstrates the range of moduli that can be assessed using the wrinkling metrology, as well as the precision of these measurements. Figure 16a shows moduli data collected along a thickness gradient library of polystyrene [PS], illustrating the ability of this technique to measure the modulus of glassy polymer films ($E \approx 1$–$5\,\mathrm{GPa}$), as well as its use in a combinatorial workflow. In the example shown in Fig. 16a, the average value for the modulus was $3.4\,\mathrm{GPa} \pm 0.1\,\mathrm{GPa}$, in excellent agreement with reported bulk values for PS measured via conventional techniques such as tensile testing [73]. The surface wrinkling metrology can also measure soft materials, such as poly(styrene–isoprene–styrene) [P(S–I–S)] block copolymers, that display moduli in the MPa range (Fig. 16b). Our surface wrinkling metrology can easily discriminate materials having less than a 5% difference in moduli, which demonstrates the unique power of this metrology for thin polymer film research. This point is illustrated in Fig. 16c, where the modulus of ultrathin PS films is shown to decrease sharply when the film thickness decreases below $\approx 40\,\mathrm{nm}$ [74].
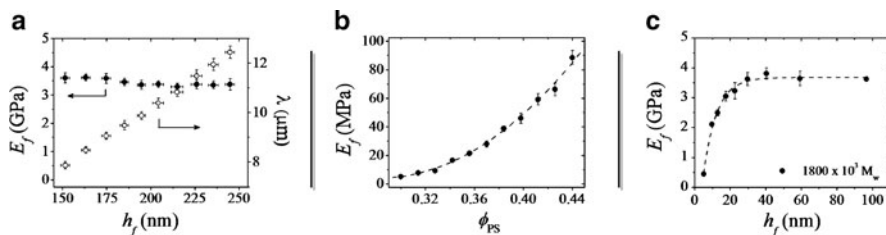

Fig. 16 Representative data from the surface wrinkling metrology, demonstrating the unprecedented range of moduli and the precision that the methodology unlocks: **a** modulus of a thickness gradient library of PS (reproduced with permission from [72]); **b** modulus as a function of composition for P(S–I–S) triblock copolymer blends; **c** modulus as a function of thickness for ultrathin PS films (reproduced with permission from [74]). The *lines* are meant to guide the eye and the *error bars* represent one standard deviation of the data, which is taken as the experimental uncertainty of the measurement

Our metrology has also been applied to particularly challenging systems, such as layer-by-layer assemblies [75–77], polymer brushes [78], and even single carbon nanotubes [79], with remarkable results.

The mechanics of surface wrinkling necessitate that there be a reasonable modulus difference between the film of interest and the soft substrate ($E_s \approx 2\,\text{MPa}$ for PDMS). In order to probe softer materials, the wrinkling metrology can be inverted, such that a sensor film of known modulus is adhered to a soft substrate of unknown modulus. Rearrangement of (1) leads to the following expression for the modulus of the soft, elastic substrate:

$$\bar{E}_s = \frac{\bar{E}_f}{3} \left(\frac{\lambda}{2\pi h_f} \right)^{-3} \tag{2}$$

Here, the unknown to be determined is the modulus of the soft elastic substrate, E_s. The thickness of the sensor film is chosen such that the wavelength of the wrinkling instability can again be measured by small angle light scattering (SALS), thus enabling high-throughput measurement of the substrate modulus. Experimental validation of this approach was conducted using a series of model crosslinked PDMS elastomers [80]. To extend the applicability of the buckling metrology as well as demonstrate its versatility, we investigated its use for determining the modulus of commonly used and commercially relevant poly(HEMA) hydrogels, which are widely used in the fields of contact lenses and biomaterials. Using this inverted geometry, we measured moduli of hydrated elastomers between $0.21\,\text{MPa} < E_s < 2.6\,\text{MPa}$, greatly extending the demonstrated range of moduli that this surface wrinkling metrology can probe. Substrates containing either discrete or continuous gradients in modulus (via gradients in composition or crosslink density, for example) can be easily integrated into this measurement workflow.

4.2 Adhesion Testing

The ability to control and tailor the adhesion at various interfaces plays a critical role in numerous technologies including electronic packaging, coatings and paints, biomedical implants, and pressure sensitive adhesives (PSAs). Previous research has shown that polymer interface formation and failure is dependent upon a range of material, processing and testing parameters. Current (traditional) approaches to the characterization of adhesion have focused on isolating a single adhesion-controlling parameter and correlating the changes in adhesion with corresponding changes in that single parameter. However, these types of approaches are time-consuming, discrete, and do not allow interplay between variables to be investigated. Indeed, one major challenge in this field is the efficient exploration of this large parameter space in order to develop an understanding of the fundamental driving forces for development of adhesive strength at polymer/polymer, polymer/metal, polymer/ceramic, and polymer/biomaterial interfaces. The ability to conduct highly parallel tests and

employ multivariant libraries is an essential step toward rapidly and efficiently identifying structure-property relationships critical for tuning adhesive performance [81, 82]. At NIST, we developed several combinatorial and high-throughput measurement platforms for probing both the fundamental origins of adhesion (e.g., interfacial interactions) as well as practical aspects of adhesion in soft materials (e.g., PSAs) as well as glassy materials and thermosets (e.g., epoxies).

4.2.1 Viscoelastic Materials: Peel Tests

The peel test is one of the most common techniques to assess the adhesive properties of PSAs. As the demand increases for combinatorial tools to test material performance rapidly, applying combinatorial and/or high-throughput approaches to the peel test could yield valuable insight into PSA structure-property relationships as well as open the door to a larger parameter space that can be rapidly and efficiently explored [83, 84]. However, there are considerable technical challenges presented by adapting conventional peel tests to include combinatorial or high-throughput concepts. To illustrate some of these challenges, we consider a simple example: measuring the adhesive strength of a commercial PSA tape adhered to a glass substrate possessing a surface energy gradient ($\Delta\gamma$) along the peel direction (see Fig. 17a). The peel force (F) is averaged across the peel width (b), thus severely limiting the ability to apply an orthogonal gradient in this geometry. However, by combining both a gradient that increases in surface energy ($+\Delta\gamma$) and one that decreases in surface energy ($-\Delta\gamma$) relative to the peel direction, we can probe the effect that the gradient itself has on the peeling process (e.g., crack acceleration or deceleration, stick-slip, etc). As shown in Fig. 17b, the resulting peel data correlate well with the changing surface energy of the substrate. While this example demonstrates
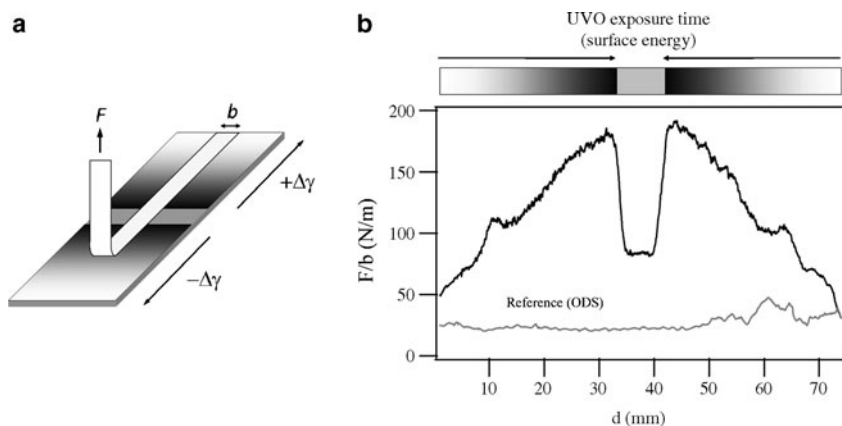

Fig. 17 a Schematic of peeling of an adhesive tape off a surface energy gradient. **b** Peel data (F/b) as a function of distance (d) along the surface energy gradient. As a reference, a traditional (non-gradient) peel test was also performed on the low surface energy substrate

the utility and value of combinatorial approaches as applied to peel tests, it also highlights a drawback: the lack of ample statistical information that is inherent in this type of measurement. For example, a conventional peel test conducted under constant conditions results in a fluctuating force to be averaged. Applying a continuous gradient of sample properties or test conditions in the peel direction implies that each data point (force) corresponds to a single point in parameter space, thus prohibiting the average force to be calculated for a given condition. To address this issue, we developed [83] a simple statistical treatment that allows a relationship between the uncertainty of the force and the domain size to be established. This statistical tool enables one to define the gradient step size (discrete gradients) or gradient steepness (continuous gradients) such that sound statistical information can be obtained and measurement uncertainties can be defined.

4.2.2 Viscoelastic Materials: Probe Tack Tests

Another common method for measuring adhesion strength in soft adhesives is the probe tack test, which involves bringing a rigid probe of known geometry into and out of contact with a flat adhesive layer while recording the applied displacement and resulting force throughout the cycle. In most cases, the probe geometry is either a cylindrical punch or a hemispherical lens. Since one needs to measure both force and displacement, it is difficult to design a parallel screening approach to this measurement platform. Therefore, the focus has been primarily on developing appropriate combinatorial libraries that span the parameter space of interest, while employing single point measurements of probe tack [85, 86]. At NIST we used this approach to examine the effect of temperature on the adhesive properties of model PSAs (see Fig. 18). In this study, a temperature gradient is established across a transparent sapphire window that is coated with a soft adhesive. The transparent substrate allowed us to image simultaneously the contact zone from below the sample, yielding valuable information about the failure mechanisms of the adhesive. Although tack tests were conducted in a serial manner across the temperature
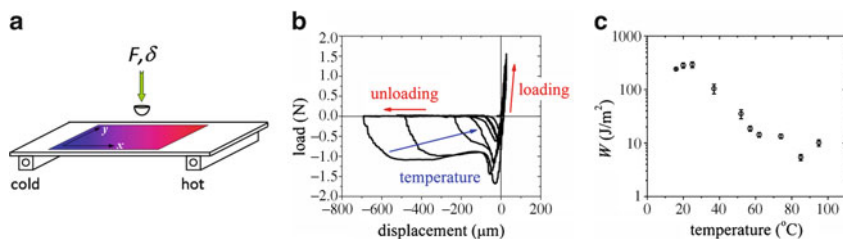

Fig. 18 a Schematic of probe tack measurements of a thin adhesive film along a temperature gradient. **b** Compilation of probe tack data during loading and unloading cycles for different temperatures. **c** Total adhesion energy, calculated from the area under the load-displacement curve shown in **b** divided by maximum contact area, as a function of temperature. The *error bars* represent one standard deviation of the data, which is taken as the experimental uncertainty of the measurement. (Reproduced with permission from [86])

gradient, our design yielded a dramatic decrease in the total measurement time to adequately survey the entire temperature range studied. For example, adhesion measurements at ten different temperatures by conventional tack tests would take 330 min [(30 min equilibration at each temperature +3 min for tack test) ×10 different temperatures], while adhesion measurements using the temperature gradient tack apparatus would only take 60 min [30 min equilibration on temperature gradient + (3 min for tack test ×10 different temperatures)]. Thus, by incorporating a temperature gradient stage, we realized more than a fivefold increase in measurement throughput. We believe this new high-throughput technique has considerable analytical utility because several critical pieces of information can be acquired simultaneously and more efficiently, thus reducing experimental uncertainties and overall measurement time. In this initial study, we conducted only 1D in situ tack measurements, opting to use the second dimension to conduct multiple identical tests for statistical purposes, but more advanced applications are possible. For example, combinatorial aging tests and kinetic studies of epoxy curing can be examined using this instrument. By introducing another parameter such as aging or curing time, 2D libraries (e.g., time and temperature) can be easily generated and screened by probe-type tack measurements.

4.2.3 Glassy Materials: Edge-Delamination Tests

Combinatorial and high-throughput measurements of adhesion in rigid coatings and films demand quite different approaches than soft adhesives such as PSAs [81, 87, 88]. For example, contact methods such as the probe tack test are not suitable for measuring the interfacial strength of a coating adhered to a substrate. To this end, NIST researchers adapted the edge-delamination test [89] to evaluate the adhesion of combinatorial coating libraries to various substrates. In the edge-delamination test, thermal stress arising from cooling of a film/substrate system can propagate an initial crack along the film–substrate interface. Debonding occurs at a critical temperature (T_c) due to the stress concentration near the crack tip. The critical stress (σ_c) necessary to debond the film can be calculated using (3):

$$\sigma_c = \frac{E_f}{1 - v}(\alpha_s - \alpha_f)(T_c - T_{ref}) \tag{3}$$

where E is the elastic modulus, α is the coefficient of thermal expansion, and T_{ref} is a reference temperature where the film is assumed to be in a stress-free state and is usually chose to be the T_g of the film. The subscripts "f" and "s" denote the film and substrate, respectively. If the failure is assumed to take place in the film very near the interface (cohesive failure), the thermal stress at the critical temperature for debonding can be related to the fracture energy (K_{IC}) of the film:

$$K_{IC} = \sigma_0 \sqrt{\frac{h_f}{2}} \tag{4}$$

Thus, K_{IC} can be used as an accurate descriptor of the interfacial strength in a film/substrate system.
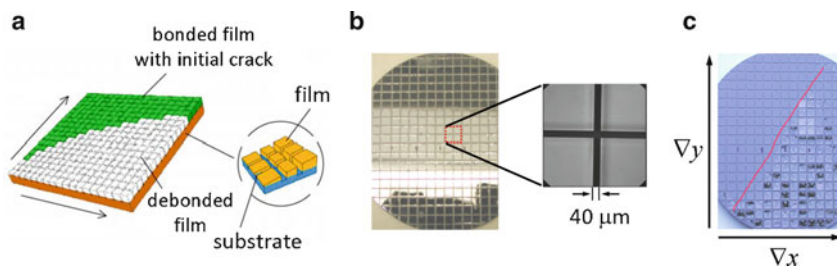
Fig. 19 **a** Schematic of the combinatorial edge-delamination test for probing interfacial adhesion strength. The gradient specimen is diced in order to mechanically isolate individual cells on the array as well as to provide an initial interfacial crack. **b** An optical micrograph of an individual element of the array illustrating the width and sharpness of the diced area. **c** Image of a gradient specimen after failure showing a distinct transition from bonded to debonded areas of the specimen. (Reproduced with permission from [91])

In order to adapt the edge-delamination test to combinatorial workflows, we first developed the framework of the metrology; this included theory, experimental design, stress analysis and simulation of the approach [90]. We could then employ combinatorial libraries that incorporate one or more adhesion-controlling parameters into the edge-delamination experimental design. For example, a film is coated onto a rigid substrate in such a way that the film has a gradient (e.g., thickness, surface energy, composition) in one direction, which is then subdivided into an array of separate edge-delamination samples, as depicted in Fig. 19a. This dicing process serves to generate a pre-crack at the film/substrate interface as well as to isolate mechanically each cell of the array from neighboring cells. A second orthogonal gradient could also be incorporated into the experimental design. The specimen is then slowly cooled and debonding events are observed for those sample cells having stresses greater than a critical value. These stresses depend on the combination of local temperature and film thickness. A map of failures can be constructed as a function of each unique combination of variable one and variable two (Fig. 19c). Subsequently, the interfacial strength between the film coating and the substrate can be deduced from the failure map using (4). We have demonstrated this methodology by probing the adhesion of thin PMMA films to a silicon substrate possessing a gradient in surface energy [91]. In that particular study, an epoxy stress-generating layer was coated directly on the PMMA films; an orthogonal thickness gradient of epoxy was applied to generate a gradient in the stress profile. We have also employed compositional gradients in epoxy films [92], as well as gradients in temperature (both curing temperature and quench temperature).

4.2.4 Elastic Materials: JKR Adhesion Tests

Oftentimes, in order to understand adhesion at the macroscale, we need to understand first the fundamental molecular interactions at interfaces. With this in mind,
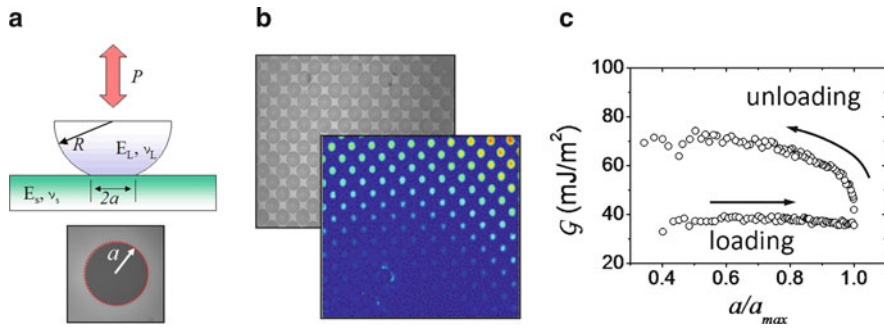
Fig. 20 a Test geometry for a single lens JKR test. The applied load (P), displacement (δ), and contact radius (a) are measured during a complete loading/unloading cycle. **b** Multilens array used for combinatorial adhesion measurements across a sample library, which can be combined with automated image analysis of the contact area across multiple lenses of the array to yield high-throughput measurements of adhesion across combinatorial libraries. **c** Representative data for $\mathcal{G}$ for both loading and unloading segments of PDMS/PDMS contact. (**b** reproduced with permission from [95])

we developed a measurement platform to study quantitatively adhesion using the Johnson, Kendall and Roberts (JKR) model [93]. In this test, a hemispherical lens of one material is brought into and out of contact with a complementary substrate while measuring the applied load, displacement, and contact area between the lens and substrate (see Fig. 20a). The energy release rate ($\mathcal{G}$) represents the amount of energy required to change the contact area a unit amount, or more simply the additional energy required to drive the separation between the two surfaces, and is given by

$$\mathcal{G} = \frac{(P' - P)^2}{8\pi E^* a^3} \tag{5}$$

where $P' = \frac{4E^* a^3}{3R}$ is the Hertzian contact load (no adhesion), P is the applied load, E^* is the system modulus, and a is the contact radius. For a JKR test, the energy required to increase surface area during the loading curve is bounded by the thermodynamic work of adhesion (W), while the unloading segment provides a measure of the adhesion hysteresis ($\mathcal{G}_{\text{HYS}}$), which reflects specific adhesion interactions that develop while the lens is in contact with the substrate.

To facilitate high-throughput measurements on combinatorial libraries, we developed means to introduce a planar array of hemispherical lenses (see Fig. 20b) into contact with a substrate possessing a gradient in material properties or environmental parameters along one or both axes of the array [94, 95]. Conversely, the hemispherical lens array could embody one of the property gradients, such as a gradient in surface energy, or the lens array itself could be comprised of a material gradient, such as composition of the lenses within in the array. If two orthogonal gradients are placed on the array, then each lens contact point yields a measurement of adhesion for a unique combination of parameters. The challenge of using

a multilens array lies in the inability to measure load on each individual lens of the array. In this case, the displacement (δ) of the lens array (not the load (P), as in (5)) is used to calculate $\mathcal{G}$:

$$\mathcal{G} = \frac{E^* (\delta' - \delta)^2}{2\pi a} \tag{6}$$

where $\delta' = \frac{a^2}{R}$ is the Hertzian contact displacement.

We have employed microlens arrays that contain 100–1,600 individual lenses per cm^2, depending on the sample size and steepness of the gradient under study. We have analyzed the effect of surface energy, crosslink density, and contact time using our multilens measurement approach. By integrating a temperature gradient into the instrument design, we can also measure temperature-dependent adhesive properties as a function of multiple variables. For example, in one study we measured the self-adhesion and fracture of polystyrene thin films using orthogonal gradients in temperature and film thickness [94]. This methodology is a powerful tool for investigating the effects of multivariable environments (e.g., surface energy, surface roughness, composition, and processing) on polymer adhesion. We are currently pursuing methods for functionalizing the PDMS lens array with different chemistries in a graded manner, such as layer-by-layer deposition of polyelectrolytes [96] and growth of polymer brushes [78], in ways that express the chemical diversity inherent in many interfaces.

5 High-Throughput Materials Synthesis and Solution Characterization: Microscale Approaches to Polymer Library Fabrication in Fluids

One of the major advantages of the techniques described above is the ability to measure materials properties with significantly reduced quantities of sample. There are few robust synthetic techniques, however, that can produce only the quantities of polymer necessary for these types of measurements. The development of microfluidic devices presented an appealing technology for adaptation to addressing this problem by producing devices that could carry out polymer synthesis in microliter volumes with cheap and flexible reactors directly interfaced with high-throughput measurement methods.

Additional potential advantages associated with performing chemical reactions in the confined space of a microfluidic channel include improved heat transfer, uniform mixing profiles, faster variable changes and improved safety [97]. Combined with a high-throughput characterization strategy this extends the versatility of a microfluidic R&D platform to studying routes for improving control of molar mass, polydispersity, architecture and composition. Previous studies demonstrate that improved control of polymer products was obtained when reactions were carried out in a microfluidic or microreactor environment [98].

The NIST program had a two-pronged approach: (1) use microfluidic devices to manipulate the stoichiometry and other conditions of reactions to produce continuous gradients in polymer chain structures, and (2) exploit the small volumes used in microfluidic channels to carry out measurements on polymer solutions that traditionally require significantly larger volumes or longer times to measure. Examples that will be presented in this section include the preparation of continuous gradients of molecular weight using ATRP, dynamic light scattering (DLS) on a chip and high-throughput interfacial tension (IFT) measurements.

5.1 Controlled Polymer Synthesis in Microchannels

With the development of controlled radical polymerization, synthetic polymer chemists dramatically expanded the range of materials that could be controlled on the molecular scale. Controlled and high-throughput techniques are essential to the systematic survey of this vast parameter space. NIST chose to pursue the use of a technique with flexibility, ease of use, and sample volumes similar to those used in the other library design and measurement methods described above. Channels fabricated in both polymer/glass (Fig. 21a) [99, 100] and metal devices [101] were used depending on the conditions necessary for the reactions. Earlier polymeric devices were replaced by metallic devices when higher temperatures and longer reaction times were required.

The first reactions were carried out at room temperature in devices fabricated from a thiolene resin cured between two glass slides. 2-Hydroxypropyl methacrylate (HPMA) was polymerized by ATRP, and reaction kinetics similar to those obtained in a traditional batch reaction were obtained by adjusting the total flow rate of the fluid through the channel and treating the residence time in the channel as the reaction time (Fig. 21b,c) [102].

The correlation of residence time to reaction time is critical in the ability to treat the volume of the channel as a continuous gradient in molecular mass. ATRP is particularly well-suited to this type of device because the reaction can be initiated at a fixed mixing element at the head of the channel where a catalyst and initiator can be brought together. By replacing a small molecule initiator with a polymer chain capable of being reinitiated, copolymers could be prepared. This was done in the thiolene/glass devices with a poly(n-butyl methacrylate) block [103].

In order to access a wider variety of monomers, higher temperatures were necessary. Using an aluminum channel capped on one wall with a Kapton film, styrene, as well as several acrylates and methacrylates, were polymerized. Furthermore, block copolymers were also prepared from these more widely used polymers, and the devices were integrated with characterization techniques as described below [104]. Similar devices have been used to carry out anionic polymerizations as well [105].
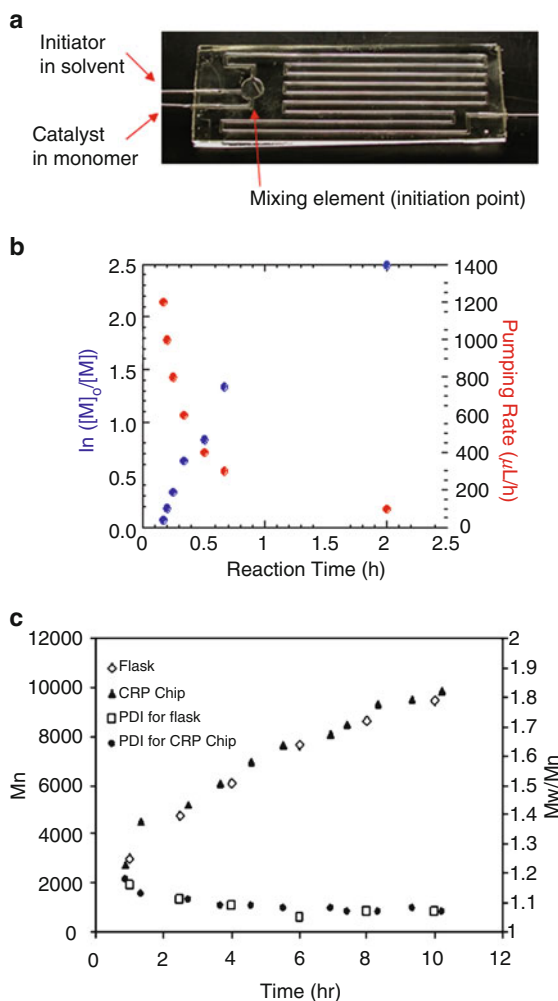
Fig. 21 Representative microfluidic device and resulting data from ATRP on a chip: **a** image of a microfluidic device (dimensions 25 mm × 75 mm) fabricated from UV curable thiolene resin between two glass slides; **b** reaction data for ATRP of HPMA synthesized on a chip showing the correlation of flow rate (or residence time) to reaction time and resulting conversion of monomer (M) to polymer ($\ln([M]_o/[M])$; **c** comparison of number average molecular mass (M_n) and polydispersity for *n*-butyl acrylate prepared in a traditional round bottom flask ('Flask') and on a chip ('CRP Chip'). (Reproduced with permission from [102])

5.2 Characterization of Interfacially-Active Polymers in Microchannels

In order to obtain the advantage of other high-throughput and combinatorial techniques in microfluidic reactors, it is critical that other processing and measurement
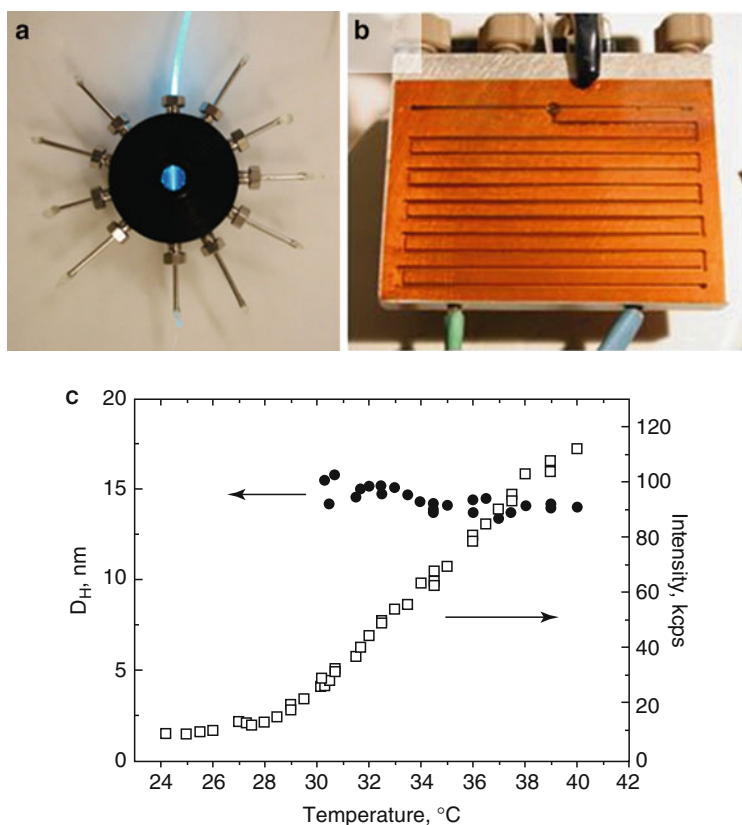
Fig. 22 Images and data representing development and application of DLS on a chip: **a** one iteration in the design of a microfluidic DLS fabricated from aluminum with the surface anodized black to reduce surface reflections; **b** image of a microfluidic chip that integrates polymer synthesis with DLS. The machined channels have been covered by a Kapton sheet fixed with adhesive; **c** data for temperature depended micelle formation of polyethylene oxide–polypropylene oxide–polyethylene oxide triblock copolymer (Pluronic P85) at 2% by volume in water. (Derived from [106] with permission)

tools be integrated into the same platform. The NIST team designed a dynamic light scattering (DLS) instrument on a chip by anodizing the inner walls of an aluminum channel to minimize reflections and plumbing the channel with fiber optics which both deliver an incident beam and detect off-axis scattering (Fig. 22a). After several iterations of design [106], the DLS was applied to detect the formation of micelles in block copolymers as a function of cosolvent fraction (polystyrene/polyisoprene diblock copolymers in hexanes/toluene) or temperature (polyethylene oxide/polypropylene oxide triblock copolymers in water; Fig. 22c).

This new DLS tool was integrated into the microreactors by placing it at the end of a chip that synthesized amphiphilic block copolymers from methyl methacrylate and either lauryl methacrylate or octadecyl methacrylate (Fig. 22b). The reaction

mixture was then diluted with a selective solvent while still on the device, which both terminated the polymerization and induced micelle or other structure formation in the fluid. The structured samples then flowed through the DLS chamber for characterization of size [101]. The total sample volume in the DLS measurement chamber was only 4 μL, and the device enabled comparatively simple alignment procedures while reducing multiple scattering.

The integrated DLS device provides an example of a measurement tool tailored to nano-scale structure determination in fluids, e.g., polymers induced to form specific assemblies in selective solvents. There is, however, a critical need to understand the behavior of polymers and other interfacial modifiers at the interface of immiscible fluids, such as surfactants in oil-water mixtures. Typical measurement methods used to determine the interfacial tension in such mixtures tend to be time-consuming and had been described as a major barrier to systematic surveys of variable space in libraries of interfacial modifiers. Critical information relating to the behavior of such mixtures, for example, in the effective removal of soil from clothing, would be available simply by measuring interfacial tension (IFT) for immiscible solutions with different droplet sizes, a variable not accessible by drop-volume or pendant drop techniques [107].

Through many iterations of design, NIST scientists developed a microfluidic chip that addressed this challenge, by forming droplets of immiscible fluids in a continuous flow stream, while systematically varying conditions that would influence the interfacial tension between the two fluids. The device consisted of three basic elements: drop formation, mixing and drop adsorption, and drop deformation, followed by detection of the drop relaxation using a charge-coupled device (CCD) camera. A variety of mixtures were characterized with these techniques, including the siloxane interface with water, air, ethylene glycol and glycerol, with and without added surfactants (Fig. 23a) [108].

Challenges associated with the proper design of the instrument on a chip included consideration and elimination of confinement effects, depletion issues when the surfactant concentration was determined by the size of the droplet (i.e., the droplet phase contained the surfactant additive) and full automation of fluid controls, image capture and data analysis. Ultimately, however, the device was demonstrated to measure both equilibrium and dynamic IFT in a fraction of the time necessary by conventional techniques and at a length-scale of greater relevance to the applications of interest. The rapid scanning of composition variation was demonstrated by measuring the IFT of water/ethylene glycol mixtures in polydimethylsiloxane oil (Fig. 23b) [109].

6   Conclusions

We provided an overview of combinatorial and high-throughput methods research at NIST, with a focus on tools and application examples that are useful for the examination of polymer surfaces, interfaces and thin films. An examination of this body
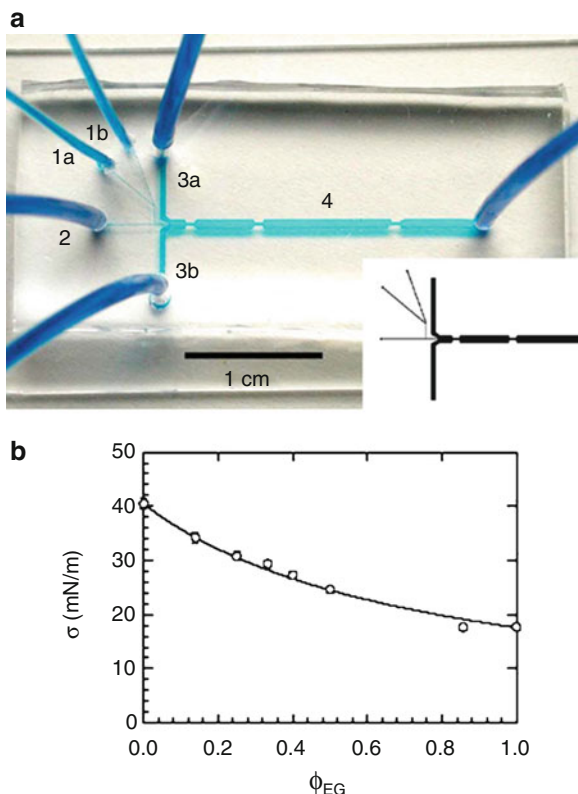
Fig. 23 a Image of a microfluidic chip used for IFT measurements filled with liquid dye to illuminate channels. To perform the measurement, drops are injected (fluid 1a and b) are injected into an immiscible stream (2). Additional immiscible matrix is added (3a and 3b) conveying the drops into channel 4 for analysis and measurement. Constrictions in channel 4 accelerate/stretch the drops. Multiple constrictions enable measurement at different interface age. The channel geometry is shown schematically in the *inset* (from [108]). **b** Interfacial tension (σ) of water/ethylene glycol mixtures (binary drops) in PDMS oil, as a function of composition (ϕ). (Reproduced with permission from [109])

of work illustrates two key points that are worth discussing in conclusion. First, it is clear that gradient and microfluidic methods are powerful tools for polymer research, and this is not only because these techniques can be more rapid (although, this is one great advantage). A more important aspect, especially for emerging polymer technologies, is that these techniques allow scientists and engineers to approach complex materials systems in ways that are impossible via traditional techniques. As illustrated in many of the examples discussed above, a library approach enables the researcher to view, often in a single specimen, an entire space of structures, behaviors and their response to influencing variables. These "big picture" snapshots can be invaluable in initiating and building a comprehensive understanding

of complex systems and the factors that govern them. In addition, gradient libraries enable the researcher to "zoom in" on specific parameter subsets to achieve more detailed analyses; this unique capability facilitates a more rigorous examination of the structure-processing-performance interrelationships that are key to materials science and engineering.

The second point is that, quite often, library approaches can provide significant advantages even if they are not integrated into extensive workflow infrastructures that are often associated with combinatorial methods. Indeed, gradient libraries and microfluidic library synthesis can provide extensive benefits both in their own right and in combination with modest automated analysis. The "self-reporting" aspect of gradient libraries is one example of this, as is the ability of continuous microreactors to create systematically changing families of polymer specimens while using miniscule amounts of reactant. Moreover, by pairing libraries with high-throughput measurement platforms researchers have access to an unparalleled, and rapid, ability to determine the factors that govern and optimize materials performance. Examples of this can be seen in our discussion of high-throughput adhesion and mechanical properties tests, which are fueled by appropriately fabricated library specimens. In addition, as we discussed, microfluidic technologies are quite powerful in this respect, since they can integrate library fabrication and high-throughput analysis of fluid specimens on a single device.

In each of these "take home" messages, the benefits of combinatorial and high-throughput approaches are gained by thinking beyond the single sample paradigm, by being aware of the opportunities afforded by developing and exploiting these tools, and by applying them with the wisdom that has always characterized successful polymers science.

References

1. Webster DC (2005) Radical change in research and development: the shift from conventional methods to high-throughput methods. JCT Coat Technol 2:24–29
2. Hanak JJ (1970) Multiple-sample-concept in materials research – synthesis, compositional analysis and testing of entire multicomponent systems. J Mater Sci 5:964
3. Meredith JC, Karim A, Amis EJ (2000) High-throughput measurement of polymer blend phase behavior. Macromolecules 33:5760–5762
4. Meredith JC, Karim A, Amis EJ (2002) Combinatorial methods for investigations in polymer materials science. MRS Bull 27:330–335
5. Stafford CM, Roskov KE, Epps TH, Fasolka MJ (2006) Generating thickness gradients of thin polymer films via flow coating. Rev Sci Instrum 77:023908
6. Zhang X, Berry BC, Yager KG, Kim S, Jones RL, Satija S, Pickel DL, Douglas JF, Karim A (2008) Surface morphology diagram for cylinder-forming block copolymer thin films. ACS Nano 2:2331–2341
7. de Gans BJ, Wijnans S, Woutes D, Schubert US (2005) Sector spin coating for fast preparation of polymer libraries. J Comb Chem 7:952–957
8. Cull TR, Goulding MJ, Bradley M (2007) Liquid crystal libraries-ink-jet formulation and high-throughput analysis. Adv Mater 19:2355–2359
9. Meier MAR, Schubert US (2005) Integration of MALDI-TOFMS as high-throughput screening tool into the workflow of combinatorial polymer research. Rev Sci Instrum 76:062211

10. Yoshioka Y, Calvert PD, Jabbour GE (2005) Simple modification of sheet resistivity of conducting polymeric anodes via combinatorial ink-jet printing techniques. Macromol Rapid Commun 26:238–246
11. de Gans BJ, Kazancioglu E, Meyer W, Schubert US (2004) Ink-jet printing polymers and polymer libraries using micropipettes. Macromol Rapid Commun 25:292–296
12. Koner L, Kofler W (1949) A heating bed for rapid determination of the melting point. Mikrochem Mikrohim Acta 34:374–381
13. Sehgal A, Karim A, Stafford CF, Fasolka MJ (2003) Techniques for combinatorial and high-throughput microscopy: part 1: gradient specimen fabrication for polymer thin films research. Micros Today 11:26–29
14. Beers KL, Douglas JF, Amis EJ, Karim A (2003) Combinatorial measurements of crystallization growth rate and morphology in thin films of isotactic polystyrene. Langmuir 19:3935–3940
15. Lucas LA, DeLongchamp DM, Vogel BM, Lin EK, Fasolka MJ, Fischer DA, McCulloch I, Heeney M, Jabbour GE (2007) Combinatorial screening of the effect of temperature on the microstructure and mobility of a high performance polythiophene semiconductor. Appl Phys Lett 90:012112
16. Eidelman N, Raghavan D, Forster AM, Amis EJ, Karim A (2004) Combinatorial approach to characterizing epoxy curing. Macromol Rapid Commun 25:259–263
17. Roberson SV, Faheya AJ, Sehgal A, Karim A (2002) Multifunctional ToF-SIMS: combinatorial mapping of gradient energy substrates. Appl Surf Sci 200:150–164
18. Smith AP, Sehgal A, Douglas JF, Karim A, Amis EJ (2003) Combinatorial mapping of surface energy effects on diblock copolymer thin film ordering. Macromol Rapid Commun 24:131–135
19. Berry BC, Stafford CM, Pandya M, Lucas LA, Karim A, Fasolka MJ (2007) Versatile platform for creating gradient combinatorial libraries via modulated light exposure. Rev Sci Instrum 78:072202
20. Elwing H, Welin S, Askendal A, Nilsson U, LundstrÖm I (1987) A wettability gradient method for studies of macromolecular interactions at the liquid/solid interface. J Colloid Interface Sci 119:203–210
21. Chaudhury MK, Whitesides GM (1992) How to make water run uphill. Science 256:1539–1541
22. Genzer J (2005) Templating surfaces with gradient assemblies. J Adhes 81:417–435
23. Zhao H, Beysens D (1995) From droplet growth to film growth on a heterogeneous surface – condensation associated with a wettability gradient. Langmuir 11:627–634
24. Liedberg B, Tengvall P (1995) Molecular gradients of omega-substituted alkanethiols on gold – preparation and characterization. Langmuir 11:3821–3827
25. Liedberg B, Wirde M, Tao YT, Tengvall P, Gelius U (1997) Molecular gradients of omega-substituted alkanethiols on gold studied by X-ray photoelectron spectroscopy. Langmuir 13:5329–5334
26. Morgenthaler S, Lee S, Zurcher S, Spencer ND (2003) A simple, reproducible approach to the preparation of surface-chemical gradients. Langmuir 19:10459–10462
27. Morgenthaler SM, Lee S, Spencer ND (2006) Submicrometer structure of surface-chemical gradients prepared by a two-step immersion method. Langmuir 22:2706–2711
28. Ashley KM, Raghavan D, Douglas JF, Karim A (2005) Wetting-dewetting transition line in thin polymer films. Langmuir 21:9518–9523
29. Fasolka MJ, Mayes AM (2001) Block copolymer thin films: physics and applications. Annu Rev Mater Res 31:323–355
30. Smith AP, Douglas JF, Meredith JC, Amis EJ, Karim A (2001) Combinatorial study of surface pattern formation in thin block copolymer films. Phys Rev Lett 87:015503
31. Ludwigs S, Schmidt K, Stafford CM, Amis EJ, Fasolka MJ, Karim A, Magerle R, Krausch G (2005) Combinatorial mapping of the phase behavior of ABC triblock terpolymers in thin films: Experiments. Macromolecules 38:1850–1858

32. Epps TH, Delongchamp DM, Fasolka MJ, Fischer DA, Jablonski EL (2007) Substrate surface energy dependent morphology and dewetting in an ABC triblock copolymer film. Langmuir 23:3355–3362
33. Roskov KE, Epps TH, Berry BC, Hudson SD, Tureau MS, Fasolka MJ (2008) Preparation of combinatorial arrays of polymer thin films for transmission electron microscopy analysis. J Comb Chem 10:966–973
34. Julthongpiput D, Fasolka MJ, Zhang WH, Nguyen T, Amis EJ (2005) Gradient chemical micropatterns: a reference substrate for surface nanometrology. Nano Lett 5:1535–1540
35. Julthongpiput D, Zhang W, Douglas JF, Karim A, Fasolka MJ (2007) Pattern-directed to isotropic dewetting transition in polymer films on micropatterned surfaces with differential surface energy contrast. Soft Matter 3:613–618
36. Gallant ND, Lavery KA, Amis EJ, Becker ML (2007) Universal chemistry for "Click" chemistry biofunctionalization. Adv Mater 19:072207
37. Kolb HC, Finn MG, Sharpless BK (2001) Click chemistry: diverse chemical function from a few good reactions. Angew Chem Int Ed 40:2004–2021
38. Lin-Gibson S, Landis FA, Drzal PL (2006) Combinatorial investigation of the structure-properties characterization of photopolymerized dimethacrylate networks. Biomaterials 27:1711–1717
39. Lin NJ, Drzal PL, Lin-Gibson S (2007) Two-dimensional gradient platforms for rapid assessment of dental polymers: a chemical, mechanical and biological evaluation. Dent Mater 23:1211–1220
40. Johnson PM, Stansbury JW, Bowman CN (2007) Photopolyrner kinetics using light intensity gradients in high-throughput conversion analysis. Polymer 48:6319–6324
41. Johnson PM, Stansbury JW, Bowman CN (2008) High-throughput kinetic analysis of acrylate and thiol-ene photopolymerization using temperature and temperature and exposure time gradients. J Polym Sci Part A Polym Chem 46:1502–1509
42. Johnson PM, Stansbury JW, Bowman CN (2008) Kinetic modeling of a comonomer photopolymerization system using high-throughput conversion data. Macromolecules 41:230–237
43. Matyjaszewski K, Miller PJ, Shukla N, Immaraporn B, Gelman A, Luokala BB, Siclovan TM, Kickelbick G, Vallant T, Hoffmann H, Pakula T (1999) Polymers at interfaces: using atom transfer radical polymerization in the controlled growth of homopolymers and block copolymers from silicon surfaces in the absence of untethered sacrificial initiator Macromolecules 32:8716–8724
44. Husseman M, Malmstrom EE, McNamara M, Mate M, Mecerreyes D, Benoit DG, Hedrick JL, Mansky P, Huang E, Russell TP, Hawker CJ (1999) Controlled synthesis of polymer brushes by "Living" free radical polymerization techniques. Macromolecules 32:1424–1431
45. Bhat RR, Tomlinson MR, Genzer J (2005) Orthogonal surface-grafted polymer gradients: a versatile combinatorial platform. J Polym Sci Part B Polym Phys 43:3384–3394
46. Genzer J, Bhat RR (2008) Surface-bound soft matter gradients. Langmuir 24(6):2294–2317
47. Wu T, Efimenko K, Genzer J (2002) Combinatorial study of the mushroom-to-brush crossover in surface anchored polyacrylamide. J Am Chem Soc 124:9394–9395
48. Wu T, Efimenko K, Vlcek P, Subr V, Genzer J (2003) Formation and properties of anchored polymers with a gradual variation of grafting densities on flat substrates. Macromolecules 36:2448–2453
49. Zhao B, Brittain WJ (2000) Polymer brushes: surface-immobilized macromolecules. Prog Polym Sci 25:677–710
50. Patten TE, Matyjaszewski K (1998) Atom transfer radical polymerization and the synthesis of polymeric materials. Adv Mater 10:901
51. Mendes PM (2008) Stimuli-responsive surfaces for bio-applications. Chem Soc Rev 37:2512–2529
52. La WH, Wang RM, He YF, Zhang HF (2008) Preparation and application of smart coatings. Prog Polym Chem 20:351–361
53. Patten TE, Xia JH, Abernathy T, Matyjaszewski K (1996) Polymers with very low polydispersities from atom transfer radical polymerization. Science 272:866–868

54. Prucker O, Ruhe J (1998) Synthesis of poly(styrene) monolayers attached to high surface area silica gels through self-assembled monolayers of azo initiators. Macromolecules 31:592–601
55. Prucker O, Ruhe J (1998) Polymer layers through self-assembled monolayers of initiators. Langmuir 14:6893–6898
56. Xu C, Wu T, Drain CM, Batteas JD, Beers KL (2005) Microchannel confined surface-initiated polymerization. Macromolecules 38:6
57. Xu C, Wu T, Batteas JD, Drain CM, Beers KL, Fasolka MJ (2006) Surface-grafted block copolymer gradients: effect of block length on solvent response. Appl Surf Sci 252:2529–2534
58. Xu C, Wu T, Drain CM, Batteas JD, Fasolka MJ, Beers KL (2006) Effect of block length on solvent response of block copolymer brushes: combinatorial study with block copolymer brush gradients. Macromolecules 39:3359–3364
59. Mei Y, Wu T, Xu C, Langenbach KJ, Elliott JT, Vogt BD, Beers KL, Amis EJ, Washburn NR (2005) Tuning cell adhesion on gradient poly(2-hydroxyethyl methacrylate)-grafted surfaces. Langmuir 21:12309–12314
60. Xu C, Barnes SE, Wu T, Fischer DA, DeLongchamp DM, Batteas JD, Beers KL (2006) Solution and surface gradients via microfluidic confinement: fabrication of a statistical copolymer brush composition gradient. Adv Mater 18:1427
61. Zhao B (2004) A combinatorial approach to study solvent-induced self-assembly of mixed poly(methyl methacrylate)/polystyrene brushes on planar silica substrates: effect of relative grafting density. Langmuir 20:11748–11755
62. Patton DL, Page KA, Xu C, Genson KL, Fasolka MJ, Beers KL (2007) Measurement of reactivity ratios in surface-initiated radical copolymerization. Macromolecules 40:6017–6020
63. Zhao JC (2006) Combinatorial approaches as effective tools in the study of phase diagrams and composition-structure-property relationships. Prog Mater Sci 51:557–631
64. Karim A, Yurekli K, Meredith C, Amis EJ, Krishnamoorti R (2002) Combinatorial methods for polymer materials science: phase behavior of nanocomposite blend films. Polym Eng Sci 42:1836–1840
65. Meredith JC, Sormana JL, Keselowsky BG, Garcia AJ, Tona A, Karim A, Amis EJ (2003) Combinatorial characterization of cell interactions with polymer surfaces. J Biomed Mater Res Part A 66A:483–490
66. Simon CG Jr, Stephens JS, Dorsey SM, Becker ML (2007) Fabrication of combinatorial polymer scaffold libraries. Rev Sci Instrum 78:0722071
67. Yang Y, Dorsey SM, Becker ML, Lin-Gibson S, Schumacher GE, Flaim GM, Kohn J, Simon CG Jr (2008) X-ray imaging optimization of 3D tissue engineering scaffolds via combinatorial fabrication methods. Biomaterials 29:1901–1911
68. Kramer EJ (1983) Microscopic and molecular fundamentals of crazing. Adv Polym Sci 52/53:1–56
69. Lauterwasser BD, Kramer EJ (1979) Microscopic mechanisms and mechanics of craze growth and fracture. Philos Mag A Phys Condens Matter Struct Defects Mech Prop 39:469–495
70. Crosby AJ, Fasolka MJ, Beers KL (2004) High-throughput craze studies in gradient thin films using ductile copper grids. Macromolecules 37:9968–9974
71. Stafford CM, Guo S, Harrison C, Chiang MYM (2005) Combinatorial and high-throughput measurements of the modulus of thin polymer films. Rev Sci Instrum 76:062207
72. Stafford CM, Harrison C, Beers KL, Karim A, Amis EJ, Vanlandingham MR, Kim HC, Volksen W, Miller RD, Simonyi EE (2004) A buckling-based metrology for measuring the elastic moduli of polymeric thin films. Nat Mater 3:545–550
73. Brandrup J, Immergut EH, Grulke EA (1999) Polymer handbook, 4th edn. Wiley, New York
74. Stafford CM, Vogt BD, Harrison C, Julthongpiput D, Huang R (2006) Elastic Moduli of ultrathin amorphous polymer films. Macromolecules 39:5095–5099
75. Nolte AJ, Cohen RE, Rubner MF (2006) A two-plate buckling technique for thin film modulus measurements: applications to polyelectrolyte multilayers. Macromolecules 39:4841–4847

76. Nolte AJ, Rubner MF, Cohen RE (2005) Determining the Young's modulus of polyelectrolyte multilayer films via stress-induced mechanical buckling instabilities. Macromolecules 38:5367–5370
77. Nolte AJ, Treat ND, Cohen RE, Rubner MF (2008) Effect of relative humidity on the Young's modulus of polyelectrolyte multilayer films and related nonionic polymers. Macromolecules 41:5793–5798
78. Huang H, Chung JY, Nolte AJ, Stafford CM (2007) Characterizing polymer brushes via surface wrinkling. Chem Mater 19:6555–6560
79. Khang DY, Xiao JL, Kocabas C, MacLaren S, Banks T, Jiang HQ, Huang YYG, Rogers JA (2008) Molecular scale buckling mechanics on individual aligned single-wall carbon nanotubes on elastomeric substrates. Nano Lett 8:124–130
80. Wilder EA, Guo S, Lin-Gibson S, Fasolka MJ, Stafford CM (2006) Measuring the modulus of soft polymer networks via a buckling-based metrology. Macromolecules 39:4138–4143
81. Chisholm B, Potyrailo R, Cawse J, Shaffer R, Brennan M, Molaison C, Whisenhunt D, Flanagan B, Olson D, Akhave J, Saunders D, Mehrabi A, Licon M (2002) The development of combinatorial chemistry methods for coating development – I. Overview of the experimental factory. Prog Org Coat 45:313–321
82. Crosby AJ (2003) Combinatorial characterization of polymer adhesion. J Mater Sci 38:4439–4449
83. Chiche A, Zhang WH, Stafford CM, Karim A (2005) A new design for high-throughput peel tests: statistical analysis and example. Meas Sci Technol 16:183–190
84. McGuiggan PM, Chiche A, Filliben JJ, Phelan FR, Fasolka MJ, Yarusso DJ (2006) High-throughput peel measurement of a pressure-sensitive adhesive. Adhes Mag 13:32–39
85. Grunlan JC, Holguin DL, Chuang HK, Perez I, Chavira A, Quilatan R, Akhave J, Mehrabi AR (2004) Combinatorial development of pressure-sensitive adhesives. Macromol Rapid Commun 25(1):286–291
86. Moon SH, Chiche A, Forster AM, Zhang WH, Stafford CM (2005) Evaluation of temperature-dependent adhesive performance via combinatorial probe tack measurements. Rev Sci Instrum 76:062210
87. Chisholm B, Potyrailo R, Shaffer R, Cawse J, Brennan M, Molaison C (2003) Combinatorial chemistry methods for coating development III. Development of a high-throughput screening method for abrasion resistance: correlation with conventional methods and the effects of abrasion mechanism. Prog Org Coat 47:112–119
88. Chisholm BJ, Potyrailo RA, Cawse JN, Shaffer RE, Brennan M, Molaison CA (2003) Combinatorial chemistry methods for coating development V. The importance of understanding process capability. Prog Org Coat 47:120–127
89. Shaffer EO, McGarry FJ, Hoang L (1996) Designing reliable polymer coatings. Polym Eng Sci 36:2375–2381
90. Chiang MYM, Wu WL, He JM, Amis EJ (2003) Combinatorial approach to the edge-delamination test for thin film reliability – concept and simulation. Thin Solid Films 437:197–203
91. Chiang MYM, Song R, Crosby AJ, Karim A, Chiang CK, Amis EJ (2005) Combinatorial approach to the edge-delamination test for thin film reliability – adaptability and variability. Thin Solid Films 476:379–385
92. Stafford CM, Kim JH, Kawaguchi D, Royston G, Chiang MYM (2006) Probing the interfacial adhesion strength in compositional libraries of epoxy films. Mater Res Soc Symp Proc 894:129–137
93. Johnson KL, Kendall K, Roberts AD (1971) Surface energy and contact of elastic solids. Proc R Soc Lond A Math Phys Sci 324:301
94. Crosby AJ, Karim A, Amis EJ (2003) Combinatorial investigations of interfacial failure. J Polym Sci Part B Polym Phys 41:883–891
95. Forster AM, Zhang WH, Crosby AJ, Stafford CM (2005) A multilens measurement platform for high-throughput adhesion measurements. Meas Sci Technol 16:81–89
96. Nolte AJ, Chung JY, Walker ML, Stafford CM (2009) In-situ adhesion measurements utilizing layer-by-layer functionalized surfaces. ACS Appl Mater Interfaces 1:373–380

97. Hessel V, Serra C, Loewe GH, Hadziioannou G (2005) Polymerizations in micro-structured reactors: overview. Chem Ing Tech 77:1693
98. Iwasaki T, Yoshida J (2005) Free radical polymerization in microreactors. Significant improvement in molecular weight distribution control. Macromolecules 38:1159–1163
99. Harrison C, Cabral J, Stafford CM, Karim A, Amis EJ (2004) A rapid prototyping technique for the fabrication of solvent-resistant structures. J Micromech Microeng 14:153–158
100. Cygan ZT, Cabral JT, Beers KL, Amis EJ (2005) Microfluidic platform for the generation of organic-phase microreactors. Langmuir 21:3629–3634
101. Chastek TQ, Iida K, Amis EJ, Fasolka MJ, Beers KL (2008) A microfluidic platform for integrated synthesis and dynamic light scattering measurement of block copolymer micelles. Lab Chip 8:950
102. Wu T, Mei Y, Cabral JT, Xu C, Beers KL (2004) A new synthetic method for controlled polymerization using a microfluidic system. J Am Chem Soc 126:7881
103. Wu T, Mei Y, Xu C, Byrd HCM, Beers KL (2005) Block copolymer PEO-b-PHPMA synthesis using controlled radical polymerization on a chip. Macromol Rapid Commun 26:1037
104. Chastek TQ, Iida K, Amis EJ, Fasolka MJ, Beers KL (2008) A microfluidic platform for integrated synthesis and dynamic light scattering measurement of block copolymer micelles. Lab Chip 8:950–957
105. Iida K, Chastek TQ, Beers KL, Cavicchi KA, Chun J, Fasolka MJ (2009) Living anionic polymerization using a microfluidic reactor. Lab Chip 9:339–345
106. Chastek TQ, Beers KL, Amis EJ (2007) Miniaturized dynamic light scattering instrumentation for use in microfluidic applications. Rev Sci Instrum 78:072201
107. Jin F, Balasubramaniam R, Stebe KJ (2004) Surfactant adsorption to spherical particles: the intrinsic length-scale governing the shift from diffusion to kinetic-controlled mass transfer. J Adhes 80:773–796
108. Hudson SD, Cabral JT, Goodrum WJ, Beers KL, Amis EJ (2005) Microfluidic interfacial tensiometry. Appl Phys Lett 87:081905
109. Cabral JT, Hudson SD (2006) Microfluidic approach for rapid multicomponent interfacial tensiometry. Lab Chip 6:427–436

Polymer Informatics

Nico Adams

Abstract Polymers are arguably the most important set of materials in common use. The increasing adoption of both combinatorial as well as high-throughput approaches, coupled with an increasing amount of interdisciplinarity, has wrought tremendous change in the field of polymer science. Yet the informatics tools required to support and further enhance these changes are almost completely absent. In the first part of the chapter, a critical analysis of the challenges facing modern polymer informatics is provided. It is argued, that most of the problems facing the field today are rooted in the current scholarly communication process and the way in which chemists and polymer scientists handle and publish data. Furthermore, the chapter reviews existing modes of representing and communicating polymer information and discusses the impact, which the emergence of semantic technologies will have on the way in which scientific and polymer data is published and transmitted. In the second part, a review of the use of informatics tools for the prediction of polymer properties and *in silico* design of polymers is offered.

Keywords Information systems · Machine learning · Ontology · Polymer markup language · Polymer informatics · QSPR · RDF · Semantic web

Contents

N. Adams (✉)
Unilever Centre for Molecular Science Informatics, University Chemical Laboratory,
University of Cambridge, Lensfield Road, Cambridge CB2 1EW, UK
email: na303@cam.ac.uk

Abbreviations

ACS	American Chemical Society
ANN	Artificial neural network
BPAC	Bisphenol A Polycarbonate
CAS	Chemical Abstracts Service
FTIR	Fourier Transform Infrared Spectroscopy
GREMAS	Genealogical Retrieval by Magnetic Tape Storage
HIM	Hamiltonian Interaction Modeling
HTE	High Throughput Experimentation
IUPAC	International Union of Pure and Applied Chemistry
LCST	Lower Critical Solution Temperature
LDPE	Low Density Polyethylene
LLDPE	Linear Low Density Polyethylene
OWL	Web Ontology Language
PCA	Principal Component Analysis
PCR	Principal Component Regression
PDF	Portable document format
PDI	Polydispersity Index
PET	Poly(ethylene terephthalate)
POLIDCASYR	Polymer Documentation System of IDC with Inclusion of Analytical and Synthetic Concept Relations
PVA	Poly(vinyl alcohol)
QSPR	Quantitative Structure Property Relationship
R^2	Correlation coefficient
R^2_{cv}	Cross-validated correlation coefficient
RBF	Radial Basis Function
RDF	Resource Description Framework
RMS	Root Mean Square Error
STM	Scientific, technical, medical
T_g	Glass transition temperature
ToF-SIMS	Time-of-Flight Secondary Ion Mass Spectrometry
TOSAR	Topological Representation of Synthetic and Analytical Relations of Concepts
UCST	Upper Critical Solution Temperature
UV	Ultraviolet
WWW	World Wide Web
XML	eXtensible Markup Language

1 Introduction

Synthetic polymers are arguably the most important class of materials of the modern age. While it is difficult to obtain precise numbers, market research suggests that the world production of polymers in 2003 was between 150 and 200 million tons a year. Within this mix, polyethylene is probably the most important commodity polymer and accounts for approximately 50 million tons a year. The consumption of linear low density polyethylene (LLDPE) in Russia alone has been predicted to increase from 90,000 metric tons in 2007 to 1,00,000 metric tons in 2008 and the percentage increase in LLDPE use in China is in double-digit figures. The significant consumption is explained by the fact that polymers have found a wide area of application in virtually all areas of life, from simple packaging and building materials to more sophisticated uses in engineering applications requiring high-performance materials as well as in medicine (both as biomaterials [1–3] and in drug-[4–11] and gene delivery [12–19]), home and personal care applications [20, 21] and as plastic and printed electronics [22–26]. The reason for the success of polymers as materials can be found in the combination of a number of reasons: (1) commodity polymers are cheap to manufacture (the average cost of crude-derived commodity polymers is approximately 1 €/kg) [27], (2) polymers are largely non-toxic, (3) polymers are easy to process, (4) polymers are easy to adapt through post-processing and additives and (5) polymers are on the whole stable and relatively tough.

For the reasons outlined above, polymer science is very much in the mainstream of both chemical and materials research and likely to remain there for the foreseeable future. However, in order to leverage all the advantages of this class of materials, polymer science must face a number of challenges and changes. The rising cost of crude oil is currently changing economics in favor of polymers based on renewable and sustainable feedstocks (biopolymers for injection molding cost about €1.60/kg) and it is reasonable to anticipate that the development of new materials from these sources will accelerate in the future and the rapid discovery of new polymeric entities will become a strategic priority [27]. Furthermore, one might speculate, that an increasing amount of work will be done on non-commodity, value-added applications of polymers, which are usually developed at the interfaces of several scientific disciplines: polymers and medicine, polymers and electronics and polymers and nano-engineering.

Another significant driver of change is the increasing use of combinatorial and high-throughput experimentation (HTE) in virtually all areas of polymer science, starting with synthesis and discovery [28–34], processing [35–40] as well as screening for chemical, physical and mechanical [41, 42] properties. While HTE has been an integral and indispensable part of the pharmaceutical industry for a significant period of time, the materials science community has mainly persisted in using "one-step-at-a-time" experimental approaches. Recently, however, a significant effort to utilize combinatorial and high-throughput technologies has been made by a number of industrial and academic laboratories, with the result that HTE is now entering standard laboratory practice.

One final force, which is currently revolutionizing science – and therefore polymer science – is the world wide web (WWW) itself. The advent of the semantic

web is currently profoundly changing the way in which scientists communicate and exchange data and it can be expected that the impact of this will also touch polymer science.

The discipline of informatics can loosely be defined as "the science of information" and is invariably coupled with both the engineering of information systems and the practice of information processing. For our purposes, this defines the scope of what polymer informatics should be and therefore also the scope of this contribution.

It has already been mentioned that one of the drivers of change in polymer science is an increasing amount of interdisciplinarity. From an informatics point of view, "interdisciplinarity" most often denotes an exercise in data integration. When attempting to develop a polymer pharmaceutical, for example, not only does the polymer chemistry have to be right, but during the development cycle, data from the synthesis laboratory must be integrated with data from other areas such as (clinical) pharmacology, toxicology, cellular biology, (pharmaco)genomics, etc. While the problem is easy to state, cross-disciplinary data integration is far from trivial. To give an example, does the term "macromolecule" mean the same thing when used in the context of (polymer) chemistry and in the context of biology (in the former case "macromolecule" often refers to a synthetic macromolecule which is a member of an ensemble of molecules which, together, make up a "polymer", whereas in the latter case "macromolecule" is often synonymous with "protein")? And therefore, what about data that is annotated with this single concept, which may have domain-specific semantics? Similarly, is the definition of "glass transition temperature" in the context of polymer science the same as in the context of mineralogy? How can we get a computer to make that decision, so that it can decide whether data from a "polymer context" and data from a "mineralogy context" is equivalent and can be combined? Interdisciplinary (polymer) science forces us to address all of these questions and hence part of the remit of polymer informatics must be to develop technologies, information architectures and ontologies that enable and facilitate data exchange between several different disciplines.

The increasing adoption of high-throughput and combinatorial experimentation approaches, too, triggers the need for sophisticated informatics support. While "high-throughput" in materials science usually implies experimental volumes, which are much smaller than those encountered in medicinal chemistry or drug discovery (HTE in polymer science typically means tens or hundreds of samples, rather than thousands or tens of thousands), materials HTE nevertheless generates significant amounts of data, which need to be administered, handled and stored. Once the necessary metadata requirements such as measurement conditions, etc. have been compounded into this, data volumes increase even further. The implication is, that the ways in which (academic) polymer science handles (by laboratory notebook and digital spreadsheet) and disseminates (by journal publication) polymer data do not scale or are inappropriate. Moreover, polymers are materials which are significantly more complex and fuzzy than small molecules. Hence, informatics solutions, which have been developed for the latter – both in the context of high-throughput and "classical" experimentation – do not translate well to the former: polymers require their own solutions. Finally, while the outcome of a HTE campaign is raw

experimental data, data on its own is quite useless. It is knowledge – the confident theoretical and practical understanding of a domain – which enables a scientist to make decisions or to develop a product. Polymer informatics, therefore, needs to develop technologies, which (1) allow the description of polymeric materials in an appropriate manner, (2) allow the attachment of knowledge and data to these descriptions and (3) allow the easy conversion of such data in knowledge.

It is worth noting that (scientific) data has intrinsic value, even if the primary purpose for which it was created, has long been fulfilled. Innovative (re-)uses of publicly available data on the internet exemplify this nicely. Scientists usually tend to produce data in the context of a specialized research project and disseminate it through the means of scientific publication in a learned journal. Once research objectives have been met or a publication has been published, scientists often lose interest in their own data as it serves no primary purpose anymore. Because of this, significant amounts of valuable scientific data either never get published and thus never become part of the "knowledge commons" or are rendered inaccessible to machines and thus effectively destroyed for informatics purposes.

By contrast, the modern internet demonstrates clearly how data that have been published openly on the web in a machine-friendly form and subsequently "mashed-up", i.e., been brought together with data from other sources or domains, can generate valuable new knowledge. Scientists are now beginning to tap into this vast potential and to generate new science and insights [43, 44]. Polymer informatics should develop technologies to enable (polymer) scientists to publish and store their data in a way that is free of access-barriers (which can be technological, financial (e.g., subscription fees) or legal (e.g., attempts to copyright data)) and that allows the easy generation of mash-ups with data from other sources.

While considerable progress has been made in the area of small molecule informatics over the past several decades, any effort in the field of polymers has been timid at best and there is considerable scope for development. The main reason for the virtual non-existence of polymer informatics is the complex nature of polymers. This review will therefore start with an examination of the particular informatics challenges posed by polymers, in particular in the area of polymer representation and will also discuss some of the peculiarities of polymer information ("the science of information"). It will look at information systems for polymers ("engineering of information systems") and a final section will review attempts to develop structure-property relationships for polymers ("practice of information processing"). The modeling of polymers either on the molecular – or meso-level – is outside the scope of this review.

2 Polymer Information is Challenging

The central dogma of chemistry is, that the structure of a molecule correlates with its physico-chemical properties. This is usually illustrated using the correlation between the boiling point of *n*-alkanes and the number of carbon atoms
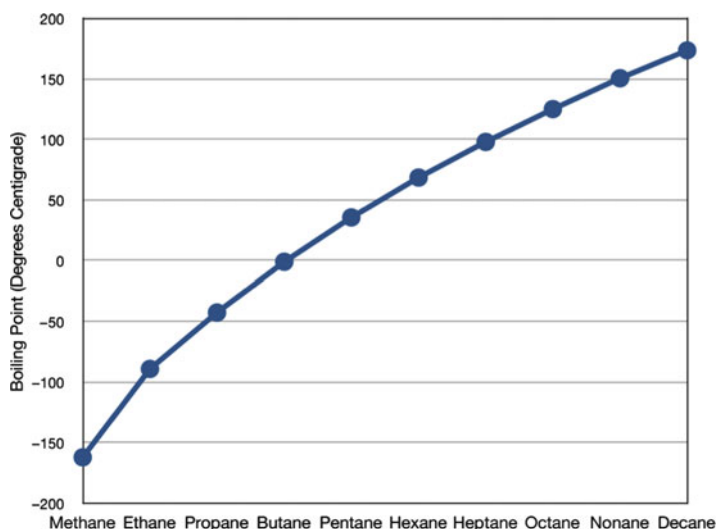
Fig. 1 The correlation between the boiling points of *n*-alkanes and number of carbon atoms in the molecule

in the molecule (Fig. 1). Knowledge of the structure of the molecule allows the calculation of "descriptors", i.e., variables, which capture information about aspects of the structure of the molecule and which can be correlated to an observed physico-chemical property.

Historically, most chemists have modeled the structure of molecules using a highly idealized "platonic" representation, where atoms are represented as vertices and bonds as paths between vertices. Chemoinformatics has very successfully adopted this representation and based many of its techniques around the metaphor of the "connection table", i.e., a list of all atoms and bonds, which occur in the molecule. While this approach is quite successful for well defined chemical entities, it begins to break down for rapidly interconverting isomers, for example, and is completely inappropriate for polymers. In the majority of cases, the successful application of chemoinformatics to a given problem depends on the availability of a connection table.

For synthetic polymers, the representation of structure by connection table essentially breaks down because polymers are collections of macromolecules, each of which is slightly different, even if only in terms of the degree of polymerization. If the central dogma of chemistry holds, though, this means that any physical quantity observed as a "polymer property" is an average over an ensemble of macromolecules. A polymer can therefore not be described by a single connection table alone. Structural heterogeneity in synthetic polymers is virtually a given: even the most well-controlled polymerization reactions yield polymers with polydispersity indices (PI) of around 1.03 (see, for example, [45]). Because no single connection table is capable of representing a polymer and because the observed physical properties of a polymer sample are the metrological sums of the properties of the

contributing entities, the connection table/data correlation approach breaks down in the case of polymers and many other materials for that matter.

Furthermore, we often know how a polymer was made, but do not know the structure of the resulting product – a famous example of this is Bakelite (phenol/formaldehyde resin). Conversely, as is often the case for industrial polymers, we may have some property data, but do not know how the polymer was made or any structural details. Polymeric materials in general have a "history" and, more often than not, it is that history which influences or completely determines its property characteristics and not the structural characteristics. The implication of this is, that a description/encoding of a polymer's history is often more relevant than an encoding of its structure.

A final factor, which complicates polymer data is the fact that crucial metadata are often missing. A significant number of polymer properties are not only dependent on the chemical nature of the constituent macromolecules of a polymeric ensemble, but also on factors such as measurement methods, measurement conditions, etc. The glass transition temperature (T_g), for example, is formally conditional on quantities such as pressure, molecular mass, tacticity and cross-linking. For low molecular weight polymers, T_g increases with increasing polymer molecular weight until an upper limit is reached and the value of T_g becomes essentially invariant to further increases in molecular weight. Furthermore the experimental method used to determine the glass transition temperature is of crucial importance: popular measurement methods include differential scanning calorimetry (DSC) or thermo mechanical analysis (TMA). DSC determines the change in heat capacity of the sample as a function of temperature, whereas TMA measures dimensional changes (length and thickness) of a sample. If, therefore, one were to determine the glass transition temperature of a polymer sample using the two different techniques, the results obtained would usually differ by several degrees Kelvin.

The first significant challenge that polymer informatics has to tackle, therefore, is to develop representations for both polymers and polymer data, which are computable, i.e., "machine-comprehensible" and to which rich metadata can be attached.

2.1 The Representation of Polymers

Early efforts in what could be termed "polymer informatics" go back to an ACS symposium on polymer nomenclature in the late 1960s [46–51]. Papers in this symposium were mainly concerned with issues of polymer nomenclature and aspects of information retrieval. A first set of seminal papers only appeared about a decade later, as a consequence of another ACS symposium on the retrieval of polymer information in 1978 [52–59]. Collectively, the papers resulting from the 1978 symposium set out the challenges still faced by polymer informatics today: the fuzzy nature of polymers and the variety of different types of descriptions and representations of polymers arising as a consequence, the problem of information

compartmentalization and the difficulty associated with information retrieval across the numerous interdisciplinary interfaces of polymer science [52]. A contribution by Fugmann, describing the POLIDCASYR polymer documentation system of the "Internationale Dokumentationsgesellschaft fuer Chemie (IDC)" (a now defunct German chemical information service founded as a joint venture between BASF, Bayer, Hoechst, Degussa and Huels) is particularly relevant, in that it examines both the important syntactical and logical concept relationships between structures and polymers and points to the use of controlled vocabularies and semantics for capturing non-structural aspects. It furthermore introduces the notion of indexing polymers as molecular fragments. The POLIDCASYR system is an extension of the GREMAS (Genealogical Retrieval by Magnetic Tape Storage) technology, also developed by IDC, which indexes molecules in terms of "molecular regions" (e.g., molecular fragments). The GREMAS system distinguishes between four distinct molecular regions, namely aliphatic carbon chains, alicycles, aromatic rings and heterocycles and uses term symbols to code for these. Typical terms include, for example, symbols for large chains of carbon atoms of statistical length (term symbol "6", Fig. 2), terms for carbon atom chains in non-polymers (term symbol:"YR", Fig. 2) terms for hydroxy-, carboxy-, carboxylic acid etc. and many other groups. This leads to an indexing of molecules as a collection of molecular terms as shown in Fig. 2.

Another POLIDCASYR extension ensures that structural features of the backbone can be distinguished from those occurring in side chains. The system furthermore augments structure codes for polymers using a controlled vocabulary of keywords, such as "epoxy resin", "aminoplast" or "phenoplast".

The POLIDCASYR paper also acknowledges the importance of the "history" of a polymer and the oftentimes incomplete information associated with a polymeric entity. This is important, because if the structure of a polymer is unknown, then an encoding of the material in fragment terms will be impossible and the information
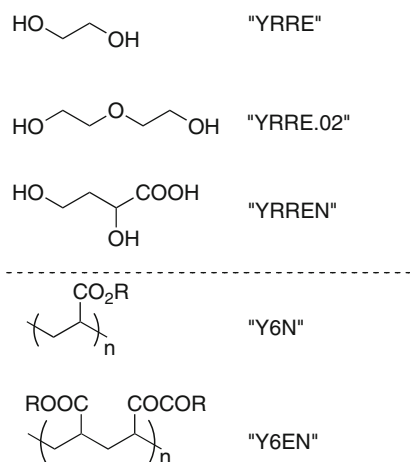
Fig. 2 Examples of GREMACS/POLIDCASYR terms for small molecules and polymers
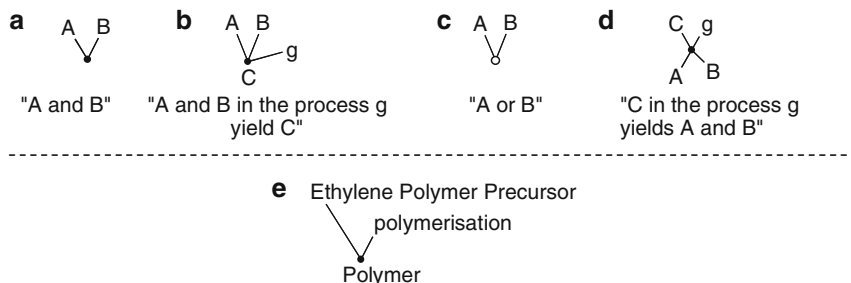
Fig. 3 Basic elements of a TOSAR graph: (**a**) "A and B", (**b**) "A and B in the process γ yield C", (**c**) "A or B", (**d**) "C in the process γ yields A and B"

scientist has little choice but to codify and index the polymer in terms of related concepts, such as the monomer a polymer was derived from. This, in turn, requires the definition of a series of syntactical and logical relationships between concepts for successful information retrieval. To this end, the IDC developed the TOSAR system (Topological representation of Synthetic and Analytical Relations of concepts) [60], which represents the relationships between concepts by means of a graph and can therefore be viewed as a precursor to modern semantic web and ontological approaches such as, for example, the Resource Description Framework (RDF) [61, 62] or the Web Ontology Language (OWL) [63]. In a TOSAR graph, concepts are represented as nodes and concept relations as edges of the graph. Concept relations can exist as either "analytical relations" or "synthetic relations" (Fig. 3) and thus the TOSAR approach is, in essence, an incarnation of Ranganathan's Colon Classification (CC) [64]. The colon classification is an 'analytico-synthetic classification", or, in modern parlance, a "faceted" classification. Furthermore, the TOSAR system allows the specification of logical operations such as "AND", "OR" and "ONLY" as well as optionality, which allows an indexer to effectively encode the history of a polymer as well the processes (e.g., synthetic reactions, grafting, sequences in time, etc.) described in a document (Fig. 4). In a sense, the resulting graph is both a structural representation of the information source it was taken from as well as a representation of the history of a polymer.

In addition to fragment and graph indexing of polymer information, the POLIDCASYR system also makes use of two distinct vocabularies for non-structural terms. The first vocabulary is, in essence, a controlled vocabulary of hierarchically ordered terms (taxonomy), supplemented by a second, more fluid vocabulary, which is subject to constant editing. The latter is used to further enhance the controlled vocabulary, e.g., the term "isomerization", which is part of the controlled vocabulary, could be defined further by the terms "racemization", "tautomerization" or "rotation isomerization". Annotation of this kind is only a short step away from techniques, which we now associate with the terms "tagging" and "folksonomies" and which are typical components of Web 2.0 systems. POLIDCASYR's controlled vocabulary is structured according to a number of semantic categories such
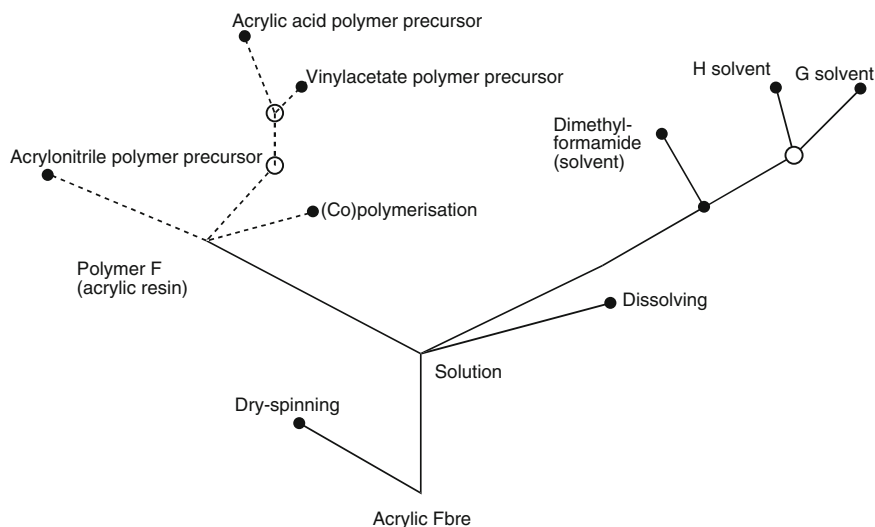
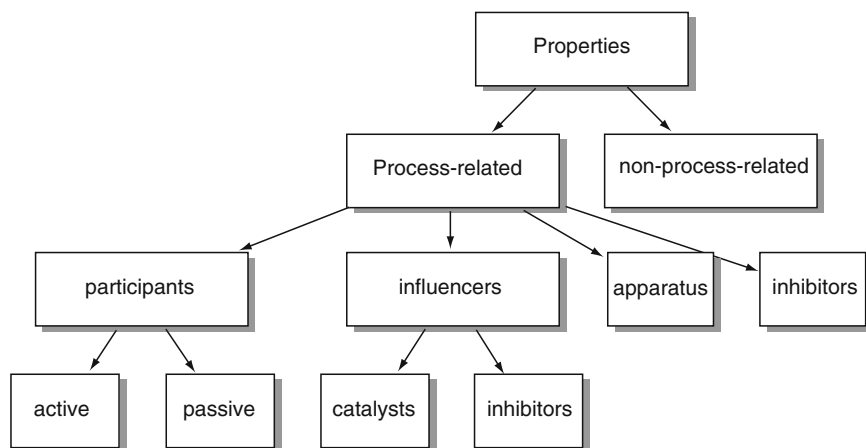**Fig. 4** TOSAR graph representing a sequence of processes

Fig. 5 Subdivision of semantic categories in the POLIDCASYR controlled vocabulary

as substances, apparatus, living entities, processes, reactions, process-related and non-process-related properties and fields of application (Fig. 5).

These top level categories can be subdivided further and establish relations between concepts (Fig. 5). Each of the subdivisions has a unique code, which can be used for indexing and searching.

Other papers from the 1978 symposium discuss the indexing of polymers in Chemical Abstracts [53], the IFI/Plenum System [59] and an in-house system for Hercules [58]. While a number of services such as the Chemical Abstracts Service

have several routes into polymer information (keyword search, search by name, search by formula index, search by general subject index), for most chemists, however, the most important route to polymer information is either *via* "search by name" or "search by structural formula".

2.1.1 Name-Based Representation of Polymers

Name-based representations of polymers normally occur in three different incarnations: (a) trade and trivial names, (b) names derived from the component monomers of a polymer ("source-based representations") and (c) names derived from the structural repeating unit of a polymer ("structure-based representations"). Trivial or trade names are often derived from the inventor of a certain material (e.g., Bakelite – developed by Baekeland) and contain no or only little chemical information and therefore very easily lead to information compartmentalization – trivial names usually cannot even be inferred. Which of the other naming conventions is used normally depends on the nomenclature philosophy of a particular community within (polymer) chemistry and there is no general agreement as to which type of nomenclature is preferable. Polybutadiene, for example, would be indexed as "1,3-butadiene, homopolymer" by the Chemical Abstracts Service (CAS) (Fig. 6). A keen observer will also have noticed that the name has been inverted, which is CAS specific. The International Union of Pure and Applied Chemistry (IUPAC) will allow the registration of the polymer as either "polybutadiene" (IUPAC source-based), "poly(but-1-ene-1,4-diyl)" (IUPAC structure-based), "1,4-polybutadiene" (IUPAC semisystematic), "poly(buta-1,3-diene)" (IUPAC source-based). Apart from particular idiosyncrasies such as name inversion or the use of brackets, nomenclature systems are also subject to historical (dis)continuities: as time passes and indexing systems evolve, nomenclature rules change: poly(ethylene terephthalate) (PET) is registered as "poly(oxyethyleneoxyterephthaloyl) in the 8th Collective Index of Chemical Abstracts, but as poly(oxy-1,2-ethanediyloxycarbonyl-1,4-phenylenecarbonyl) in the 9th Collective Index.

While different nomenclature conventions and historical discontinuities are at best confusing to the human searcher, they lead to serious problems in terms of multiple registration of entities in registration systems as well as information compartmentalization: a mapping of "polybutadiene" onto "poly(but-1-ene-1,4-diyl)" is not straightforward for a human and even less so for a machine (polybutadiene does not indicate the position of the double bond in the polymer backbone) and therefore any data associated with either registration may or may not be equivalent.
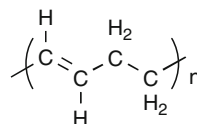

Fig. 6 Polybutadiene repeating unit

Ontologies could go some way towards solving this problem since they assist in the specification of parthood relationships (e.g., between a single concept and multiple labels).

2.1.2 Structure-Based Representation of Polymers

Apart from simple name-based representations, polymer information systems also use chemical structure diagrams to register polymeric entities. We have already discussed the breakdown of the structure diagram metaphor for polymers in the sections above and the situation currently encountered in many polymer information systems is reflective of this: polymers are either registered using the structure of the corresponding monomer(s) or a greatly reduced representation in the form of the repeating unit of one of the macromolecular constituents.

Structure representations of polymers based on monomer structures are the least desirable, because they reference one concept in terms of another and necessarily lose all polymer-specific information: often, monomers undergo significant structural change upon polymerization (e.g., going from cyclic to linear structures during ring-opening metathesis polymerizations (ROMP)) and potentially important information such as endgroups, post-modification procedures such as grafting, etc., cannot be encoded. Representation by repeating unit structure is problematic too: while the repeating unit is at least indicative of the major structural features of the polymer backbone (end group information, post-processing, etc., is still not encoded), often the problem of unambiguous representation arises. When considering the structure of a poly-1,3-butadiene macromolecule, for example, it becomes evident that several valid repeating unit structures can be drawn (Fig. 7).

The fact that several representations are possible automatically necessitates the development of rules which would allow a researcher to decide upon a preferred representation. To this end, IUPAC has developed an elaborate rules-based system using the "seniority of subunits", the direction of citation, etc. [65]. However, rules-based systems are subject to the same limitations as nomenclature systems in that they, too, suffer from (potential) historical discontinuities and require acceptance by a broad community.
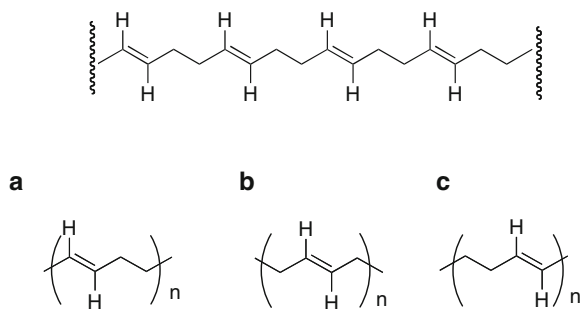

Fig. 7 Possible repeating unit representations (**a, b, c**) for poly-1,3-butadiene

One paper arising from the 1978 symposium points out another central and unsolved problem in polymer informatics today, namely the scarcity of polymer data [56]. The paper suggests that three things are needed to develop a successful polymer information system: (1) the availability of good data models, (2) the long-term commitment of both industry and academia to generate comprehensive and metadata rich materials data, which adheres to the data model and (3) "the commitment of national data centers to act as repositories of such information." The important message here is that the successful development of information systems for materials is mainly a "political" problem: communities of practice need to agree to produce and share data and to preserve and curate it for the long term. Good technology is essential, but is hardly ever the real limiting factor. For polymers, none of these requirements have been met so far. However, developments on the WWW such as an increasing emphasis on community-developed or community-created information and data (e.g., Wikipedia and Freebase) together with developing technologies for linking and "mashing-up" data might go some way towards meeting the above requirements.

While the 1978 symposium on polymers highlighted many of the problems associated with polymer information and also discussed some possible solutions, papers submitted for another ACS symposium on the topic entitled "Polymer Information: Storage for Retrieval, or Hide and Seek?" suggest, that nothing much has changed [66].

One notable exception to this is a paper by Gushurst et al. introducing MDL's (now Symyx) proprietary Sgroup notation [67]. "Sgroup" is an acronym for "substructure group" and represents a "persistent collection of atoms and bonds" which is a part of a larger connection table. Sgroups subdivide into two types, "chemical Sgroups" and "data Sgroups". The Sgroup notation can be used for the description of polymers, formulations and other materials. Sgroup representations of both a structure-based (Fig. 8a) and a source-based (Fig. 8b) block copolymer of polystyrene and polyethylene oxide are shown in Fig. 8.

In Sgroups, repeating units are enclosed in square brackets and a subscript "n" is placed to the right of the closing bracket. The subscript "blk" indicates a block copolymer and "mon" a monomer in a source-based representation. Superscripts indicate the orientation of the repeating units (hh = head-to-head, ht = head-to-tail, eu = either unknown) in a structure-based description. Crossing bonds (bonds
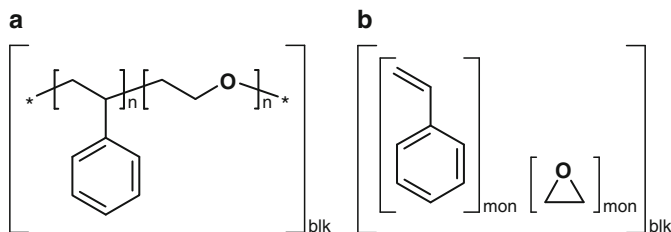

Fig. 8 (**a**) Structure-based and (**b**) source-based Sgroup representation of a polystyrene/polyethylene oxide block-copolymer

crossing the square brackets) indicate known connectivity. Data Sgroups may be associated with these structural descriptions and can hold information about, for example, the percent composition and distribution of building blocks in a polymer, modifications, etc. Sgroups therefore go some way towards being able to describe the history of a polymer as much as its composition. When searching for a particular polymer using a structure-based representation, MDL's proprietary "flexmatch" algorithm cyclizes all possible repeating unit representations. If multiple valid repeat units can be written, the cyclization process creates a set of molecules, which are "phase-shifted" with respect to each other. This means that all structures are effectively identical, which removes the need for rules for choosing a preferred repeating unit representation.

A paper by Kaback re-enforces the previously made point that "there's more to a polymer than just its build" [68] and that it is the history of a polymer that is often more important for information retrieval than any complex structure representation. As an example, Kaback points out, that, for a polymer, it makes a significant difference whether the polymer was synthesized in a stirred autoclave or a tubular flow-through system, as this will lead to polymers of vastly different physical characteristics, even if all else is equal. This information, however, is hardly ever encoded as metadata in information systems. The same is true for other types of metadata – it is currently very difficult to distinguish information about elastomeric ethylene/propylene copolymers from data referring to, for example, rigid thermoplastic ethylene/propylene copolymer, etc. In Kaback's own words: "Polymers are both chemicals and materials. In viewing a polyolefin as a chemical reactant, it is critical for me to know if it was produced by a catalyst system that gives a product in which residual chain unsaturation is overwhelmingly at the chain end, rather than one or more units into the chain. In viewing it as a thermoplastic, it is critical for me to know whether the molecular weight distribution is broad, implying good flow properties, or narrow, suggesting possible melt processing difficulties" [68]. In other words, what determines the value of a polymer information system is the "axiomatization" of the polymeric entity and the context-aware "lens" onto the information that the system should provide. Other papers in the 1991 symposium series are essentially descriptions of a number of proprietary information systems, such as the Derwent Plasdoc System [69], the IFI/Plenum Polymer Indexing System [70] the Rapra Abstracts Rubber and Plastics Database [71], with side-by-side comparisons of all these systems [72, 73] and a discussion of the particular challenges associated with searching for information on condensation polymers [74].

2.1.3 The Semantic Web of Polymer Data

Many of the challenges described so far can be addressed using technologies developed in the context of the "semantic web" or "web 3.0" [75]. The semantic web is currently revolutionizing the way in which we structure, handle, present, and exchange scientific data and information. Unlike the current incarnation of the web, which is mainly a web of documents, the semantic web is a vision of a web of

data, in which software robots are able not only to discover information, but also to understand its meaning and therefore to act on it autonomously. Currently, the way in which we communicate polymer information is similar to the way in which we treat information on the web. Most polymer information is contained in unstructured documents (equivalent on the web: webpages) such as scientific papers, theses, patents. etc. Because these documents are unstructured (a machine does not *a priori* understand that the symbol combination "°C" denotes a temperature unless this is explicitly stated in machine comprehensible language), it is extremely hard for machines to discover information in these documents. Moreover, information about a given polymer is often scattered across several sources (web analogy: many webpages on different servers/sites talking about the same concept) and hard to combine into a single picture. The semantic web is developing some technical solutions to address these problems in the web domain and it is reasonable to assume that these can also be applied to the domain of polymer information.

In a typical scenario, a polymer scientist wishing to design a new polymer for a given application would specify an application/property profile of that polymer. A semantic web agent (software that acts on behalf of a user), in turn, would be able to "understand" the specification and to collect relevant information from the "cloud" (e.g., the web, in-house data sources, proprietary and open databases, scientific publications, etc.). The agent might then reconcile the gathered information against the requirements profile and use existing quantitative structure-property relationships or rules to infer other properties. Finally, the agent would present a list of polymers with a property profile closely matching the original specification. To achieve this vision, a software agent would not only have to find information (i.e., information must be present in a structured form), but also understand its meaning (i.e., the information must be computable). On a technology level, therefore, we require the three components of (1) publication (data needs to be available digitally), (2) semantics (data needs to be semantically rich), and (3) data interoperability (which can be achieved via the use of semantics).

The technological foundations of this vision currently consist of eXtensible Markup Language (XML) [76], XML Schema [77], the Resource Description Framework (RDF) [61], RDF Schema [62], and the Web Ontology Language [63]. These technologies are interdependent and can thus be arranged in the form of a "semantic layer cake" (Fig. 9).

One way to impart structure to otherwise unstructured documents is to utilize a suitable markup language. The function of markup languages is to combine the text of a document with further information about the text (markup languages typically add "metadata" – data about data) and while metadata is normally hidden from the view of a human reader, it is available to processing software. XML allows an author to add arbitrary metadata to documents through the use of tags, which are user-defined and annotate data sources.

With XML providing the mechanism for structuring, the Resource Description Framework (RDF) provides the machinery for data integration and lightweight axiomatization. A "resource" in informatics terminology is anything that can be named, addressed, or handled and the language provides a framework for making
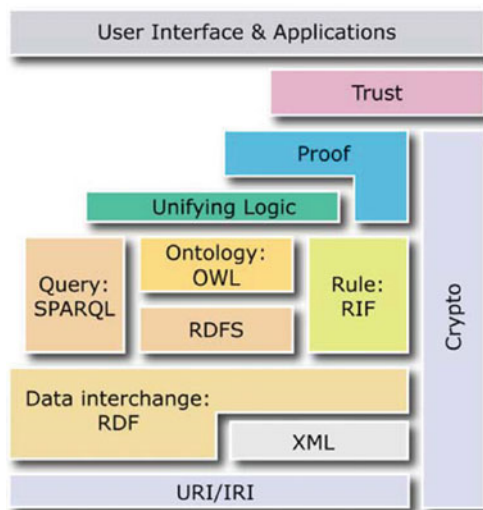
Fig. 9 The semantic layer-cake. (Copyright 2008 World Wide Web Consortium, (Massachusetts Institute of Technology, European Research Consortium for Informatics and Mathematics, Keio University). All Rights Reserved. http://www.w3.org/Consortium/Legal/2002/copyright-documents-20021231. Reproduced with permission)

statements about these resources. Statements are made in the form of "triples", i.e., almost human-language like *subject-predicate-object* constructs. RDF therefore allows simple assertions of the type: "polystyrene is a polymer" to be made. The web ontology language (OWL), finally, extends this expressivity even further by allowing the addition of first-order-logic. This, in turn, means that relationships between resources, such as disjoints, cardinality, equality and symmetry, etc., can be described.

Semantic technologies are highly significant for polymer (data) representation, because they are now being applied in the field of chemistry and polymer science. As XML is indeed extensible, a number of markup languages have been developed over the last decade, which are of relevance in the general area of chemistry and which can also be used to structure polymer information. The most significant of these languages are Chemical Markup Language (CML) [78–83], Analytical Markup Language (AnIML), and ThermoML (markup language for thermochemical and thermophysical data) [84]. Some papers detailing the beginnings of an alternative to CML as a general chemical markup language have also recently been published [85, 86].

Chemical Markup Language was pioneered by Murray-Rust and Rzepa and is designed to manage mainly molecular information, such as chemical structure as well as spectral, analytical-, computational-, and crystallographic data. CML is currently being investigated by Microsoft Research as a way of introducing semantically rich chemistry features within the Microsoft Office Word package [87]. Adams and Murray-Rust recently reported the development of Polymer Markup Language as a polymer-specific extension to CML [88, 89]. Like the Sgroup approach, the

language is a fragment-based representation and addresses considerations such as the composition of a given polymer, the structure of a polymer or macromolecule (if known), as well as the records of a computational experiment, physical or other properties of a polymer or macromolecule, experimental metadata, and reaction information. At the moment, PML does not consider polymer processing such as compounding, but may well be extended to cover these areas in the future. The design criteria of PML include the re-use of CML whenever possible, full namespace awareness, interoperability with other mature STM languages, the avoidance of implicit semantics, the treatment of polymer-specific phenomena such as the ensemble nature of polymers, ambiguous repeating units, tacticity, double bond isomerism, macromonomers as well as the description of all commonly encountered structural motifs such as homopolymers, copolymers (statistical, alternating, block), branched polymers (combs, hyperbranched systems, dendrimers) as well as cross-linked polymers and graft polymers. Figure 10 shows a PML document for a simple styrene heptamer.

The construction of the molecule starts with a root fragment which, in the particular document in Fig. 10, is a methyl group (<molecule ref = "g:me">). The "g:me" pointer links to a fully atomistic description of the methyl fragment in CML, which in turn allows the annotation of individual atoms if needed – this could be important when wishing to specify differential reactivity of backbone atoms for grafting and post-processing, for example. The methyl group joins onto a CH-group (<molecule ref = "g:ch">), which is connected to a methylene fragment (<molecule ref = "g:ch2">) and a phenyl fragment (<molecule ref = "g:benzene">). The construction thus defines a full repeating unit, though this is completely accidental and not required by the language – the user is free to choose any type of fragment, such as multiple repeating units, macroinitiator fragments, etc.

The <fragment> container, which is a child of the root element, contains a countExpression attribute, which indicates to PML processing software that the fragment definition is to be repeated another six times. The countExpression attribute is, in fact, a computable variable. This is a new concept for markup languages, which have hitherto been used in a completely declarative way. The countExpression element can evaluate either deterministically (specifying a macromolecule) or stochastically (specifying distributions of macromolecules). In general, PML can either be implicitly or explicitly computed, which means that it is possible to create documents containing free variables. As such, it is possible to embed XSL Transformations [90] into PML documents and to evaluate the resulting expressions in a lazy manner.

PML can also represent polymers at different levels of certainty: where the structure is known, it can be encoded and where this information is not available, a polymer can be codified in terms of other concepts, such as the monomers it was prepared from. Furthermore, PML provides essentially a coarse-grained representation: larger structural fragments can be mapped back to fully atomistic fragments, if desired. PML, therefore, allows data to be associated with a polymer representation at the atom, molecular fragment, molecule and molecule ensemble level, and,
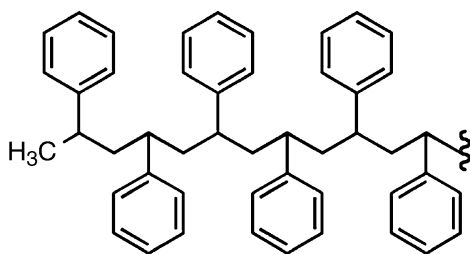
```xml
<?xml version="1.0" encoding="UTF-8"?>
<fragment convention='cml:PML-basic'
 xmlns='http://www.xml-cml.org/schema'
 xmlns:g='http://www.xml-cml.org/mols/geoml'>
 <fragment id="f0">
   <fragment>
     <molecule ref='g:me' />
   </fragment>
   <join moleculeRefs2="PREVIOUS NEXT" atomRefs2="r1 r1">
     <torsion>90</torsion>
   </join>
   <fragment countExpression="*(6)">
     <join moleculeRefs2="PREVIOUS NEXT" atomRefs2="r1 r1">
       <torsion>90</torsion>
     </join>
     <fragment>
       <molecule ref="g:ch">
         <join moleculeRefs2="PARENT CHILD"
           atomRefs2="r3 r1">
           <torsion>90</torsion>
           <molecule ref="g:benzene" />
         </join>
       </molecule>
       <join moleculeRefs2="PREVIOUS NEXT" atomRefs2="r2 r2">
         <torsion>90</torsion>
       </join>
       <molecule ref="g:ch2" />
     </fragment>
   </fragment>
  </fragment>
</fragment>
```

Fig. 10 A simple PML document showing the construction of a styrene oligomer

as such, it can be considered to be a "normal" (though not a canonical) form of a polymer description. The authors have recently published a "polymer builder" prototype application, making use of polymer markup language and the associated processing software [88]. As part of one of their papers, Adams et al. also briefly present the development of polymer ontologies, which contain basic polymer science terms, although no formal publication has appeared yet. To date, ontologies are severely underused in chemistry and chemical data management, although there are a few attempts at constructing ontologies in the domain. Probably the most prominent chemical ontology is the European Bioinformatics Institute's "Chemical

Entities of Biological Interest" (ChEBI) [91]. ChEBI is a small-molecule "database" of natural products or synthetic entities, which have been used to interfere in biological processes and encompasses an ontological classification specifying relationships between molecular entities. Information about chemical entities is derived from a number of datasources, such as COMPOUND [92], the Chemical Ontology (CO), and IntEnz [93]. Other EBI ontologies in the chemistry domain are REX [94] and FIX [95], which describe physicochemical processes and methods respectively. Other groups have also reported efforts to model chemical structure [96], reactions [85, 86], and laboratory processes [97–99]. Further ontologies for the general scientific domain encompass ontologies of the scientific experiment as such [100], as well as a number of upper ontologies, which are suitable for science (e.g., SUMO [101], General Formal Ontology [102]). When taken together, it is reasonable to assume that these will be useful for describing and capturing much of the metadata that many of the "early" polymer informaticians requested from their information systems and that concepts from these ontologies can also contribute to the development of computable (i.e., "machine comprehensible") definitions of what a polymer, a glass transition temperature, etc., is.

A typical example of the possible definition of a macromolecule in the OWL ontology language is shown in Fig. 11. Here, a macromolecule is modeled in terms of sets: a macromolecule is a molecule which has a high relative molecular mass and which is derived from either a molecule of low molecular mass or from an oligomer or from molecules of low molecular mass and oligomers. It is now easy to see how one can develop axiomatizations such as those envisaged by the TOSAR system (see above) using modern semantic web technologies and how information about the history of a material can be encoded in a machine comprehensible way, which is subsequently available for reasoning and knowledge discovery [88].

2.2 Access to Polymer Information

So far, all of the discussion in this review has focused on the representation of polymer structure and polymer information. However, another significant challenge in the development of polymer informatics is access to polymer data. In this context, the term "access" takes on two distinct meanings, namely "access" to data in terms of access-barriers (e.g., proprietary data, copyright considerations, etc.) and "access" in terms of the formats in which polymer data is communicated, handled and exchanged.

2.2.1 Access and Technical Access-Barriers

The first and obvious technical access barrier is the availability of data in digital form. While most modern documents are "born digital", a lot of libraries will still only archive paper copies of scientific literature, although more and more

```
:Macromolecule
    a       owl:Class ;
    rdfs:comment "A molecule of high relative molecular mass, the structure of which essentially
comprises the multiple repetition of units derived, actually or conceptually, from molecules of low
relative molecular mass." , "http://goldbook.iupac.org/M03667.html" ;
    rdfs:subClassOf :Molecule ;
    rdfs:subClassOf
            [ a        owl:Restriction ;
              owl:onProperty :hasStructuralComponent ;
              owl:someValuesFrom :Endgroup
            ] ;
    rdfs:subClassOf
            [ a        owl:Restriction ;
              owl:onProperty :hasStructuralComponent ;
              owl:someValuesFrom :MainChain
            ] ;
    owl:equivalentClass
            [ a        owl:Class ;
              owl:unionOf ([ a        owl:Class ;
                    owl:intersectionOf (:Molecule [ a        owl:Restriction ;
                              owl:onProperty :hasRelativeMolecularWeight ;
                              owl:someValuesFrom :High
                            ] [ a        owl:Restriction ;
                              owl:onProperty :isDerivedFrom ;
                              owl:someValuesFrom :SmallMolecule
                            ])
                  ] [ a        owl:Class ;
                    owl:intersectionOf (:Molecule [ a        owl:Restriction ;
                              owl:onProperty :hasRelativeMolecularWeight ;
                              owl:someValuesFrom :High
                            ] [ a        owl:Restriction ;
                              owl:onProperty :isDerivedFrom ;
                              owl:someValuesFrom :OligomerMolecule
                            ])
                  ] [ a        owl:Class ;
                    owl:intersectionOf (:Molecule [ a        owl:Restriction ;
                              owl:onProperty :hasRelativeMolecularWeight ;
                              owl:someValuesFrom :High
                            ] [ a        owl:Restriction ;
                              owl:onProperty :isDerivedFrom ;
                              owl:someValuesFrom :SmallMolecule
                            ] [ a        owl:Restriction ;
                              owl:onProperty :isDerivedFrom ;
                              owl:someValuesFrom :OligomerMolecule
                            ])
                  ])
            ] .
```

Fig. 11 Possible ontological description of the concept "Macromolecule" in the OWL ontology language

institutions now require documents to be submitted to institutional repositories in digital form. Furthermore, the increasing use of open access and self-archiving mandates by universities contributes to the availability of data. However, this is a gradual process and it is only now that a growing number of university libraries engage in the development of institutional repositories. Some sources of polymer information, such as the Polymer Handbook [103], are available on paper only.

Even if a document containing polymer information is available digitally, the format of the document is critical. While most scientific documents are authored using a word processing system such as Microsoft Word or Open Office or a typesetting system such as LaTeX, this is not normally the format they are subsequently disseminated in. In the majority of cases, these documents are converted to portable document format (pdf) for publication and dissemination. It is this very step which is problematic for automated information extraction. Portable document format has been designed as a purely presentational format: "The PDF design is very tailored to the creator being able – quite directly and without ambiguity – to specify the exact

output desired" and even its developers admit, that it is extremely difficult to extract information [104]. Essentially, pdf converts text to a set of graphical objects without semantics, i.e., there are no well-defined relationships between these objects and the conversion process is "lossy" in terms of information content. A consequence of this is, that a lot of vital scientific information is lost when converting back to text: frequently subscripts and superscripts disappear, a loss of vital information when attempting to teach a computer to recognize molecular formulae in text, and data tables are often completely destroyed. An example of this is a recent paper by Feniri et al. in which the authors reported the synthesis and spectroscopic character-ization of a large library (630 compounds) of polystyrenes [105]. Each compound in the library was characterized by both IR and Raman spectroscopy and the re-sulting data was published as spectral plots in pdf format. The result of this form of data publishing is that the spectral data associated with the polymers is lost: the data is only useful for human inspection and effective machine learning and data mining as well as the possibility of generating mashups with other data sources has been destroyed. In this particular case, the authors had little choice but to publish in this format (although archival of the raw spectral data in an institutional repository would also be an option): the chemical and polymer science community has simply not yet evolved mechanisms for publishing its data and not "just" its papers.

Even if the document is produced in a format suitable for information extraction and does not of itself destroy information, it is often the reporting scientist who does. A good example is the way in which NMR data of organic molecules are currently reported: the digital signal obtained from the NMR machine, even when processed, contains significantly more information than is reported using the standard journal publication procedures (i.e., peak positions, splitting patterns and coupling con-stants). It is not possible to reconstruct the original spectrum from this data and any information that may have been contained in the original signal and which is not captured in the reported data is lost. In the era of digital documents, virtually free and unlimited storage and pervasive computing and network access, scientists should be much less willing to simply throw data (and thus potentially information) away, in particular if the data has been produced at great cost. (Chemical) Crystal-lography is exemplary in this regard: as a community, the discipline has evolved data standards (cif file format [106] and the crystallographic information framework) and tools and mechanisms for data preservation, sharing, and archiving (e.g., the Cam-bridge Crystallographic Database [107], CrystalEye [108]). There are currently no technical obstacles to doing the same for polymer data. What is severely lacking, though, is an understanding of data ("I am a chemist and shouldn't have to worry about data (formats)") as such, a willingness to become educated, and community agreement on how to deal with scientific data.

Another challenge to data access is presented by the unstructured nature of the data contained in many documents. From "the point of view of a computer", an unstructured document is a collection of symbols without any semantics, i.e., the phrase "polystyrene has a glass transition temperature of 95° C" is, in the absence of further structuring data, i.e. metadata, meaningless and even the presence of data is hard to detect.

We have already discussed that a technical solution to this is to provide metadata in the form of markup. Markup can be introduced into a document either at the time

of authoring (a priori) or once the document has been prepared (a posteriori). As the authoring of markup is potentially complex, good semantic authoring tools are required. At the moment these are largely absent, although the Chem4Word project aims to fill this gap [87]. If markup is introduced a posteriori, one usually has to engage in a significant amount of "information archaeology" and utilize technologies such as natural language processing, entity extraction, and parts-of-speech tagging. An example of this is the OSCAR 3 system, which is currently being developed by Corbett and Murray-Rust and extended to polymers by Jessop and Adams [109]. OSCAR 3 is an open and extensible system for the automated markup of chemistry in documents. The markup is XML-based and designed to support browsing and chemistry-aware searching.

Table 1 shows an example of markup, generated using the OSCAR 3 system. The abstract of a polymer research paper has been parsed by OSCAR and the resulting markup for the first sentence of the abstract is shown in-line with the text (Table 1B). The first chemical entity encountered in the sentence is "oleic acid", which has been marked up as type = CM (Chemical Moiety) and a number of other annotations, such as in-line representations of chemical structure (InChI, SMILES) have been attached.

2.2.2 Access and "Political/Cultural" Access-Barriers

While any technical problems associated with access to polymer data can be overcome with comparative ease, the real access problem is politico-cultural in nature. We have already alluded to the fact that scientists often produce data for the single

Table 1 An abstract ([174]) (A) prior to markup, (B) after markup with OSCAR 3

(A) Elaboration of PLLA-based superparamagnetic nanoparticles: Characterization, magnetic behavior study and in vitro relaxivity evaluation Abstract. Oleic acid-coated magnetite has been encapsulated in biocompatible magnetic nanoparticles (MNP) by a simple emulsion evaporation method.

```
(B)<?xml version = "1.0" encoding = "UTF-8"?>
<PAPER><TITLE>Elaboration of PLLA-based superparamagnetic
nanoparticles: Characterization, magnetic behaviour
study and in vitro relaxivity evaluation.</TITLE> [175]
<ne surface= "Oleic acid" type= "CM" provenance=
"unknown" SMILES = "CCCCCCCC\C=C/CCCCCCCC(O)=O"
InChI="InChI=1/C18H34O2/c1-2-3-4-5-6-7-8-9-10-11-
12-13-14-15-16-17-18(19) 20/h9-10H, 2-8, 11-17H2, 1H3, (H,
19, 20)/b10-9-" cmlRef="cml1" ontIDs="CHEBI:16196">Oleic
acid</ne>-coated<ne surface="magnetite" type= "CM"
provenance="nGramScore" weight="0.09220993385201925">magnetite</ne>has
been encapsulated in biocompatible magnetic nanoparticles (MNP)
by a simple emulsion<ne surface="evaporation" type= "ONT"
provenance="oscarLexicon" ontIDs="REX:0000178">evaporation
</ne>method....</ABSTRACT>
```

purpose of accomplishing the aims of the research project they are working on at the time of data production. Once this has been achieved, the data produced during the project becomes virtually obsolete and its main value for the scientist lies in the proof of the fact that project work has been carried out at all and that it has been carried out with scientific integrity [110]. There is very little return in taking any further steps beyond "standard" journal publication to ensure that his data is easily accessible and reusable by other scientists, even when there are no commercial or other obstacles to data sharing.

Apart from very simple considerations of return or reward, the very system of scientific publishing, which science has evolved, now represents a *de facto* obstacle to data sharing and dissemination. Scientific publishing is historically a response to a scaling problem: in the early days of modern science, data and results were communicated through letters sent between scientists. With the growth of the community of scientists and the breadth of scientific endeavor, letter writing clearly did not scale any more and the twin institutions of the "learned society" and the scientific journal publication were developed [111]. The remit of the scientific journal was to collect manuscripts, to organize some form of verification of the "reasonableness" of the publication's content and to print and distribute the resulting journal issue. The journal subscription fee formed the economic basis of the system. Much of the value proposition of current STM publishing is still rooted in this business model. With the advent of the digital document, the internet and the set of technologies currently subsumed under the "Web 2.0" label, the economic foundation for this model has all but collapsed and the internet now fulfils many of the functions a traditional publisher used to perform. Document collection can be automated (users upload their digital manuscripts into an electronic workflow) as can, in principle, peer review (a weblog ("blog") with a commenting function is nothing other than a publication system with built-in peer review) and, of course, virtually cost-free publication and distribution can be achieved by simple publication of papers on a website. Pervasive computing and networks mean that the economic cost associated with each of these activities is minimal and tending towards zero. Publishers are therefore increasingly attempting to shift their value proposition to content and data: the subscription to an electronic journal is often redefined as a subscription to a database. This redefinition is particularly problematic because once the subscription is discontinued, so is access to the content. Physical copies of paper-based journals, by contrast, remain in the subscribing institution's library even after discontinuation of the subscription and access is therefore secure. The shift to content as the main value proposition is furthermore exemplified by what appears to be an attempt to apply copyright statements to factual data, which is now effectively preventing scientists from accessing their own data in all but the most technologically backward way.

Copyright was originally conceived to protect the property rights of an author and to facilitate the governance of the use of an expression of an idea, but neither the idea itself nor factual data. Although copyright subsists in the particular expression

of the idea of an anthropomorphic mouse (e.g., Mickey Mouse), copyright law does not stop other parties from developing different expressions of the same idea and from subsequent exploitation.

This discussion is relevant here, because the act of publication of a scientific paper containing polymer data means that the publisher merely owns the expression of the facts and data, but not the fact or the data itself. Unfortunately, publishers increasingly appear to attempt to claim copyright on scientific data by attaching copyright statements to, for example, supplementary data which is almost completely factual. In an optimistic interpretation of these practices, one might assume that it only gives an impression that the data is copyrighted and the copyright statement merely refers to the layout of the supplementary information. In the worst possible interpretation, this can be viewed as a data grab by the publishers, who are trying to erect barriers to data access which universities or private institutions would not have the appetite to test in court. The practice of appending copyright statements to supplementary information in any case obfuscates the data access situation. Other disciplines, such as biology, environmental science, and physics, have long evolved both a discipline and an ethics of data sharing and open access to data. Although there are examples to the contrary (e.g., PubChem), chemistry and polymer science are astoundingly backward in their approach and attitude to caring about their data as well as to sharing and dissemination. Ultimately, the successful development of polymer informatics will require access to polymer data and hence a culture of "data awareness" and sharing needs to be developed in the polymer science community.

3 Making Use of Polymer Data

Another aspect of polymer informatics, beyond the representation and registration of polymer information and data, is the conversion of data into knowledge and thus into the power to make decisions. To this end, the same tools, which are common in small molecule informatics, have also been used to study polymer data. The work that has been reported so far subdivides into two categories, namely classification and chemometrics problems and property prediction.

3.1 Classification and Chemometrics Problems

The rapid classification of polymeric species is an important problem in the area of analytical chemistry in general and of particular relevance to recycling and waste management. To accomplish classification tasks, a combination of spectral data and principal component analysis (PCA) is often employed.

Principal component analysis is a simple vector space transform, allowing the dimensionality of a data set to be reduced, while at the same time minimizing

the concurrent information loss [112–114]. In essence, PCA transforms data from one coordinate system to another in such a way that the greatest data variance comes to lie on the first axis of the new coordinate system (the first principal component with the highest eigenvalue), the second largest variance on the second axis (the second principal component) and so forth. There are as many principal components in the system as there are dimensions. Data reduction is achieved by discarding components with variances below a certain threshold.

Van den Eynde and Bertrand described the use of PCA for the determination of molecular weights from time-of-flight secondary ion mass spectrometry (ToF-SIMS) spectra of polystyrene samples [115]. ToF-SIMS spectrometry is well established for the characterization of polymer surfaces, but the quantification of the resulting spectra has proved to be difficult. In a previous study, the authors had recognized an influence of the molecular weight of their polymer samples on the intensities of observed secondary ions. In the present study, the researchers used 18 polystyrene samples of different molecular weights and different butyl endgroups (*n*-butyl, *sec*-butyl, *tert*-butyl), which were spin-coated onto silicon wafers and subsequently subjected to ToF-SIMS analysis. After pre-processing, the spectral data was subjected to PCA. The results showed, that the first two principal components were sensitive to both the molecular weight and the chemical structure of the endgroups. The most significant ions in the spectrum can be detected from the corresponding loading plots and the score plots allow samples to be categorized in terms of end-group structure and molecular weights. Furthermore, a universal calibration curve could be found by plotting the first principal component, which is independent of the structure of the endgroup, as a function of molecular weight. This can then be used for the determination of the molecular weight of an unknown polystyrene sample from its secondary ion mass spectrum. A similar approach was reported for the characterization of hyperbranched aliphatic polyesters [116].

Batur et al. also used a number of machine learning tools, including PCA, and a set of different experimental techniques in a bid to quantify the crystallinity of low-density polyethylene (LDPE) films [117]. In a multistep experiment, a first set of training data was produced by heating a thin film of LDPE to 120°C in order to produce a completely amorphous sample. The sample was then cooled in steps of 2°C and a Raman spectrum was recorded at each temperature step. The spectra were subsequently used as inputs for principal component analysis and neural network modeling. The inputs were correlated to crystallinity values derived from small angle light scattering (SALS) experiments, which were carried out at the same time and calibrated by DSC. The authors developed a linear regression model of crystallinity by correlating the factor loadings of the significant factors to the experimentally determined crystallinity values. It could be shown, that models determined in this way validated well with respect to experimental data and also predicted the crystallinities of test samples subjected to different cooling rates with satisfactory accuracy. Modeling using neural networks led to comparable results.

Miranda et al. used a combination of Fourier-Transform Infrared Spectroscopy (FT-IR) and PCA to elucidate the chemistry that occurs when poly(vinyl alcohol)

(PVA) is cross-linked under ultraviolet (UV) irradiation using sodium benzoate as an initiator [118]. An aqueous solution of PVA and sodium benzoate was cast onto a glass plate and the solvent was allowed to evaporate. After irradiation of the samples for 1, 2, 3, and 4 h, the IR spectra of the films were determined and analyzed by PCA. A detailed analysis of the scores and loadings led to the conclusion that upon irradiation the sodium benzoate is decomposed in an initial step. The resulting radical subsequently abstracts a hydrogen atom from the PVA chain to produce a polymeric radical. The latter reacts with available hydroxy groups to form ether bond linkages between PVA chains. Furthermore, it was found that there is a good linear correlation between the mean of the scores of one of the significant principal components and irradiation time, which means that the irradiation time of an unknown sample can be determined from the IR spectrum.

The use of PCA for the classification of both natural and synthetic polymers was demonstrated by Vazquez et al. [119]. In their work, the researchers recorded Total X-Ray Fluorescence (TXRF) spectra of scleroglucan, xanthan, glucomannan, poly(ethylene oxide), and polyacrylamide and subjected the resulting spectral data to PCA. To the naked eye, the X-ray fluorescence spectra of the polymers look virtually identical. However, when subjected to PCA it could be shown that the first two principal components contain approximately 96% of the variance in the dataset. When plotting the scores of the two components against each other, six distinct clusters are observed, which clearly differentiate the individual polymers.

Principal Component Regression (PCR) was used by Tuchbreiter and Muelhaupt to determine the composition of a number of random ethane/propene, ethane/1-hexene, and ethane/1-octene copolymers [120]. After polymerization, the polymers were characterized by both Attenuated Total Reflection Fourier Transform Infrared Spectroscopy (ATR-FT-IR) and ^{13}C NMR and multivariate calibration models using PCR were subsequently developed to estimate the co-monomer content.

The data generated by other experimental techniques is also amenable to decomposition/analysis by PCA. Lukasiak et al. reported the use of several classification techniques, such as PCA, k-means and hierarchical clustering, linear discriminant analysis, k-nearest neighbors as well as distance metrics using Euclidean and Mahalanobis measures on data generated by Dynamic Mechanical Analysis (DMA) of several types of polymers (polypropylene, LDPE, polystyrene, acrylonitrile-butadiene-styrene) of several different grades [121]. In their paper, the authors determined the damping factor (tan δ) of the polymers as a function of temperature and showed that this data, in combination with several of the machine learning techniques listed above, can be used to classify polymers into types and grades.

All of these studies suffer from the fact that they were carried out on relatively small datasets of more or less homogeneous polymers and are generally not well validated. As such, they indicate that there may be useful chemometric methods here, but there is considerable scope for further studies on much larger and heterogeneous sample sets to demonstrate general applicability and usefulness.

3.2 Property Prediction

A more common use of informatics for data analysis is the development of (quantitative) structure-property relationships (QSPR) for the prediction of materials properties and thus ultimately the design of polymers. Quantitative structure-property relationships are multivariate statistical correlations between the property of a polymer and a number of variables, which are either physical properties themselves or descriptors, which hold information about a polymer in a more abstract way. The simplest QSPR models are usually linear regression-type models but complex neural networks and numerous other machine-learning techniques have also been used.

Two very simple types of QSPR have been developed early on in the evolution of polymer property prediction, namely van Krevelen's group contribution methods [122] and Bicerano's system [123], which mainly relies on the use of topological descriptors. Group contributions regard the overall properties of the polymer as the scalar sum of the properties of the chemical groups contained in the molecules making up the polymer.

While both the Bicerano and van Krevelen systems model a significant number of polymer properties, most QSPR studies have focused on only a small number of key properties (which is mainly correlated to the availability of data for model development).

3.2.1 Glass Transition Temperature (T_g)

The glass transition temperature is a central property of polymers and of considerable importance in both fundamental polymer science as well as polymer engineering and processing. Below the glass transition temperature, macromolecules in bulk are fairly rigid, as they only have the freedom to vibrate and oscillate around fixed positions, creating a small amount of free volume. Significant translational movement, however, is usually not possible. The glass transition occurs at the temperature at which the free volume in the bulk material becomes large enough for macromolecular chains to move relative to each other. At this point the polymer backbone relaxes and the material undergoes a transition from a solid to a quasiliquid state [124].

Van Krevelen's group contributions are widely used for the prediction of T_g and perform reasonably well. When experimentally determined T_g values for 600 polymers are compared to predictions from group contributions, it could be shown that approximately 80% of the calculated T_g values were within $\pm 20\,\mathrm{K}$ of the experimental result [122]. A serious limitation of any group contribution method, however, is that only polymers with structural groups for which contributions have been developed can be predicted.

The group contribution methodology was extended by Hopfinger and Koehler through combination with molecular modeling [125, 126]. In these papers the main determinants of the glass transition temperature are considered to be the

conformational entropy and mass moments of the polymer, which the authors estimate from molecular mechanics and conformational energy calculations. Results show, that T_g can be correlated with the intramolecular flexibility of the polymer chain, which can be broken down into linear contributions of conformational entropies of the repeat units and intermolecular interactions arising mainly from electrostatics.

Katritzky and co-workers reported a descriptor-based attempt to develop QSPR models of T_g for low-molecular weight homopolymers [127]. The authors used the CODESSA suite [128] to calculate a set of 238 molecular descriptors for a set of 22 simple homo- and co-polymers with little structural diversity. To eliminate highly correlated descriptors, a pairwise comparison of descriptors was carried out and only those with descriptors with pairwise correlation coefficients $R_{ij}^2 < 0.1$ were used for the development of QSPR models. Linear regression techniques produce a four parameter model with important contributions from descriptors such as DPSA (the difference between the positive and negative partial surface areas normalized by the number of electrons), the topological Randic index, the number of OH groups present in the molecules, and the partial negative charge surface area weighted by the total charge. The authors point out that molecules with large DSPA values have stronger intermolecular electrostatic interactions and thus higher glass transition temperatures. The Randic index can be interpreted to be a measure of branching of the molecule. The regression model determined by the authors suggests, that the higher the degree of branching, the higher T_g, which is commensurate with our current understanding of the glass transition temperature in polymers. The appearance of the OH group count may be specific to the set of polymers chosen by the researchers, but could also be interpreted as a measure of the hydrogen bonding in the system. The partial negative surface area, like the DSPA descriptor, may be interpreted to be a measure of the electrostatic interactions between polymer chains. Unfortunately, the authors do not provide any type of validation of their QSPR model, and therefore it is difficult to assess how general the model is.

A subsequent paper expands this work by considering a larger and more diverse set of polymers and by validating constructed models [129]. The work only considers linear polymers and uses trimers as input models. Descriptors were again calculated using the CODESSA package on the middle fragment of the trimer. Linear regression modeling gave rise to a five-parameter model. The most significant descriptors were found to be the moment of inertia (measuring the mass distribution around the principal axis of rotation), the Kier shape index (coding for the number of skeletal atoms, molecular branching etc.), the most negative atomic charge in the molecule, the HSA/TSFA descriptor (measuring hydrogen bond forming ability), and the fractional positive partially charged surface area (describing electrostatic interactions between molecules), thus confirming the physical picture emerging from the first study. While the reported correlations are good ($R^2 = 0.946$, $R_{cv}^2 = 0.938$ for the best model) and additional cross-validation was also satisfactory, no validation using a text/external data set (i.e., data not used for developing the regression model) was reported, which again makes it somewhat difficult to assess the stability of the model. The standard error of prediction was 32.9 K.

Yet another expansion of this work was reported by Cao et al. who developed a set of descriptors based on the rotation of the polymer side chain, the bond count of the freely rotating part of the side chain, the polarizability effect index, and a descriptor containing information relating to hydrogen bonding [130]. The authors applied the descriptors to the polymer set reported by Katritzky and found good correlations between predicted and observed values with a standard deviation of approximately 21 K and an absolute average error of 15.30 K. While this is somewhat better than the results obtained by Katritzky, it is still a very significant error and underlines the difficulty associated with the task of accurately predicting the glass transition temperature for polymers.

An attempt to design polymers with specific properties, thus solving the "inverse" structure-property relationship problem, was presented by Reynolds in an elegant piece of work [131]. In a first step, Reynolds constructed a library of 17 polymers, chosen from a larger collection of 112 diphenol/diacid condensation polymers, using a diversity search method in order to derive quantitative structure-property relationships for T_g and the contact angle (CA). The QSPRs were then evaluated against the remaining polymers in the large library and could be shown to be performing well ($R^2 = 0.89$, RMS error $= 7$ K (validation set)). In a subsequent step, the validated models were used to build focused libraries of new condensation polymers with specific glass transition temperatures and contact angles.

Following on from Reynolds' work, Brown and co-workers also developed a solution to the inverse QSPR problem using models built on the signature molecular descriptor and targeting polymer properties such as T_g, heat capacity, density, molar volume, and cohesive energies [132]. The "forwards" equations are comparable to other work discussed here in terms of predictive ability. The researchers subsequently use their models to "design" polymers within a given property target range and to validate their approach by the "re-disovery" of Nylon-6,10 from an inverse QSPR model.

Apart from regression techniques, artificial neural networks (ANNs) have also been investigated for the development of predictive systems for T_g. ANNs are mathematical constructs, which are designed to mimic loosely information processing in the brain and in particular the functions of neurons [133] and are commonly used in statistics to model complex and often non-linear relationships between data. While there is a plethora of different neural network architectures, there are some common features. All neural networks have a number of interconnected processing nodes, which store knowledge by a dynamic response to external inputs and also make information available for use [134]. Knowledge is contained in the weighted distribution between processing nodes and a learning algorithm is used to determine and change the weights of the processing units during the learning process (Fig. 12).

In an early paper, Osguthorpe et al. investigated the use of ANNs of several different architectures for the prediction of the glass transition temperature of linear homopolymers, using descriptor values computed from the structure of the corresponding monomers [135]. The problem with any prediction from a monomer structure is, of course, that it ignores the history of a polymer, which can significantly influence its glass transition temperature as well as physical factors such as
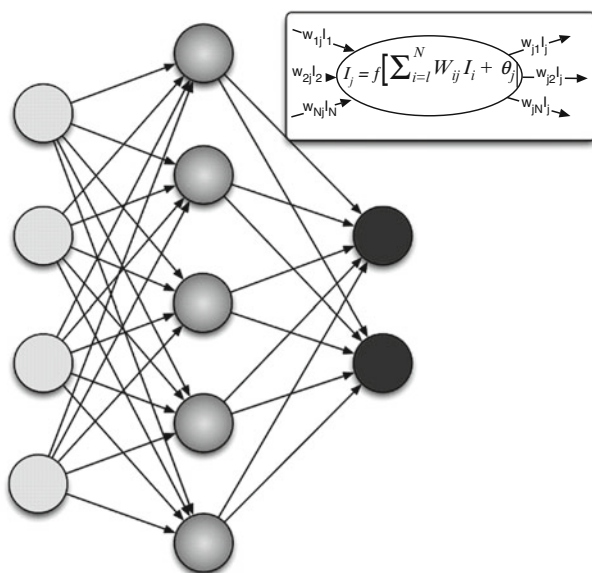
Fig. 12 The structure of a simple ANN together with an illustration of neuron microstructure (*inlaid box*)

Fig. 13 General chemical structure of the Brocchini-Kohn Library of polyarylates (R, Y = points of structural variability in the pendent chain and the backbone) [3]
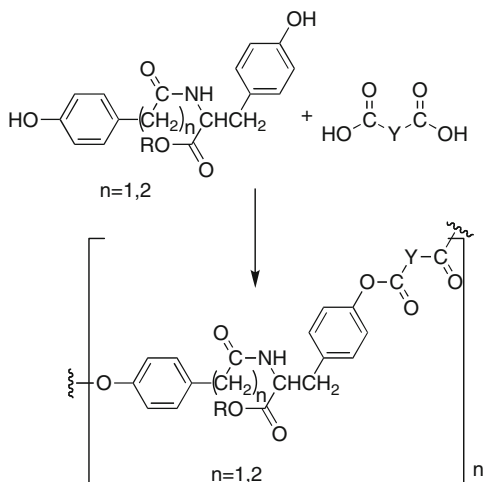
the molecular weight dependence of T_g and others. Consequently, the best result obtained by this approach gives RMS errors of 35 K in a validation set with maximum errors as large as 130 K. Nevertheless, and probably as expected, the study shows that the monomer does carry some information about the glass transition temperature of the corresponding polymer.

In a subsequent study, Mattioni and Jurs compared prediction approaches, which take the structure of a monomer as an "input structure" vs those starting from the

polymer repeating unit structure [136]. In the first part of their study, numerical descriptors for a set of 165 monomers were calculated and the set was subsequently split into a training and test set. The best linear regression model was a 10-component model with an RMS error of 25.87 K in the training set and 26.68 K in the test set. The authors found that descriptors which encode molecular size and branching were particularly relevant as was a descriptor counting the number of single bonds in the monomer molecule (which may hold information about the degree of flexibility of the corresponding polymer backbone). The most relevant descriptors from linear modeling were used as inputs into several NNs with different architectures. The best NN-generated models produced an RMS error of 15.67 K for the training and 21.76 K for the test set, which is an improvement when compared to Osguthorpe's work. The use of genetic algorithms or simulated annealing procedures to select relevant input descriptors did not lead to a significant improvement in prediction accuracy of the NNs. In the second part of the study, descriptors derived from the repeating unit structure of a macromolecule were used. The best linear models constructed from this data had RMS errors of 40.06 K in the training and 43.16 K in the test set, which is significantly worse than the results achieved using the monomer structures. The use of neural networks improves the situation somewhat with RMS errors of 27.33 K and 32.96 K for training and test set. For models derived from repeating units, the use of descriptors selected using feature selection methods, in particular simulated annealing, as inputs led to significant improvements in performance with the best NN models achieving RMS errors of 21.14 and 21.94 for training and test sets respectively.

An unconventional approach to the prediction of T_g (other properties, such as degradation temperature, tensile strength, Izod impact, Rockwell hardness, compressive strength, maximum elongation and refractive index were also considered) using neural networks was presented by Ulmer et al., who combined the use of "custom" descriptors for polymers with the notion of bootstrap cross-validation and "property experts" in an attempt to develop new polycarbonate polymers with defined physical properties [137]. The authors argue that traditional topological and theoretical descriptors do not provide an optimum way to represent polymers, as they tend to neglect aspects of polymer structure such as tacticity, entanglement, cross-linking, etc. They therefore introduce a new type of vector representation of molecular structure and atomic composition, which is referred to as "Hamiltonian Interaction Modeling" (HIM). HIM is based on the assumption that the combination of inter- and intramolecular interactions describes the behavior of both the atomistic and the condensed phase of a polymer. A "molecular Hamiltonian" for a repeating unit is constructed by fusing descriptions of atomic, valence and mass connectivity with an interaction site model based on cell models and the polymer reference interaction site model (PRISM) [138]. This yields several descriptors, which are used as inputs into neural networks using "bootstrap resampling". Furthermore, the authors compared the HIM descriptors to other descriptor systems, such as the Porter [139] and Bicerano [123] descriptors. Bootstrap resampling is used to subdivide the dataset into a training and test set. The algorithm works by creating a new dataset of N data points by randomly sampling an original dataset N times with the possi-

bility of sample repetition. Unique training sets are generated by comparing the sets produced by bootstrap resampling to the original dataset and selecting only unique data points. Once a significant number of training and test sets have been created in this way, neural networks are trained for each training set and evaluated against an ensemble of test sets. Predicted values for the property under consideration are then produced by averaging over the output of each of the individual networks. The trained networks were used to design novel bisphenol A polycarbonate (BPAC) polymers with increased impact resistance.

Afantitis et al. investigated the use of radial basis function (RBF) neural networks for the prediction of T_g [140]. Radial basis functions are real-valued functions, whose value only depends on their distance from an origin. Using the dataset and descriptors described in Cao's work [130] (see above), RBF networks were trained. The best performing network models showed high correlations between predicted and experimental values. Unfortunately the authors do not formally report an RMS error, but a cursory inspection of the reported data in the paper would suggest approximate errors of around 10 K.

A slew of almost identical papers by a Chinese group reported the use of quantum mechanical methods for the calculation of descriptors for several classes of polymers and their subsequent correlation to the glass transition temperature and other polymer properties via artificial neural networks [141–144]. The general conclusions, which can be drawn from these contributions are that NNs usually show better performance in predicting glass transition temperatures than regression models, and that descriptors which codify for inter- and intramolecular interactions, conformational freedom and the presence and size of a side chain, are the most suitable for predicting T_g. This confirms results from prior studies using computationally less expensive methods.

Solaro et al. reported the use of a direct structure representation (chemical trees), rather than descriptors, as an input into a recursive neural network using a narrow dataset composed of methacrylate polymers containing alkyl, thioalkyl and fluoroalkyl ester groups as well as polyacrylamides and α-substituted polyacrylics. This seems to lead to good prediction results in both training and test sets, though further validation using larger and more diverse datasets will be required [145].

3.2.2 Refractive Index

The refractive index is another important polymer property and is defined as the ratio of the velocity of light traveling in a vacuum to that of light traveling in a material [123]. As polymers are increasingly used in optical applications, this quantity is of considerable importance. The refractive index is also an important quantity in light scattering experiments which, in turn, are used for the determination of molecular weights, molecular shapes, and molecular dimensions. As is the case for all major polymer properties, both the van Krevelen [122] and Bicerano [123] methodologies allow the estimation of the quantity.

One of the first QSPR models was developed by Katritzky using a dataset consisting of 95 mainly homochain polymers, though polyoxides, polyamides, and polycarbonates were also represented [146]. The homochain polymers subdivide into polyethylenes, polyacrylates, polymethacrylates, and polystyrenes. The model was developed from standard CODESSA descriptors using multilinear regression, which gave rise to a five-parameter equation ($R^2 = 0.940, s^2 = 0.00013$). The significant parameters are the HOMO-LUMO energy gap, the AM1 heat of formation, the maximum nuclear repulsion for a C–H bond, the partial negative surface area, and the relative number of fluorine atoms. The researchers interpret the presence of the AM1 heat of formation and the positive contribution this factor makes to the "looseness" of electrons in the molecule and therefore to a greater amount of freedom to interact with light. They note that less stable compounds have higher refractive indices. The presence of the maximum nuclear repulsion energy for C–H bonds is taken to encode information containing the hybridization state of the carbon atoms in the molecule and thus presumably also holds information concerning how electromagnetic radiation interacts with the electrons contained in the molecules. The partial negative surface area encodes information about the charge distribution and thus the size of the repeating unit. The presence of the fluorine atom count can be rationalized by the very unusual electronic properties this atom imparts on molecules (fluorinated polymers have unusually low refractive indices).

Subsequent work was mainly reported by a cluster of Chinese workers who outlined the development of a four-parameter model [147], the use of descriptors derived from high-level density functional theory calculations [148], the use of cyclic dimer structures rather than repeat unit structures for the purposes of descriptor calculation [149], and the development of a more specialized QSPR model for the refractive indices of conjugated polymers [150] and vinyl polymers [148]. For the purposes of the development of their four-parameter model, Xu et al. used monomer structures rather than repeating unit structures. While they do not report the details of the software used to calculate their descriptors, four quantities seem to be of importance: the sum of the valence degrees, the degree of unsaturation, the relative number of halogen atoms, and the intermolecular electrostatic attraction or hydrogen bonding of the molecules. Conceptually, many of these descriptors encode similar types of information as those used by Katritzky et al. and thus support earlier findings. There is, however, only a marginal improvement of predictive accuracy. The other papers in this series mainly confirm and repeat these results without adding significant new insights or improvements in predictive ability.

3.2.3 Lower Critical Solution Temperature (LCST)

The lower critical solution temperature is another crucial polymer property, which, together with the Upper Critical Solution Temperature (UCST), defines the two solubility boundaries of polymers in solution. Typically, systems are completely miscible below the LCST but only partially miscible above the LCST and completely immiscible above the UCST.

Liu and Zhong introduced a number of QSPR models based on molecular connectivity indices [151, 152]. In a first iteration, the researchers developed polymer-dependent correlations: descriptors were calculated for a set of solvents and models were developed per polymer type [151]. Polymer classes under consideration were polystyrene, polyethylene, poly-1-butene, poly-1-pentene, poly(4-methyl-1-pentene), polydimethylsiloxane, and polyisobutylene. As the authors fail to provide any validation for their models, it is difficult to asses their predictive power. In a subsequent iteration and general expansion of this study, mixed and therefore more general models based on the calculated connectivity indices of both solvent and polymers were developed. While it is unclear from the paper which polymer representation was used for the calculation of the connectivity indices, the best regression model (eight parameter model) yields only acceptable predictive power ($R^2 = 0.77$, $R^2_{cv} = 0.77$, $s = 34.47$ for the training set, $R^2 = 0.75$ for a test set) [152]. Using the same dataset, Afantitis and co-workers subsequently expanded this work by expanding the descriptor space and providing more rigorous validation [153]. The researchers produced a nine-parameter model, which shows improvements over the equation put forward by Liu et al. ($R^2 = 0.8860$, $R^2_{cv} = 0.8546$ for the training set, $R^2 = 0.8738$ for the test set). Xu et al. tested the dataset previously used by Liu and Afantitis using a set of 199 topological Dragon descriptors [154]. This leads to a linear 10-factor model which shows approximately the same predictive power as that developed by Afantitis et al. ($R^2 = 0.8874$, $R^2_{cv} = 0.8658$, $s = 24.57$). In a further paper, Xu et al. investigated an even larger descriptor set and the use of neural networks for the prediction of LCSTs [155]. The researchers showed that the development of an initial linear model on the basis of the enlarged descriptor space does not lead to significant improvements in predictive ability in comparison to earlier work, but that the use of neural networks can lead to further improvements in the predictive ability of a model ($R^2 = 0.9625$, $s = 13.43$ for the training and $R^2 = 0.9524$ for the test set). The obvious drawbacks here are the lack of interpretability and reproducibility of neural network models.

3.2.4 Intrinsic Viscosity

Like the lower critical solution temperature, the intrinsic viscosity of a polymer solution is dependent on both the nature of the polymer and that of the solvent. The intrinsic viscosity contains information about the volume associated with a given amount of polymer in dilute solution and thus encodes information about the conformational properties of a polymer chain. The quantity is therefore of importance for those engaged in both polymer synthesis and processing [123, 156]. Using the same methodology the researchers exploited for the development of their LCST model, Afantitis et al. report the construction of a linear eight-component model for the intrinsic viscosity [157]. The correlation was developed using a dataset containing 65 different polymer-solvent combinations and 10 different polymers. A total of 30 physicochemical, topological, and structural descriptors were calculated and the polymers were represented as their corresponding monomers for the purposes

of descriptor generation. As was the case with LCST, the prediction of the intrinsic viscosity is difficult: the best performing model showed $R^2 = 0.759$, $R^2_{cv} = 0.601$, and a root mean square (RMS) error of 34.67 for the training set ($R^2 = 0.751$, RMS $= 49.39$, test set). Both the HOMO and LUMO values as well as the topological index of the solvent and the principal moment of inertia along the x-axis of the solvent, together with the dipole length, Conolly molecular surface area, the LUMO energy, and the molecular weight of the polymer are significant factors, thus indicating that the intrinsic viscosity depends on the molecular weights of both the polymer and that of the solvent, the polymer and solvent structure, the interactions between polymer and solvent as well as the electronic properties of both polymer and solvent.

Gharagheizi subsequently expanded the work by Afantitis et al. by expanding the descriptor space (calculating 1664 descriptors for both solvent and polymer) and investigating the use of radial basis function neural networks, but using the same data set. Parameter selection through genetic-algorithm based multilinear regression leads to a five-parameter model with an $R^2 = 0.8112$ and $R^2_{cv} = 0.7714$. The important descriptor types in this model are electrotopological state descriptors (polymer), information content descriptors (polymer), radial distribution function descriptors (polymer), as well as a weighted total accessibility index descriptor (solvent). When these descriptors are used as inputs into a neural network, a further improvement in R^2 can be observed.

3.2.5 Biomaterials

Polymer-based biomaterials are becoming increasingly important, whether they are used as medical supplies (pipes, catheters, bags), prostheses, or dental materials, or in a pharmaceutical context as drug conjugates [4, 7, 158–160], protein conjugates [6, 158, 159, 161], synthetic vectors [12, 14, 18, 162, 163], or as immuno-adjuvants [164, 165].

Early and prescient work to develop correlations between biological observables and the physico-chemical properties of polymers were reported by Brocchini and Kohn [3, 32, 166]. Prior to the development of the models, the authors had been engaged in the combinatorial synthesis of a 112-member library of polyarylates, prepared through the condensation of diphenols with diacids (Fig. 12).

The library was evaluated with respect to a number of physicochemical properties such as glass transition temperatures and contact angles, and a number of correlations were developed. Furthermore, the polymers in the library were screened with respect to fibrinogen absorption and fibroblast proliferation on a thin polymer film and good correlations between proliferation, contact angle, and the backbone architecture of the polymer could be established: fibroblasts proliferate effectively when seeded on polymers in which oxygen substitutions are present in the side chain and the main chain and when the contact angle is large. However, proliferation decreases upon increasing contact angle in the absence of oxygen substitution. More recently, Kohn et al. built on this work and reported the in silico design and preparation of

a polymethacrylate library. The library was screened against fibrinogen adsorption and the attachment and growth of fibroblast-like NIH3T3 cells. Descriptors were calculated on the polymer structures using the Molecular Operating Environment (MOE) program and models were developed using polynomial neural networks. While validation data are provided, the authors fail to communicate both the models they developed and the precise nature of some of the descriptors involved in the correlations (presumably for commercial reasons). This makes the comparison and assessment of this work difficult though the authors assert that factors similar to those observed for the polyarylates, namely the hydrophilicity/hydrophobicity of the polymer and the presence of heteroatoms as well as measures of electrostatic behavior, make a significant contribution to the models describing the biological responses [167].

3.2.6 Other Polymer Properties

There have been isolated QSPR studies of a number of other polymer properties. These include the dielectric constant [144], the dielectric dissipation factor (tan δ) [168], the solubility parameter [169], the molar thermal decomposition function [170], the vitrification temperature of polyarylene oxides [171], and quantities relating to molecularly imprinted polymers [172, 173]. The interested reader is referred to the literature for further information.

4 Summary and Conclusions

Informatics in the domain of polymer science is an exciting and multifaceted challenge. Many problems remain unsolved: there are still significant issues in the representation of fuzzy materials such as polymers. The move away from the paradigm of the connection table is absolutely necessary, but also requires a rethink of the traditional ways of information representation in chemistry. Some of the technological solutions may be found in the realm of the semantic web, which is already impacting the way in which scholarly information and scientific data are communicated and transmitted. The main problem, however, is a cultural one: unlike in other disciplines, there is currently no culture of data sharing and data re-use in chemistry and much of the materials sciences. Furthermore, the current scholarly publication process is profoundly dysfunctional – even scientists who wish to share data do not currently have the tools or the infrastructure to do so. All of this directly impedes the development of polymer informatics. In spite of all of these obstacles, work to tackle both the technological and cultural problems associated with polymer data is ongoing. Work is being carried out which attempts to relate polymer properties to their (chemical structure) representation. One should therefore remain optimistic, that progress towards the ultimate goal, namely the use of informatics to aid the understanding of the physico-chemical behavior of polymers and their *in silico* design is inexorable.

References

1. Yoshida M, Langer R, Lendlein A et al. (2006) From advanced biomedical coatings to multi-functionalized biomaterials. Polym Rev 46:347–375
2. Dewez JL, Lhoest JB, Detrait E et al. (1998) Adhesion of mammalian cells to polymer surfaces: from physical chemistry of surfaces to selective adhesion on defined patterns. Biomaterials 19:1441–1445
3. Brocchini S, James K, Tangpasuthadol V et al. (1998) Structure-property coorrelations in a combinatorial library of degradable biomaterials. J Biomed Mat Res 42:66–75
4. Cuchelkar V, Kopecek J (2006) Polymer-drug conjugates. In: Uchegbu IF and Schaetzlein AG (ed) Polym Drug Deliv, CRC Press, Boca Raton
5. Torchilin VP (2006) Polymorphic micelles as pharmaceutical carriers. Polym Drug Deliv 111–130
6. Haag R, Kratz F (2006) Polymer therapeutics: concepts and applications. Angew Chem Int Edn 45:1198–1215
7. Khandare J, Minko T (2006) Polymer-drug conjugates: progress in polymeric prodrugs. Prog Polym Sci 31:359–397
8. Way JL, Petrikovics I, Jiang J et al. (2001) Application of dendrimeric polymers as a drug carrier in pharmacology. Abstracts of Papers, 221st ACS National Meeting, San Diego, CA, United States, April 1–5, 2001 IEC-316
9. Kataoka K, Kwon GS, Yokoyama M et al. (1993) Block copolymer micelles as vehicles for drug delivery. J Contr Rel 24:119–132
10. Malmsten M (2006) Soft drug delivery systems. Soft Matter 2:760–769
11. Qiu LY, Bae YH (2006) Polymer architecture and drug delivery. Pharm Res 23:1–30
12. Kang HC, Lee M, Bae YH (2007) Polymeric gene delivery vectors. In: Peppas NA, Hilt JZ, Thomas JB (ed) Nanotechnology in therapeutics Taylor and Francis, New York
13. Alexis F, Zeng J, Wang S (2007) PEI nanoparticles for targeted gene delivery. Gene Transfer 473–478
14. Leong KW (2006) Polymer design for nonviral gene delivery. BioMEMS Biomed Nanotechnol 1:239–263
15. Mahato RI (2005) Water insoluble and soluble lipids for gene delivery. Adv Drug Deliv Rev 57:699–712
16. Mahato RI, Kim SW (2005) Water soluble lipopolymers for gene delivery. In: Ammiji MM (ed) Polym Gene Deliv, CRC Press, Boca Raton
17. Adams ML, Lavasanifar A, Kwon GS (2003) Amphiphilic block copolymers for drug delivery. J Pharm Sci 92:1343–1355
18. Wagner E, Kloeckner J (2006) Gene delivery using polymer therapeutics. Adv Polym Sci 192:135–173
19. Joester D, Losson M, Pugin R et al. (2003) Amphiphilic dendrimers: novel self-assembling vectors for efficient gene delivery. Angew Chem Int Ed 42:1486–1490
20. Bjornerg HC, Derici L, Haggman BH et al. (2006) Hair care compositions comprising a dendritic polymer. 2005-EP7017 2006018064
21. Derici L, Harcup JP, Khoshdel E (2006) Hair care composition comprising a dendritic macromolecule. 2005-EP7016 2006018063
22. Goosey M (2007) An overview of polymers as key enablers in electronics assembly-a printed circuit board perspective. Polymers in Electronics 2007: Paper9/1-Paper9/5, Munich, Germany
23. Rost H (2007) Printed electronic circuits. Kunstst 97:97–101
24. Xing R-b, Ding Y, Han Y-c (2007) Patterning of polymer by inkjet printing and its application in the fabrication of organic electronic devices. Fenzi Kexue Xuebao 23:75–81
25. Liang Z, Wang Q (2007) Patterning of conjugated polymers for organic electronics and opto-electronics. In: Naiwa HS (ed) Polym Nanostruct Their Appl, American Scientific Publishers, Stevenson Ranch, California

26. Bock K (2005) Polytronics – electronics and systems on flexible substrates. IEEE VLSI-TSA International Symposium on VLSI Technology, Hsinchu, Taiwan, pp 53–56
27. Stafford N (2007) Large-scale biopolymer production. http://www.rsc.org/chemistryworld/News/2007/May/14050701.asp, Accessed Dec 12 2008
28. Zhang H, Hoogenboom R, Meier MAR et al. (2004) High-throughput experimentation in polymer chemistry. Trans Mater Res Soc Jpn 29:319–324
29. Zhang H, Hoogenboom R, Meier MAR et al. (2005) Combinatorial and high-throughput approaches in polymer science. Meas Sci Technol 16:203–211
30. Hoogenboom R, Fijten MWM, Wijnans S et al. (2006) High-throughput synthesis and screening of a library of random and gradient copoly(2-oxazoline)s. J Comb Chem 8:145–148
31. Hoogenboom R, Schubert US (2005) High-throughput synthesis equipment applied to polymer research. Review of Scientific Instruments 76:062202/062201–062202/062207
32. Brocchini S, James K, Tangpasuthadol V et al. (1997) A combinatorial approach for polymer design. J Am Chem Soc 119:4553
33. Wiesbrock F, Hoogenboom R, Leenen MAM et al. (2005) Investigation of the living cationic ring-opening polymerization of 2-methyl-, 2-ethyl-, 2-nonyl-, and 2-phenyl-2-oxazoline in a single-mode microwave reactor. Macromolecules 38:5025–5034
34. Wiesbrock F, Hoogenboom R, Abeln CH et al. (2004) Single-mode microwave ovens as new reaction devices: accelerating the living polymerization of 2-ethyl-2-Oxazoline. Macromol Rapid Commun 25:1895–1899
35. Gilman JW, Bourbigot S, Shields JR et al. (2003) High throughput methods for polymer nanocomposites research: extrusion, NMR characterization and flammability property screening. J Mat Sci 38:4451
36. Davis RD, Bur AJ, McBearty M et al. (2004) Dielectric spectroscopy during extrusion processing of polymer nanocomposites: a high-throughput processing/characterization method to measure layered silicate content and exfoliation. Polymer 45:6487–6493
37. Gilman JW, Davis RD, Bellayer S et al. (2005) Use of optical probes and laser scanning confocal fluorescence microscopy for high-throughput characterization of dispersion in polymer layered silicate nanocomposites. PMSE Prepr 92:168–169
38. Gilman JW, Davis RD, Shields JR et al. (2004) Development of high-throughput methods for polymer flammability property characterization. International SAMPE Symposium and Exhibition:460–469
39. Gilman JW, Maupin PH, Harris RH et al. (2004) High throughput methods for nanocomposite materials research. Extrusion and visible optical probes. PMSE Prepr. 90:717–718
40. Adams N, Moneke M, Gulmus SA et al. (2006) Combinatorial compounding. Mater Res Soc Symp Proc 894:171–179
41. Kranenburg JM, Tweedie CA, Hoogenboom R et al. (2007) Elastic moduli for a diblock copoly(2-oxazoline) library obtained by high-throughput screening. J Mater Chem 17:2713–2721
42. Kranenburg JM, van Duin M, Schubert US (2007) Screening of EPDM cure states using depth-sensing indentation. Macromol Chem Phys 208:915–923
43. Cheung K-H, Yip KY, Townsend JP et al. (2008) HCLS 2.0/3.0: health care and life sciences data mashup using Web 2.0/3.0. J Biomed Inform 41:694–705
44. Walkingshaw AD, White TOH, Day NE et al. (2008) Representing, indexing and mining scientific data with XML and RDF: Golem and CrystalEye. XTech 2008: Dublin, Ireland
45. Ma H, Melillo G, Oliva L et al. (2005) Aluminum alkyl complexes supported by [OSSO] type bisphenolato ligands: synthesis, characterization and living polymerization of rac-lactide. Dalton Trans 721–727
46. Huggins ML (1969) Macromolecular nomenclature: general background and perspective. J Chem Doc 9:230–231
47. Livingston HK, Fox RB (1969) Nomenclature of organic polymers. J Chem Doc 9:232–234
48. Cohn WE (1969) Representation of macromolecules and polymers of biological importance. J Chem Doc 9:235–241
49. Block BP, Thomas PM, Donovan KM (1969) Problems in the nomenclature of inorganic polymers. J Chem Doc 9:242–244

50. Bikales NM (1969) Polymer nomenclature in industry. J Chem Doc 9:245–247
51. Loening KL, Metanomski WV, Powell WH (1969) Indexing of polymers in Chemical Abstracts. J Chem Doc 9:248–251
52. Metanomski WV (1979) Symposium on retrieval of polymer information: introductory remarks. J Chem Inf Comput Sci 19:59
53. Langstaff EM, Ostrum K (1979) Access to polymer information in chemical abstracts. J Chem Inf Comput Sci 19:60–64
54. Fugmann R (1979) POLIDCASYR: the polymer documentation system of IDC. J Chem Inf Comp Sci 19:64–68
55. Donaruma LG (1979) Some problems encountered in interdisciplinary searches of the polymer literature. J Chem Inf Comp Sci 19:68–70
56. Nardone J (1979) Computerized numeric data for polymers. J Chem Inf Comp Sci 19:71–73
57. Roush PF, Seitz JT, Young LF (1979) An on-line system for storage and retrieval of polymer data. J Chem Inf Comp Sci 19:73–76
58. Skolnik H (1979) A classification system for polymer literature in an industrial environment. J Chem Inf Comp Sci 19:76–79
59. Zurbach Balent M, Lotz JW (1979) Polymers and patents don't mix-easily. J Chem Inf Comp Sci 19:80–83
60. Fugmann R (1974) Representation of concept relations using the TOSAR system of the IDC. J Am Soc Inf Sci 25:287–307
61. Manola F, Miller E (2004) RDF Primer. http://www.w3.org/TR/rdf-primer/. Accessed Jul 10 2007
62. Brickley D, Guha RV (2004) RDF vocabulary description language 1.0: RDF schema. http://www.w3.org/TR/rdf-schema/. Accessed Dec 30 2008
63. McGuiness D, van Harmelen F (2004) OWL web ontology language overview. http://www.w3.org/TR/owl-features/.Accessed Dec 30 2008
64. Ranganathan SR (1963) Colon classification. Asia Publishing House, Bombay, India
65. Metanomski WV (1991) Compendium of macromolecular nomenclature (the purple book). Blackwell Scientific Publications, Oxford
66. Kaback SM (1991) Polymer information: storage for retrieval, or hide and seek? Introduction. J Chem Inf Comput Sci 31:439–443
67. Gushurst AJ, Nourse JG, Hounshell WD et al. (1991) The substance module: the representation, storage and searching of complex structures. J Chem Inf Comp Sci 31:447–454
68. Kaback SM (1991) There's more to a polymer than just its build. J Chem Inf Comput Sci 31:439–443
69. Briggs JA, Ferns EA, Shenton KE (1991) Improvements in Derwent Plasdoc system. J Chem Inf Comput Sci 31:454–458
70. Rieder MD (1991) The IFI polymer indexing system: its past, present and future. J Chem Inf Comput Sci 31:458–462
71. Green C (1991) The Rapra abstracts rubber and plastics database. J Chem Inf Comput Sci 31:476–481
72. Herz M (1991) Polymer searching in different databases. J Chem Inf Comput Sci 31:469–475
73. Lambert N (1991) Online searching of polymer patents: precision and recall. J Chem Inf Comput Sci 31:443–446
74. Wilke RN, Buntrock RE (1991) Condensation polymer information: problems and opportunities. J Chem Inf Comput Sci 31:463–468
75. Berners-Lee T, Hendler J, Lassila O (2001) The semantic web. Sci Am 284:34–44
76. Bray T, Paoli J, Sperberg-McQueen CM et al. (2006) Extensible markup language (XML) 1.1 (Second Edition). http://www.w3.org/TR/REC-xml/.Accessed Jul 10 2007
77. W3C (2004) XML schema part 0: primer. Second edition http://www.w3.org/TR/xmlschema-0/. Accessed Dec 12 2008
78. Holliday GL, Murray-Rust P, Rzepa HS (2006) Chemical markup, XML, and the world wide web. 6. CMLReact, an XML vocabulary for chemical reactions. J Chem Inf Model 46:145–157

79. Murray-Rust P, Rzepa HS, Williamson MJ et al. (2004) Chemical markup, XML, and the world wide web. 5. Applications of chemical metadata in RSS aggregators. J Chem Inf Comput Sci 44:462–469
80. Murray-Rust P, Rzepa HS (2003) Chemical markup, XML, and the world wide web. 4. CML schema. J Chem Inf Comput Sci 43:757–772
81. Gkoutos GV, Murray-Rust P, Rzepa HS et al. (2001) Chemical markup, XML and the world-wide web. 3. Toward a signed semantic chemical web of trust. J Chem Inf Comput Sci 41:1124–1130
82. Murray-Rust P, Rzepa HS (2001) Chemical markup, XML and the world-wide web. 2. Information objects and the CMLDOM. J Chem Inf Comput Sci 41:1113–1123
83. Murray-Rust P, Rzepa H (1999) Chemical markup, XML, and the world-wide web. 1. Basic principles. J Chem Inf Comput Sci 39:928–942
84. Frenkel M, Chiroco RD, Diky V et al. (2006) XML-based IUPAC standard for experimental, predicted, and critically evaluated thermodynamic property data storage and capture (ThermoML) (IUPAC Recommendations 2006). Pure Appl Chem 78:541–612
85. Sankar P, Aghila G (2006) Design and development of chemical ontologies for reaction representation. J Chem Inf Model 46:2355–2368
86. Sankar P, Aghila G (2007) Ontology aided modeling of organic reaction mechanisms with flexible and fragment based XML markup procedures. J Chem Inf Model 47:1747–1762
87. Microsoft (2008) Chem4Word project. http://research.microsoft.com/projects/chem4word/. Accessed Dec 30 2008
88. Adams N, Murray-Rust P (2008) Engineering polymer informatics: towards the computer-aided design of polymers. Macromol Rapid Commun 29:615–632
89. Adams N, Murray-Rust P, Winter J et al. (2008) Chemical markup, XML and the world wide web. 8. Polymer Markup Language. J Chem Inf Model 48:2118–2128
90. Clark J (1999) XSL Transformations (XSLT). http://www.w3.org/TR/xslt. Accessed Aug 04 2008
91. de Matos P, Ennis M, Zbinden M et al. (2006) ChEBI – Chemical entities of biological interest. http://www3.oup.co.uk/nar/database/summary/646, Accessed Dec 12 2008
92. Kanehisa M, Goto S, Kawashima S et al. (2004) The KEGG resource for decipering the genome. Nucleic Acids Res 32:D277–D280
93. Fleischmann A, Darsow M, Degtyarenko K et al. (2004) IntEnz, the integrated relational enzyme database. Nucleic Acids Res 32:D434–D437
94. Degtyarenko K (2007) The Rex ontology. http://obofoundry.org/cgi-bin/detail.cgi?id=rex, Accessed Dec 30 2008
95. Degtyarenko K (2007) The FIX ontology. http://obofoundry.org/cgi-bin/detail.cgi?id=fix, Accessed Dec 30 2008
96. Feldman HJ, Dumontier M, Lng S et al. (2005) CO: a chemical ontology for identification of functional groups and semantic comparison of small molecules. FEBS Lett 579:4685–4691
97. Frey JG, Hughes GV, Mills HR et al. (2003) Less is more: lightweight ontologies and user interfaces for smart labs. UK e-Science All Hands Meeting:500–507, Nottingham, UK
98. Frey JG, de Roure D, Schraefel MC et al. (2003) Context slicing the chemical aether. First International Workshop on Hypermedia and the Semantic Web:9, Nottingham, UK
99. Taylor KR, Gledhill RJ, Essex JW et al. (2006) Bringing chemical data onto the semantic web. J Chem Inf Model 46:939–952
100. Soldatova LN, Clare A, Sparkes A et al. (2006) An ontology for a robot scientist. Bioinformatics 22:e464–e471
101. Niles I, Pease A (2001) Towards a standard upper ontology. Proceedings of the 2nd International Conference on Formal Ontology in Information Systems (FOIS-2001): Ogunquit, Maine, United States
102. Heller B, Herre H (2004) Ontological categories in GOL. Axiomathes 14:57–76
103. Brandrup J, Immergut EH (1989) Polymer handbook. Wiley, New York
104. King J (2008) Text content in pdf files. http://blogs.adobe.com/insidepdf/2008/07/text_content_in_pdf_files.html. Accessed Dec 28 2008

105. Fenniri H, Chun S, Terreau O et al. (2007) Preparation and infrared/Raman classification of 630 spectroscopically encoded styrene copolymers. J Comb Chem 10:31–36

106. Hall SR, Allen FH, Brown ID (1991) The Crystallographic Information File (CIF): a new standard archive file for crystallography. Acta Cryst A 47:655–685

107. CCDC (2008) The Cambridge Crystallographic Data Centre. http://www.ccdc.cam.ac.uk/. Accessed Dec 12 2008

108. Day NE (2008) CrystalEye. http://wwmm.ch.cam.ac.uk/crystaleye/index.html. Accessed Dec 12 2008

109. Corbett P, Murray-Rust P (2006) High-throughput identification of chemistry in life science texts. Computational Life Sciences II. Lecture Notes in Computer Science, vol 4216, pp 107–118

110. Atkinson D (1992) The evolution of medical research writing from 1735 to 1985: the case of the Edinburgh Medical Journal. Appl Linguist 13:337–374

111. Zaye DF, Metanomski WV (1986) Scientific communication pathways: an overview and introduction to a symposium. J Chem Inf Comput Sci 26:43–44

112. Suh C, Rajagopalan A, Li X et al. (2002) The application of principal component analysis to materials science data. Data Sci J 1:19

113. Bajorath J (2001) Selected concepts and investigations in compound classification, molecular descriptor analysis and virtual screening. J Chem Inf Comput Sci 41:233

114. Wold S, Esbensen K, Geladi P (1987) Principal component analysis. Chemom Intell Lab Syst 2:37

115. Vanden Eynde X, Bertrand P (1997) ToF-SIMS quantification of polystyrene spectra based on principal component analysis (PCA). Surf Interface Anal 25:878

116. Coullerez G, Lundmark S, Malmstroem E et al. (2003) ToF-SIMS for the characterization of hyperbranched aliphatic polyesters: probing their molecular weight on surfaces based on principal component analysis (PCA). Surf Interface Anal 35:693–708

117. Batur C, Vhora MH, Cakmak M et al. (1999) On-line crystallinity measurement using laser Raman spectrometer and neural network. ISA Trans 38:139–148

118. Miranda TMR, Goncalves AR, Amorim MTP (2001) Ultraviolet-induced crosslinking of poly(vinyl alcohol) evaluated by principal component analysis of FTIR spectra. Polym Int 50:1068–1072

119. Vazquez C, Boeykens S, Bonadeo H (2002) Total reflection X-ray fluorescence polymer spectra: classification by taxonomy statistic tools. Talanta 57:1113–1117

120. Tuchbreiter A, Marquardt J, Zimmermann J et al. (2001) High-throughput evaluation of olefin copolymer composition by means of attenuated total reflection fourier transform infrared spectroscopy. J Comb Chem 3:598–603

121. Lukasiak BM, Faria R, Zomer S et al. (2006) Pattern recognition for the analysis of polymeric materials. Analyst 131:73–80

122. van Krevelen DW (1990) Properties of polymers: their correlation with chemical structure, their numerical estimation and prediction from additive group contributions. Elsevier, Amsterdam

123. Bicerano J (2002) Prediction of polymer properties. Marcel Dekker Ltd, New York

124. Stevens MP (1990) Polymer chemistry. An introduction. Oxford University Press, Oxford

125. Koehler MG, Hopfinger AJ (1989) Molecular modelling of polymers: 5. Inclusion of intermolecular energetics in estimating glass and crystal-melt transition temperatures. Polymer 30:116–126

126. Hopfinger AJ, Koehler MG, Pearlstein RA (1988) Molecular modling of polymers. IV. Estimation of glass transition temperatures. J Polym Sci Part B 26:2007–2028

127. Katritzky AR, Rachwal P, Law KW et al. (1996) Prediction of polymer glass transition temperatures using a general quantitative structure-property relationship treatment. J Chem Inf Comput Sci 36:879–884

128. Ivanciuc O (1997) CODESSA version 2.13 for Windows. J Chem Inf Comput Sci 37:405–406

129. Katritzky AR, Sild S, Lobanov V et al. (1998) Quantitative structure-property relationship (QSPR) correlation of glass transition temperatures of high molecular weight polymers. J Chem Inf Comput Sci 38:300–304

130. Cao C, Lin Y (2003) Correlation between the glass transition temperatures and repeating unit structure for high molecular weight polymers. J Chem Inf Comput Sci 43:643–650
131. Reynolds CH (1999) Designing diverse and focused combinatorial libraries of synthetic polymers. J Comb Chem 1:297–306
132. Brown WM, Martin S, Rintoul MD et al. (2006) Designing novel polymers with targeted properties using the signature molecular descriptor. J Chem Inf Model 46:826–835
133. Gurney K (1997) An introduction to neural networks. Routledge, London
134. Sumpter BG, Getino C, Noid DI (1994) Theory and applications of neural computing in chemical science. Annu Rev Phys Chem 45:439–481
135. Joyce SJ, Osguthorpe DJ, Padgett JA et al. (1995) Neural network prediction of glass-transition temperatures from monomer structure. J Chem Soc Faraday Trans 91:2491–2496
136. Mattioni BE, Jurs PC (2002) Prediction of glass transition temperatures from monomer and repeat unit structure using computational neural networks. J Chem Inf Comput Sci 42:232–240
137. Ulmer II CW, Smith DA, Sumpter BG et al. (1998) Computational neural networks and the rational design of polymeric materials: the next generation polycarbonates. Comput Theor Polym Sci 8:311–321
138. Schweizer KS, Curro JG (1994) PRISM theory of the structure, thermodynamics, and phase transitions of polymer liquids and alloys. Adv Polym Sci 116:319–377
139. Porter D (1995) Group interaction modeling of polymer properties. Marcel Dekker, New York
140. Afantitis A, Melagraki G, Makridima K et al. (2005) Prediction of high weight polymers glass transition temperature using RBF neural networks. J Mol Struct: THEOCHEM 716:192–198
141. Yu X, Yi B, Wang X et al. (2007) Correlation between the glass transition temperatures and multipole moments for polymers. Chem Phys 332:115–118
142. Gao J, Wang X, Li X et al. (2006) Prediction of polyamide properties using quantum-chemical methods and BP artificial neural networks. J Mol Model 12:513–520
143. Liu W, Yi P, Tang Z (2006) QSPR Models for various proeprties of polymethacrylates based on quantum chemical descriptors. QSAR Comb Sci 25:936–943
144. Liu A, Wang X, Wang L et al. (2007) Prediction of dielectric constants and glass transition temperatures of polymers by quantitative structure-property relationships. Eur Polym J 43:989–995
145. Duce C, Michell A, Starita A et al. (2006) Prediction of polymer properties from their structure by recursive neural networks. Macromol Rapid Commun 27:711–715
146. Katritzky AR, Sild S, Karelson M (1998) Correlation and prediction of the refractive indices of polymers by QSPR. J Chem Inf Comput Sci 38:1171–1176
147. Xu J, Chen B, Zhang Q et al. (2004) Prediction of refractive indices of linear polymers by a four descriptor QSPR model. Polymer 45:8651–8659
148. Yu X, Yi B, Wang X (2007) Prediction of the refractive index of vinyl polymers by using density functional theory. J Comp Chem 28:2336–2341
149. Xu J, Liang H, Chen B et al. (2008) Linear and nonlinear QSPR models to predict refractive indices of polymers from cyclic dimer structures. Chemom Intell Lab Syst 92:152–156
150. Gao J, Xu J, Chen B et al. (2007) A quantitative structure-property relationship study for refractive indices of conjugated polymers. J Mol Model 13:573–578
151. Liu H, Zhong C (2005) Modeling of the theta (lower critical solution temperature) in polymer solutions using molecular connectivity indices. Eur Polym J 41:139–147
152. Liu H, Zhong C (2005) General correlation for the prediction of theta (lower critical solution temperature) in polymer solutions. Ind Eng Chem Res 44:634–638
153. Melagraki G, Afantitis A, Sarimveis H et al. (2007) A novel QSPR model for predicting theta (lower critical solution temperature) in polymer solutions using molecular descriptors. J Mol Model 15:55–64
154. Xu J, Liu L, Xu W et al. (2007) A general QSPR model for the prediction of theta (lower critical solution temperature) in polymer solutions with topological indices. J Mol Graph Model 26:352–359

155. Xu J, Chen B, Liang H (2008) Accurate prediction of theta (lower critical solution temperature) in polymer solutions based in 3D descriptors and artificial neural networks. Macromol Theory Simul 17:109–120
156. Rushing TS, Hester RD (2004) Semi-empirical model for polyelectrolyte intrinsic viscosity as a function of ionic strength and polymer molecular weight. Polymer 45:6587–6594
157. Afantitis A, Melagraki G, Sarimveis H et al. (2006) Prediction of intrinsic viscosity in polymer-solvent combinations using a QSPR model. Polymer 47:3240–3248
158. Duncan R (2006) Polymer conjugates as anticancer nanomedicines. Nat Rev Cancer 6:688–701
159. Duncan R, Ringsdorf H, Satchi-Fainaro R (2006) Polymer therapeutics: polymers as drugs, drug and protein conjugates and gene delivery systems: past, present and future opportunities. Adv Polym Sci 192:1–8
160. G.S. Kwon, K. Kataoka (1995) Block copolymer micelles as long-circulating drug vehicles. Adv Drug Delivery Rev 16:295
161. Hoffman AS, Stayton PS (2004) Bioconjugates of smart polymers and proteins: synthesis and applications. Macromol Symp 207:139–151
162. Putnam D (2006) Polymers for gene delivery across length scales. Nat Mater 5:439–451
163. Godbey WT, Wu KK, Mikos AG (1999) Poly(ethylenimine) and its role in gene delivery. J Controlled Release 60:149–160
164. Hunter R, Strickland F, Kezdy F (1981) The adjuvant activity of nonionic block polymer surfactants. J Immunol 127:1244–1250
165. Hunter RL, Bennett B (1984) The adjuvant activity of nonionic block polymer surfactants. II. Antibody formation and inflammation related to the structure of the triblock and octablock copolymer. J Immunol 133:3167–3175
166. Brocchini S (2001) Combinatorial chemistry and biomedical polymer development. Adv Drug Delivery Rev 53:123–130
167. Kholodovych V, Gubskaya A, Bohrer M et al. (2008) Prediction of biological response for large combinatorial libraris of biodegradable polymers: polymethacrylates as a test case. Polymer 49:2435–2439
168. Yu X, Yi B, Liu F et al. (2008) Prediction of the dielectric dissipation factor tan delta of polymers with an ANN model based on DFT calculation. React Funct Polym 68:1557–1562
169. Yu X, Wang X, Wang H et al. (2006) Prediction of solubility parameters for polymers by a QSPR model. QSAR Comb Sci 25:156–161
170. Yu X, Xie Z, Yi B et al. (2007) Prediction of the thermal decomposition property of polymers using quantum chemical descriptors. Eur Polym J 818–823
171. Toropov AA, Nurgaliev IN, Balakhonenko OI et al. (2004) QSPR modeling of vitrification temperatures for polyarylene oxides. J Struct Chem 45:706–712
172. Nantasenamat C, Isarankura-Na-Ayudhya I, Naenna T et al. (2007) Quantitative structure-imprinting factor relationship of molecularly imprinted polymers. Biosens Bioelectron 2007:3309–3317
173. Si HZ, Zhang KJ, Hu ZD et al. (2007) QSAR model for prediction capacity factor of molecular imprinting polymer based on gene expression programming. QSAR Comb Sci 26:41–50
174. Hamoudeh M, Faraj AA, Canet-Soulas E et al. (2007) Elaboration of PLLA-based superparamagnetic nanoparticles: characterization, magnetic behaviour study and in vitro relaxivity evaluation. Int J Pharm 338:248–257
175. Service CA (1997) Chemical Abstracts Index Guide 1997. Columbus

Index